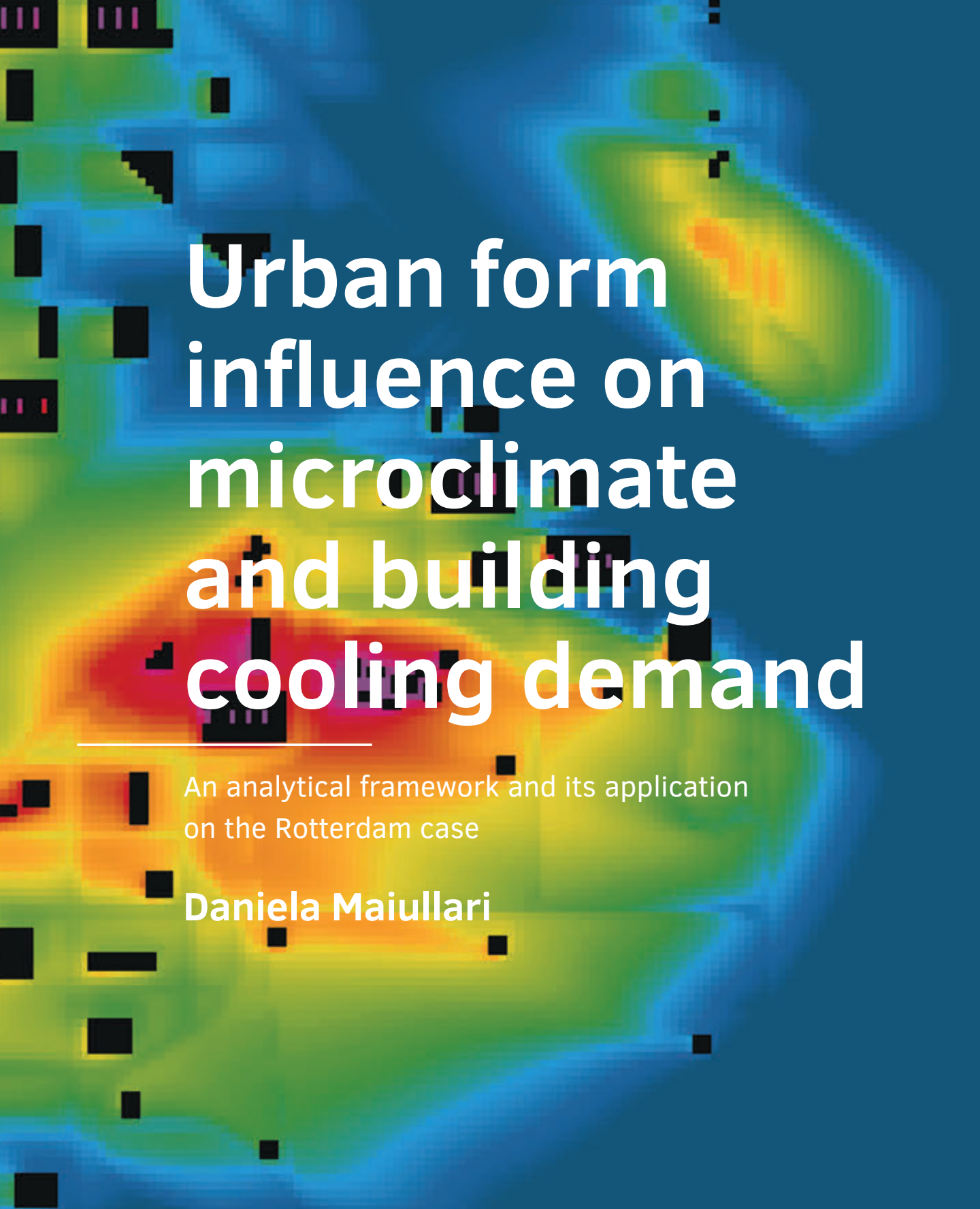


Urban form influence on microclimate and building cooling demand

An analytical framework and its application on the Rotterdam case

Daniela Maiullari

Urban form influence on microclimate and building cooling demand

An analytical framework and its application on the Rotterdam case

Daniela Maiullari

TOC

A+BE | Architecture and the Built Environment | TU Delft BK

23#04

Design | Sirene Ontwerpers, Véro Crickx

ISBN 978-94-6366-669-5
ISSN 2212-3202

© 2023 Daniela Maiullari

This dissertation is open access at https://doi.org/10.7480/abe.2023.04

Attribution 4.0 International (CC BY 4.0)

This is a human-readable summary of (and not a substitute for) the license that you'll find at:
https://creativecommons.org/licenses/by/4.0/

You are free to:
Share — copy and redistribute the material in any medium or format
Adapt — remix, transform, and build upon the material
for any purpose, even commercially.
This license is acceptable for Free Cultural Works.
The licensor cannot revoke these freedoms as long as you follow the license terms.

Under the following terms:
Attribution — You must give appropriate credit, provide a link to the license, and indicate if changes were made. You may do so in any reasonable manner, but not in any way that suggests the licensor endorses you or your use.

Unless otherwise specified, all the photographs in this thesis were taken by the author. For the use of illustrations effort has been made to ask permission for the legal owners as far as possible. We apologize for those cases in which we did not succeed. These legal owners are kindly requested to contact the author.

TOC

Urban form influence on microclimate and building cooling demand

An analytical framework and its application on the Rotterdam case

Dissertation

for the purpose of obtaining the degree of doctor
at Delft University of Technology
by the authority of the Rector Magnificus, prof.dr.ir. T.H.J.J. van der Hagen
chair of the Board for Doctorates
to be defended publicly on
Friday, 10 March 2023 at 12:30 o'clock

by

Daniela MAIULLARI
Master of Architecture, Università IUAV di Venezia, Italy
born in Bari, Italy

TOC

This dissertation has been approved by the promotors.

Composition of the doctoral committee:

Rector Magnificus,	chairperson
Prof.dr.ir. A. van Timmeren	Delft University of Technology, promotor
Dr.ir. M.M.E. van Esch	Delft University of Technology, copromotor

Independent members:

Prof.dr. J.E. Stoter	Delft University of Technology
Emeritus Prof. S.C. Roaf	Heriot Watt University, England
Dr. M.Y. Berghauser Pont	Chalmers University of Technology, Sweden
Prof.dr. H.A.E.E. Khalil	Cairo University, Egypt
Prof.dr.dipl.ing. S. Lenzholzer	Wageningen University, the Netherlands
Prof.dr. E.M. van Bueren	Delft University of Technology, reserve member

This study was co-financed by JPI Urban Europe & NWO (438.15.413)

To

my given and chosen family

Acknowledgements

This thesis would not have been possible without the support and encouragement of the following people throughout my Ph.D. journey. First and foremost, I would like to express my sincere gratitude to my thesis promoters **Arjan van Timmeren** and **Marjolein van Esch**, for their invaluable guidance, support, and encouragement throughout my academic journey. Beyond your insightful suggestions and constructive feedback, which were essential to shaping this thesis, I'm deeply grateful for your dedication and genuine interest in my research. I would also like to thank **Jorge Gil**, for the stimulating discussions that have enriched this thesis methodology and inspired new research paths.

This research was made possible thanks to the collaboration between TU Delft, ETH Zurich and the University of Bergen in the SPACERGY project. The project provided financial support and key learning opportunities. Thanks to **Akkelies van Nes** and **Arno Schlueter** for initiating this collaboration and welcoming me to their teams during visiting periods. **Martin Mosteiro** and **Remco de Koning,** fellow students in the SPACERGY adventure, also deserve a special mention for their dedication to the project and for providing empirical evidence that there is life outside Ph.D. life.

I would like to thank all my colleagues in the BK Urbanism Department. Their constructive criticism, suggestions, and support have been invaluable in helping me to develop my ideas and research. I am especially grateful to **Birgit Hausleitner, Alexander Wandl, Ioana Ionescuu, Claudiu Forgaci, Ulf Hackauf, Yan Song and Rusne Šileryté,** who have been a constant source of support and inspiration. To my former ETD colleagues **Kristel Aalbers, Abdullah Aldakheelallah, Arnout Sabbe, Foteini Setaki, Fransje Hooimeije, Mariette Overschie** and **Tanya Tsui,** thanks for making our workspace feel like a home.

I am also deeply grateful to **René van der Velde, Michiel Pouderoijen, Rebecca Price, Gül Aktürk, Clara Garcia Sanchez, Martijn Lugten** and **Lukas Beuster**. Working with you has been an honor and a source of inspiration. To **Liane Thuvander, Holger Wallbaum, Maja Kovacs** and all my other current and former colleagues at ACE, thank you for welcoming me at Chalmers and for supporting me during the last year of this journey.

I would like to extend my sincere gratitude to my colleagues and friends **Daniele, Cecilia, Giorgio, Luca, Bri, Bretty, Flávia, Tiago** and **Alex** for their friendship, encouragement, and support. I am truly grateful for all that you have done for me, and I will never forget your kindness and generosity.

I would like to express also my heartfelt gratitude to my friends outside academia, for their understanding and patience during these years. **Ema, Marine, Pau, Rachel, Silvio, Ylenia, Futura, Mania, Raffaella, Jessica** and **Tijn**, thanks for your love and for bringing joy and crazy adventures into my life. Thanks also for sharing lessons from the architectural/design practice and encouraging explorations of the world outside academia.

I cannot be more proud of having with me as paranymphs **Luiz Carvalho** and **Taneha Kuzniecow Bacchin**. I can't find the words to express my gratitude to them. I met **Taneha** on a rainy day in Venice before my Master graduation and I would have never imagined that encounter would end up being the beginning of a new life. She gave me the opportunity to discover my passion and talents for research and encouraged me to come to TU Delft. **Luiz** has been a Ph.D.–brother during these years, we have shared struggles and exciting achievements, along with a passion for urban morphological studies. He guided me to unexplored research and life territories that have greatly influenced my personal and professional growth. Basically, my story would have been completely different without you two. I'm eternally thankful for your mentorship, support and friendship.

I am also deeply grateful to my family, who have always been my source of strength and inspiration. Their 'amore incodizionato', support, and encouragement have pushed me forward. I'm especially thankful to my mamma **Paola** and my papá **Michele** for showing me how to embrace every challenge with braveness and a pinch of irony; to my sister **Elena** for teaching me every day that where there is a will there is a way; and to my siblings **Silvia** and **Fabio** for always been there for me, no matter what.

This achievement would not have been possible without the unconditional support of my beloved wife. **Marta**. I am deeply grateful for your love and patience, for believing in the relevance of this work, and for inspiring its development. This thesis is dedicated to you, my compass and my safe harbor throughout this turbulent journey.

Contents

List of Tables 13
List of Figures 14
Summary 17
Samenvatting 19

1 Introduction 21

1.1 **Cooling Demand, Climate and Urban Form** 23
1.1.1 Climate Drivers of Building Cooling Demand 23
1.1.2 Building Energy Demand and Urban Form 25

1.2 **Problem definition and objectives** 27
1.3 **Case study** 29
1.4 **Research questions** 31
1.5 **Thesis outline** 32

2 Urban Form and Building Energy Demand in Urban Climate 41

A Review of Energy-Relevant Form Attributes, Their Operation and Performance

2.1 **Introduction** 42
2.2 **Literature Search and Selection** 44

2.3 **Energy-Relevant Form Attributes and Parameters** 46
2.3.1 Building Unit 46
2.3.1.1 Size 47
2.3.1.2 Orientation 49
2.3.1.3 Building compactness 52
2.3.2 Street Canyon Unit 57
2.3.2.1 Proportion 58
2.3.2.2 Direction 62
2.3.3 Urban Fabric Unit 64
2.3.3.1 Density 65

2.3.3.2 Vertical Openness 71
2.3.3.3 Surface Roughness 73
2.3.3.4 Greenery 75

2.4 **Multivariable Approach** 78
2.5 **Discussion and Conclusions** 79

3 **A Quantitative Morphological Method for Mapping Local Climate Types** 95

3.1 **Introduction** 96

3.2 **Methodological Framework** 100
3.2.1 Case Study Description 100

3.3 **Classification of Building and Context Types** 101
3.3.1 Data Preparation for Morphological Quantification 101
3.3.2 Quantification of Morphological Attributes 102
3.3.3 Urban Form Characterisation 104
3.3.3.1 Description of the Building and Context Types 104
3.3.4 Archetype Selection 109

3.4 **Microclimate Assessment** 109
3.4.1 Data Preparation for Microclimate Modelling 109
3.4.2 Microclimate Quantification Results and Discussions 112
3.4.3 Characterization of Microclimate Patterns in Types 114
3.4.3.1 Indoor Temperature Patterns for the Different Building Types 115
3.4.3.2 Wind Speed Patterns for the Different Building Types 118
3.4.3.3 Air Temperature Patterns for Different Context Types 118

3.5 **Limitations** 120
3.6 **Conclusions** 121

4 **An Integrated Microclimate-Energy Demand Simulation Method for the Assessment of Urban Districts** 129

4.1 **Introduction** 130
4.2 **Background and state of the art** 132

4.3 **Methodology** 134
4.3.1 Step 1: Microclimate Modeling in ENVI-met 135
4.3.2 Step 2: Energy Demand Modelling in CEA and Main Environmental Parameters 137
4.3.2.1 Outdoor Air Temperature and Sensible Loads 137
4.3.2.2 Latent Load Calculation and Relative Humidity 139
4.3.2.3 Wind Speed Effects on Air Infiltration 139
4.3.2.4 Wind speed effects on convective heat transfer at exterior building surfaces 141

4.4 **Case Study Description** 142
4.4.1 Baseline Climate Dataset 143
4.4.2 Microclimate Dataset: ENVI-met Model Construction and Parameters 145
4.4.3 CEA Database and Model Construction 147

4.5 **Results** 148
4.5.1 Validation of the ENVI-met Model 149
4.5.2 Microclimate Characteristics of the Hochschulquartier 150
4.5.3 Comparison of the Space Cooling Demand for Each Weather Case 153

4.6 **Limitations** 157
4.7 **Conclusions** 158

5 **Energy Performance in Local Climate Types** 163

Application of an Integrated Microclimate-Energy Demand Simulation Method in a Dutch Context

5.1 **Introduction** 164

5.2 **Methodological Framework** 166
5.2.1 Building and context types' description 168
5.2.2 Baseline and Microclimate Datasets 172
5.2.3 City Energy Analyst: modelling and settings 174

5.3 **Results** 175
5.3.1 Outdoor and indoor conditions of Rotterdam archetypes 176
5.3.1.1 Correlations between morphological characteristics and temperatures 178
5.3.2 Space cooling demand in Baseline and Microclimate scenarios 180
5.3.2.1 Average daily cooling demand in building types 180
5.3.2.2 Sensitivity of cooling demand to microclimate 181
5.3.2.3 Sensitivity of cooling demand to Context Types 184
5.3.2.4 Hourly cooling demand 184

5.3.3 Analysis of the correlation between diurnal cooling demand, morphological and climate variables. 186

5.4 **Limitations** 187
5.5 **Conclusions** 188

6 **Discussion** 193

6.1 **Local Climate Type Classification** 193
6.2 **Microclimate assessment** 195
6.3 **Relationship between form and microclimate** 197
6.4 **Energy assessment** 198
6.5 **Cooling energy demand among Rotterdam LCTs** 200
6.6 **Relationship between cooling demand, urban form and climate characteristics** 203
6.7 **Potential applications of the results** 206

7 **Conclusions** 211

7.1 **Answering the research sub-questions** 211
7.1.1 Sub-questions 1 and 2 211
7.1.2 Sub-question 3 212
7.1.3 Sub-question 4 214
7.1.4 Sub-question 5 215
7.1.5 Sub-question 6 217

7.2 **Main research question** 219

7.3 **Recommendations** 221
7.3.1 Recommendations for future research 221
7.3.2 Recommendations for planning and design 224

7.4 **Final words** 225

Appendix 227
Curriculum vitae 249
Publications 253

List of Tables

1.1 Research questions 31

3.1 Summary of the selected morphological parameters. 103

3.2 Patterns of indoor temperatures per building type. 115

3.3 Patterns of wind speed per building type. 118

3.4 Patterns of outdoor air temperature per context type. 119

4.1 ENVI-met model settings. 145

4.2 Physical properties of the vegetation used in the ENVI-met model. 146

4.3 Physical properties of the soil materials used in the ENVI-met model. 146

4.4 Physical properties of the wall materials used in the ENVI-met model. 147

4.5 CEA model settings used in the case study. 148

5.1 Rotterdam Material Database 173

5.2 CEA inputs from Dutch standards 174

5.3 Occupancy schedule 175

5.4 Results of the linear regression analysis on Microclimate energy estimation in order of significance. 186

6.1 Key studies on urban climate related cooling penalty 201

List of Figures

1.1 Research outline 34

2.1 Classification framework of energy-relevant form parameters 45

2.2 Energy-relevant form attributes and parameters for the building unit 47

2.3 Energy-relevant form attributes and parameters for the street canyon unit 58

2.4 Schematic representation of H/W and SAO values 62

2.5 Energy-relevant form attributes and parameters for urban fabric unit 66

3.1 Methodological framework. 99

3.2 Hierarchical classification results: Building types (left) and Context types (right). 105

3.3 Standardized (z-score) numerical profiles of the building types (left) and context types (right). 106

3.4 Numerical thresholds for the description of the building types (left) and context types (right). 108

3.5 Visualization of the building archetypes in the five context types. 110

3.6 Building average air temperature (left), relative humidity (centre), and wind speed (right) near façade. 114

3.7 Indoor temperature values and wind speed values for each building type; outdoor air temperature values for each context type. 116

4.1 Diagram showing the proposed integration method between ENVI-met and CEA for each of the climatic cases considered. 134

4.2 Resistance-capacitance (RC) model used in CEA (adapted from SIA Merkblatt 2044). 138

4.3 Aerial representation of the case study area and functional distribution of the buildings under consideration. The functions shown as “Office” include both research and hospital spaces. The buildings selected for this study are colored red for university buildings and blue correspond to the hospital. The yellow circle marks the location of the temperature sensor in the case study area. 143

4.4 Data from the weather station SMA for the time period under analysis. 144

4.5 Outdoor air temperature results from the microclimate simulations for Model A and Model B compared to measured data from the sensor on the ML building. 150

4.6 Simulated mean air temperature, relative humidity and wind speed in the area compared to data from Baseline climate values. 151

4.7 Spatial distribution of air temperature at 2 m height. 152

4.8 Spatial distribution of wind speed at 2 m height. 152

4.9 Simulated mean air temperature, relative humidity and wind speed around buildings. 153

4.10 Box plots showing the space cooling demand and peak cooling power on the selected day when using weather station data compared to using local microclimate simulations. The total space cooling demand comprises the sensible and latent demands. 154

4.11 Box plots showing the change in space cooling demand and peak cooling power on the selected day when replacing the weather station data with simulated local microclimate results. The total space cooling demand comprises the sensible and latent demands. 154

4.12 Hourly space cooling demand in the district on the selected day for each of the climate cases. The boxplots at each hour show the distribution in the space cooling demand per conditioned floor area for all buildings in the area, whereas the lines show the entire district's demand per square meter for each case. 156

4.13 Change in total and peak cooling demand on the selected day due to the effect of microclimate for each building in the area. 156

5.1 Scheme of the methodological framework 167

5.2 Visualization of the 25 archetypes based on the five building types and the five context types. 169

5.3 Standardized (z-score) numerical profiles of building types (left) and context types (right). 170

5.4 Plotting of hourly air temperature, relative humidity and wind speed values at KNMI weather station at Rotterdam airport (June 29th-30th 2018) 172

5.5 Building average air temperature (left), relative humidity (center), wind speed (right) near façade 176

5.6 Urban Heat Island maximum intensity for building types (left), and for context types (right) 177

5.7 Average daytime Indoor temperature in building types cases 178

5.8 Standardized coefficient of the relation between temperatures and form parameters. 179

5.9 Daily cooling demand in Baseline and Microclimate scenarios grouped for building type (left) and cooling demand variation between Baseline and Microclimate scenarios (right). 182

5.10 Average and total cooling demand of each building type; cooling demand variation between Baseline and Microclimate scenarios for the two days analyzed. 183

5.11 Daily patterns of cooling demand in Baseline and Microclimate scenarios 185

TOC

Summary

As a determinant of urban microclimate and building energy performance, urban form plays a critical role when planning city transitions toward decarbonization. Even though energy use for cooling has tripled between 1990 and 2016 globally, and global increase in temperature is reinforcing this trend, the complex relationship between urban form and cooling demand remains understudied. Additionally, in urban climate conditions where the Urban Heat Island (UHI) further contributes to a temperature increase, a comprehensive quantification of form-dependent microclimate impacts on building cooling demand is limited by the methodological approaches employed.

The thesis aims at providing conceptual and methodological instruments to better understand the nature and the magnitude of the urban form-energy link by addressing the question '*How does urban form influence building cooling demand in urban microclimate conditions, and how can the magnitude of the relationship be assessed?'.*

By answering the main research question, the thesis contributes to the conceptualization and understanding of both the intrinsic and the extrinsic energy role of urban form. Furthermore, it proposes a novel methodological framework for increasing the accuracy of the numerical assessment of urban form-related climate and energy performance. The application of this framework on the city of Rotterdam provides an understanding of how and to what extent building and context form influence building cooling demand, illustrating the magnitude of UHI impacts in temperate climates and proving the relevance of informing planning and design practice.

In a first instance a transdisciplinary literature review (Chapter 2) identifies nine energy-related form attributes and over 54 descriptive parameters related to building, street canyon and urban fabric units. The analysis of the associated thermal processes highlights a twofold role of urban form in determining the cooling demand of buildings. The intrinsic role of form lies in building characteristics, which directly influence energy loads by impacting thermal gains and losses. The extrinsic role of form lies in the indirect effect of canyon and urban fabric on microclimate (e.g. by altering wind flows, radiation, sensible heat fluxes) which determine the conditions of the context in which a building energy system operates.

Following, the thesis addresses the limitations in assessing the magnitude of urban form influence on building cooling demand for analysing the direct effects of building characteristics and the indirect, microclimate effects of context characteristics . Informed by existing morphological approaches in the climatology and energy domains, the thesis concludes that to assess urban microclimate conditions from a morphological perspective, four conditions should be met. The morphological approach should i) allow for multi-variables, ii) allow for a multi-scalar description, iii) use analytical units of proximity, and iv) acknowledge heterogeneity of the fabric in the selection of representative form patterns. Additionally, the thesis suggests that building demand calculations should include the use of microclimate boundary conditions for a more precise cooling demand estimation. Based on this list of requirements, the framework developed enables the identification of Local Climate Types (LCTs), the assessment of the microclimate influence of buildings and context types within these LCTs (Chapter 3), and the simulation of building cooling demand within local microclimate conditions (Chapter 5). The latter method for coupling microclimate and energy demand models is initially tested on a case study in Zurich, Switzerland (Chapter 4)

The application of the framework on the case study of Rotterdam helps to identify five building types and five context types, which together make combined 25 LCTs. The microclimate assessment during two representative hot days shows that urban form variables result in a change in urban air temperature up to 2.5°C, 3m/s change in wind speed and 5% change in relative humidity. As a consequence, daily cooling demand is on average 23-32% higher in urban microclimate conditions compared to rural conditions, and among the analysed buildings the increase in cooling loads varies between 3.6% and 100%. A sensitivity analysis showed which building and context form parameters determine the variations.

Finally, the general outcomes of the study are discussed, interlinked and placed within the context of the existing body of knowledge (Chapter 6). Conclusions are presented, providing recommendations for future research and applications of the thesis results in planning and design (Chapter 7).

Samenvatting

Als bepalende factor voor zowel het microklimaat van steden als de energie-efficiëntie van gebouwen speelt de stedelijke vorm een belangrijke rol bij de transitie naar een koolstofarme economie. Hoewel het energieverbruik voor koeling van gebouwen tussen 1990 en 2016 wereldwijd is verdrievoudigd – en de opwarming van de aarde deze trend versterkt – is de complexe relatie tussen stadsvorm en koudevraag nog te weinig bestudeerd. Daarbovenop komt dat binnen de huidige methodologieën een uitgebreide kwantificering van vormafhankelijke microklimaateffecten op de koudevraag van gebouwen, in hoeverre het hitte-eilandeffect (urban heat island, UHI) verder bijdraagt aan temperatuurstijging, beperkt is.

Dit proefschrift beoogt conceptuele en methodologische instrumenten aan te reiken om de aard en omvang van de relatie tussen stadsvorm en energiebehoefte beter te begrijpen door de vraag te beantwoorden: Hoe beïnvloedt stadsvorm de koudevraag van gebouwen in een stedelijk microklimaat en hoe kan de omvang van die invloed bepaald worden? Door deze onderzoeksvraag te beantwoorden draagt het proefschrift bij aan de conceptualisering van- en kennis over de intrinsieke en extrinsieke energie effecten van de stedelijke vorm. Bovendien levert het een nieuw methodologisch kader om de klimaat- en energie-effecten van stadsvorm nauwkeuriger te bepalen. De toepassing hiervan op de stad Rotterdam belicht hoe en in welke mate gebouw- en contextvorm de koudevraag van gebouwen beïnvloeden naast de omvang van UHI-effecten daarop in gematigde klimaten, en bewijst het de relevantie voor de plannings- en ontwerppraktijk.

Allereerst identificeert een transdisciplinair literatuuronderzoek (hoofdstuk 2) negen energiegerelateerde vormelementen en meer dan 54 beschrijvende parameters met betrekking tot gebouwen, straten en stedelijk weefsel. De analyse van de bijbehorende thermische processen brengt de tweeledige rol van stedelijke vorm bij het bepalen van de koudevraag van gebouwen in beeld. De intrinsieke rol van vorm bestaat uit gebouwkenmerken, die de energiebehoefte rechtstreeks beïnvloeden door warmtewinsten en -verliezen. De extrinsieke rol bestaat uit het indirecte effect van straten en stedelijk weefsel op het microklimaat (bijvoorbeeld door verandering van windstromen, straling of voelbare warmtefluxen), en bepaalt daarmee de context waarin een gebouwenergiesysteem werkt.

Vervolgens gaat het proefschrift in op de beperkingen bij het bepalen van de invloed van de stadsvorm op de koudevraag van gebouwen via directe effecten (gebouwkenmerken) en indirecte microklimaateffecten (contextkenmerken). Gebaseerd op bestaande morfologische benaderingen uit de klimatologie en energiedomeinen is de conclusie dat om een stedelijk microklimaat vanuit een morfologisch perspectief te kunnen beoordelen, aan vier voorwaarden moet worden voldaan. De morfologische benadering moet i) multi-variabelen toestaan, ii) een multi-scalaire beschrijving toestaan, iii) analytische eenheden van nabijheid gebruiken, en iv) heterogeniteit van het stedelijk weefsel erkennen bij de selectie van typische vormpatronen. Daarnaast stelt het proefschrift voor dat om schattingen van de koudevraag van gebouwen preciezer te maken, de grensvoorwaarden van het microklimaat moeten worden gebruikt. Op basis van deze lijst met vereisten maakt het ontwikkelde kader het mogelijk om voor stedelijke contexten lokale klimaattypen (local climate types, LCT's) te identificeren, de invloed van gebouw- en contexttypen op het microklimaat van deze LCT's te bepalen (hoofdstuk 3), en de koudevraag van gebouwen binnen de voorwaarden van het lokale microklimaat te simuleren (hoofdstuk 4).

De toepassing van het kader op de casestudy van Rotterdam (hoofdstuk 5) helpt bij het identificeren van de vijf voornaamste gebouwtypen en vijf voornaamste contexttypen, die gecombineerd 25 LCT's vormen. De concrete effecten, door middel van berekeningen aangaande het microklimaat gedurende twee representatieve hete dagen, laten zien dat variabelen in de stadsvorm resulteren in mogelijke verandering in luchttemperatuur tot 2,5 °C, een verandering in windsnelheid tot 3 m/s en een mogelijke verandering in relatieve vochtigheid van 5%. Bijgevolg is de dagelijkse koudevraag in een stedelijk microklimaat gemiddeld 23 tot 32% hoger dan bij landelijke omstandigheden. Voor de geanalyseerde gebouwen varieert de toename tussen 3,6% en 100%. Een uitgevoerde gevoeligheidsanalyse toont tenslotte welke gebouw- en contextvormparameters deze variaties bepalen.

Tot slot worden de algemene uitkomsten van het onderzoek besproken, aan elkaar gerelateerd en in de context van eerder onderzoek geplaatst (hoofdstuk 6). Conclusies worden gepresenteerd en vergezeld van aanbevelingen voor toekomstig onderzoek en mogelijke toepassingen van de onderzoeksresultaten in de plannings- en ontwerppraktijk (hoofdstuk 7).

1 Introduction

"*Every nation builds houses for its own climate. At this time of international interpenetration of scientific techniques, I propose one single building for all nations and climates, the house with respiration exacte*" (Le Corbusier, 1930).

With this statement in 1930, Le Corbusier proclaimed the final fracture between the modernist *machine à habiter* and climate-sensitive vernacular architecture; a break that has been perpetrated and consolidated in the design practice of the following decades, and that subordinates the relation between buildings and outdoor climate in favour of the creation of an artificial indoor comfort, enabled by technological advances in mechanical equipment for air-conditioning. Said in other words, "building form and function can be considered to have been liberated from its climate driven form" (Mills & Futcher, 2021).

The consequences of the scaling-up of this design paradigm are still visible today. The building sector consumes more than 55% of global electricity and accounts for up to 28% of total global energy-related CO_2 emissions (IEA, 2020). From an environmental perspective, the massive transition from passive to mechanical ventilation has been a major driver of change in the energy consumption of the building sector, despite advances in envelope insulation and system efficiency (IEA, 2018). From a design and research perspective, knowledge on the relationship between climate and building design has remained the core of bio-climatic and passive architecture, showcasing good practices for achieving energy efficiency. On the other hand, thermal comfort studies have clearly demonstrated the negative effects of mechanical ventilation on occupants' well-being and the influence of thermal comfort standards on building energy consumption increase (Roaf et al., 2010). As such, both perspectives suggest a need for a critical reflection on the role of climate-sensitive design and planning to meet decarbonization targets in cities (Manzano-Agugliaro et al., 2015; Aghimien et al., 2022).

Like the energy crisis in the 1970s that called for urgent energy savings on indoor conditioning, following energy crises represented opportunities to advance knowledge and practice towards novel, diverse and finally more sustainable energy use. Ultimately, the ongoing energy transition builds on these premises. In the last few decades, the debate around a low-carbon society and related policy interventions has been growing in intensity due to the urgent need to control

anthropogenic greenhouse gas emissions and their impact on global warming. Having analysed the cumulative effects of human activities on the climate system, the special IPCC report in 2018 Masson-Delmotte et al. (2018) introduced new targets for limiting global temperature change to 1.5°C, and analysed an array of pathways to this goal. Since the reduction of CO_2 emissions involves different portfolios of climate change mitigation measures, it has been argued that diverse levels of balance can be achieved by lowering energy demand and supplying energy via decarbonized sources (Rogelj et al., 2018).

However, regardless of the pathways chosen to limit global warming, rapid and structural implementation of new strategies is required in the energy, land use, building and infrastructure sectors. These sectors are called to address the multidimensional challenge (Santamouris, 2020) of 1) complying with the new targets for reducing energy consumption, 2) ensuring affordable and secure energy supply, 3) improving efficiency of use, and 4) adapting to the effects of climate change. These challenges appear even more intense in urban systems, where energy transitions require a deep rethinking of the structure and functioning of the built environment (Davoudi et al., 2009), and where energy-related technical measures and urban planning practices have to confront the spatial accommodation of new performances (Sijmons et al., 2014) while developing resilience and adaptive capacity for future climate conditions. As a consequence, urban energy transitions increasingly demand to advance knowledge on reciprocal influences between urban spatial structure, climate conditions and energy performance (Emmanuel & Steemers, 2018; Futcher & Mills, 2013). Building on this requirement, the development of integrated energy strategies provides a renewed occasion for a paradigm shift in urban planning and design towards re-establishing a positive synergy between spatial and environmental properties and reconciling buildings' performance with their outdoor climate.

In this context, this thesis aims to contribute to an understanding of the relationship between the spatial characteristics of the built environment and building energy demand, while recognising the key role of climatic conditions. This multidisciplinary discourse builds on previous studies in urban morphology, urban climatology and energy-related fields. Acknowledging the wide and complex nature of the topic, this research focuses specifically on the energy-related characteristics of urban form and their influence on building cooling demand within an urban climate context. Building cooling demand is here defined as the energy in watt-hours required to extract sensible and latent heat through a cooling system to maintain a constant temperature and humidity in a building during a given period of time (ISO 13790, 2008; ASHRAE, 2022).

In this chapter, Section 1.1 provides the basic definitions and concepts on which this thesis builds. The research context is introduced by presenting the climate-related drivers of future cooling demand and advances in energy studies using both a climatological and morphological approach. Section 1.2 focuses on the problem definition and the research objectives that drive the thesis. Section 1.3 introduces the case study of Rotterdam (the Netherlands). Finally, Sections 1.4 and 1.5 present the research questions and outline of the thesis, respectively.

1.1 Cooling Demand, Climate and Urban Form

1.1.1 Climate Drivers of Building Cooling Demand

Global energy use for space cooling in buildings has tripled between 1990 and 2016, and is the fastest-growing form of energy use in buildings (IEA, 2018). In terms of future pressures on energy consumption, climate factors become even more critical as an increase in temperatures will likely further reinforce this trend. Moreover, from the previously mentioned multidimensional perspective, warmer climate conditions can increase the overall energy consumption of buildings, undermine the achievement of energy targets, and affect a secure supply of energy, especially during extremely hot periods. This is aggravated in cities, as both macro-scale processes at the global level and the urban heat island effect at the urban meso-scale cause warmer climates in cities (Santamouris, 2020; Nik et al., 2021).

At the macro-scale, climate change is expected to be one of the strongest drivers of energy consumption change in the building sector, affecting the need for space heating and predominately the need for space cooling. As summarised by Bazazzadeh et al. (2021), three trends will probably lead to an exponential rise in cooling demand:

- insufficient natural ventilation in hotter climate conditions or during extreme weather events will likely result in a gradual growth of HVAC (heating, ventilation and air conditioning) system installation, including in existing buildings;

TOC

- a decrease in days when heating is required and an increase in days when cooling is required will result in an overall increase in cooling demand in the building sector;
- peak electricity demand may increase due to extreme events and related demand for cooling.

Additionally, urban overheating processes are expected to further contribute to an increase in building cooling demand. At the urban climate meso-scale, there is a distinctive change in atmospheric characteristics associated with the properties of the built environment and with anthropogenic emissions (Pijpers-van Esch, 2015). The heat created by human activity, the trapping of solar energy, the increased thermal storage, and the influence on wind speed (often reduction) due to urban fabric properties, as well as the reduction in evapotranspiration resulting from the lack of vegetation and permeable paving materials, all result in higher surface and air temperatures in urban environments compared with rural environments. This phenomenon, studied for over two centuries (Stewart, 2019), is today known with the term given by Peppler (1929): urban heat island (UHI) effect.

Due to the city energy balance (Mills et al.,2022) buildings in urban environments are exposed to complex processes of heat and mass exchange between surfaces and the atmosphere, which influence the energy needs for space cooling. A literature review by Santamouris (2014) concluded that the UHI effect contributes to an increase in the average cooling load of typical urban buildings by 13%. However, Santamouris also observed that in cooling-dominated zones the growth in cooling demand due to UHI is much higher than the decrease in heating demand, while in heating-dominated zones UHI mainly contributes to lower heating loads. A more recent review by Li et al. (2019) indicates that UHI can increase cooling consumption by a median of 19% in a range between 10% and 120%, and can decrease heating consumption by a median of 18.7% in a range between 3% and 44.6%. However, despite the variations found in global case studies, the analysis did not identify a geographical and temporal pattern. Further studies also demonstrate the impact of UHI on peak electricity consumption. For instance, Santamouris et al. (2015) estimated that for each degree of temperature increase, peak electricity demand for space cooling increases by between 0.45% and 4.6%.

Therefore, it appears evident that advancing a systemic understanding of the urban climate and related energy performance of buildings is necessary to develop effective low-carbon adaptive strategies to control the increase in energy consumption for cooling purposes, including in climate zones traditionally considered to be temperate. Overlooking an adaptive perspective might negatively influence the overall decrease in energy consumption in the long term (Mauree et al., 2018). However, available studies in which decarbonization guidelines and measures are

framed for the building stock are largely built on assessments using typical weather data, and thus past climatic conditions rather than future conditions, and very often neglect the urban climate and the morphological context in which the building operates (Nik et al., 2021). Consequently, disregarding climate warming and UHI in energy analyses and assessments leads to an important underestimation of cooling demand (Allegrini et al., 2012; Sun & Augenbroe, 2014), and might lead decisions towards the adoption of energy efficient solutions that are mostly heating-oriented (for example, retrofitting building envelopes), and therefore further increase space-conditioning loads (Gunawardena et al., 2019) and outdoor temperatures (van Hooff et al., 2016). Furthermore, the increase in space cooling demand due to increased global temperatures is expected to create a 'vicious cycle' (Ashie et al., 1999; Kikegawa et al. 2003) by causing more anthropogenic heat emission which will intensify the UHI effect and therefore the need for mechanical cooling (Afshari & Liu, 2017).

Although researchers have proved that climate phenomena are determining factors of building energy demand, "cities affect climate at a hierarchy of scales" (Mills & Futcher, 2021) that need further research. At the microclimate scale—the scale representing the direct urban context of buildings—atmospheric variables can substantially deviate from the climatic conditions prevailing over a larger urban area (i.e. at the meso level) as they are governed by geometry, materialization and landscaping conditions (Pijpers-van Esch, 2015). These three factors influence air temperature (Lan & Zhan, 2017; Yu et al., 2020), shadow and wind patterns (Wang et al., 2017), the reflection and absorption of solar radiation (Morganti, Salvati, Coch, & Cecere, 2017), and the evaporative cooling (Chun & Guldmann, 2018; Wang et al., 2016). All these microclimate properties of the built environment and related mechanisms, mostly been analysed in isolation, have been found to be critical in determining building energy performance, although they are only partially included in the common practice of energy demand estimation. A systemic and quantitative analysis of the climatic environment in buildings' surroundings can support the development of more comprehensive energy strategies to control building energy demand and specifically space cooling loads.

1.1.2 Building Energy Demand and Urban Form

The importance of the surroundings on the energy performance of buildings has been recognised in energy studies with an urban morphology perspective. Expanding on the work of Baker & Steemers (2000) which identified occupants' behaviour, system design and building design as the major factors shaping building energy

demand, Ratti et al. (2005) acknowledged the relevance of the urban context for building energy demand, defining the urban context as the combination of urban geometry and related urban microclimate processes. However, due to technical limitations, their model only allowed a partial computation of microclimate factors—they could only calculate light availability. This attempt to quantify form-related energy consumption, together with others that followed, showed that building design and the urban context together might account for up to a factor of 5 (Ratti, et al., 2005) or 6 (Rode et al., 2014a) in reducing building energy use. Compared to system efficiency and occupants' behaviour, which were estimated to each account for a factor 2 variation in energy consumption, the physical dimension thus appears to be the factor most relevant to the realisation of a drastic reduction of building energy consumption (Salat, 2007).

Other quantitative morphological approaches have been employed in studies that analyse urban form parameters and the related energy performance of cities (Ahmadian et al., 2021; Bourdic et al., 2012; Mashhoodi, 2019; Rode et al., 2014b; Silva, et al., 2018). These studies have focused on different scales of analysis. For example, at the building scale, empirical and parametric studies have demonstrated that increases in envelope area and plan depth (Steadman et al., 2014) as well as building height (Godoy-Shimizu et al., 2018) increase energy demand. By analysing street canyon and district characteristics, Li et al., (2018), Futcher et al. (2018), and Leng et al., (2020), among others, have shown that *height-to-width ratio* and *density* influence the cooling and heating demand of buildings. Other scholars, such as Wong et al. (2011), have measured the form characteristics of building surroundings in units of vicinity in order to specifically investigate energy load variations resulting from context change.

Following the categorisation of urban morphology research by Gauthier and Gilliland (2006), these energy-focused morphological studies find their position in the branch of *space morphology*, which, according to Moudon (1994), uncovers the fundamental geometrical characteristics of the urban fabric components (buildings, blocks, districts, and plots). Inspired by the seminal work of Martin and March (1972), morpho-energy studies employ a mathematical approach to describe urban forms and attempt to identify and assess energy-relevant form characteristics. However, while these studies have proven that building energy performance is largely dependent on urban form characteristics, spatially-explicit analyses are needed to quantify the magnitude of urban form influence (Silva, 2017), as it has been suggested that it is an energy management parameter (Futcher et al., 2013) and thus key to understanding the specificity of energy use in different urban areas (Grubler, 2012) and to developing sustainable urban plans for more resource efficient cities. Additionally, building energy demand due to space cooling needs and

urban microclimate factors have only been partially addressed or even overlooked in morphological studies. Urban microclimate factors have been acknowledged as a component of the conditions of the urban context in which buildings operate (Natanian, 2020; Tsirigoti & Tsikaloudaki, 2018), nevertheless quantification of their impact has largely been limited.

1.2 Problem definition and objectives

This thesis acknowledges that urban form—together with behaviour adjustment, technological advancement and design considerations—is a key area of intervention to reduce building energy demand in urban environments. As we have seen in the previous section, in a warmer future cooling demand is a driver of change in the building energy sector. For a successful energy transition, it is fundamental that the application of measures to reduce energy demand, and in particular those related to cooling, re-establishes the connection between the design of the physical form of buildings and the climatic context in which they perform.

Overall, the relationship between urban form and building energy performance is well established in literature. However, the size of the influence and the complex nature of the environmental processes involved remain understudied (Ko, 2013; Silva, et al., 2017), especially regarding space cooling. The reasons for this have a multivariable, multiscale and multidomain nature. Firstly, a comprehensive explanation of the influence of urban form on building cooling demand relies on a detailed understanding of the thermal mechanisms triggered by both buildings and the characteristics of their contexts. However, for decades, studies have employed a sectoral approach by investigating the energy relevance of building form factors (Anderson et al., 2015). These attributes generally describe the geometrical properties of single buildings and their direct impact on loads and gains. In contrast, urban context characteristics do not seem to act directly on building energy loads, but rather shape the urban microclimate conditions in which buildings operate. Secondly, these indirect effects of the urban context on urban climate, and thus on energy consumption, are addressed in a fragmented body of literature that focuses on only a few form and climate variables at a time (Kolokotroni & Salvati, 2021). Thirdly, most of the studies that have demonstrated that urban warming phenomena such as UHI have a significant effect on space cooling demand have overlooked the micro-scale of climate phenomena by focusing predominately on

comparing temperature-dependent loads in urban and rural environments (Toparlar et al., 2018).

As a result, the degree of interaction between urban form characteristics remains largely unknown (Silva et al., 2017), and the understanding of the overall magnitude of urban fabric impacts on energy performance remains limited (Quan & Li, 2021). Ewing and Cervero (2010) also argue that "the effect of each variable of urban form has a relatively small effect on the overall urban energy demand, but that their combined effect is expected to be more significant and worth controlling". Furthermore, Adolphe (2001) has pointed out that although there is an evident relation between form factors, climatic conditions and energy supply, the "characterization of this complex link remains critical, especially because of the extreme morphological heterogeneity".

The problems just described partly result from the limitations of the methodological instruments used to quantify the influence of form on energy demand. Generally, the models and techniques developed to analyse the energy behaviour of buildings have adopted an architectural design perspective by focusing on individual building entities, "neglecting the importance of phenomena that occur at the urban scale" (Ratti et al., 2005). Thus, computational energy demand models have largely overlooked urban microclimate and UHI effect, instead representing the city as a collection of stand-alone objects (Anderson et al., 2015) in a static setting and employing rural weather data and typical meteorological years for the estimation of energy demand (Afshari & Liu, 2017; Yang et al., 2020). Additionally, the studies that have addressed the interactions between the urban climatic context and building thermal performance have been limited by the availability of measured climate data from only a few urban stations (Hassid et al., 2000; Kolokotroni et al., 2006, Su et al., 2021), or by climate modelling techniques with limited computational capacity for simulating large areas of cities (Huang et al., 2020).

These limitations of the methodological instruments also affect morphological approaches. In the literature on the relationship between the energy performance of buildings and urban climate, quantitative morphological approaches have helped to describe and classify urban form characteristics and analyse the relationships among variables. These approaches, however, generally take one of two methodological paths. The first is based on a selection of urban samples with homogeneous characteristics (Rode et al., 2014b; Salvati et al., 2019) and generic patterns created by the repetition of building and canyon types (Ahmadian et al., 2021; Zhang & Gao, 2021), which limits the investigation of urban morphological complexity. The second measures form characteristics usually at the city scale, making use of spatial units of aggregation such as blocks or administrative districts (Mashhoodi

et al., 2020) that do not permit the impact of building form to be separated from that of the urban context. Thus, specifically in urban climate research, more effective frameworks are needed to assess the influence of urban form on urban microclimate, support an understanding of the morphological complexity of cities and allow investigations of the relationship between climate-related performance of buildings and the characteristics of their contexts.

In conclusion, understanding the interactions between urban form, building energy performance and climatic conditions which occur in urban systems is fundamental to advancing energy transition strategies. The study of the interplay between these aspects is challenging as it requires a multidisciplinary approach on multiple scales, and until now has only been addressed in a fragmented way in urban morphology, urban climatology and energy-focused research.

As a consequence, the overall thermal mechanisms triggered by the form characteristics of buildings and their contexts have not been fully analysed. Furthermore, due to the limitations of methodological instruments, a comprehensive explanation and quantification of the influence of urban form on building cooling demand in urban microclimatic environments is largely lacking. In this context, the main objectives of this thesis are:

- To identify urban form characteristics that influence cooling demand, including those that contribute to shaping urban microclimates.
- To describe the thermal mechanisms triggered by the urban form characteristics identified.
- To develop and test a morphological approach to classifying and assessing urban microclimate conditions.
- To develop and test an energy assessment method to quantify the impacts of building and urban context on cooling loads.

1.3 Case study

In this thesis, a case study will be employed to test the developed methods. The city of Rotterdam was selected to test whether novel assessment methods can contribute to an understanding of how and to what extent urban form influences building cooling demand. Rotterdam is the second largest city in the Netherlands. Despite being in a temperate climate zone (Kottek et al., 2006) studies have shown

that the city experiences a significant UHI effect (Roodenburg, 1983; Steeneveld et al., 2011). According to Klok et al. (2012) the surface UHI effect can reach up to 10°C, while van Hove et al. (2015) found that the atmospheric UHI effect can vary from 4.3°C to 8°C depending on local urban characteristics.

As with the rest of Europe, in the Netherlands climate change is expected to cause average temperatures to rise, resulting in hotter summers and the increased magnitude, frequency and duration of extreme heat events (KNMI, 2015). Research on heat-related risks and vulnerability levels (eg. Albers et al., 2015; Hoeven & Wandl, 2015) in recent years has highlighted the need for heat adaptation action. At the national level this need has been translated into goals to be achieved by 2050 (Delta Programme, 2015). A couple of studies have pointed out that at the municipal level there is insufficient understanding of risks related to increased heat stress and of the urgent need to adapt urban environments to it (Runhaar et al., 2012; Klok & Kluck, 2018).

Additionally, from an energy perspective, although van Hooff et al. (2016) have shown that cooling demand will likely increase in the future due to climate change, the Integraal Nationaal Energie Klimaatplan 2021-2030, (2021) does not address cooling, and focuses primarily on heating-related goals and measures. As a consequence, municipalities are not guided towards the acknowledgement of cooling-related energy consumption and the development of strategies to reduce future cooling demand.

The urgent need to quantify the possible consequences of urban warming on energy loads is exacerbated also by urban development initiatives to accommodate increased housing demand. The recent program for building one million homes is promoting the re-densification of existing urban areas in the Netherlands, which will result in an increase in the heterogeneity of the built environment and will require the broadening of knowledge on the effects of higher building density on UHI magnitude and energy demand. Therefore, it becomes evident that addressing the relationships between form, urban microclimate and building cooling loads, and supporting analytical and planning instruments for municipal decision-making processes, is crucial to ensure a decarbonized future.

1.4 Research questions

To address the above objectives, the main research question of this thesis is as follows:

How does urban form influence building cooling demand in urban microclimate conditions, and how can the magnitude of the relationship be assessed?

The main research question has a twofold nature. The first part of the question focuses on the relationships between urban form characteristics, urban microclimate processes and energy demand for building cooling, while the second part drives the exploration of conceptual and methodological instruments to quantify this relationship. As stated in the previous section, the city of Rotterdam will be used as case study to test these instruments.

TABLE 1.1 Research questions

Main Research question	Research sub-questions (theory and methods)	Research sub-questions (case study)
How does urban form influence building cooling demand in urban microclimate conditions?	**SQ1:** What urban form characteristics influence building cooling demand?	
	SQ2: What thermal mechanisms drive this influence?	
and how can the magnitude of the relationship be assessed?	**SQ3:** How to assess urban microclimate conditions influenced by urban form characteristics?	**SQ4:** How and to what extent do urban form characteristics influence summer outdoor and indoor thermal conditions in the Rotterdam case?
	SQ5: How to include the effects of urban microclimate in the assessment of building cooling demand?	**SQ6:** How and to what extent do urban microclimate and urban form impact building cooling demand in the Rotterdam case?

As shown in Table 1.1, the main research question is answered through six sub-questions.

To begin building an interdisciplinary understanding, the sub-questions SQ1 and SQ2 enhance the theoretical base and prompt a review of the literature on energy-relevant form characteristics. The review aims to analyse the existing body of knowledge in the fields of urban morphology, energy studies and climatology in order to compile a comprehensive list of energy-relevant form characteristics. The description of these characteristics, also called form attributes, will unfold the thermal mechanisms they trigger and their effects on building energy performance.

The following sub-questions were derived from the need to explore new methodological instruments in order to measure the influence of form on urban microclimate (SQ3), and to quantify the influence of urban microclimate on building energy demand (SQ5). These questions drive an analysis of available existing methods, and will explore the potential of novel morphological and modelling approaches to overcome the existing limitations. Ultimately, two assessment methods will be developed on this basis. The first method focuses on the necessity of addressing the morphological complexity of cities and analysing the impacts of urban form on microclimate, while the second method allows urban microclimate boundary conditions to be used in building energy modelling.

In a feedback loop with the previous questions, sub-questions SQ4 and SQ6 drive the use the new assessment instruments to investigate the influence of urban form on building cooling demand in the Rotterdam case study. The choice of a case study allows the novel methods to be tested and also advances the understanding of the role of urban form and the magnitude of its impacts on microclimate and building energy loads, thus contributing to the answering of the main research question.

1.5 Thesis outline

As shown in Figure 1.1, the thesis is divided into seven chapters.

Following this first chapter, which introduces the context and structure of the research, Chapter 2 addresses SQ1 and SQ2. It describes the results of a systematic literature review on energy-relevant morphological characteristics. Form characteristics (or attributes) with an influence on building energy demand are classified into three units of analysis: building, street canyon and texture. For each unit, the attributes are described from the point of focus of the triggered thermal mechanisms and their effects on building energy performance. Furthermore, the review is enriched by a list of the quantitative parameters that have been used in previous studies for the measurement of energy- and climate-related form attributes.

Chapter 3, addressing SQ3 and SQ4, describes the development and application of a novel method for classifying and assessing urban climate conditions based on urban form characteristics. Inspired by the Local Climate Zone (LCZs) framework, the proposed Local Climate Types (LCT) method explores the application of

morphological unsupervised classification in the field of urban climatology. This approach addresses the heterogeneity of cities and identifies building and context types separately. The classification of types is based on parameters which describe building form characteristics and parameters which describe the characteristics of the surrounding urban fabric forms. Furthermore, an assessment of the climate performance of each type is carried out through numerical microclimate simulations.

Chapter 3 also demonstrates the use of the Local Climate Types method in the Rotterdam case study, allowing an understanding and description of the role of form characteristics in microclimatic thermal processes. Daily thermal patterns for 25 form archetypes are modelled using the ENVI-met microclimate tool for a hot summer period. Additionally, a sensitivity analysis highlights the relationship between form characteristics and urban outdoor air temperature.

Chapter 4, driven by SQ5, explores a novel energy modelling approach that enhances the assessment of building cooling demand by using urban microclimate boundary conditions. The chapter describes the development of a method for coupling a microclimate tool (ENVI-met) and an energy modelling tool (City Energy Analyst) that allows the consideration of local wind speed, relative humidity and air temperature when estimating building cooling demand. First, the equations and procedures for the numerical simulations are described, then the coupling is tested on an urban district in Zurich, Switzerland.

Addressing SQ6, Chapter 5 describes the application of the coupling method on the Rotterdam case, to study the effect and the magnitude of urban form and microclimate on cooling loads. The types previously identified in Chapter 3 are modelled through the coupled microclimate-energy procedure described in Chapter 4. An analysis of the results enables the comparison of cooling demand between Rotterdam's types and allows identification of the form-related patterns of building cooling energy consumption behaviours. A sensitivity analysis highlights the correlation between morphological factors, microclimate variables and building cooling need.

Finally, in Chapter 6 the general outcomes of the study are discussed, interlinked and placed within the context of the existing body of knowledge, while Chapter 7 presents final conclusions.

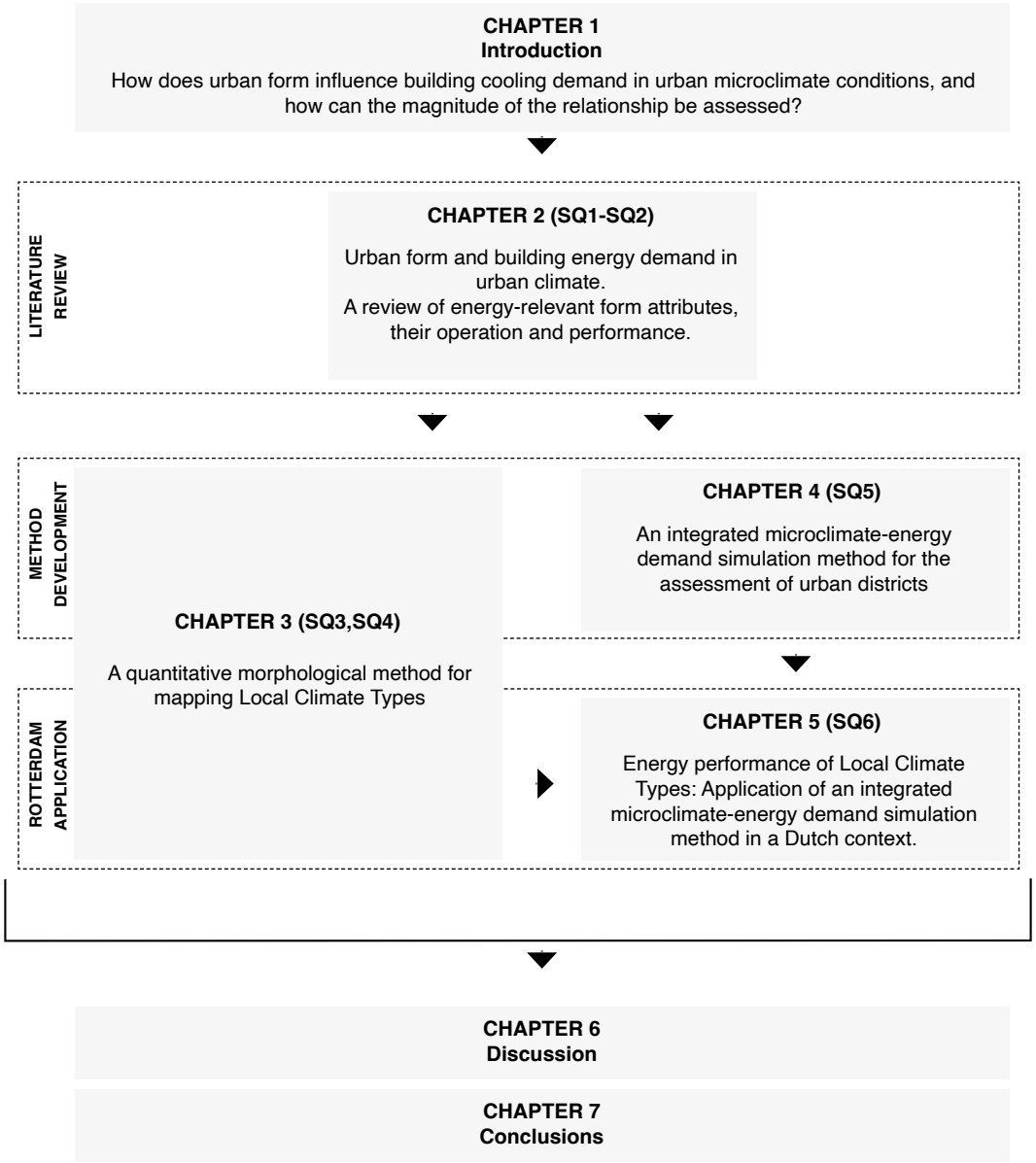


FIG. 1.1 Research outline

TOC

References

Adolphe, L. (2001). A simplified model of urban morphology: Application to an analysis of the environmental performance of cities. *Environment and Planning B: Planning and Design*, *28*(2), 183–200. https://doi.org/10.1068/b2631

Afshari, A., & Liu, N. (2017). Inverse modeling of the urban energy system using hourly electricity demand and weather measurements, Part 2: Gray-box model. *Energy and Buildings*, *157*, 139–156. https://doi.org/10.1016/j.enbuild.2017.01.052Aghimien, E. I., Li, D. H. W., & Tsang, E. K. W. (2022). Bioclimatic architecture and its energy-saving potentials: a review and future directions. *Engineering, Construction and Architectural Management*, *29*(2), 961–988. https://doi.org/10.1108/ECAM-11-2020-0928

Ahmadian, E., Sodagar, B., Bingham, C., Elnokaly, A., & Mills, G. (2021). Effect of urban built form and density on building energy performance in temperate climates. *Energy and Buildings*, *236*, 110762. https://doi.org/10.1016/j.enbuild.2021.110762

Albers, R. A. W., Bosch, P. R., Blocken, B., van den Dobbelsteen, A. A. J. F., van Hove, L. W. A., Spit, T. J. M., … Rovers, V. (2015). Overview of challenges and achievements in the climate adaptation of cities and in the Climate Proof Cities program. *Building and Environment*, *83* (December 2014), 1–10. https://doi.org/10.1016/j.buildenv.2014.09.006

Allegrini, J., Dorer, V., & Carmeliet, J. (2012). Influence of the urban microclimate in street canyons on the energy demand for space cooling and heating of buildings. *Energy and Buildings*, *55*, 823–832. https://doi.org/10.1016/j.enbuild.2012.10.013

Anderson, J. E., Wulfhorst, G., & Lang, W. (2015). Energy analysis of the built environment - A review and outlook. *Renewable and Sustainable Energy Reviews*, *44*, 149–158. https://doi.org/10.1016/j.rser.2014.12.027

Ashie, Y., Thanh Ca, V., Asaeda, T. (1999). Building canopy model for the analysis of urban climate, *Journal of Wind Engineering and Industrial Aerodynamic* . *81*(1), 237–248.

ASHRAE (2022). Cooling demand. ASHRAE Terminology. A Comprehensive Glossary of Terms for the Built Environment. Retrieved January 10, 2023, from https://terminology.ashrae.org

Baker, N., & Steemers, K. (2000). *Energy and Environment in Architecture - A Technical Design Guide*. London & New York: Taylor & Francis Group.

Bazazzadeh, H., Nadolny, A., & Safaei, S. S. H. (2021). Climate Change and Building Energy Consumption: A Review of the Impact of Weather Parameters Influenced by Climate Change on Household Heating and Cooling Demands of Buildings. *European Journal of Sustainable Development*, *10*(2), 1–12. https://doi.org/10.14207/ejsd.2021.v10n2p1

Boezeman, D., & Kooij, H.J., 2015. Heated debates: the transformation of urban warming into an object of governance in the Netherlands. In Beunen, R., Van Assche, K., Duineveld, M. (Eds.), Evolutionary Governance Theory: Theory and Applications (pp. 185–203). Springer, New York. http://dx.doi.org/10.1007/978-3-319-12274-8_13.

Bourdic, L., Salat, S., & Nowacki, C. (2012). Assessing cities: A new system of cross-scale spatial indicators. *Building Research and Information*, *40*(5), 592–605. https://doi.org/10.1080/09613218.2012.703488

Chun, B., & Guldmann, J. M. (2018). Impact of greening on the urban heat island: Seasonal variations and mitigation strategies. *Computers, Environment and Urban Systems*, *71*(September 2017), 165–176. https://doi.org/10.1016/j.compenvurbsys.2018.05.006

Delta Programme, 2015. Working on the Delta. The Decisions to Keep the Netherlands Safe and Liveable. Publication of the Ministry of Infrastructure and the Environment and the Ministry of Economic Affairs. http://www.deltaportaal.nl/ programfiles/154/programfiles/DeltaProgramme2015English_tcm310-358177.pdfN, p.175).

Davoudi, S., Crawford, J., & Mehmood, A. (2009). Climate change and spatial planning response. In Davoudi, S., Crawford, J., & Mehmood, A. (Eds.), Planning for climate change : strategies for mitigation and adaptation for spatial planners (pp. 7-18). Earthscan, London. http://bvbr.bibbvb.de:8991/F?func=service&doc_library=BVB01&local_base=BVB01&doc_number=018620647&line_number=0001&func_code=DB_RECORDS&service_type=MEDIA

Emmanuel, R., & Steemers, K. (2018). Connecting the realms of urban form, density and microclimate. *Building Research and Information*, *46*(8), 804–808. https://doi.org/10.1080/09613218.2018.1507078

Ewing, R., & Cervero, R. (2010). Travel and the built environment. *Journal of the American Planning Association*, *76*(3), 265–294. https://doi.org/10.1080/01944361003766766
Futcher, J. A., Kershaw, T., & Mills, G. (2013). Urban form and function as building performance parameters. *Building and Environment*, *62*, 112–123. https://doi.org/10.1016/j.buildenv.2013.01.021
Futcher, J. A., & Mills, G. (2013). The role of urban form as an energy management parameter. Energy Policy, 53, 218-228. https://doi.org/10.1016/j.enpol.2012.10.080
Futcher, J., Mills, G., & Emmanuel, R. (2018). Interdependent energy relationships between buildings at the street scale. *Building Research and Information*, *46*(8), 829–844. https://doi.org/10.1080/09613218.2018.1499995
Gauthier P, Gilliland J (2006) Mapping urban morphology. *Urban Morphology, 10*, 41–50.
Grubler, A., Bai, X., Buettner, T., Dhakal, D., Fisk, D.K., Ichinose, T., Keirstead, J.E., Sammer, G., Satterthwaite, D., Schulz, N.B., et al. (2012). Chapter 18: Urban Energy Systems. In Johansson T.B., Patwardhan A., Nakicenovic N., Gomez-Echeverri L. (Eds.), *Global Energy Assessment - Toward a Sustainable Future* (pp. 1307–1400). Cambridge University Press.
Gunawardena, K., Kershaw, T., & Steemers, K. (2019). Simulation pathway for estimating heat island influence on urban/suburban building space-conditioning loads and response to facade material changes. *Building and Environment*, *150*(October 2018), 195–205. https://doi.org/10.1016/j.buildenv.2019.01.006
Hassid, S., Santamouris, M., Papanikolaou, N., Linardi, A., Klitsikas, N., Georgakis, C., & Assimakopoulos, D. N. (2000). Effect of the Athens heat island on air conditioning load. *Energy and Buildings*, *32*(2), 131–141. https://doi.org/10.1016/S0378-7788(99)00045-6
Hoeven, F. Van Der, & Wandl, A. (2015). Hotterdam , mapping the Rotterdam urban heat island. *Project Baikal*, (45), 138–145. https://doi.org/http://dx.doi.org/10.7480/projectbaikal.45.906.858
Howard, L., 1833. The Climate of London Deduced from Meteorological Observations, Made in the Metropolis, and at Various Places Around It. Vol. 1–3. Harvey and Darton, London Huang, J., Jones, P., Zhang, A., Peng, R., Li, X., & Chan, P. (2020). Urban Building Energy and Climate (UrBEC) simulation: Example application and field evaluation in Sai Ying Pun, Hong Kong. *Energy and Buildings*, *207*. https://doi.org/10.1016/j.enbuild.2019.109580
IEA. (2018). *The Future of Cooling. Opportunities for energy efficient air conditioning.* https://doi.org/10.1787/9789264301993-en
IEA (2020). *IEA World Energy Balances, World Energy Balances and Statistics.* https://www.iea.org/subscribe- to-data-services/world-energy-balances-and-statistics
ISO 13790 (2008). Energy Performance of Buildings –Calculation of Energy Use for Space Heating and Cooling. Geneva: International Organization for Standardization
Kikegawa, Y., Genchi, Y., Yoshikado, H., Kondo, H. (2003). Development of a numerical simulation system toward comprehensive assessments of urban warming countermeasures including their impacts upon the urban buildings' energy-demands, *Applied. Energy, 76*(4), 449–466
Klok, E. J., & Kluck, J. (2018). Reasons to adapt to urban heat (in the Netherlands). *Urban Climate*, *23*, 342–351. https://doi.org/10.1016/j.uclim.2016.10.005
Klok, L., Zwart, S., Verhagen, H., & Mauri, E. (2012). The surface heat island of Rotterdam and its relationship with urban surface characteristics. *Resources, Conservation and Recycling*, *64*, 23–29. https://doi.org/10.1016/j.resconrec.2012.01.009
KNMI, 2015. *14 Climate Change Scenarios for the Netherlands.* http://www.climatescenarios.nl/ images/Brochure_KNMI14_EN_2015.pdfN, p.36)
Ko, Y. (2013). Urban Form and Residential Energy Use: A Review of Design Principles and Research Findings. *Journal of Planning Literature*, *28*(4), 327–351. https://doi.org/10.1177/0885412213491499
Kolokotroni, M., Giannitsaris, I., & Watkins, R. (2006). The effect of the London urban heat island on building summer cooling demand and night ventilation strategies. *Solar Energy*, *80*(4), 383–392. https://doi.org/10.1016/j.solener.2005.03.010
Kolokotroni, M., & Salvati, A. (2021). Comfort and energy implications of urban microclimate in high latitudes. In M. Palme & A. Salvati (Eds.), *Microclimate Modelling for Comfort and Energy Studies* (pp. 79-104). Springer. https://doi.org/10.1007/978-3-030-65421-4
Kottek, M., Grieser, J., Beck, C., Rudolf, B., & Rubel, F. (2006). World map of the Köppen-Geiger climate classification updated. Meteorologische Zeitschrift, 15, 3, 259-263.

Lan, Y., & Zhan, Q. (2017). How do urban buildings impact summer air temperature? The effects of building configurations in space and time. *Building and Environment*, *125*, 88–98. https://doi.org/10.1016/j.buildenv.2017.08.046

Le Corbusier (1930) Precisions, Paris. In R. Banham (Ed.), *The Architecture of the Well-Tempered Environment* (2nd ed., p. 159). University of Chicago Press.

Leng, H., Chen, X., Ma, Y., Wong, N. H., & Ming, T. (2020). Urban morphology and building heating energy consumption: Evidence from Harbin, a severe cold region city. *Energy and Buildings*, *224*, 110–143. https://doi.org/10.1016/j.enbuild.2020.110143

Li, C., Song, Y., & Kaza, N. (2018). Urban form and household electricity consumption: A multilevel study. *Energy and Buildings*, *158*, 181–193. https://doi.org/10.1016/j.enbuild.2017.10.007

Li, X., Zhou, Y., Yu, S., Jia, G., Li, H., & Li, W. (2019). Urban heat island impacts on building energy consumption: A review of approaches and findings. *Energy*, *174*, 407–419. https://doi.org/10.1016/j.energy.2019.02.183Manzano-Agugliaro, F., Montoya, F. G., Sabio-Ortega, A., & García-Cruz, A. (2015). Review of bioclimatic architecture strategies for achieving thermal comfort. *Renewable and Sustainable Energy Reviews*, *49*, 736–755. https://doi.org/10.1016/j.rser.2015.04.095

Martin, L. & March, L. (Eds.) (1972). *Urban space and structures*. Cambridge University Press.

Mashhoodi, B. (2019). Local and national determinants of household energy consumption in the Netherlands. *GeoJournal*, *9*. https://doi.org/10.1007/s10708-018-09967-9

Mashhoodi, B., Stead, D., & van Timmeren, A. (2020). Land surface temperature and households' energy consumption: Who is affected and where? *Applied Geography*, *114* (April 2019), 102–125. https://doi.org/10.1016/j.apgeog.2019.102125

Masson-Delmotte, V., Zhai, P., Pörtner, H.-O., Roberts, D., Skea, J., Shukla, P. R., … Waterfield, T. (2018). Global Warming of 1.5 Degrees Celcius. In *IPCC-Summary for Policymakers*. https://doi.org/10.1017/CBO9781107415324

Mauree, D., Coccolo, S., Perera, A. T. D., Nik, V., Scartezzini, J. L., & Naboni, E. (2018). A new framework to evaluate urban design using urban microclimatic modeling in future climatic conditions. *Sustainability (Switzerland)*, *10*(4), 1–20. https://doi.org/10.3390/su10041134

Mills, G., & Futcher, J. (2021). Integrating urban climate knowledge: the need for a new knowledge infrastructure to support climate-responsive urbanism. In M. Palme & A. Salvati (Eds.), Microclimate Modelling for Comfort and Energy Studies (pp. 183-192). Springer. https://doi.org/10.1007/978-3-030-65421-4

Mills, G., Stewart, I. D., & Niyogi, D. (2022). The origins of modern urban climate science: reflections on 'A numerical model of the urban heat island.' Progress in Physical Geography, 46(4), 649–656. https://doi.org/10.1177/03091333221107212

Ministerie van Economische Zaken en Klimaat. (2021). *Integraal Nationaal Energie - en Klimaatplan 2021-2030*. Netherlands.

Morganti, M., Salvati, A., Coch, H., & Cecere, C. (2017). Urban morphology indicators for solar energy analysis. *Energy Procedia*, *134*, 807–814. https://doi.org/10.1016/j.egypro.2017.09.533

Moudon AV (1994) Getting to know the built landscape: typomorphology. In: Franck, K. & Schneekloth, L. (Eds.), *Ordering space: types in architecture and design* (pp. 289–311). Van Nostrand Reinhold.

Natanian, J. (2020). Beyond Zero Energy Districts: A Holistic Energy and Environmental Quality Evaluation, TU Munich.

Nik, V. M., Perera, A. T. D., & Chen, D. (2021). Towards climate resilient urban energy systems: A review. *National Science Review*, *8*(3). https://doi.org/10.1093/nsr/nwaa134

Oke, T.R. (1991). Climate of Cities. In: F. Baer, N. L Canfield, & J. M. Mitchell (Eds.) *Climate in Human Perspective. Atmospheric and Oceanographic Sciences Library*, vol 15. Springer. https://doi.org/10.1007/978-94-011-3320-3_6

Oke, T. R., Mills, G., Christen, A., & Voogt, J. A. (2017). *Urban Climates*. Cambridge University Press.

Palme, M., & Salvati, A. (2021). Urban Microclimate Modelling for Comfort and Energy Studies. *Urban Microclimate Modelling for Comfort and Energy Studies*, (January), 4–5. https://doi.org/10.1007/978-3-030-65421-4

Peppler, A., 1929. Das Auto als Hilfsmittel der meteorologischen Forschung [The auto as an aid to meteorological investigation]. Zeitschrift für angewandte Meteorologie 46, 305–308.

Pijpers-van Esch, M. (2015). Designing the Urban Microclimate. A framework for a design-decision support tool for the dissemination of knowledge on the urban microclimate to the urban design process. https://journals.open.tudelft.nl/index.php/abe/article/view/pijpers/1067

Quan, S. J., & Li, C. (2021). Urban form and building energy use: A systematic review of measures, mechanisms, and methodologies. *Renewable and Sustainable Energy Reviews*, *139* (January), 110–662. https://doi.org/10.1016/j.rser.2020.110662

Ratti, C., Baker, N., & Steemers, K. (2005). Energy consumption and urban texture. *Energy and Buildings*, *37*(7), 762–776. https://doi.org/10.1016/j.enbuild.2004.10.010

Roaf, S., Nicol, F., Humphreys, M., Tuohy, P., & Boerstra, A. (2010) Twentieth century standards for thermal comfort: promoting high energy buildings, Architectural Science Review, 53:1, 65-77, DOI: 10.3763/asre.2009.0111

Rode, P., Burdett, R., Robazza, G., Schofield, J., Keim, C., Bahu, N., … Bahu, J. M. (2014b). *Cities and energy. Urban morphology and heat energy demand*.

Rode, P., Keim, C., Robazza, G., Viejo, P., & Schofield, J. (2014). Cities and energy: Urban morphology and residential heat-energy demand. *Environment and Planning B: Planning and Design*, *41*(1), 138–162. https://doi.org/10.1068/b39065

Rogelj, J., Shindell, D., Jiang, K., Fifita, S., Forster, P., Ginzburg, V., … Vilarino, M. V. (2018). Mitigation Pathways Compatible With 1.5°C in the Context of Sustainable Development. In *Global Warming of 1.5°C: An IPCC Special Report [...]* (p. 82). https://www.ipcc.ch/site/assets/uploads/sites/2/2019/02/SR15_Chapter2_Low_Res.pdf

Roodenburg, J. (1983). Adaptation of rural minimum temperature forecasts to an urban environment. *Archives for Meteorology, Geophysics, and Bioclimatology Series B*, *32*(4), 395–401. https://doi.org/10.1007/BF02324659

Runhaar, H., Mees, H., Wardekker, A., van der Sluijs, J., Driessen, P., 2012. Adaptation to climate change-related risks in Dutch urban areas: stimuli and barriers. *Regional Environmental Change. 12*, 777–790.

Salat, S. (2007). Energy and bioclimatic efficiency of urban morphologies : towards a comparative analysis of Asian and European cities. *International Conference on Sustainable Building Asia*, p. 6.

Salvati, A., Monti, P., Coch Roura, H., & Cecere, C. (2019). Climatic performance of urban textures: Analysis tools for a Mediterranean urban context. *Energy and Buildings*, *185*, 162–179. https://doi.org/10.1016/J.ENBUILD.2018.12.024

Santamouris, M. (2014). On the energy impact of urban heat island and global warming on buildings. *Energy and Buildings*, *82*, 100–113. https://doi.org/10.1016/j.enbuild.2014.07.022

Santamouris, M., Cartalis, C., Synnefa, A., & Kolokotsa, D. (2015). On the impact of urban heat island and global warming on the power demand and electricity consumption of buildings—A review. *Energy and Buildings*, *98*, 119–124. https://doi.org/10.1016/J.ENBUILD.2014.09.052

Santamouris, M. (2020). Recent progress on urban overheating and heat island research. Integrated assessment of the energy, environmental, vulnerability and health impact. Synergies with the global climate change. *Energy and Buildings*, 207. https://doi.org/10.1016/j.enbuild.2019.109482

Sijmons, D., Hugtenburg, J., Hoorn, A. van, & Feddes, F. (2014). *Landscape and energy : designing transition*. Nai010 Publishers.

Silva, M. (2017). A Multi-Scale Decision-Support Model to Integrate Energy in Urban Planning. *FEUP*. http://ezproxy.umuc.edu/login?url=https://search.proquest.com/docview/2084518934?accountid=14580%0Ahttp://sfx.umd.edu/uc?url_ver=Z39.88-2004&rft_val_fmt=info:ofi/fmt:kev:mtx:dissertation&genre=dissertations+%26+theses&sid=ProQ:ProQuest+Dissertations+%26+T

Silva, M. C., Horta, I. M., Leal, V., & Oliveira, V. (2017). A spatially-explicit methodological framework based on neural networks to assess the effect of urban form on energy demand. *Applied Energy*, *202*, 386–398. https://doi.org/10.1016/j.apenergy.2017.05.113

Silva, M., Oliveira, V., & Leal, V. (2017). Urban Form and Energy Demand: A Review of Energy-relevant Urban Attributes. *Journal of Planning Literature*, *32*(4), 346–365. https://doi.org/10.1177/0885412217706900

Silva, M., Leal, V., Oliveira, V., & Horta, I. M. (2018). A scenario-based approach for assessing the energy performance of urban development pathways. *Sustainable Cities and Society*, *40* (October 2017), 372–382. https://doi.org/10.1016/j.scs.2018.01.028

Steadman, P., Hamilton, I., & Evans, S. (2014). Energy and urban built form: An empirical and statistical approach. *Building Research and Information, 42*(1), 17–31. https://doi.org/10.1080/09613218.2013.808140

Steeneveld, G. J., Koopmans, S., Heusinkveld, B. G., Van Hove, L. W. A., & Holtslag, A. A. M. (2011). Quantifying urban heat island effects and human comfort for cities of variable size and urban morphology in the Netherlands. *Journal of Geophysical Research Atmospheres*, *116*(20), 1–14. https://doi.org/10.1029/2011JD015988Stewart, I. D. (2019). Why should urban heat island researchers study history? Urban Climate, 30(April), 100484. https://doi.org/10.1016/j.uclim.2019.100484

Su, M. A., Ngarambe, J., Santamouris, M., & Yun, G. Y. (2021). Empirical evidence on the impact of urban overheating on building cooling and heating energy consumption. IScience, 24(5), 102495. https://doi.org/10.1016/j.isci.2021.102495

Sun, Y., & Augenbroe, G. (2014). Urban heat island effect on energy application studies of office buildings. *Energy and Buildings*, *77*, 171–179. https://doi.org/10.1016/j.enbuild.2014.03.055

Toparlar, Y., Blocken, B., Maiheu, B., & van Heijst, G. J. F. (2018). Impact of urban microclimate on summertime building cooling demand: A parametric analysis for Antwerp, Belgium. *Applied Energy*, *228*, 852–872. https://doi.org/10.1016/J.APENERGY.2018.06.110

Tsirigoti, D., & Tsikaloudaki, K. (2018). The effect of climate conditions on the relation between energy efficiency and urban form. *Energies*, *11*(3). https://doi.org/10.3390/en11030582

van Hooff, T., Blocken, B., Timmermans, H. J. P., & Hensen, J. L. M. (2016). Analysis of the predicted effect of passive climate adaptation measures on energy demand for cooling and heating in a residential building. *Energy*, *94*, 811–820. https://doi.org/10.1016/j.energy.2015.11.036

van Hove, L. W. A., Jacobs, C. M. J., Heusinkveld, B. G., Elbers, J. A., Van Driel, B. L., & Holtslag, A. A. M. (2015). Temporal and spatial variability of urban heat island and thermal comfort within the Rotterdam agglomeration. *Building and Environment*, *83*, 91–103. https://doi.org/10.1016/j.buildenv.2014.08.029

Wang, B., Cot, L. D., Adolphe, L., Geoffroy, S., & Sun, S. (2017). Cross indicator analysis between wind energy potential and urban morphology. *Renewable Energy*, *113*, 989–1006. https://doi.org/10.1016/j.renene.2017.06.057

Wang, Y., Berardi, U., & Akbari, H. (2016). Comparing the effects of urban heat island mitigation strategies for Toronto, Canada. *Energy and Buildings*, *114*, 2–19. https://doi.org/10.1016/j.enbuild.2015.06.046

Wong, N. H., Jusuf, S. K., Syafii, N. I., Chen, Y., Hajadi, N., Sathyanarayanan, H., & Manickavasagam, Y. V. (2011). Evaluation of the impact of the surrounding urban morphology on building energy consumption. *Solar Energy*, *85*(1), 57–71. https://doi.org/10.1016/j.solener.2010.11.002

Yang, X., Peng, L. L. H., Jiang, Z., Chen, Y., Yao, L., He, Y., & Xu, T. (2020). Impact of urban heat island on energy demand in buildings: Local climate zones in Nanjing. *Applied Energy*, *260*(30), 114279. https://doi.org/10.1016/j.apenergy.2019.114279

Yu, Z., Chen, S., & Wong, N. H. (2020). Temporal variation in the impact of urban morphology on outdoor air temperature in the tropics: A campus case study. *Building and Environment*, *181*(April), 107–132. https://doi.org/10.1016/j.buildenv.2020.107132

Zhang, M., & Gao, Z. (2021). Effect of urban form on microclimate and energy loads: Case study of generic residential district prototypes in Nanjing, China. *Sustainable Cities and Society*, *70* (March), 102–930. https://doi.org/10.1016/j.scs.2021.102930

TOC

2 Urban Form and Building Energy Demand in Urban Climate

A Review of Energy-Relevant Form Attributes, Their Operation and Performance

ABSTRACT Understanding how urban form influences individual buildings' energy use is crucial to informing urban planning and design in the global transition towards carbon-neutral cities. The complex relation between the physical and the performative dimensions of the urban environment has been proved in previous studies. However, the understanding of the mechanisms that govern the relationship between form characteristics and the final thermal performance of buildings in urban environments remains largely embedded in a fragmented body of studies in the fields of morphology, climatology and energy. More precisely, the limitations lie in i) the variety of energy-relevant form characteristics and their descriptive parameters, ii) the multiple spatial scales used for analysis, and iii) the complexity of the tradeoffs between urban form, climate and building energy use. Thus, this article offers a comprehensive review of the existing literature on energy-relevant form attributes of *buildings*, *street canyons* and *urban fabric units*. The systematic classification identifies nine urban form attributes and 54 related quantitative parameters for the three spatial units of analysis. Additionally, the review provides an updated understanding of the thermal mechanisms that directly determine building cooling and heating demand, and the ones that intervene indirectly by influencing the urban climatic context. Finally, the study discusses knowledge gaps and directions for future research.

2.1 Introduction

Decades of research on the energy performance of the built environment have largely demonstrated the role of urban form characteristics in shaping energy consumption in the building and mobility sectors (Oliveira, 2016). According to Vettorato (2011), spatial structures and configurations of street and building elements are responsible for variations in districts' energy performance due to their influence on uses, efficiency and conservation capability. For transport-related consumption, key metrics such as built-up area density, land use mix, connectivity and accessibility are well-established urban form attributes that, in large cities, drive GHG emissions in the mobility sector (Cervero & Kockelman, 1997; Seto et al., 2015).

Regarding building-related consumption, the quantification of the overall degree of influence of urban form on energy demand is widely debated in the research community. Several studies have proved that the form attributes of the urban fabric, such as density and compactness, determine different levels of cooling and heating demand, and thus have a relevant impact on GHG emissions (Lee & Lee, 2014) and climate change (Blanco et al., 2011). Among others, Ratti, Baker, & Steemer (2005) showed that form characteristics can lead to a 10% variation in annual energy consumption. By comparing 20 urban morphology samples in four cities, Rode et al. (2014), found variations in heating-related energy demand up to a factor 6, while Silva et al. (2017), by applying a high-resolution methodology with a spatially explicit character, concluded that urban form characteristics explain the 78% variation in the overall energy needed for ambient heating and mobility in the city of Porto.

As of today, however, the research effort hasn't delivered a comprehensive understanding of the impacts that the urban physical structure has on building energy use (Silva et al., 2017). The magnitude of the influence and the complex nature of environmental processes involved remain unclear (Ko, 2013; Lee & Lee, 2014; Quan & Li, 2021). This gap in knowledge can be attributed to interconnected problems that arise from the multiscale nature of the relationship, as well as from the methodological approaches employed in different fields of study (Mouzourides et al., 2019). Additionally, in the literature, there is a lack of structure in connecting multiple energy-relevant form parameters and in describing their intercorrelations (Ahmadian, Sodagar, Bingham, Elnokaly, & Mills, 2021).

From a morphological perspective, quantitative approaches have been devoted to identifying simple parameters to describe the energy-relevant form characteristics of the built environment or simply analyse the relationships between form and

consumption patterns (Depecker et al., 2001). In this direction, however, a twofold setback has been encountered. On the one hand, empirical studies have been confronting the lack of city building consumption data and the difficulty of isolating morphological factors from the other factors that lead to energy performance variation, namely building design, system efficiency and occupant behaviour (Baker & Steemers, 2000); on the other hand, studies using simulations and parametric approaches have focused on a few form characteristics at a time (Quan & Li, 2021). As a result, the understanding of the energy-performative values of urban form and the knowledge translation in design and planning practices results to be 'controversial' (Silva et al.,2017).

From an energy perspective, models and techniques have been developed for decades to assess energy loads of buildings, mostly, however, with a limited design perspective and a focus on single-building entities, neglecting the relevance of interrelated mechanisms on a larger urban scale (Ratti, Baker, & Steemer, 2005) and the 'external influence energy consumption' affected by the contextual environment (Leng et al., 2020). As a consequence, links and processes that concern the interactions between the urban form characteristics of the surrounding environment and building thermal performance have been studied only partially.

In this regard, however, decades of studies in climatology have advanced the understanding of the influence of the surrounding environment by focusing on the role of urban form in shaping urban and local climatic phenomena (Palme & Salvati, 2021). Overall urban form is recognised to influence thermal and aerodynamic processes, being one of the factors that contribute to the trapping of solar energy and anthropogenic heat, the increase of thermal storage and the reduction of wind speed and evaporative cooling. These mechanisms explain why air and surface temperatures are higher in cities than in rural areas, or in other words, the phenomenon known as Urban Heat Island (UHI) effect. Although interdisciplinary studies have further investigated the relationship between form parameters and urban climate patterns, Lan & Zhan (2017); Yu, Chen, & Wong (2020), and others have demonstrated that urban climate conditions have an impact on building cooling and heating loads (Kolokotroni et al., 2010; Santamouris, 2014, 2020; Santamouris et al., 2015). The disciplinary fragmentation and the focus of studies on a few form and climate variables at a time (Kolokotroni & Salvati, 2021) haven't allowed a comprehensive and clear understanding of the tradeoffs between form characteristics, climate patterns and energy demand.

These limitations confirm that the problem of relating form and energy demand is a multidimensional and multivariable one (Ratti, Baker, & Steemer, 2005). However, the identification of specific form parameters connected with energy demand is

fundamental to providing designers with action perspective and to supporting 'operative knowledge' in an early project phase (Depecker et al., 2001), and to supporting urban planners in defining urban energy strategies. Additionally, as argued by Futcher, Kershaw, & Mills (2013), a 'form-first approach' could help to decrease the impact of urban warming on building energy use and could help in understanding the suitability of building types for a specific urban context.

The present study aims to address these limitations and to provide a systematic understanding of the relations between the form characteristics and the energy demand of buildings, by reviewing the existing literature and by offering a comprehensive analysis of the state of inter- and trans-disciplinary research in urban morphology, climatology and energy-related fields. The review investigates the scales, processes and patterns of these relations: i) by giving an overview of studies that focus on building, canyon and urban fabric form; ii) by listing energy-relevant form attributes and descriptive parameters; iii) by describing the thermal mechanisms that drive urban form influence on building heating and cooling loads; and iv) by examining the magnitude and the patterns of variations in building thermal performance.

2.2 Literature Search and Selection

This literature review focuses on studies that investigated the climate and energy performance of urban form, using quantitative morphological parameters as descriptors, or energy consumption indicators. A three-step procedure is implemented to identify, classify and analyse energy-relevant form attributes and parameters.

In the first step, studies were retrieved from scientific databases (Scopus and Google Scholar) based on a search by the keywords "urban form" OR "urban morphology" AND "building energy demand" OR "building energy consumption". A second search was performed to include climate-related studies by adding "UHI" OR "urban climate'' as search keywords. Further queries and analysis of the abstracts allowed to identify and exclude irrelevant studies, such as studies on renewable energy production and transportation energy use. This led to a preliminary list of energy-relevant form parameters, after which an additional search was performed using the names of the parameters as keywords, and the abstracts were screened to ensure relevance.

Second, articles were categorised based on i) the spatial unit in which the parameter was measured, and ii) the form attribute that the parameter described. As shown in Figure 2.1, three main units of analysis were identified: building, street canyon and urban fabric. The building is the basic unit, for which the form attributes of size, orientation and compactness were identified. The street canyon is the first unit of aggregation that assembles building and street profile, and its form is characterised by the attributes of proportion and direction. The second aggregation unit, urban fabric, embeds parameters measured in multiple land division units, such as plot, block or island, and district. For the urban fabric unit, density, vertical openness, surface roughness and greenery were identified as form attributes that influence the energy performance of buildings.

In the final step, a review of the full text was carried out for the list of selected studies. A backward search was used to ensure the inclusion of the relevant publications cited in the reviewed studies. Form attributes were systematically analysed to understand both their thermodynamic mechanisms and their influence on building cooling and heating demand. This two-level analysis allowed to unfold the complexity of the data, since the same form attribute can deliver different performances by establishing a number of operative processes in the energy field and in the climate field. A clear example of this complexity is the attribute of density, which, from an energy perspective, operates on a building's solar gains, and from a microclimate perspective, contributes to the phenomenon of UHI. Clarifying the operations also allowed, therefore, to reveal potential performative values when a direct correlation with heating and cooling loads had not yet been established. A final list of 218 studies is reviewed in this article.

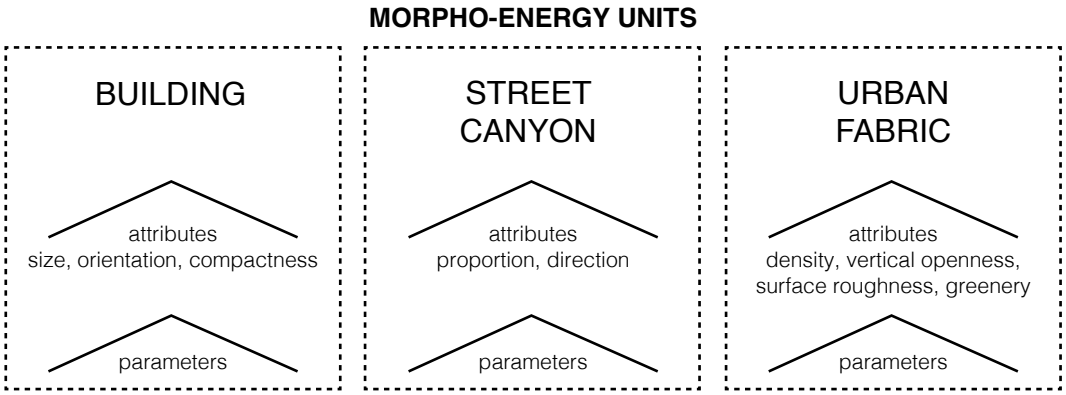


FIG. 2.1 Classification framework of energy-relevant form parameters

TOC

2.3 Energy-Relevant Form Attributes and Parameters

2.3.1 Building Unit

Energy-related form parameters that refer to the building unit are the most acknowledged in design and planning literature. As energy research traditionally has a focus on individual buildings, the energy performance is usually investigated in relation with direct geometrical characteristics of the building envelope and the space enclosed by it (volume, floor plan, etc.).

These characteristics, which regulate the balance between thermal gains and losses, have been described through parameters that measure the form attributes of size, orientation and compactness (Figure 2.2). Parameters of building size are generally employed for policy purposes, as primary analytical (Hu et al., 2017) and energy modelling factors (Turhan et al., 2014; Kesten et al., 2012), or to define standards and building typologies (Gui et al., 2018; Steadman et al., 2000). In design studies, building size parameters are used, among other purposes, to unravel the performance regarding sustainability and consequently to optimise building form (Caruso, Fantozzi, & Leccese, 2013; Camporeale & Mercader-Moyano, 2019). Parameters of orientation and compactness are also commonly used as optimisation factors for building shape, supporting studies on passive design strategies in various climate contexts (Inanici & Demirbilek, 2000). In addition, compactness variables find a wide use in energy modelling to assess heating and cooling loads (Baker & Steemers, 2000; Lim & Kim, 2018), but also as environmental metrics for different kinds of sustainability assessments on larger urban scales (Bourdic, Salat, & Nowacki, 2012; Salat, 2009; Mashhoodi, 2019).

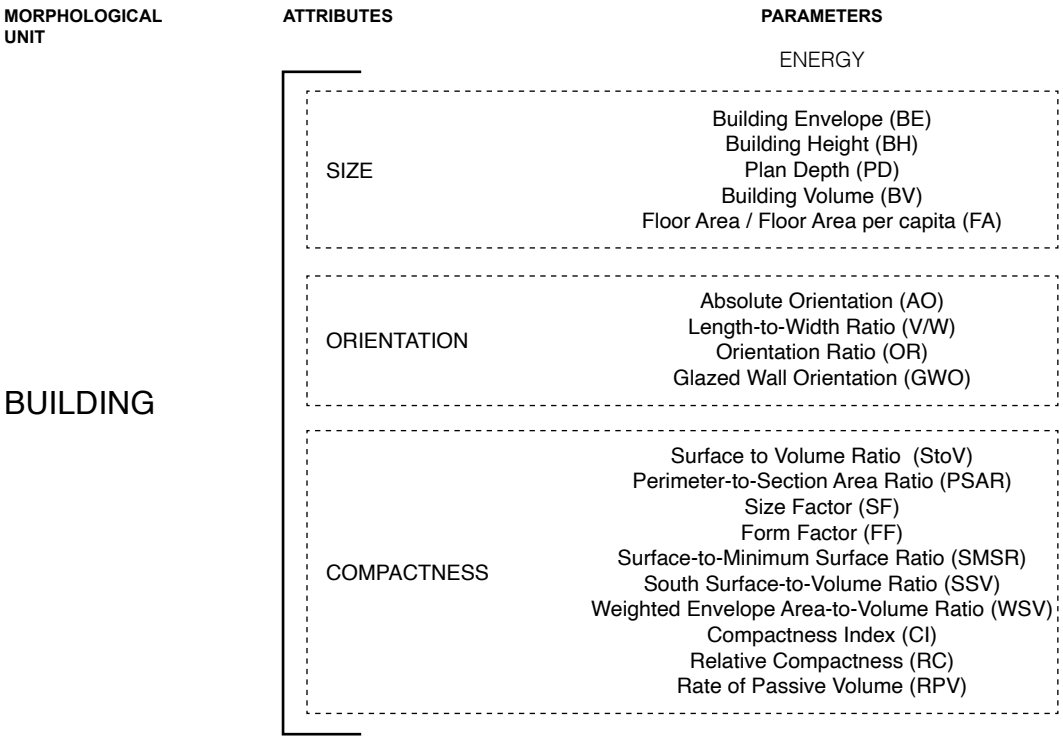


FIG. 2.2 Energy-relevant form attributes and parameters for the building unit

2.3.1.1 Size

Building *size* is one of the primary building attributes that influence energy consumption. *Size* operates through two main processes on energy demand. The size of the building shell influences the thermal exchange between the indoor and outdoor space, while the size of the indoor space defines the amount of air to be heated and cooled by energy systems. These two size-specific operational natures differently affect building energy performance. The impact of building shell *size* on heating and cooling energy performance depends on the balance between solar radiation gains and the thermal dispersion to the outside. Well-established morphological parameters describe the size of the shell, viz. *Building Envelope Area, Building Height,* and *Plan Depth.*

TOC

Building Envelope (BE) is the key spatial apparatus that defines the thermal transfer between indoor and outdoor space. Overall energy use tends to increase with the increase of envelope area. Empirical studies, such as the one by Steadman, Hamilton, & Evans (2014) on the non-domestic building stock of London, found a significant positive correlation between envelope area and both electricity and gas consumption. The same trend is found for cooling demand, for example in the study by Choi, Cho, & Kim (2012), which show that electricity consumption in summer increases for high-rise buildings that have a larger envelope surface.

Building Height (BH) expresses the vertical dimension of a building object. Through modelling assessment of different configurations, Mangan et al. (2021) concluded that in temperate humid zones, an increase in building height corresponds to a decrease of heating and lighting energy consumption, but to an increase in cooling loads. This result is explained by the fact that building height allows higher solar gains during both summer and winter. However, from an urban microclimate perspective, buildings' air infiltration rate depends upon air speed and turbulence, which generally increase with the increase of building height. Thus, from an energy perspective, this means that the higher the building, the higher the heat losses due to air infiltration. Jurelionis & Bouris (2016) demonstrated that the air infiltration rate is higher for buildings between 16 and 36 m high, resulting in a 40% increase in heat loads (compared to buildings lower than 16m) in order to cover thermal losses. However, the study by Saroglou et al. (2017) suggested that for high-rise buildings, while heating loads tend to increase, cooling loads tend to decrease from ground floor to top as a result of the decrease in ambient air temperature with height.

Plan Depth (PD) is a shape parameter usually correlated with solar accessibility and natural light provision. The deeper the building, the lower the contribution of solar radiation to internal gains. Steemers (2003) predicted with the LT method that increasing the depth from 12 to 24 m doubles the energy demand of office buildings. A threshold was identified in the study by Steadman et al. (2014), who argued that electricity for air-conditioning and lighting increase for buildings that exceed 14 m in plan depth.

The size of the indoor space determines the overall energy consumption for offices and housing. For residential uses it is well established that energy consumption increases with house size (Ewing & Rong, 2008). Historical analyses have also shown that the trend of growth in median house size can drastically reduce the energy saving achieved through other energy efficiency policies (Fournier et al., 2019). Variables of floor area and dwelling type, together, have also been shown to explain 39% of the variation in energy consumption for English households (Huebner et al., 2015). The main metrics employed to describe the size of the indoor space

are *Volume* and *Floor Area Ratio* or *Floor Area per capita.* The *Building Volume* (BV) parameter conveys the indoor volumetric dimensions of the space to be heated and cooled. The analysis by Steadman et al. (2014) for London employs a classification of volume size. The statistical correlation with electricity and gas consumption shows that volume size positively relates with a factor 0,92 and 0,88, respectively.

The *Floor Area* and *Floor area per capita* (FA) descriptors are used to measure the horizontal usable area of buildings. Numerous studies have concluded that an increase in floor area results in increased residential consumption of electricity (Zhou & Teng, 2013) and gas (Brounen, Kok, & Quigley, 2012). According to Gui et al. (2018), this parameter strongly correlates (0,92) with energy consumption in hot and cold zones of China, while the study by Theodoridou, Papadopoulos, & Hegger (2011) found a weaker correlation (0,43) for the Greek residential building stock. Moreover, floor area has been largely used in studies that aimed to determine drivers that contribute to energy demand related to larger scales of focus -national or regional/urban- (Jones, Fuertes, & Lomas, 2015). In an analysis of historical European data, Serrano et al. (2017) highlighted a trend of increasing floor area per capita in the 20 years between 1990 and 2010, while the energy consumption per capita generally decreased, probably due to the implementation of efficiency measures. However, projections of energy use by Ürge-Vorsatz et al. (2015) showed that floor area per capita is an important driver of future heating and cooling consumption. In these scenarios, it is expected to increase by 50% between 2010 and 2050, contributing, together with other drivers, to an overall increase in global energy consumption of 80%.

2.3.1.2 Orientation

Building *orientation* is a form attribute that describes the position of a building in relation to the cardinal directions, determining its exposure to the sun. Building orientation operates on the penetration and absorption of solar radiation through the components of the building envelope: wall, roof and windows. This attribute is used frequently for energy modelling (Bektas Ekici & Aksoy, 2011), as well as for energy optimisation studies (Ying & Li, 2020), as the orientation can help to reduce cooling loads in summer by minimising solar gains, and to decrease heating loads during cold months, but can also influence natural daylight access, and consequently electricity consumption for lighting (Mangkuto, Rohmah, & Asri, 2016). It has been estimated that the optimisation of building orientation, together with other envelope properties, can reduce energy consumption by 36% in cold regions (Aksoy & Inalli, 2006) and 27.6 % in temperate regions (Jaber & Ajib, 2011). Other studies have estimated

that cooling demand for specific building types can vary between -31% and +24%, depending on the orientation (Vasaturo et al., 2018). To measure orientation and its related effects, the main form parameters that emerge from the literature are Absolute Orientation and Length-to-Width Ratio, which are usually analysed together (Pacheco, Ordóñez, & Martínez, 2012), Orientation Ratio, and Glazed Wall Orientation.

Absolute Orientation (AO) usually describes the predominant orientation of building façades measured in degrees from true north (or south), and it is commonly used in parametric studies that employ energy modelling techniques. Many studies (for instance, Jaber & Ajib, 2011; Adeli, Farahat, & Sarhaddi, 2020; Fuentes-Bargues et al., 2020) make use of selected building types that are rotated and exposed to different orientations. The assessment of the resulting heating and cooling energy demand allows an understanding of the impact of orientation on annual energy consumption, and the further optimisation of the building design through passive or renewable production measures. Optimal orientation of the building has also been assessed by looking only at the predominant energy use during the year. Similarly, Ascione et al. (2019) identified the orientation that contributes to the reduction of space heating by maximising solar radiation, while Shao & Jin (2019) demonstrated that the impact of orientation on heating is consistent even when the insulation characteristics of the envelope are changed.

The impact of orientation on energy use mainly depends on the geographical position of the building and the solar azimuth angle throughout the year. Rules of thumb have been developed in passive design practice to guide designers at different latitudes. In general, for the northern hemisphere, solar radiation is more intense on the southern facades for latitudes greater than 22.450. As Caruso, Fantozzi, & Leccese (2013) summarise, the highest intensity of solar radiation in temperate and subtropical climates is received by south-facing walls in winter and east- and west-facing walls in summer. Parametric studies, such as the one by Vasaturo et al. (2018), highlight that in temperate climates in the northern hemisphere, buildings having a predominant orientation north, northeast or northwest have a higher heating demand, while the same orientations are found the most effective to reduce cooling demand. However, other studies to optimise solar control show that south is the orientation that works better to increase solar heat gains in winter and control solar heat gains in summer (Bourass & Et-Tahir, 2019; Mingfang, 2002).

Length to Width Ratio (L/W) captures the quantitative proportion between the length of a building object and its width in the form of a ratio (1:2) or in the form of a decimal number (0.5). L/W is usually used in combination with Absolute Orientation to describe the percentage of building envelope exposed to each cardinal point. Mangan et al. (2021), who investigated the influence of building length and

width on solar irradiation, concluded that the impact of orientation is stronger on rectangular floor plan buildings than on square floor plan buildings, on which impacts are negligible. Similarly, Hemsath & Bandhosseini (2015) concluded that the most efficient geometry for residential buildings is a compact one with a 1:1 ratio. However, when increasing the L/W from 1:1 to 3:1, orientation has a small impact on energy demand (0.3 %) for the four US cities considered in this study. In addition, the study confirmed that for rectangular floor-plan buildings, the exposure of the larger facades to the east and west contributes to higher cooling loads, due to incoming solar radiation during the morning and afternoon. Regarding cold climates, parametric studies on rectangular buildings with larger ratios (1:8) also confirm that exposing the longest facades to the north and south leads to the lowest annual energy demand (Nicholson, Shohet, & Fung, 2019). Similarly, for elongated building shapes, exposing the long side to the south lowers annual energy consumption in temperate climates, according to Florides et al. (2002). While these studies focused on free-standing single buildings, others surrounded the selected geometry with identical building blocks – simulating a neighbourhood configuration – and therefore took mutual shadowing into consideration. For the temperate-humid zones of Istanbul (Turkey), through the investigation of 120 configurations, Mangan et al. (2021) showed that long facades exposed to the east and west lower both cooling and heating demand by between 2% and 28% compared to other orientations.

A variable that seems to combine the previous ones is the *Orientation Ratio* (OR), as proposed by Rodríguez-Álvarez (2016) in a study that developed a morphological energy assessment method for a large urban area. The orientation ratio was defined as the 'ratio between the perimeter on the main orientation and its orthogonal' and can be considered a refined parameter of aspect ratio, since it gives an indication of a predominant and secondary orientation.

Glazed wall orientation (GWO) is a parameter that describes the predominant orientation of window surfaces. This parameter can be expressed in absolute terms as the Orientation Angle to which the glazed part is exposed or as the Glazing Ratio for a building side. This parameter has a clear design value for optimisation studies intended to obtain high-performance buildings. As Méndez Echenagucia et al. (2015) pointed out, controlling this parameter in an early design stage contributes to minimising heating, cooling and lighting needs. Thus, it is used to assess the thermal performance of buildings in exploratory studies. For example, Lapisa (2019), using a comparative approach in France, calculated that in the oceanic climate of Poitiers, orienting the glazed walls to the east, west and south reduces energy demand by 22%, while in the Mediterranean climate of Marseille, where heating and cooling needs are more balanced, exposing glazed walls to the east, south and north results in energy savings of 27%. Finally, the study showed that the same building, when located in the tropical climate of Jakarta, reduces its cooling need

by 6% when the glazed walls are oriented to the south and north. At the same time, however, Hassid et al. (2000) showed for the city of Athens (Greece) that the impacts of orientation on both peak power and cooling energy are negligible if opposite facades have the same amount of glazed surface. A variation of the GWO is the so-called South Window Size (SWS), which is expressed by the ratio between the window surface facing south and the full south façade area (Inanici & Demirbilek, 2000).

2.3.1.3 Building compactness

Compactness is a topological property that describes the degree of enclosure of a space. A large body of studies has demonstrated a relation between building compactness and heating and cooling demand and has found this property to be associated with the potential of buildings to interact with the climate. In fact, this attribute captures the building processes of energy loss and gain that act through the interface between the outdoor and indoor environment and that are responsible for controlling heat, light and ventilation flows. Since heat losses and gains are proportional to the thermal envelope area, buildings with a smaller thermal envelope per volume unit are more compact and interact less with the outdoor environment. Thus, when the compactness of a building is increased, heat, losses by radiation or convection through the envelope are reduced. However, greater compactness usually results in a reduction of solar gains and daylight, as well as a decreased potential for natural ventilation techniques (Ratti, Baker, & Steemers, 2005; Salat, 2007).

In the reviewed studies, it has been extensively proved that the compactness of a building influences both heating and cooling loads to different extents. Regarding space heating demand, the general findings are that the higher the building compactness, the lower the expected energy demand. For residential buildings, statistical analyses have shown that compactness explains 60% of heating demand (Caldera, Corgnati, & Filippi, 2008), while for office buildings, Gratia & De Herde (2003) showed a difference of 24.9% in heating demand among five types with different compactness values. Other studies, such as Catalina, Virgone, & Iordache (2011) only found a reduction between 6% and 10% in heating demand when office buildings had a more compact shape (in the hot–humid and temperate French climates of Nice and Lyon). Despite the recognition of the influence of this morphological characteristic, few attempts have been made to quantify the relation between building compactness and cooling demand. Studies in cooling-dominated climates have confirmed that the higher the building compactness, the lower the energy consumption for cooling (Hassid et al., 2000; AlAnzi, Seo, & Krarti, 2009). In the general debate on the impact of this form attribute on building energy

consumption, several authors have argued that compactness is a local determinant (Mashhoodi, 2019) or climate-dependent parameter (Salat, 2007), since the degree of influence on heating and cooling loads depends on the meso-climate context, outdoor temperatures and the availability of solar radiation (Depecker et al., 2001).

As building compactness is a widely acknowledged energy-related form attribute, it has been described by a large number of parameters, the main of which is *Surface-to-Volume ratio (StoV).* Derived from StoV are the parameters of *Perimeter-to-Section Area Ratio, Size Factor, Form Factor, Surface-to-Minimum Surface Ratio, South Surface-to-Volume Ratio* and *Weighted Envelope Area-to-Volume Ratio.* In literature StoV is also used in its reverse form of *Compactness Index* or *Relative Compactness.* Finally, another descriptor, named *Rate of passive volume,* indirectly derived from *Surface-to-volume ratio* embeds the concept of passivity.

Surface to Volume Ratio (StoV**)**, also named *'shape coefficient'*, *'shape factor'* or '*coefficient ratio'*, is a traditional indicator for compactness and is largely used in energy-related design and planning studies. Although its nature is to describe an intrinsic characteristic of building geometry, StoV has been used at larger scales to describe the compactness of districts and cities (Mashhoodi, Stead, & van Timmeren, 2020) and proposed as an environmental indicator (Salat, 2009). This parameter measures the proportion between the exposed envelope of a building and its volume. The higher the value of StoV, the larger the envelope area in proportion to the building volume. StoV has shown to positively correlate with total building heat gains (Araji, 2019) and to be proportional to heat loss coefficients (Szodrai, Lakatos, & Kalmar, 2016), but also to influence the variation of heating and cooling loads. The comparative study by Rode et al. (2014) on dominant residential building typologies including 20 samples and 20 idealised archetypal samples in four cities – London (United Kingdom),Paris(France), Berlin (Germany) and Istanbul (Turkey) – has shown that 'increasing surface-to-volume ratio increases the range of energy demand in buildings'. In fact, for highly compact buildings with a StoV ratio of 0.15, the range in energy performance is found to vary between 35 and 80 kWh/m^2/a; with a StoV ratio of 0.4, this range increases to 110-200 kWh/m^2/a.

It has been argued that StoV is more accurate in describing heating demand in colder climates than in mild climates. In Paris, Depecker et al. (2001) found a strong linear positive correlation (r=0.91) between the compactness index of 14 building typologies and heating demand. However, applying the same analysis in the case of Carpentras, near Montreux (France), the authors concluded that the relation cannot be stated in milder climates, supporting the concept of balance between predominant factors: The envelope area is a predominant factor in determining the thermal balance in cold climates, where weak heat gains do not perturbate

the heating demand-dominated energy balance. Inversely, mild temperatures and sunny periods lead to a reduced predominance of heat losses through the envelope in favour of solar energy gains though the glazing surfaces. On the contrary, other studies have found significant correlations also in temperate climates. Albatici & Passerini (2010), by calculating heating loads for four buildings in different Italian climate zones, found that a relation between heating loads and building compactness existed also for mild climates. In this study, high values of StoV (0.78 m^2/m3) corresponded to higher heating demands in all the climate conditions under consideration. In the same study, buildings that had a StoV with a range between 0.54 m^2/m3 and 0.64 m^2/m3 had very similar performances in the same climatic context. However, regarding the impact of StoV on energy demand in temperate climates, conflictual results have also been found in recent research. While Mashhoodi (2019) estimated that in only 13% of Dutch neighbourhoods StoV was significantly correlated with household energy consumption, (Taleghani et al., 2013) demonstrated the importance of the ratio to achieve annual energy efficiency through energy simulations, comparing the heating and lighting performance of building typologies in the same temperate Dutch context.

Studies investigating the StoV parameter have largely focused on heating demand. A few investigations have been done on annual energy demand and (only) cooling energy demand, using parametric and modelling analysis. Martilli (2014) concluded that low StoV minimises both heating and cooling loads in hot, dry climates, while Vartholomaios (2017) arrived at the same conclusion for the Mediterranean climate of Thessaloniki (Greece). The latter study also concluded that maintaining a low StoV was a key strategy for low-energy design, in particular when high compactness was combined with a predominant orientation towards the south. The comparative analysis by Rashdi & Embi (2016) investigated the dependency of cooling capacity on compactness and showed that building types with large StoV used more energy for mechanical cooling systems. Similarly, Hassid et al. (2000), in their study on the effect of UHI on energy consumption, concluded that the cooling load of Athens's (Greece) buildings was strongly influenced by their compactness value. Contrastingly, others, such as Xiong, Fu, & Dong (2014), found a nonsignificant relation between StoV and summer loads. However, Vartholomaios (2017), through a sensitivity analysis on annual energy demand, concluded that the correlation between compactness and heating loads was two times stronger than that between compactness and cooling loads.

A few research studies have shown that the magnitude of StoV impacts on energy demand is sensitive to other factors, such as the vertical building dimension and the thermal properties of the envelope materials. In a parametric study in Indian climate contexts, Bansal & Bhattacharya (2009) concluded that with equal values of StoV,

the energy consumption increased significantly with building height increase, while the energy demand increased only slightly with increasing building length or width. Moreover, envelope characteristics were found to influence the impacts of StoV on heating consumption. For Nordic climate zones, Danielski, Fröling, & Joelsson (2012) showed that variations in compactness accounted for 10% to 21% of the energy demand, by simulating the energy performance of five residential types with different StoV ratios. The study also showed that the impact of StoV was lower for highly insulated buildings: heat demand varied according to the shape factor by 18 to 21% for buildings with low insulation, 15 to 19% for buildings with medium insulation and 11 to 16% for buildings with high insulation. In addition, strong winds were found to increase the impact of the shape factor on heat demand.

Another research path has focused on the testing of descriptors that can better capture building compactness. As shown in Figure 2.2, a large number of parameters are derived from StoV and have been proposed with three main purposes: simplifying the calculations, removing the size bias, and including orientation or envelope characteristics to give specificity to the StoV. With the intention of simplifying the estimation method, de Trocóniz et al. (2012) argued that the 3D nature of StoV can be reduced to a 2D geometrical problem since, for elongated buildings, the form factor is equivalent to the Perimeter-to-Section Area Ratio (PSAR). According to the authors, the so-called method of the sections can be used for a preliminary simplified comparative assessment of energy measures. Other studies have pointed out that since StoV is a scale-dependent parameter, its use is limited for comparative morphological analysis. In fact, the calculation for two cubes of different size will result in different values: the greater the size of the building, the smaller the StoV value. Thus, alternative variables have been proposed to measure building compactness.

Salat, Vialan, & Nowacki (2010) and Bourdic et al. (2012) introduced the variables of *Size Factor* (SF) and *Form Factor* (FF). SF quantitatively describes the cube equivalent to the building volume, while the derived a-dimensional FF removes the bias of the object size from the calculation of StoV. In addition, D'Amico & Pomponi (2019) proposed a dimensionless parameter applicable to rectangular building shapes, called *Surface-to-Minimum Surface Ratio* (SMSR). This compactness parameter describes the relation between the building envelope and the minimum (spherical or cuboid) envelope required to enclose the building volume.

Finally, variations of StoV have been investigated by embedding characteristics of orientation and transmittance. The *South Surface-to-Volume ratio* (SSV) is an index with an explicit reference to the solar irradiation for one predominant orientation. Albatici & Passerini (2010) argued that the exposure is less important for low

values of StoV than for high values of StoV, while in the case of equal compactness, space heating is lower for larger exposure of the envelope area to the south. Using a different approach, de Trocóniz et al. (2012) developed a new parameter that integrates insulation value and envelope configuration, focusing on the problem that these properties are usually addressed separately. The proposed *Weighted Form Factor* (WSV), also called *Weighted Envelope Area-to-Volume Ratio*, by multiplying the transmittance coefficient for the area of the envelope, allows for an understanding of the thermal efficacy of different design solutions. The smaller the value of this parameter, the more thermally effective the building is.

In the study by Pacheco, Ordóñez, & Martínez (2012), two other descriptors were introduced: *Compactness Index* (CI) and *Relative Compactness* (RC). CI can be seen as the reverse of StoV and is calculated as the ratio between the heated (or cooled) volume and the building envelope. RC measures the ratio between a building's compactness index and that of a reference building. The reference building is usually the most compact one with an equal volume. These two parameters were used together by Catalina, Virgone, & Iordache (2011) for the energy optimisation process of office buildings in Nice and Lyon (France). The results showed that increasing the compactness through CI and RC had the most impact on heating energy savings in the hot climate of Nice. While CI is rarely employed alone (Gratia & De Herde, 2003), RC has been used independently in studies that estimate the impact of building form on energy demand. Werner & Mahdavi (2003) found a significant correlation between RC and heating loads. Ourghi, Al-Anzi, & Krarti (2007) employed as a reference building the cube of the actual building volume to predict the impact on annual energy demand. The energy assessment method based on this compactness variable was found to be accurate, in particular for cooling demand-dominated climates. Similarly, Al Anzi, Seo, & Krarti (2009) made use of the RC to analyse and compare the cooling demand of office buildings in a hot and-arid climate zone. Among the different building types, the results confirmed that energy demand in office buildings decreased exponentially with increasing RC values.

Finally, a variable that describes the indirect capability of compactness to influence active and passive operational energy can be found in the literature. *The Rate of Passive Volume* (RPV) describes a building's potential for passively using natural light and ventilation in the space(s) adjacent to the building façade; it is expressed as the proportion between the passive zone and the total building volume. A building's passive zone is defined as the volume within the first 6 meters' distance from an exterior wall, as this part of the building can potentially benefit from passive lighting, ventilation, cooling and heating. The active zone is the remaining building volume that requires the use of energy systems for climatisation. Derived from StoV, this parameter is also a function of the envelope area exposed to the

outside environment. According to Ratti, Baker, & Steemers (2005), RPV is a better descriptor of form-related energy consumption than StoV. However, as Salat (2007) pointed out, the importance of this parameter is climate-dependent, as it describes the mediation between the two phenomena of losing heat and receiving gains through facades. In cold climates at very high latitudes, the supply of natural ventilation and daylight is, in fact, secondary to the need for heat conservation. In these latitudes, the energy budget of buildings depends mostly on the reduction of the exposed envelope, while at lower latitudes, minimising the building envelope is beneficial for reducing radiation gains and cooling needs. Bourdic, Salat, & Nowacki (2012) argued that 'the passivity potential', despite being a building property, can also be analysed at the larger scales of neighbourhoods and blocks for environmental assessment. However, the attempt to consider the RPV an indicator of sustainability needs further testing.

2.3.2 Street Canyon Unit

The street canyon is a spatial unit traditionally used in urban climate analysis; it allows for observation of the thermal and aerodynamic mechanisms created by the interaction between building vertical surfaces, street horizontal surfaces and the air confined between them. Defined by Oke (1988) as the basic geometric unit, the form characteristics of a street canyon determine the primary microclimate environment of a building and thus affect building thermal losses and gains. Compared to a standalone building, a building in a canyon is subjected to three key thermal mechanisms that enhance Urban Heat Island effect and thus influence building energy demand. First, the total radiation budget (diffuse, direct, reflected radiation) is higher in a street canyon because of the interreflection between surfaces. Second, the canyon geometry facilitates the trapping of long wave radiation (Oke 1981, 1988). Third, the canyon influences the speed of wind flows and generally reduces convective heat transfer from building facades. These three mechanisms in a canyon generally result in higher surface temperatures of building facades during diurnal hours and higher air temperatures during nocturnal hours compared to standalone buildings. As a result, space cooling demand tends to be higher for buildings in a street canyon than for standalone ones (Allegrini, Dorer, & Carmeliet, 2012; Vallati et al., 2016).

For this unit, form parameters describe characteristics of *proportion and direction* of a canyon (Figure 2.3) with their related influence on the climate and energy performance of buildings. Quantitative parameters measuring proportion and direction are commonly used in analytical and design-oriented studies that employ

both measurements and modelling approaches to estimate the effects of form changes on climatic factors and energy demand variations (Tsoka et al., 2020). Additionally, proportion and direction parameters have been extensively employed for analysing the contribution of street design to outdoor thermal comfort (Abdollahzadeh & Biloria, 2021; Abreu-Harbich, Labaki, & Matzarakis, 2014; Ali-Toudert, & Passerini, 2010; Deng & Wong, 2020; Lobaccaro et al., 2019; Muniz-Gäal et al., 2020).

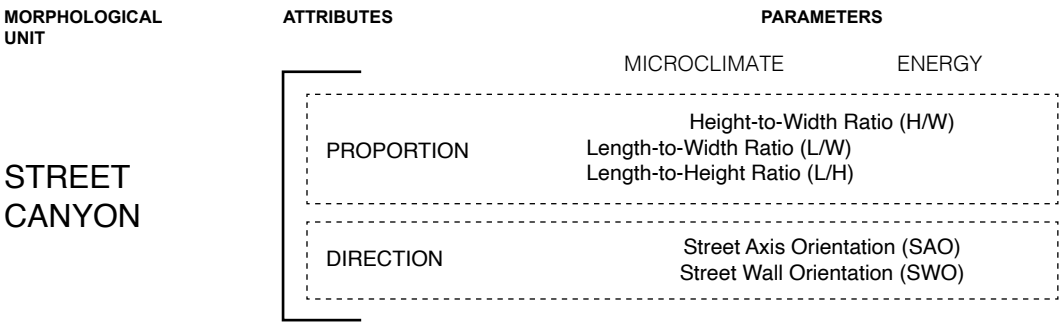


FIG. 2.3 Energy-relevant form attributes and parameters for the street canyon unit

2.3.2.1 Proportion

Street canyon proportion can be defined as the attribute that describes the geometrical relation between the three dimensions of a canyon: length, width and height. From a climate perspective, proportion determines the solar access in a canyon, the reflection of long-wave and shortwave radiation, and convective heat flow patterns, and thus it influences air and surface temperature. From an energy perspective, these processes affect heat gains and losses mediated by building envelopes. On the one hand, by influencing the penetration of solar radiation and thus multiple shortwave reflections (Vallati, Mauri, & Colucci, 2018), the canyon proportion directly determines the distribution of wall temperatures (Theeuwes et al., 2014) and the contribution of solar gains on building energy loads (Kolokotroni, Zhang, & Watkins, 2007). On the other hand, the canyon proportion determines the degree of trapping of long-wave radiation (Nazarian & Kleissl, 2015). When more long-wave radiation is trapped, the result is generally higher outdoor air temperatures and thus higher thermal gains through building facades. Additionally, during the night, this process, combined with the lower convective heat transfer

TOC

in canyons, results in a reduced heat dissipation from building surfaces. As a consequence, the impacts of canyon proportion on building heating and cooling energy performance can be considered indirect, as they primarily depend on the urban microclimate processes enhanced by the canyon. In the reviewed literature, the three main form parameters that describe canyon proportion are *Height-to-Width ratio*, *Length-to-Width Ratio and Length-to-Height Ratio.*

Height to Width Ratio (H/W) is a well-established parameter describes the proportion in a vertical section between the (average) building height and the street width. A large H/W value corresponds to deep street canyons, while a low H/W value describes shallow ones. Shallow canyons enhance the entering of more solar radiation, causing higher radiation absorption on building facades and higher trapping through reflection, while narrow street canyons, by creating overshadowing, block the entering of solar radiation. Studies such as those by Allegrini, Dorer, & Carmeliet (2012) and Chen et al. (2020) showed that during the daytime, wall temperatures are the highest in street canyons with H/W=0.5 and H/W=1. These studies also observed that compared to wall temperatures in narrow canyons (H/W=2–3), wall temperatures in wide canyons quickly decrease during the nighttime. However, according to Nazarian & Kleissl (2015), despite the fact that narrow canyons reduce the penetration of shortwave radiation, wall temperatures can increase as a result of the decreased convective cooling (convective heat transfer).

Additionally, a few studies have confirmed the relation between street canyon proportion, air temperature and UHI magnitude. According to Salvati, Coch Roura, & Cecere (2017) the difference in H/W in a Mediterranean context can determine air temperature variation between 0.8 and 1.7 °C, while Andreou & Axarli (2012) showed that in the same climate, the variation can range between 1 and 3 °C during the daytime and between 3 and 4 °C during the night. Bakarman & Chang (2015) observed that in hot–arid climates, air temperature in canyons is higher than in rural environments; viz. 5% higher in deep canyons and 15% higher in shallow ones. Furthermore, the analysis by Goh & Chang (1999) in Singapore highlighted a high degree of interdependence among these factors, concluding that the median H/W ratio explains 28% of UHI variation.

Several studies have confirmed that maximum diurnal air temperatures decrease with the increase of H/W because deep street canyons provide larger shaded area (Deng & Wong, 2020). On the other hand, nocturnal temperatures increase with the increase of H/W, meaning that deep canyons show higher temperatures than shallow ones during night hours. Thus, the correlation between UHI intensity (at night) and H/W has a positive sign (Oke 1987; Salvati, Coch Roura, & Cecere, 2017). The fact that higher H/W is linked to higher nocturnal temperature in canyons is

explained by the fact that a narrow canyon facilitates the trapping of solar radiation during daytime hours and hinders radiative heat loss during nighttime hours. In other words, the narrower the canyons (high H/W) the slower the heat dissipation. However, a study by Marciotto et al. (2010) suggested the presence of thresholds, observing in the context of San Paulo a positive correlation between H/W and nocturnal temperature until H/W=3.5, and then a curve inversion with further increase of H/W. Furthermore, Theeuwes et al. (2014) showed, by assessing the balance between the two mechanisms, that shadowing is a dominating effect on long-wave radiation trapping, meaning that in narrow streets (H/W>1) that receive less direct radiation during the day, nighttime temperature and UHI are more stable and can even decrease.

Street canyon proportion, by creating temperature differences in the canyon, also influences the flow field structure, specifically the spiral flow created by the downward vertical component and the longitudinal one. de Lieto et al. (2014) observed, in a comparative analysis for Milan, that H/W influences the natural convective vortex, and specifically that higher H/W increases the impacts of convective flows. Others have pointed out that the deeper the canyon, the larger the range of wind speed and temperature values (Jareemit & Srivanit, 2019; Chen et al. 2020).

Not only is H/W a traditional parameter in climatology, but it has also been widely used in parametric and modelling energy studies to compare the influence of different street geometries on cooling and heating loads. Numerous studies have confirmed what was previously pointed out by Oke (1987): narrow canyons (with high H/W) reduce the cooling needs of buildings because of shadowing during the day. For the Swiss city of Basel, Allegrini, Dorer, & Carmeliet (2012) calculated that annual building cooling demand is lower for narrow canyons (H/W=2) that for wide ones (H/W=0.5). Futcher et al. (2018) showed, by simulating daytime demand under London weather conditions, that increasing the H/W of a street canyon is beneficial for reducing the cooling loads of office spaces, specifically those with H/W>2. Huang & Li (2017) also highlighted that H/W has a greater effect than other factors, such as orientation and vegetation density, on peek cooling consumption in the subtropical climate of Taipei. Buildings in deep street canyons (H/W=2) have a 28.6% lower cooling demand than buildings in shallow canyons (H/W=0.5). Krüger, Pearlmutter, & Rasia (2010) confirmed for the hot–arid climate of Israel that deep canyons (H/W=2) contribute to a drop in air conditioning energy demand due to reduced diffuse and direct solar radiation received by building facades. Shallow canyons (H/W= 0.33), on the contrary, can increase energy demand for cooling by up to 250% compared to a base case (H/W= 0.6). Similarly, Strømann-Andersen & Sattrup (2011), through thermal simulations in Copenhagen (Denmark), found that high H/W ratio contributes to a decreased cooling demand due to overshadowing,

while increasing the energy demand for heating and artificial lighting. Generally, annual energy consumption (including lighting, heating and cooling) varies from free horizon (H/W=0) to H/W=3 by between +2,1% and +30.2% for office buildings and by between +2 and +19% for housing buildings.

Other studies have used combined measurements and modelling to analyse UHI impacts on energy loads. Kolokotroni et al. (2007) assessed the annual heating and cooling load of a typical office building in 24 locations in London, showing that in urban areas, the cooling load is up to 25% higher than in rural areas, while heating demand is up to 22% lower. A classification of the urban areas under study, based on the canyon aspect ratio (H/W) showed that mean temperatures during the daytime correlate with H/W. Salvati, Coch Roura, & Cecere (2017) found that for Barcelona (Spain), the maximum UHI intensity during the nighttime occurred in narrow canyons and that overall UHI caused a daily-average increase in cooling demand of between 19% and 24%. Although UHI is higher in narrow canyons, the absolute increase in UHI-related cooling demand depends on solar gains, as energy loads are less related to outdoor temperature when solar gains are high.

The Length to Width Ratio (L/W) and *Length to Height Ratio* (L/H) parameters are indices (non-dimensional) that describe the proportion between canyon length and width, and between canyon length and building height respectively, where length is the distance between two intersections and width is the distance between building facades.

These descriptors have been used predominantly to analyse wind flows in canyons within empirical and parametric morphological studies, and applied for wind computational modelling (Georgakis & Santamouris, 2008), analysis on pollution dispersion (Kastner-Klein, Berkowicz, & Britter, 2004) and outdoor comfort at pedestrian level (Arkon & Özkol, 2014).

From an energy perspective, L/W and L/H have been related to potential natural ventilation through passive cooling techniques for buildings in urban configurations (Assimakopoulos, Georgakis, & Santamouris, 2006). Overall wind flows have reduced speed in canyons, compared to those in undisturbed locations, and thus in urban environments, the natural ventilation potential is limited (Georgakis & Santamouris, 2006). However, as found by Kitous, Bensalem, & Adolphe (2012) and Jareemit & Srivanit (2019), longer canyons contribute to higher wind speed compared to short ones. Although these parameters can potentially describe urban heat dissipation due to wind flow velocity, and thus thermal losses and gains through envelopes, they are not directly used in energy studies for analysing aerodynamic and thermal effects on building energy loads.

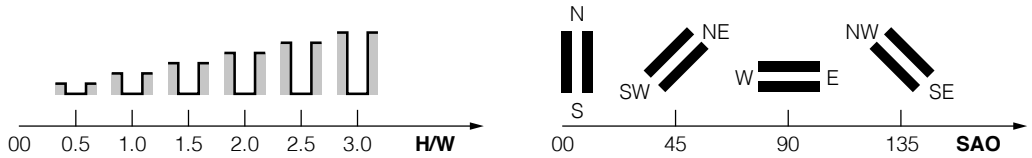


FIG. 2.4 Schematic representation of H/W and SAO values

2.3.2.2 Direction

Direction is a form attribute that conveys the orientation of canyon components (street and facades) and relates to the penetration of solar radiation and wind flows. Thus, from an energy perspective, the canyon direction influences buildings' thermal gains and losses, which are due to direct radiation and convective air movement respectively. The main parameters used to describe and measure direction are *street axis orientation* and *street–wall orientation*.

Street Axis Orientation (SAO) describes the direction of a street canyon's long axis in degrees from true north (or south) or through the four cardinal points (or compass directions). This parameter is often used to evaluate, through parametric studies, radiative exchange between surfaces in street canyons (Battista et al., 2021) and wind flows patterns. Design-oriented studies have explored SAO as an optimisation parameter to mitigate outdoor thermal stress (Chatzidimitriou & Yannas, 2017; De & Mukherjee, 2018).

Many climate studies have highlighted that air temperature is more sensitive to change in H/W than to street orientation. The comparison between east–west and north–south streets with similar H/W in Algeria by Ali-Toudert & Mayer (2006) confirmed minor temperature differences. However, it has been observed that with the increase of H/W, air in east–west canyons becomes warmer than in north–south canyons because of a longer exposure to direct solar radiation in east–west canyons. This pattern is also observed in the Nanjing central district (China), where, according to Deng & Wong (2020), canyons oriented east–west register the highest temperatures as H/W increases. Northeast–southwest orientation is indicated as the more performative orientation to deliver a cooler thermal environment. Similarly, in the Dutch climate context of De Bilt (Holland), Van Esch, Looman, & De Bruin-Hordijk (2012) found that the canyon orientation hardly influenced the total level of direct and diffuse radiation, as differences in orientation caused variation no greater than 5%. However, while global radiation is almost constant in canyons regardless

TOC

of their orientation, the distribution and pattern of irradiation change. In north–south canyons, the radiation at façade is constant during the year, and no shadow is present during the hottest hours in summer, while for east–west canyons, the relative radiation at façade increases during summer. Street surfaces receive more direct radiation during the morning and the afternoon but also provide shade during the hottest hours.

SAO is also one of the main parameters used to analyse wind flow behaviour in urban areas. Wind speed increases in canyons oriented parallel to the prevailing wind direction, while it strongly decreases if the street orientation is perpendicular to the prevailing wind direction (Huang & Li, 2017; Jareemit & Srivanit, 2019). In the former case, deep canyons will further contribute to wind channelling and increase wind velocity (Deng & Wong, 2020). High wind velocity can contribute to the removal of warm air from the canyon in a shorter time but may also increase the convective heat transfer from building surfaces. Moreover, as shown by Andreou & Axarli (2012) in Tinos (Greece), the matching between street orientation and wind direction has a large influence on air temperature. At a high wind speed of 10 m/s, changing the wind direction from parallel to perpendicular to the street results in a 3.5°C air temperature change.

From an energy perspective, Vallati, Mauri, & Colucci (2018), analysing a generic canyon in the climate context of Rome (Italy), concluded that north–south oriented street canyons (H/W=2) increased cooling demand by up to 35% compared to east–west oriented canyons, because of multiple shortwave reflections. Similarly, Huang & Li (2017) found in their study on the average peak cooling consumption in Taipei (Taiwan) for different canyon orientations, that a north–south canyons resulted in the highest cooling demand for buildings, while a southwest–northeast canyon orientation contributed to the lowest energy consumption (17% lower than the former). Southwest–northeast and east–west orientations provide more shading during the daytime; however, the authors argued that cooling loads may increase for those orientations with H/W lower than 0.5, due to the greater heat storage provided by paving materials. Furthermore, Krüger, Pearlmutter, & Rasia (2010) showed that east–west canyons require relatively low cooling loads and are less sensitive than north–south ones to H/W variation. Additionally, their study highlighted that in Israel, hot-climate cooling loads can be reduced in north–south street canyons by increasing H/W.

Similar energy-related results are found for *Street Wall Orientation* (SWO), which describes the cardinal orientation of the building facades in a canyon. Allegrini, Dorer, & Carmeliet (2012) observed, in a parametric analysis for the Basel (Switzerland) climate, that for buildings in a canyon with facades exposed north and south, cooling demand is lower than

for building facades exposed east and west with H/W=1. East–west facades generally have longer exposure to direct solar radiation, which leads to higher cooling demand. Strømann-Andersen & Sattrup (2011) showed in Copenhagen (Denmark) that a southern building orientation is more sensitive to variations in canyon geometry than other orientations with regard to cooling and heating demand. A canyon with H/W>1.5 reduced cooling demand by 150% compared to free horizon. Generally, east–west facing buildings have a yearly energy demand that increases with the increase in H/W. Similarly, Chen et al. (2020) observed that street–wall orientation strongly influences wall temperature and can determine a maximum difference up to 12.7 C (east–west) in Guangzhou, P.R. (China). Additionally, east- and west-oriented walls determine asymmetric wall heating during diurnal hours because direct solar radiation reaches east facades in the morning and west facades in the afternoon, thus enhancing horizontal wind circulation.

2.3.3 Urban Fabric Unit

Urban fabric attributes convey characteristics of units that differ from the building and the canyon. These attributes have an aggregative nature that allows to describe the relations between different urban elements, for example, between building and land division features. Urban fabric characteristics have been found to influence both climate patterns and (indirectly) building energy performance, and have been described through parameters that measure *density, vertical openness, surface roughness and greenery* (Figure 2.5).

Parameters that describe *density* are commonly used in planning-oriented studies for evaluating the energy performance (Álvarez, 2013; Kolodiy & Capeluto, 2021; Rodríguez-Álvarez, 2016) or the climate behaviour (Adelia, Yuan, Liu, & Shan, 2019; Bardhan, Debnath, Gama, & Vijay, 2020; Sharifi & Lehmann, 2014) of different urban areas. Density parameters can also be found in many design-oriented studies that focus on parametric performance evaluations (Natanian, 2020) and mitigation measures to reduce air temperature or to optimise the energy efficiency of buildings (Bardhan et al., 2020; Mahmoud & Ragab, 2021; Z. Shi, Fonseca, & Schlueter, 2017). *Roughness* parameters find a minor application in energy-related studies. Similarly, *vertical openness* parameters are well established in the literature and are used mostly in climate and thermal comfort studies (Deevi & Chundeli, 2020; He et al., 2015; Drach, Krüger, & Emmanuel, 2018) and in design-oriented studies (F. Yang & Chen, 2016; Zhang et al., 2012). Finally, parameters of *greenery* find wide use in climate studies to describe the effect of vegetation on the UHI effect and urban warming, but also to guide heat mitigation actions through comparative scenario analysis (Aboelata & Sodoudi, 2019; Bumseok, Chun & Guldmann, 2018).

Many reviewed studies combined multiple parameters to describe the energy and climate performance of urban environments. A systematisation of multiple quantitative descriptors has been pursued for assessments at the city scale. Among others Adolphe (2001, 2009) proposed a set of assessment indicators to link the morphological complexity with the environmental performance of cities. Ahmadian, Sodagar, Bingham, Elnokaly, & Mills (2021) defined a Form Signature to correlate density indicators with various geometrical parameters, while Rodríguez-Álvarez (2016) developed a method to assess the Urban Energy Index of urban areas.

2.3.3.1 Density

The energy role of urban fabric density is still controversial (Quan & Li, 2021) as a consequence of its multiscale and multivariable nature (Pont & Haupt, 2010) and the complexity of the thermal mechanisms involved. Traditionally, climate-oriented studies have reported that highly dense urban areas consume more energy than dispersed urbanisations and thus that there is a relation between the radial distance from the centre of cities (which generally have higher densities) and building heating and cooling loads (Kolokotroni, Davies, Croxford, Bhuiyan, & Mavrogianni, 2010). Annual loads tend to increase with the increased degree of density and the consequent rise of UHI magnitude (Kolokotroni, Zhang, & Watkins, 2007; Zinzi & Carnielo, 2017). The main reasons are that high urban density translates to a higher capacity for absorbing direct and reflected solar radiation and a more limited capacity for releasing the accumulated heat (Sun, Gao, Li, Wang, & Liu, 2019). Wind speed in cities is generally lower than in less dense areas, where wind flows encounter fewer obstacles. Consequently, dense urban areas tend to maintain high surface temperatures for longer periods, increasing UHI magnitude. The energy result of this process is that high density is associated with lower heating demand and higher cooling demand (Ahmadian et al., 2021).

However, the density of the urban fabric also changes the incidence of shortwave radiation reaching the urban surfaces and the extent of interreflection processes between surfaces (Lima, Scalco, & Lamberts, 2019; Pakarnseree, Chunkao, & Bualert, 2018). Thus, larger shaded areas (with reduced solar access) in high-density areas can provide a cooling effect and thus reduce buildings' heat gains during the daytime. In this regard, a few studies have pointed out that increasing density (for example, through high-rise buildings) can result in lower daytime temperatures (Beraldi & Wang, 2016) and reduced cooling loads (Loibl et al., 2021; Mirkovic & Alawadi, 2017).

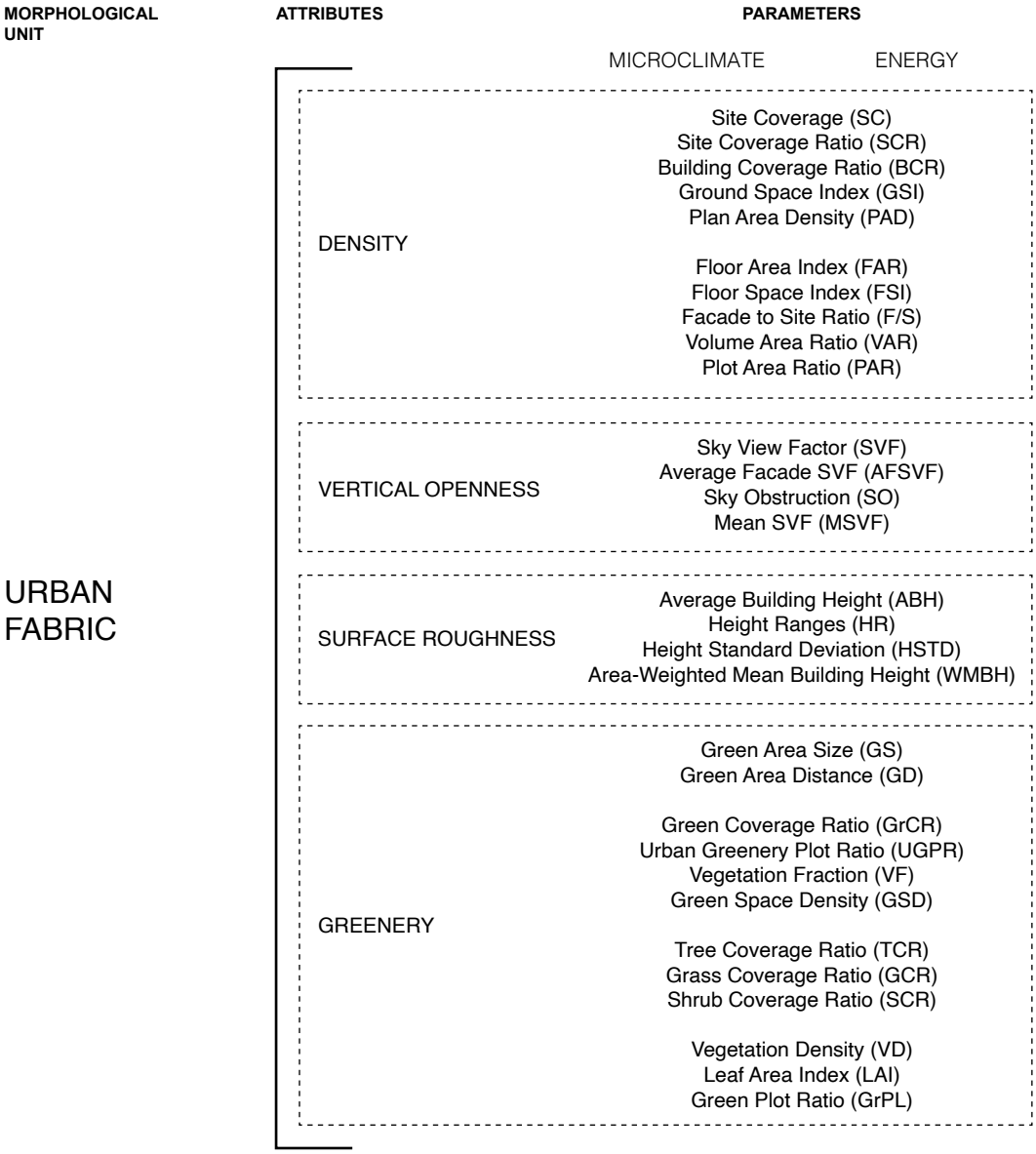


FIG. 2.5 Energy-relevant form attributes and parameters for urban fabric unit

TOC

The density of the built environment is a well-known energy-related attribute, and it has been described through a large number of parameters in both energy and climate studies. Density parameters can be classified into two main subgroups: 1) parameters that describe urban fabric *compactness* and thus the degree of building coverage on a horizontal plane (in other words, building footprint density)—namely *Site Coverage, Building and Site Coverage Ratio, Ground Space Index, and Plan Area Density*; and 2)traditional parameters that describe building *intensity* and imply a three-dimensional occupation of an urban area—namely *Floor Area Ratio and Floor Space Index.*

All parameters of building compactness describe the relation between building footprint area and the total area of the site under analysis, or in other words, horizontal building density. *Site Coverage* (SC) is usually measured in percentages ranging from 0% (no buildings on the site) to 100% (building footprint occupying the full site), while *Site Coverage Ratio* (SCR), *Building Coverage Ratio* (BCR), *Ground Space Index* (GSI) and *Plan Area Density* (PAD) describe the ratio of land occupied by buildings and are expressed in decimal numbers ranging from 0 (no buildings on the site) to 1 (building footprint occupying the full site). Regardless of the measuring unit, the higher the value, the higher the compactness of an urban area.

All of these parameters are used in energy and climate studies. Climate studies generally confirm that air temperatures are positively correlated with compactness (Sun et al., 2019; Lan & Zhan, 2017; Mavrogianni et al., 2009). Hadavi & Pasdarshahri (2021), by comparing three cases in Teheran (Iran), showed that higher PAD reduces ventilation and heat dissipation, leading to higher UHI intensity. Specifically, in the case of a generic pattern of elongated buildings, a change in PAD from 0.4 to 0.73 results in a UHI increase up to 3.8 ^{o}C. With regard to land surface temperature (LST), the study by Chun & Guldmann (2014) concluded that in Columbus (Ohio, USA), a 1% increase in SC led to a temperature increase of 0.06% for a 480-m grid. Additionally, Pakarnseree et al. (2018), by comparing climate data in Bangkok (Thailand) from rural and urban weather stations, found that UHI magnitude correlates to BCR during winter and summer with similar significance. On the other hand, Salvati, Monti, Coch Roura, & Cecere (2019), working in the Mediterranean context of Rome (Italy) and Barcelona (Spain), showed that SCR is the most important parameter correlated to air temperature and UHI in winter (with a coefficient of 0.9), while during the summer it becomes the second most important parameter (with a coefficient of 0.42). These findings highlight the fact that increasing SCR overall increases UHI intensity but that the weight of this factor can change according to seasons and geographical position.

This positive relation between compactness parameters and urban temperatures generally translates to increased cooling demand and decreased heating demand. Salvati, Palme, Chiesa, & Kolokotroni (2020), in a study performed in the Mediterranean climate of Rome (Italy) confirmed a positive correlation between SCR and higher nighttime temperatures, which also translates to a positive correlation between SCR and building cooling demand. By coupling a climate and energy model, Kamal et al. (2021) showed that in the hot–arid climate of Lusail (Qatar), with an increase in SCR from 0.2 to 0.5, cooling demand increased by up to 50%. In London (UK), a study on domestic energy consumption by Godoy-Shimizu, Steadman, & Evans (2021) found that natural gas use fell with the increase of compactness, with a threshold at GSI=0.3. This means that less compact areas (GSI<0.3) have a 9% higher rate of consumption than more compact areas (GSI>0.3). A few exceptions, however, have been found. For example, by comparing the energy performance of two urban models with SC of 87.5% and 35.8% in Stockholm (Sweden), K Javanroodi & Nik (2019) showed that in less compact areas, lower wind speed and turbulence intensity (-27%), together with higher temperature (+14%) resulted in lower energy demand (mainly due to heating).

Energy analyses that do not take into consideration urban climate temperatures and reduced wind flow velocity usually find correlations of opposite sign. Among the studies reviewed, a few showed that increasing compactness resulted in increasing heating demand and decreasing cooling demand. Eicker, Tereci, & Kesten (2010), in a study done in the cold climate of Stuttgart (Germany), found a 10% increase in energy demand when the building context changed from SC= 0% to SC= 60%, mainly due to heating. In London (UK) Rodríguez-Álvarez (2016) calculated that an increase in GSI from 0.1 to 0.9 increased domestic heating demand by 30%. On the contrary, negative correlations are observed between compactness parameters and cooling loads, meaning that the higher the compactness, the lower the cooling demand. Kesten, Tereci, Strzalka, & Eicker (2012), in a study carried out in the cold climate of Stuttgart (Germany), showed that at 60% SC, annual cooling loads were 36% lower than at 30% SC. Eicker et al. (2010) observed in the hot climate of Hong Kong a reduction in cooling loads by 30% when context SC increased from 0% to 60%. (mainly because of cooling). Huang & Wang (2015) confirmed in their study of Wuhan (China) the negative correlation between cooling loads and SCR, finding the lowest cooling demand at SCR=0.6. Lima et al. (2019), working in the hot and humid climate of Maceio (Brazil), found that shading and low-reflectance environments led to a reduction in cooling loads by up to 21% when SC increased from 0 to 28% in the building's surroundings. J. Li, Zheng, Bedra, Li, & Chen (2022) observed that Increasing PAD from 0.06 to 0.7 reduced indoor temperature on average by up 4.7C in Singapore. The correlation is stronger during the daytime, suggesting an association with solar access and consequent gains.

The importance of solar access has also been confirmed in studies that address urban temperature changes caused by variations in compactness. The majority of these studies find a negative correlation between diurnal UHI and compactness parameters. For example, Lin, Lau, Qin, & Gou (2017) in Hong Kong, showed that when SC varied from 30% to 40%, daytime UHI was reduced by 077 ^{o}C. By modelling a building context with a PAD between 0 and 0.44, J. Liu, Heidarinejad, Gracik, & Srebric (2015) showed that the shading effect increases heating loads by 32%, and decreases cooling loads by over 24% for five American cities in different climate zones (San Francisco, Miami, Phoenix, Philadelphia and Chicago). Mirkovic & Alawadi (2017) showed that for Abu Dhabi (UAE), heat gains could be reduced by up to 50% by changing the compactness of the building context.

Floor Area Ratio (FAR), *Floor Space Index* (FSI) are the main parameters that describe building intensity of the urban fabric. Despite the different names, both measure the total building floor area divided by the total site area, or in other words, the floor area per unit area. Many climate studies have used these parameters to describe the influence of building intensity on UHI effect. Some studies reported a cooling benefit due to reduced solar access (J. Li et al., 2022; Bourbia & Awbi, 2004). For instance, Sun et al. (2019) found a negative correlation between FAR and surface temperature in Ningbo (China), explaining the result with the fact that high building intensity produces larger shadow areas. In the tropical climate of Hong Kong, Lin et al. (2017) found that change in FAR (from 4 to 7) explains 32.7% of daytime UHI and that with an increase of 1 FAR, UHI magnitude decreases by 0.39 ^{o}C. However, the majority of the studies reported that with an increase in FAR, urban temperature also increased (mainly during the nighttime) as a consequence of the trapping of long-wave radiation and reduced wind speed. In Wuhan (China), Lan & Zhan (2017) showed, through urban measurements and regression analysis, that FAR was positively correlated with urban air temperatures and it was able to explain 45% of the variance in air temperature during nighttime hours. Similar results were also found by Pakarnseree et al. (2018) in Bangkok (Thailand), with a 0.5 correlation coefficient, and by J. Yang et al. (2021) in Shenyang (China). Chokhachian, Perini, Giulini, & Auer (2020) analysed the environmental impacts of building intensity in the context of Munich (Germany). The high correlation between UHI and FAR also showed that up to FAR=4, the UHI effect is limited.

Some studies have suggested that, as a consequence of the higher temperature in urban areas, cooling demand increases with FAR increase. Li, Song, & Kaza (2018), working in Ningbo (China), found a positive correlation between FAR and electricity consumption for residential buildings in the summer, explained as the result of UHI magnitude. In their study in the hot–humid climate of Amaravati (India), Bardhan et al. (2020) suggested that reducing FSI below 2 could support the reduction of

UHI-related cooling demand for residential buildings by up to 80%. Others, however, who have disregarded urban climate warming, have suggested that high building intensity, and thus high shadow density, can benefit cooling saving. For example, Galal Ahmed & Hossein Alipour (2019) analysed the cooling demand associated with increased FAR in the hot–arid climate of Al Ghreiba and Al Dhaher (UAE) and estimated that increasing FAR from 0.11 to 0.53 and from 0.24 to 0.51 would result in a cooling load reduction of 37% and 50%, respectively.

Differently, on the influence of building intensity on heating demand, studies tend to be in agreement. Rodríguez-Álvarez (2016) in London (UK) and Leng, Chen, Ma, Wong, & Ming (2020) in Herbin (China) found that FSI was negatively correlated with heating demand. Also in London, but by using measured energy data, Godoy-Shimizu et al. (2021) showed that for residential buildings, at FSI<0.6, median gas and electricity consumption were 11% and 6% higher than that at FSI>0.6. One of the most comprehensive studies that have been completed on the heating demand of various urban forms is the one by Rode et al. (2014), which explored the different performances of form patterns in London, Paris, Berlin and Istanbul. FAR was found to be a good predictor of heating loads, with a negative correlation sign. Greater variations in heating demand were found at FAR=1, while areas with FAR <4 had the lowest annual heating demand of all studied areas: 30 to 50 kWh/m^2. A previous study by Yannas (1994) argued that a heat savings up to 40% could be achieved by changing FAR and concluded that FAR 2.5 represented the more efficient intensity. However, Quan, Economou, Grasl, & Yang (2020) suggested that the relation between building intensity and energy loads is more complex. The study observes, through a parametric analysis of areas with FAR between 1 and 20, that increasing FAR decreases annual energy demand only up to a turning point. When the threshold is reached (FAR=4.0 for 50% site coverage), demand starts increasing gradually.

There are also other parameters of density, which appear sporadically in the reviewed studies. For example, Salvati et al. (2019), conducting a study in the Mediterranean context of Rome (Italy) and Barcelona (Spain), identified *Façade to Site Ratio* (F/S) as the second most important parameter for describing UHI during the wintertime. In summer, however, F/S became the most impactful variable on UHI. In a parametric study for the city of Teheran (Iran), Javanroodi, Mahdavinejad, & Nik (2018) described the density of buildings' surroundings through combined variables and considered the resulting microclimate conditions. The parameter of *Volume Area Ratio* (VAR) is calculated as the total volume of surrounding buildings divided by the total site area, while *Plot Area Ratio* (PAR) is the result of the total floor area of the surrounding buildings divided by the total site area. Cooling demand was found to be lower in maximum-density scenarios (Par=2.91, Var=11.64) than in minimum-density scenarios (Par=0.72, Var=2.88). Compared to an average

density scenario the Max density reduces annual cooling demand by 3.9%. Sharifi & Lehmann (2014) made use of Open Plot Ratio (total horizontal open space divided by site area), finding in Sydney (Australia) a correlation between this parameter and surface temperatures.

2.3.3.2 Vertical Openness

Vertical openness is a form attribute that conveys the degree of urban fabric's openness to the sky and determines the amount of incoming shortwave radiation as well as the amount of long-wave radiation returned to the sky. In climatology, limited sky view is reported to increase UHI as a result of the latter factor. Not only buildings but also trees affect the vertical openness of the urban fabric, limiting outgoing long-wave radiation. From an energy perspective, high exposure to the sky is beneficial for daylight. However, the larger incidence of solar radiation also leads to higher surface and air temperatures and increased energy demands for space cooling. On the contrary, greater vertical openness potentially reduces heating demand.

The main parameter that describes vertical openness is the *Sky View factor* (SVF). The SVF is used in climate studies to understand the impact of vertical openness on climate phenomena such as UHI (Unger, 2004) and on methods and technologies for improving its calculation (Jiang, You, & Ding, 2017; de Morais et al., 2018; Jhaldiyal et al., 2018). Further, SVF is also employed in climate modelling for predicting mean radiant temperature (Lindberg & Grimmond, 2011; Lindberg et al., 2008).

SVF describes the fraction of the sky that is visible, but as some have argued, it also provides an indication of so-called urban fabric density (Dirksenet al., 2019). Specifically, SVF measures the ratio between sky voltage visible from a given point on the ground and the entire sky dome (Oke 1988) or in other words, the 'degree to which the sky is obscured by the surroundings for a given point' (Grimmond et al., 2001). This parameter is a dimensionless one, ranging from 0 to 1. The higher the value, the more open is the urban fabric to the sky. This 'geometric definition' (J. Zhang et al., 2012) is based on the assumption that every part of the sky dome is of equal importance and translates in the measuring by the ratio between angle of sky visibility from a point and its solid angle of hemisphere. In climatology studies, however, SVF has also been described as the ratio between the radiation received from a planar surface and the radiation emitted by the sky dome (Watson & Johnson, 1987). Based on this definition, SVF calculation can introduce a weight factor for the part of the sky closer to the zenith.

Having a climatologic origin, SVF is widely used in studies that address surface and air temperature in cities (Unger, 2004). Oke, Johnson, Steyn, & Watson (1991) showed that the cumulative results of early studies in different continents featured a negative correlation between nocturnal Maximum UHI and SVF. Other studies concluded that the relation between air temperature and SVF changed between nighttime and daytime. During diurnal hours, the correlation was positive because with increased openness, a larger amount of solar radiation hit the surfaces, while during nocturnal hours, the correlation was negative, because the lower the SVF, the higher the trapping of heat in form of longwave radiation. In Tehran (Iran) Baghaeipoor & Nasrollahi (2019), by analysing a high-density residential area, confirmed a positive correlation between SVF and air temperature during the daytime, while an inverse correlation was found during the night. Additionally, the study suggested that areas could be classified in three categories according to their climate behaviour: SVF<0.25 (corresponding to dense space), SVF that ranging between 0.25 and 0.5 (corresponding to semi-open space) and SVF>0.5 (corresponding to open space). However, other studies have not found a correlation difference between night and day. Liu, Xu, Weng, Zhang, & Shu, (2021) working in Beijing (China), concluded that with an SVF ranging between 0.4 and 1, SVF and UHI were negatively correlated during the full 24-hour period, though the correlation was clearly stronger during night hours. Bourbia & Boucheriba (2010), in a study in Constantine (Algeria), observed a positive correlation during all 24 hours of analysis for SVF = 0.076-0.58.

Regarding the degree of influence of this parameter, Erdem, Okumus & Terzi (2021) argued, based on their study for Istanbul (Turkey), that the effect of SVF on surface UHI remains low (SVF= 0.37-0.97). This weak correlation was confirmed by H. Li et al. (2021) in Wuhan (China). In fact, they observed a maximum effect of 0.4 C on LST for SVF between 0.5 and 1. However, this study also showed that SVF had a seasonally varying influence on LST. For example, in summer, the correlation has a U shape, meaning an initial positive correlation where SVF= 0.5–0.8 and a subsequent negative correlation where SVF>0.8. This result was explained by the increased wind speed due to the increased openness. Daramola & Balogun (2019) found that for Akure (Nigeria), SVF ranging between 0.42 and 0.97 accounted for 36% of the variation in LST, 32% of sensible heat flux and 37% of latent heat flux. Chun & Guldmann (2014) found that in Columbus Ohio (USA), a 1% increase in SVF led to a 0.31% decrease in LST as a result of increased wind circulation. The results of a study conducted by Giridharan et al. (2004) in subtropical climate conditions indicated that a 1% reduction in SVF might reduce the daytime UHI intensity by up to 4%.

The impact on energy demand can be influenced by openness as result of the thermal mechanisms driven by it. Higher SVF (meaning higher exposure to the sky), implies a higher incidence of shortwave radiation and thus higher solar gains for buildings. Additionally, as the degree of openness influences air temperature and wind flows in cities, an indirect effect is expected on the heating and cooling demand of buildings through convective heat loss (or gain). However, the review has identified only a few relevant studies. A possible explanation for this gap is that the parameter of SVF is difficult to apply to energy studies because it describes the relation between a single point and the sky, rather than a surface or volume. For example, Chatzipoulka, Compagnon, Kaempf, & Nikolopoulou (2018) used the parameter of *Average Façade SVF* (AFSVF) to evaluate the solar irradiance (direct, diffuse and reflected radiation) of facades in the climates of Athens, London and Helsinki (Finland). The results confirmed a very strong linear correlation (R^2= 0.8) for all 24 areas studied, in all climates and for all the orientations examined. Using the same parameter, Morganti, Salvati, Coch, & Cecere (2017) analysed 14 urban patterns in Rome and Barcelona, finding that GSI, façade-to-site-ratio and SVF explained 91% of solar incidence at façade, and thus potentially explained solar gains. A positive correlation was found between AFSVF and solar incidence. Additionally, *Horizontal and Vertical Sky Obstruction* (SO) was used by A. Salvati et al. (2020) in Rome (a Mediterranean climate) and Antofagasta (Chile—a subtropical desert climate) to explain the increase in minimum temperature in areas with low urban SVF and its influence on the final increase in cooling demand, despite the cooling effect due to shadow. Zhang & Gao (2021) used the parameter of *Mean SVF* (MSVF) to describe eight generic urban patterns in the climate of Nanjing (China); these urban patterns had MSVF ranging between 0.18 and 0.56. Through coupling a climate model with an energy model, the study found a positive correlation between MSVF and cooling and heating demand. In summer, this result was explained by higher solar gains and air temperature (for higher MSVF), while in winter, MSVF negatively correlates with air temperature because of high wind speed.

2.3.3.3 Surface Roughness

Roughness is a form attribute of the urban fabric and its elements (such as trees and buildings) that influence air movement through friction or due to buoyancy induced by solar heating on surfaces (Bonan 2018). In climatology, micrometeorological approaches traditionally employ parameters such as *roughness length* and *zero-plane displacement* (Oke, 1988), while morphometric approaches rely on simplified parameters such as *frontal area ratio* and *average element height* (Grimmond and Oke 1999; Oke, Mills, Christen, & Voogt, 2017). However, within the reviewed

articles, only a few of these roughness parameters have been found. Thus, it is difficult to reach conclusions related to the cooling and heating performance of buildings determined by this attribute.

A few energy analyses and climate analyses refer to *Average Building Height* (ABH). This parameter is used as an ambivalent descriptor of roughness and density. Building height affects air flows and influences solar gains. Chokhachian, Perini, Giulini, & Auer (2020) showed that for Munich (Germany), maximum UHI during nighttime was highly influenced by building height. Lan & Zhan (2017) found a positive correlation between ABH and night air temperature in Wuhan (China), determining that the optimal scale for analysis of this parameter is a squared buffer area of 200–250m. Salvati et al. (2020) found that for Antofagasta (Chile), ABH had the strongest influence on maximum air temperature and solar gains, resulting in a negative correlation with cooling demand. Similar findings were confirmed by Wong, Jusuf, Syafii, & Chen (2011) through a parametric study conducted in Singapore; they found that increasing the height of the surroundings up to 60m reduced cooling load by up to 4.70%.

Height is also analysed through other parameters. By using a classification of *Height Ranges* (HR), Jurelionis & Bouris (2016) modelled air infiltration impact on building energy consumption at constant building volume and modified building heights (18m, 16–36 m, 6–16 m) Zurich (Switzerland), Kaunas (Lithuania) and Athens (Greece). The results showed that the area with the highest ABH had a higher air exchange rate and a larger range of values, thus resulting in a higher energy demand to cover heat losses. Li et al. (2021) also employed a classification of height (low rise=3–10m, mid-rise=10–25m, high-rise >25m) and found that height is a season-stable factor influencing LST in Wuhan (China). The study also found a height threshold of 10m, which determined a switch from a heating to a cooling effect.

By using building *Height Standard Deviation* (HSTD), the comprehensive sensitivity analysis carried out by Martins, Faraut, & Adolphe (2019) in three districts of Toulouse (France) showed that the effect of building height on cooling (0.2–1.5 %) was slightly lower than the effect on heating (0.3–2%). Palusci, Monti, Cecere, Montazeri, & Blocken (2022) used Area-Weighted Mean Building Height (WMBH) and showed a strong correlation between this parameter and urban wind velocity and ventilation in compact urban environments.

Finally, the study by Adolphe (2001) proposed a set of original form parameters to describe and assess the climate performance of the urban fabric. Among these parameters, the ones that describe urban surface roughness are *porosity, sinuosity* and *rugosity*. The first two relate to the capacity of wind flows to infiltrate in the

urban fabric, while the last conveys the level of friction that urban elements will oppose to air flows. Porosity is calculated as the open volume divided by the urban fabric total volume (built and non-built), assuming that the street axes (or open spaces) are parallel to wind flow direction. If the street axes are not oriented parallel to the predominant wind direction, the relative sinuosity describes how the urban 'pores' diverge from wind direction. This parameter is calculated as the sum of street segments weighted through the angle (x) against wind direction, divided by the total length of the street. Absolute rugosity is described by Adolphe (2001) as the average height of the canopy layer (built and non-built), while relative rugosity is calculated as 'the mean square deviation of canopy height (built and non-built), for a given direction, weighted by the width of each element in the cross section plane'.

2.3.3.4 Greenery

Vegetation in cities influences both cooling and heating loads, and thus greenery can be considered an energy-related attribute of the urban fabric. It is also well known that greenery influences urban climate through various processes. First, trees, by shading, reduce the exposure to sun radiation and the thermal storage of built surfaces (such as walls and paving); this effect also reduces long-wave exchange with a building's surroundings. Second, the evapotranspiration process, which is enhanced by vegetation, lowers air temperatures through evaporative cooling and increases the air moisture content. Third, trees are also known as roughness elements, meaning that they modify air flows in the canopy layer.

Thus, by enhancing shade, vegetation can reduce solar gains for buildings, while evapotranspiration and the effect of roughness on wind speed influence the microclimate context of a building and thus influence losses through convective movements at the façade. Although greenery can reduce wind speed, it is overall considered a passive cooling measure during hot seasons because shade and evaporative cooling can lead to lower cooling demand for buildings (Morakinyo, Lau, Ren, & Ng, 2018).

Many parameters have been used to describe greenery coverage in the urban fabric, and overall, there is wide agreement on the negative correlation between these parameters and urban temperatures, and thus on the cooling loads of buildings. This means that the lower the vegetation coverage, the higher the temperature and cooling demand. The most common parameters found in the literature are *Green Area Size* (GS) and *Green Area Distance* (GD), *Green Coverage Ratio* (GrCR), *Tree Coverage Ratio* (TCR), *Grass Coverage Ratio* (GCR), *Shrub Coverage Ratio* (SCR), *Vegetation Density* (VD), *Leaf Area Index* (LAI) and *Green Plot Ratio* (GrPL).

A few studies have used size parameters that describe GS and GD, focusing on the relationship between the size of the green area/park and the cooling effect at a certain distance from it. For example, Aram, Higueras García, Solgi, & Mansournia (2019) and Chen et al. (2012) found decreased temperature at a 300-m distance from large parks (>10ha) and negligible change in temperature for small parks (<1ha). However, Lin et al. (2017), by analysing the performance of parks in dense areas of Hong Kong, concluded that the size of the green area does not necessarily influence UHI magnitude. This finding was also confirmed by other studies, which found a beneficial effect of small green areas in terms of temperature decrease, for instance, Yan et al. (2012). Additionally, shorter radii of 20m and 30m have been used to analyse the climate effect of green areas in studies by Emmanuel (1997) and Saito, Ishihara, & Katayama (1990).

Green Coverage Ratio (GrCR), also called *Urban Greenery Plot Ratio* (UGPR) or *Vegetation Fraction* (VF) or *Green Space Density* (GSD) is a parameter that describes the ratio of urban surface occupied by vegetation to the total area under analysis as a percentage. The higher the value, the higher is the percentage of land occupied by vegetation. Sharifi & Lehmann (2014), using UGPR in a study conducted in Sydney (Australia), found a negative correlation (-0.40) with surface UHI. Morakinyo et al. (2018), in a parametric study in Hong Kong, analysed an increase in GrCR from 7 % to 30%, revealing a reduction of maximum temperature by up 1^{o}C.

Energy studies have highlighted the effects of vegetation on cooling and heating demand. Among others, Feng, Li, Ruan, & Xu (2016) found that in Qingdao (China), cooling energy use in summer was primarily affected by occupant behaviour and household characteristics, followed by GrCR which contributed to reducing consumption. Martilli (2014), by analysing 22 idealised cities with hot–dry climate, compared the energy demand for areas with VF ranging from 80% to 0%. Results confirmed a negative correlation, in particular for cooling in summer. Ko & Radke (2014), conducting a study in Sacramento (California, US), determined through a statistical model that GSD significantly correlates with electricity use. GSD was calculated as the green area per unit area from a landcover image in a buffer zone with a 30-m radius and was found to have a negative correlation with electricity use for space cooling. Zhou et al. (2017), working in Shanghai, used GrCR to confirm the negative correlation with UHI, finding that for each degree of reduction in GrCR, heating demand decreases by 5%.

A few studies have adapted GrCR in order to analyse the contribution of different vegetation types, such as trees, shrubs and grass. The parameter of *Tree Coverage Ratio* (TCR) describes the ratio of the foliage area projected on a horizontal floor to the total land area. Similar calculations are used for *Grass Coverage Ratio* (GCR) and

Shrub Coverage Ratio (SCR). Many studies using these parameters have indicated a relation between coverage and air temperature.

The majority of the studies under review confirmed a negative correlation between TCR and urban air temperature. The parametric study conducted in Hong Kong by Ng, Chen, Wang, & Yuan (2012) concluded that a TCR higher than 33% reduces air temperature by about 1°C. Similarly, other studies showed that a TCR between 25% and 40% reduced temperature by 1 °C and that the impact on UHI tended to flatten above 40% (Giridharan, Lau, Ganesan, & Givoni, 2008). Taha (1997), working in four Canadian, cities reported a temperature decrease of 5°C with TCR=33% and a decrease of up to 10°C with TCR=67%. Wang, Berardi, & Akbari (2016) and Wang & Akbari, (2016) concluded that increasing urban vegetation by 10% reduces temperature by up to 0.8°C. Other studies, such as the one by Ibsen, Jenerette, Dell, Bagstad, & Diffendorfer (2022) reported an air temperature reduction of 0.026°C during daytime and 0.016°C during the nighttime per 1% change in cover in the semi-arid climate of Denver (Colorado, US). Giridharan et al. (2008) also report that at a similar coverage ratio, shrub-covered areas were 0.5 to 1.0°C warmer than tree-covered areas. Lin et al. (2017) did not find a significant relationship between UHI and SCR. Aboelata & Sodoudi (2019), by modelling a high-density urban district in Cairo (250mx250m), compared the effects of green coverage scenarios. During the daytime, TCR=50 % contributed to a maximum reduction of 1°C in air temperature, while TCR=30% and TCR=30%+GCR=70% led to a reduction of only 0.5°C. However, during the nighttime, the impact is similarly around 0.5°C. Onishi, Cao, Ito, Shi, & Imura (2010) in a study conducted in Nagoya (Japan), found that GCR=70%+TCR=30% could reduce LST by up to 9°C, while 100% GCR resulted in a 6.4°C reduction. Aboelata & Sodoudi (2019), analysing an area with 50% TCR, calculated a reduction of air conditioning of 1044kWh for a commercial building.

Finally, other studies have explored the use of different vegetation parameters. Nichol, Wong, Fung, & Leung (2006) proposed the parameter of Vegetation Density (VD) as a substitute for LAI (Leaf Area Index) to measure the 'vegetation amount in all vertical layers above ground'. The application of this parameter in a study conducted in Hong Kong showed that with an increase of VD, surface temperature decreases. LAI was explored by Carlson & Ripley (1997) for large-scale climate analysis and later evolved into *Green Plot Ratio* (GrPL) (Ong, 2003). GrPL, calculated as the ratio of LAI to total lot area, was used by Wong et al. (2011) to analyse the effect of urban surroundings on a building's cooling load. This study concluded that in the tropical climate of Singapore, increasing GnPL of 1 reduces minimum temperature of 0.2 C, and overall GnPL 4 contributes to reduce cooling loads by up 6%.

2.4 Multivariable Approach

The present review addresses various energy-relevant form attributes and parameters through a structured classification. However, a combination of multiple parameters was found in many studies to describe the climate and the energy performance of buildings in urban environments. A few studies departed from the Local Climate Zone (LCZ) framework (Stewart & Oke, 2012) which classifies urban areas based on compactness, building height and building intensity. For instance, the study by Benjamin, Luo, & Wang (2021) analysed energy demand patterns in London, concluding that cooling demand is the highest in LCZ 2, while L. Shi et al. (2019), in a study conducted in Hong Kong, confirmed that sensible cooling loads decrease while following the LCZ classification.

Other studies referred to the Spacemate chart (Berghauser-Pont & Haupt, 2010), which draws comprehensive relationships between variables that describe density, such as FSI, GSI and OSR. A few studies have adopted and adapted the Spacemate approach to energy-related studies (Godoy-Shimizu et al., 2021; Martins et al., 2019); while Ahmadian et al., (2021) developed a 'form signature', adding on the correlation with building parameters and aiming to identify the impacts on building energy performance (demand and renewable solar energy production). The study used site coverage and plot ratio as descriptive parameters for urban areas. However, the results showed that for similar density levels, the annual energy performance varies according to the building type (courtyard, pavilion, etc) and the buildings' geometrical characteristics. Consequently, the authors suggested a simultaneous analysis of urban density and building form.

A few studies have also used multiple parameters and multiple units of analysis. For example, Chokhachian et al. (2020) compared different form scenarios in Munich with the goal of identifying optimal configurations and informing performance-based planning. Their study showed that parameters of building height, canyon width and building size need to be considered together to describe UHI form performance. For example, the lowest UHI (equivalent to 7°C) was found when the ratio between canyon width and building linear size (w/x) was equal to 1.14 and the buildings were 9 storeys high, while for FAR 3, UHI can reach 10 °C for w/x= 1 with buildings of 12 storeys. Sun & Augenbroe (2014) also employed a combination of form parameters at multiple scales—canyon height, canyon aspect ratio, vegetation coverage and building coverage—in order to represent urban density in tall-building districts and high-, medium- and low-density cities. Representative samples were then used to estimate the effect of form on UHI through modelling, confirming

that the median annual UHI is higher in large city centres than in suburban areas. However, the final estimation of energy demand, reported to an aggregated level, does not allow a reflection on the detailed energy impacts of urban form. In fact, results are reported in terms of an increase in cooling degree-days of 25.3% and in heating degree-days by 31.7 %, leading to an average decrease in total demand of 17 % for the 15 US locations. Leng et al. (2020) concluded that the urban forms surrounding the 14 office buildings under study in a cold region explains the 62% of the heating energy consumption. Among floor area ratio, building height, H/W and total wall surface, density (FAR) showed to have the greatest impact (50%) on heating consumption. Multiple morphological attributes were also employed in the study by K Javanroodi, Mahdavinejad, & Nik (2018), which investigated urban design variables associated with building cooling load and ventilation potential. Four high-rise building forms were inserted into urban contexts generated by variations of canyon aspect ratio and density patterns, resulting in 1600 case studies. A combination of CFD and energy simulations finally demonstrated that higher density resulted in lower cooling loads and that urban pattern parameters induced a 10% reduction in cooling loads; it also suggested that high density, when combined with a low H/W ratio, contributed to a decrease in building cooling loads in districts in hot–arid climates.

2.5 Discussion and Conclusions

This article addresses the existing knowledge fragmentation regarding the relationships between urban form and building energy demand for space cooling and heating. Through a literature review, it recognises nine energy-relevant urban form attributes and 54 quantitative parameters, while describing the form-dependent thermal and aerodynamic mechanisms that influence buildings' energy performance.

In the studies reviewed, energy-relevant form attributes were identified for building, street canyon and urban fabric units. Building energy demand for heating and cooling was found to be influenced by i) building size, compactness and orientation, ii) street canyon proportion and direction, and iii) urban fabric density, vertical openness, surface roughness and greenery. Building size and compactness determine the thermal exchange between the indoor and outdoor space, as well as the amount of air to be heated and cooled by energy systems, while building orientation regulates the building's exposure to the sun by operating

on the penetration and absorption of solar radiation through building envelope components. Street canyon proportion and direction were found to influence outdoor air and surface temperature and in turn, thermal gains and losses through building envelopes, by determining the penetration of solar radiation and wind flows in a canyon, the reflection of long-wave and shortwave radiation, and convective heat flow patterns. Similarly, density, vertical openness, roughness and greenery of the urban fabric influence urban climate conditions and in turn, building energy loads. Some attributes have a more limited role: roughness interacts primarily with urban airflow movements, and vertical openness acts primarily to determine the balance between incoming shortwave radiation and long-wave radiation returning to the sky. Other attributes, like density and greenery, have a larger spectrum of urban climate effects: they influence radiation absorption and reflection, wind velocity and air and surface temperature. Thus, the analysis of energy-relevant form attributes and related thermal mechanisms reveal both an intrinsic and an extrinsic energy role for urban form. The intrinsic role lies primarily in building form characteristics that have a direct impact on thermal losses and gains, while the extrinsic role lies in street canyon and urban fabric characteristics that impact heating and cooling loads indirectly by modifying the contextual climate conditions around a building.

Additionally, this article compiles a list of quantitative parameters used in the reviewed articles to describe the form attributes under discussion. However, the parameters identified were not equally present in heating- and cooling-oriented studies. For example, at the building unit where a larger body of literature was found on heating-related form characteristics, only a few studies used Plan Depth, Building Volume and Rate of Passive Volume in relation to cooling loads. On the contrary, at the street canyon and urban fabric unit, a larger body of studies was found to address cooling-related form characteristics, and thus the corresponding parameters (except the ones that describe density) were found only in a few heating-related studies. The review also suggests that many street canyon and urban fabric parameters are generally well established in climate studies but find only a minor use in energy studies, such as the ones describing canyon proportion and surface roughness. This fact, however, may be due to the limitations of the review method, since parameters are not always included in the keywords or the abstract and title, but instead are used in the unfolding of the paper to describe the characteristics of the areas under study or are later analysed through sensitivity analysis.

This review also reports on the magnitude and sign of the correlations between form parameters and energy loads, when available. Across the reviewed studies, a general agreement was found on the positive correlation between heating loads and building envelope, volume, floor area, and plan depth, and on the negative correlation between cooling loads and canyon height-to-width ratio. A general agreement was

also shown regarding the building and street orientations in the northern hemisphere that control winter and summer solar gains. Surface-to-volume ratio was found to positively correlate with both heating and cooling loads, meaning that the lower the building compactness, the higher the thermal gains and losses. Contradictory results were observed for building height in relation to heating and cooling, because increasing building height results in higher solar gains but potentially also in higher infiltration losses. Regarding urban fabric parameters, the majority of the studies suggested that heating loads decrease and cooling loads increase with the increase of building compactness and intensity (as a consequence of UHI effect). Cooling demand was found to correlate positively with sky view factor, as a result of the increased incidence of solar radiation, and to correlate negatively with parameters describing greenery, because of the cooling effect of vegetation in urban settings.

This study offers a comprehensive overview of the complex trade-offs between urban form and energy performance of buildings in urban climates. Overall, the findings confirm the importance of a better understanding of the multiple synergies in urban environments to guide planning and design decisions toward a decarbonised future. Future studies should continue addressing the relationship with a transdisciplinary approach. Specifically, scholars are encouraged to explore the energy influence of form attributes traditionally considered climatological ones. Additionally, the research focus should be directed toward comprehensive energy assessments to investigate the ways urban form simultaneously influences both the heating and the cooling demand of buildings.

References

Abdollahzadeh, N., & Biloria, N. (2021). Outdoor thermal comfort: Analyzing the impact of urban configurations on the thermal performance of street canyons in the humid subtropical climate of Sydney. *Frontiers of Architectural Research*, *10*(2), 394–409. https://doi.org/10.1016/j.foar.2020.11.006

Aboelata, A., & Sodoudi, S. (2019). Evaluating urban vegetation scenarios to mitigate urban heat island and reduce buildings' energy in dense built-up areas in Cairo. *Building and Environment*, *166*(August), 106407. https://doi.org/10.1016/j.buildenv.2019.106407

Abreu-Harbich, L. V., Labaki, L. C., & Matzarakis, A. (2014). Thermal bioclimate in idealized urban street canyons in Campinas, Brazil. *Theoretical and Applied Climatology*, *115*(1–2), 333–340. https://doi.org/10.1007/s00704-013-0886-0

Adelia, A. S., Yuan, C., Liu, L., & Shan, R. Q. (2019). Effects of urban morphology on anthropogenic heat dispersion in tropical high-density residential areas. *Energy and Buildings*, *186*, 368–383. https://doi.org/10.1016/j.enbuild.2019.01.026

Adolphe, L. (2001). A simplified model of urban morphology: Application to an analysis of the environmental performance of cities. *Environment and Planning B: Planning and Design*, *28*(2), 183–200. https://doi.org/10.1068/b2631

Adolphe, L. (2009). Morphometric Integrators of a Sustainable City. *PLEA2009,- Passive and Low Energy Architecture*, (June), 22–24. Quebec City.

Ahmadian, E., Sodagar, B., Bingham, C., Elnokaly, A., & Mills, G. (2021). Effect of urban built form and density on building energy performance in temperate climates. *Energy and Buildings*, *236*, 110762. https://doi.org/10.1016/j.enbuild.2021.110762

AlAnzi, A., Seo, D., & Krarti, M. (2009). Impact of building shape on thermal performance of office buildings in Kuwait. *Energy Conversion and Management*, *50*(3), 822–828. https://doi.org/10.1016/j.enconman.2008.09.033

Aksoy, U. T., & Inalli, M. (2006). Impacts of some building passive design parameters on heating demand for a cold region. *Building and environment*, *41*(12), 1742-1754

Albatici, R., & Passerini, F. (2010). BUILDING SHAPE AND HEATING REQUIREMENTS : A PARAMETRIC APPROACH IN ITALIAN CLIMATIC. *CESB 2010 Prague - Central Europe towards Sustainable Buildings*.

Ali-Toudert, F., & Mayer, H. (2006). Numerical study on the effects of aspect ratio and orientation of an urban street canyon on outdoor thermal comfort in hot and dry climate. *Building and Environment*, *41*(2), 94–108. https://doi.org/10.1016/j.buildenv.2005.01.013

Allegrini, J., Dorer, V., & Carmeliet, J. (2012). Influence of the urban microclimate in street canyons on the energy demand for space cooling and heating of buildings. *Energy and Buildings*, *55*, 823–832. https://doi.org/10.1016/j.enbuild.2012.10.013

Álvarez, J. R. (2013). Energy and urban form : A top-down assessment tool. *PLEA 2013: Sustainable Architecture for a Renewable Future*, (September).

Andreou, E., & Axarli, K. (2012). Investigation of urban canyon microclimate in traditional and contemporary environment. Experimental investigation and parametric analysis. *Renewable Energy*, *43*, 354–363. https://doi.org/10.1016/j.renene.2011.11.038

Araji, M. . T. (2019). Surface-to-volume ratio : How building geometry impacts solar energy production and heat gain through envelopes envelopes. *SUSTAINABLE BUILT ENVIRONMENT CONFERENCE 2019*. https://doi.org/10.1088/1755-1315/323/1/012034 Arkon, C. A., & Özkol, Ü. (2014). Effect of urban geometry on pedestrian-level wind velocity. *Architectural Science Review*, *57*(1), 4–19. https://doi.org/10.1080/00038628.2013.835709

Aram, F., Higueras García, E., Solgi, E., & Mansournia, S. (2019). Urban green space cooling effect in cities. *Heliyon*, *5*(4), e01339. https://doi.org/10.1016/j.heliyon.2019.e01339

Ascione, F., Bianco, N., Maria Mauro, G., & Napolitano, D. F. (2019). Building envelope design: Multi-objective optimization to minimize energy consumption, global cost and thermal discomfort. Application to different Italian climatic zones. *Energy*, *174*, 359–374. https://doi.org/10.1016/j.energy.2019.02.182

Assimakopoulos, V. D., Georgakis, C., & Santamouris, M. (2006). Experimental validation of a computational fluid dynamics code to predict the wind speed in street canyons for passive cooling purposes. *Solar Energy*, *80*(4), 423–434. https://doi.org/10.1016/j.solener.2005.07.007

Baghaeipoor, G., & Nasrollahi, N. (2019). The effect of sky view factor on air temperature in high-rise urban residential environments. *Journal of Daylighting*, *6*(2), 42–51. https://doi.org/10.15627/jd.2019.6

Bakarman, M. A., & Chang, J. D. (2015). The Influence of Height/width Ratio on Urban Heat Island in Hot-arid Climates. *Procedia Engineering*, *118*, 101–108. https://doi.org/10.1016/j.proeng.2015.08.408

Baker, N., & Steemers, K. (2000). *Energy and Environment in Architecture - A Technical Design Guide*. London & New York: Taylor & Francis Group.

Bansal, N. K., & Bhattacharya, A. (2009). Parametric equations for energy and load estimations for buildings in India. *Applied Thermal Engineering*, *29*(17–18), 3710–3715. https://doi.org/10.1016/j.applthermaleng.2009.07.002

Bardhan, R., Debnath, R., Gama, J., & Vijay, U. (2020). REST framework: A modelling approach towards cooling energy stress mitigation plans for future cities in warming Global South. *Sustainable Cities and Society*, *61*(January), 102315. https://doi.org/10.1016/j.scs.2020.102315

Battista, G., de Lieto Vollaro, E., Ocłoń, P., & Vallati, A. (2021). Effect of mutual radiative exchange between the surfaces of a street canyon on the building thermal energy demand. *Energy*, *226*. https://doi.org/10.1016/j.energy.2021.120346

Bektas Ekici, B., & Aksoy, U. T. (2011). Prediction of building energy needs in early stage of design by using ANFIS. *Expert Systems with Applications*, *38*(5), 5352–5358. https://doi.org/10.1016/j.eswa.2010.10.021

Benjamin, K., Luo, Z., & Wang, X. (2021). Crowdsourcing urban air temperature data for estimating urban heat island and building heating/cooling load in london. *Energies*, *14*(16). https://doi.org/10.3390/en14165208

Berardi U., Wang Y., (2016). The effect of a denser city over the urban microclimate: the case of Toronto, Sustainability 8(8) Art. no. 8. 10.3390/su8080822.

Berghauser-Pont, M., & Haupt, P. (2010). *Spacematrix: space, density and urban form*. https://doi.org/9789052693750

Blanco, H., McCarney, P., Parnell, S., Schmidt, M., & Seto, K. C. (2011). The role of urban land in climate change. Climate Change and Cities. In S. M. C. Rosenzweig, W. D. Solecki, S. A. Hammer (Ed.), *First Assessment Report of the Urban Climate Change Research Network*. https://doi.org/10.5771/9783845272078-358

Bonan, G. B., Patton, E. G., Harman, I. N., Oleson, K. W., Finni- gan, J. J., Lu, Y., and Burakowski, E. A. (2018). Modeling canopy- induced turbulence in the Earth system: a unified parameteriza- tion of turbulent exchange within plant canopies and the rough- ness sublayer (CLM-ml v0), Geosci. Model Dev., 11, 1467– 1496, https://doi.org/10.5194/gmd-11-1467-2018.

Bourass, O., & Et-Tahir, A. (2019). The impact of building orientation on energy consumption in a domestic house in desert climate. *International Journal of Innovative Technology and Exploring Engineering*, *9*(1), 1087–1096. https://doi.org/10.35940/ijitee.A4347.119119

Bourbia, F., Awbi, H. (2004). Building cluster and shading in urban canyon for hot dry climate: Part 2: shading simulations. Renew. Energy 29, 291–301.

Bourbia, F., & Boucheriba, F. (2010). Impact of street design on urban microclimate for semi arid climate (Constantine). *Renewable Energy*, *35*(2), 343–347. https://doi.org/10.1016/j.renene.2009.07.017

Bourdic, L., Salat, S., & Nowacki, C. (2012). Assessing cities: A new system of cross-scale spatial indicators. *Building Research and Information*, *40*(5), 592–605. https://doi.org/10.1080/09613218.2012.703488

Brounen, D., Kok, N., & Quigley, J. M. (2012). Residential energy use and conservation: Economics and demographics. *European Economic Review*, *56*(5), 931–945. https://doi.org/10.1016/j.euroecorev.2012.02.007

Ca, T. V., Asaeda, T., & Abu, E. M. (1998). Reductions in air conditioning energy caused by a nearby park. *Energy and Buildings*, *29*(1), 83–92. https://doi.org/10.1016/s0378-7788(98)00032-2

Caldera, M., Corgnati, S. P., & Filippi, M. (2008). *Energy demand for space heating through a statistical approach : application to residential buildings*. *40*, 1972–1983. https://doi.org/10.1016/j.enbuild.2008.05.005

Camporeale, P. E., & Mercader-moyano, P. (2019). Towards nearly Zero Energy Buildings : Shape optimization of typical housing typologies in Ibero-American temperate climate cities from a holistic perspective. *Solar Energy*, *193*(October), 738–765. https://doi.org/10.1016/j.solener.2019.09.091

Carlson, T. N., & Ripley, D. A. (1997). On the relation between NDVI, fractional vegetation cover, and leaf area index. *Remote Sensing of Environment*, *62*(3), 241–252. https://doi.org/10.1016/S0034-4257(97)00104-1

Caruso, G., Fantozzi, F., & Leccese, F. (2013). Optimal theoretical building form to minimize direct solar irradiation. *Solar Energy*, *97*, 128–137. https://doi.org/10.1016/j.solener.2013.08.010

Catalina, T., Virgone, J., & Iordache, V. (2011). Study on the impact of the building form on the energy consumption. *Proceedings of Building Simulation 2011: 12th Conference of International Building Performance Simulation Association*, 1726–1729.

Cervero, R., & Kockelman, K. (1997). Travel demand and the 3Ds: Density, diversity, and design. *Transportation research part D: Transport and environment*, *2*(3), 199-219

Chatzidimitriou, A., & Yannas, S. (2017). Street canyon design and improvement potential for urban open spaces; the influence of canyon aspect ratio and orientation on microclimate and outdoor comfort. *Sustainable Cities and Society*, *33*(June), 85–101. https://doi.org/10.1016/j.scs.2017.05.019

Chatzipoulka, C., Compagnon, R., Kaempf, J., & Nikolopoulou, M. (2018). Sky view factor as predictor of solar availability on building façades. *Solar Energy*, *170*(June), 1026–1038. https://doi.org/10.1016/j.solener.2018.06.028

Chen, X., Su, Y., Li, D., Huang, G., Chen, W., & Chen, S. (2012). Study on the cooling effects of urban parks on surrounding environments using Landsat TM data: A case study in Guangzhou, southern China. International Journal of Remote Sensing, 33(18), 5889–5914.

Chen, G., Wang, D., Wang, Q., Li, Y., Wang, X., Hang, J., … Wang, K. (2020). Scaled outdoor experimental studies of urban thermal environment in street canyon models with various aspect ratios and thermal storage. *Science of the Total Environment*, *726*, 138147. https://doi.org/10.1016/j.scitotenv.2020.138147

Chen, G., Yang, X., Yang, H., Hang, J., Lin, Y., Wang, X., … Liu, Y. (2020). The influence of aspect ratios and solar heating on flow and ventilation in 2D street canyons by scaled outdoor experiments. *Building and Environment*, *185*(July), 107159. https://doi.org/10.1016/j.buildenv.2020.107159

Cheung, P. K., & Jim, C. Y. (2019). Differential cooling effects of landscape parameters in humid-subtropical urban parks. *Landscape and Urban Planning*, *192*(September). https://doi.org/10.1016/j.landurbplan.2019.103651

Choi, I. Y., Cho, S. H., & Kim, J. T. (2012). Energy consumption characteristics of high-rise apartment buildings according to building shape and mixed-use development. *Energy and Buildings*, *46*, 123–131. https://doi.org/10.1016/j.enbuild.2011.10.038

Chokhachian, A., Perini, K., Giulini, S., & Auer, T. (2020). Urban performance and density: Generative study on interdependencies of urban form and environmental measures. *Sustainable Cities and Society*, *53*(November 2019), 101952. https://doi.org/10.1016/j.scs.2019.101952

Chun, B., & Guldmann, J. M. (2014). Spatial statistical analysis and simulation of the urban heat island in high-density central cities. *Landscape and Urban Planning*, *125*, 76–88. https://doi.org/10.1016/j.landurbplan.2014.01.016

Chun, Bumseok, & Guldmann, J. M. (2018). Impact of greening on the urban heat island: Seasonal variations and mitigation strategies. *Computers, Environment and Urban Systems*, *71*(September 2017), 165–176. https://doi.org/10.1016/j.compenvurbsys.2018.05.006

D'Amico, B., & Pomponi, F. (2019). A compactness measure of sustainable building forms. *Royal Society Open Science*, *6*(6). https://doi.org/10.1098/rsos.181265

Danielski, I., Fröling, M., & Joelsson, A. (2012). The Impact of the Shape Factor on Final Energy Demand in Residential Buildings in Nordic Climates. *World Renewable Energy Forum 2012*, (November 2014).

Daramola, M. T., & Balogun, I. A. (2019). Analysis of the urban surface thermal condition based on sky-view factor and vegetation cover. *Remote Sensing Applications: Society and Environment*, *15*(July), 100253. https://doi.org/10.1016/j.rsase.2019.100253

De, B., & Mukherjee, M. (2018). "Optimisation of canyon orientation and aspect ratio in warm-humid climate: Case of Rajarhat Newtown, India." *Urban Climate*, *24*(April 2017), 887–920. https://doi.org/10.1016/j.uclim.2017.11.003

de Lieto Vollaro, A., de Simone, G., Romagnoli, R., Vallati, A., & Botillo, S. (2014). Numerical study of urban canyon microclimate related to geometrical parameters. *Sustainability (Switzerland)*, *6*(11), 7894–7905. https://doi.org/10.3390/su6117894

de Morais, M. V. B., de Freitas, E. D., Marciotto, E. R., Guerrero, V. V. U., Martins, L. D., & Martins, J. A. (2018). Implementation of observed sky-view factor in a mesoscale model for sensitivity studies of the urban meteorology. *Sustainability (Switzerland)*, *10*(7), 1–15. https://doi.org/10.3390/su10072183

Deevi, B., & Chundeli, F. A. (2020). Quantitative outdoor thermal comfort assessment of street: A case in a warm and humid climate of India. *Urban Climate*, *34*(October), 100718. https://doi.org/10.1016/j.uclim.2020.100718

de Trocóniz, F., Revuelta, A. J., Huerta, M. A. G., & López, T. G. (2012). A Simple Way to Assess and Compare the Thermal Efficacy in Elongated Building Designs. *Sustainability in Energy and Buildings*, *12*, 285–294. https://doi.org/https://doi.org/10.1007/978-3642-27509-8_24

Deng, J. Y., & Wong, N. H. (2020). Impact of urban canyon geometries on outdoor thermal comfort in central business districts. *Sustainable Cities and Society*, *53* (November 2019), 101966. https://doi.org/10.1016/j.scs.2019.101966

Depecker, P., Menezo, C., Virgone, J., & Lepers, S. (2001). Design of buildings shape and energetic consumption. *Building and Environment*, *36*, 627–635.

Dirksen, M., Ronda, R. J., Theeuwes, N. E., & Pagani, G. A. (2019). Sky view factor calculations and its application in urban heat island studies. *Urban Climate*, *30*(July), 100498. https://doi.org/10.1016/j.uclim.2019.100498

Drach, P., Krüger, E. L., & Emmanuel, R. (2018). Effects of atmospheric stability and urban morphology on daytime intra-urban temperature variability for Glasgow, UK. *Science of the Total Environment*, *627*, 782–791. https://doi.org/10.1016/j.scitotenv.2018.01.285

Eicker, U., Tereci, A., & Kesten, D. (2010). Energy Performance of Buildings in Urban Areas. *SET2010 - 9th International Conference on Sustainable Energy Technologies;*, (August). Shanghai, China.

Emmanuel R. (1997). Summertime Heat Island Effects of Urban Design Parameters, Ph.D. Thesis, The University of Michigan.

Erdem Okumus, D., & Terzi, F. (2021). Evaluating the role of urban fabric on surface urban heat island: The case of Istanbul. *Sustainable Cities and Society*, *73*(February), 103128. https://doi.org/10.1016/j.scs.2021.103128

Ewing, R., & Rong, F., (2008). The impact of urban form on U.S. residential.

Feng, F., Li, Z., Ruan, Y., & Xu, P. (2016). An Empirical Study of Influencing Factors on Residential Building Energy Consumption in Qingdao City, China. *Energy Procedia*, *104*, 245–250. https://doi.org/10.1016/j.egypro.2016.12.042

Florides, G. A., Tassou, S. A., Kalogirou, S. A., & Wrobel, L. C. (2002). Measures used to lower building energy consumption and their cost effectiveness. *Applied Energy*, *73*(3–4), 299–328. https://doi.org/10.1016/S0306-2619(02)00119-8

Fournier, E. D., Federico, F., Porse, E., & Pincetl, S. (2019). Effects of building size growth on residential energy efficiency and conservation in California. *Applied Energy*, *240* (June 2018), 446–452. https://doi.org/10.1016/j.apenergy.2019.02.072

Fuentes-Bargues, J. L., Vivancos, J. L., Ferrer-Gisbert, P., & Gimeno-Guillem, M. Á. (2020). Analysis of the impact of different variables on the energy demand in office buildings. *Sustainability (Switzerland)*, *12*(13). https://doi.org/10.3390/su12135347

Futcher, J. A., Kershaw, T., & Mills, G. (2013). Urban form and function as building performance parameters. *Building and Environment*, *62*, 112–123. https://doi.org/10.1016/j.buildenv.2013.01.021

Futcher, J., Mills, G., & Emmanuel, R. (2018). Interdependent energy relationships between buildings at the street scale. *Building Research and Information*, *46*(8), 829–844. https://doi.org/10.1080/09613218.2018.1499995

Galal Ahmed, K., & Hossein Alipour, S. M. (2019). Investigating the Effect of Urban Compactness on Energy Efficiency in Recent Urban Communities in UAE. *IOP Conference Series: Materials Science and Engineering*, *603*(2). https://doi.org/10.1088/1757-899X/603/2/022092

Georgakis, C., & Santamouris, M. (2008). On the estimation of wind speed in urban canyons for ventilation purposes-Part 1: Coupling between the undisturbed wind speed and the canyon wind. *Building and Environment*, *43*(8), 1404–1410. https://doi.org/10.1016/j.buildenv.2007.01.041

Georgakis, Ch, & Santamouris, M. (2006). Experimental investigation of air flow and temperature distribution in deep urban canyons for natural ventilation purposes. *Energy and Buildings*, *38*(4), 367–376. https://doi.org/10.1016/j.enbuild.2005.07.009

Giridharan, R., Ganesan, S., & Lau, S. S. Y. (2004). Daytime urban heat island effect in high-rise and high-density residential developments in Hong Kong. *Energy and Buildings*, *36*(6), 525–534. https://doi.org/10.1016/j.enbuild.2003.12.016

Giridharan, R., Lau, S. S. Y., Ganesan, S., & Givoni, B. (2008). Lowering the outdoor temperature in high-rise high-density residential developments of coastal Hong Kong: The vegetation influence. *Building and Environment*, *43*(10), 1583–1595. https://doi.org/10.1016/j.buildenv.2007.10.003

Godoy-Shimizu, D., Steadman, P., & Evans, S. (2021). Density and morphology: from the building scale to the city scale. *Buildings and Cities*, *2*(1), 92–113. https://doi.org/10.5334/bc.83

Goh, K. C., & Chang, C. H. (1999). The relationship between height to width ratios and the heat island intensity at 22:00 h for Singapore. *International Journal of Climatology*, *19*(9), 1011–1023. https://doi.org/10.1002/(SICI)1097-0088(199907)19:9<1011::AIDJOC411>3.0.CO;2-U

Gratia, E., & De Herde, A. (2003). Design of low energy office buildings. *Energy and Buildings*, *35*(5), 473–491. https://doi.org/10.1016/S0378-7788(02)00160-3

Grimmond, C. S. B., Potter, S. K., Zutter, H. N., & Souch, C. (2001). Rapid methods to estimate sky view factors applied to urban areas. *International Journal of Climatology*, *21*, 903–913. https://doi.org/10.1002/joc.659

Grimmond, C. S. B., & Oke, T. R. (1999). Aerodynamic properties of urban areas derived from analysis of surface form. *Journal of Applied Meteorology and Climatology*, *38*(9), 1262-1292.

Gui, X. chen, Ma, Y. teng, Chen, S. qin, & Ge, J. (2018). The methodology of standard building selection for residential buildings in hot summer and cold winter zone of China based on architectural typology. *Journal of Building Engineering*, *18*(April), 352–359. https://doi.org/10.1016/j.jobe.2018.04.006

Hassid, S., Santamouris, M., Papanikolaou, N., Linardi, A., Klitsikas, N., Georgakis, C., & Assimakopoulos, D. N. (2000). Effect of the Athens heat island on air conditioning load. *Energy and Buildings*, *32*(2), 131–141. https://doi.org/10.1016/S0378-7788(99)00045-6

Hadavi, M., & Pasdarshahri, H. (2021). Investigating effects of urban configuration and density on urban climate and building systems energy consumption. *Journal of Building Engineering*, *44*(March). https://doi.org/10.1016/j.jobe.2021.102710

He, X., Miao, S., Shen, S., Li, J., Zhang, B., Zhang, Z., & Chen, X. (2015). Influence of sky view factor on outdoor thermal environment and physiological equivalent temperature. *International Journal of Biometeorology*, *59*(3), 285–297. https://doi.org/10.1007/s00484-014-0841-5

Hemsath, T. L., & Alagheband Bandhosseini, K. (2015). Sensitivity analysis evaluating basic building geometry's effect on energy use. *Renewable Energy*, *76*, 526–538. https://doi.org/10.1016/j.renene.2014.11.044

Hu, S., Yan, D., Guo, S., Cui, Y., & Dong, B. (2017). A survey on energy consumption and energy usage behavior of households and residential building in urban China. *Energy and Buildings*, *148*(2017), 366–378. https://doi.org/10.1016/j.enbuild.2017.03.064

Huang, K. T., & Li, Y. J. (2017). Impact of street canyon typology on building's peak cooling energy demand: A parametric analysis using orthogonal experiment. *Energy and Buildings*, *154*, 448–464. https://doi.org/10.1016/j.enbuild.2017.08.054

Huang, Y., & Wang, Z. (2015). Comparative Study on Traditional and Modern Urban Textures : Form , Energy and Climate. *ICUC9 - 9th International Conference on Urban Climate Jointly with 12th Symposium on the Urban Environment Comparative*, 1–6.

Huebner, G. M., Hamilton, I., Chalabi, Z., Shipworth, D., & Oreszczyn, T. (2015). Explaining domestic energy consumption - The comparative contribution of building factors, socio-demographics, behaviours and attitudes. *Applied Energy*, *159*, 589–600. https://doi.org/10.1016/j.apenergy.2015.09.028

Ibsen, P. C., Jenerette, G. D., Dell, T., Bagstad, K. J., & Diffendorfer, J. E. (2022). Urban landcover differentially drives day and nighttime air temperature across a semi-arid city. *Science of The Total Environment*, *829*, 154589. https://doi.org/10.1016/j.scitotenv.2022.154589

Inanici, M. N., & Demirbilek, F. N. (2000). Thermal performance optimization of building aspect ratio and south window size in five cities having different climatic characteristics of Turkey. *Building and Environment*, *35*(1), 41–52. https://doi.org/10.1016/S03601323(99)00002-5

Jaber, S., & Ajib, S. (2011). Optimum, technical and energy efficiency design of residential building in Mediterranean region. *Energy and Buildings*, *43*(8), 1829–1834. https://doi.org/10.1016/j.enbuild.2011.03.024

Jareemit, D., & Srivanit, M. (2019). Effect of Street Canyon Configurations and Orientations on Urban Wind Velocity in Bangkok Suburb Areas. *IOP Conference Series: Materials Science and Engineering*, *690*(1). https://doi.org/10.1088/1757-899X/690/1/012006

Javanroodi, K, & Nik, V. M. (2019). Impacts of microclimate conditions on the energy performance of buildings in urban areas. *Buildings*, *9*(8). https://doi.org/10.3390/buildings9080189

Javanroodi, Kavan, Mahdavinejad, M., & Nik, V. M. (2018). Impacts of urban morphology on reducing cooling load and increasing ventilation potential in hot-arid climate. *Applied Energy*, *231*(September), 714–746. https://doi.org/10.1016/j.apenergy.2018.09.116

Jhaldiyal, A., Gupta, K., Gupta, P. K., Thakur, P., & Kumar, P. (2018). Urban Morphology Extractor: A spatial tool for characterizing urban morphology. *Urban Climate*, *24*(December 2017), 237–246. https://doi.org/10.1016/j.uclim.2018.04.003

Jiang, Z., You, W., & Ding, W. (2017). Calculation of Ground View Factor as an Index for Urban Thermal Environment Optimization. *Energy Procedia*, *142*, 2996–3001. https://doi.org/10.1016/j.egypro.2017.12.375

Jones, R. V., Fuertes, A., & Lomas, K. J. (2015). The socio-economic, dwelling and appliance related factors affecting electricity consumption in domestic buildings. *Renewable and Sustainable Energy Reviews*, *43*, 901–917. https://doi.org/10.1016/j.rser.2014.11.084

Jurelionis, A., & Bouris, D. G. (2016). Impact of urban morphology on infiltration-induced building energy consumption. *Energies*, *9*(3), 1–13. https://doi.org/10.3390/en9030177

Kamal, A., Abidi, S. M. H., Mahfouz, A., Kadam, S., Rahman, A., Hassan, I. G., & Wang, L. L. (2021). Impact of urban morphology on urban microclimate and building energy loads. *Energy and Buildings*, *253*, 111499. https://doi.org/10.1016/j.enbuild.2021.111499

Kastner-Klein, P., Berkowicz, R., & Britter, R. (2004). The influence of street architecture on flow and dispersion in street canyons. *Meteorology and Atmospheric Physics*, *87*(1–3), 121–131. https://doi.org/10.1007/s00703-003-0065-4

Kesten, D., Tereci, A., Strzalka, A. M., & Eicker, U. (2012). A method to quantify the energy performance in urban quarters. *HVAC and R Research*, *18*(1–2), 100–111. https://doi.org/10.1080/10789669.2011.583307

Kitous, S., Bensalem, R., & Adolphe, L. (2012). Airflow patterns within a complex urban topography under hot and dry climate in the Algerian Sahara. *Building and Environment*, *56*, 162–175. https://doi.org/10.1016/j.buildenv.2012.02.022

Ko, Y. (2013). Urban Form and Residential Energy Use: A Review of Design Principles and Research Findings. *Journal of Planning Literature*, *28*(4), 327–351. https://doi.org/10.1177/0885412213491499

Ko, Y., & Radke, J. D. (2014). The effect of urban form and residential cooling energy use in Sacramento, California. *Environ. Plann. B Plann. Des.*, *41*(4), 573–593. https://doi.org/10.1068/b12038p

Kolodiy, O., & Capeluto, G. (2021). Towards zero-energy residential complexes in high-density conditions. *Indoor and Built Environment*, *30*(10), 1751–1765. https://doi.org/10.1177/1420326X20962161

Kolokotroni, M., Davies, M., Croxford, B., Bhuiyan, S., & Mavrogianni, A. (2010). A validated methodology for the prediction of heating and cooling energy demand for buildings within the Urban Heat Island: Case-study of London. *Solar Energy*, *84*(12), 2246–2255. https://doi.org/10.1016/j.solener.2010.08.002

Kolokotroni, M., Zhang, Y., & Watkins, R. (2007). The London Heat Island and building cooling design. *Solar Energy*, *81*(1), 102–110. https://doi.org/10.1016/j.solener.2006.06.005

Kolokotroni, M., Salvati, A. (2021). Comfort and Energy Implications of Urban Microclimate in High Latitudes. In: Palme, M., Salvati, A. (eds) Urban Microclimate Modelling for Comfort and Energy Studies. Springer, Cham. https://doi.org/10.1007/978-3-030-65421-4_5

Krüger, E., Pearlmutter, D., & Rasia, F. (2010). Evaluating the impact of canyon geometry and orientation on cooling loads in a high-mass building in a hot dry environment. *Applied Energy*, *87*(6), 2068–2078. https://doi.org/10.1016/j.apenergy.2009.11.034

Lan, Y., & Zhan, Q. (2017). How do urban buildings impact summer air temperature? The effects of building configurations in space and time. *Building and Environment*, *125*, 88–98. https://doi.org/10.1016/j.buildenv.2017.08.046

Lapisa, R. (2019). The effect of building geometric shape and orientation on its energy performance in various climate regions. *International Journal of GEOMATE*, *16*(53), 113–119. https://doi.org/10.21660/2019.53.94984

Lee, S., & Lee, B. (2014). The influence of urban form on GHG emissions in the U.S. household sector. *Energy Policy*, *68*, 534–549. https://doi.org/10.1016/j.enpol.2014.01.024

Leng, H., Chen, X., Ma, Y., Wong, N. H., & Ming, T. (2020). Urban morphology and building heating energy consumption: Evidence from Harbin, a severe cold region city. *Energy and Buildings*, *224*, 110143. https://doi.org/10.1016/j.enbuild.2020.110143

Li, C., Song, Y., & Kaza, N. (2018). Urban form and household electricity consumption: A multilevel study. *Energy and Buildings*, *158*, 181–193. https://doi.org/10.1016/j.enbuild.2017.10.007

Li, H., Li, Y., Wang, T., Wang, Z., Gao, M., & Shen, H. (2021). Quantifying 3D building form effects on urban land surface temperature and modeling seasonal correlation patterns. *Building and Environment*, *204*(February), 108132. https://doi.org/10.1016/j.buildenv.2021.108132

Li, J., Zheng, B., Bedra, K. B., Li, Z., & Chen, X. (2022). Effects of residential building height, density, and floor area ratios on indoor thermal environment in Singapore. *Journal of Environmental Management*, *313*(December 2021), 114976. https://doi.org/10.1016/j.jenvman.2022.114976

Lim, H. S., & Kim, G. (2018). Analysis of Energy Performance on Envelope Ratio Exposed to the Outdoor. *Advances in Civil Engineering*, *2018*.

Lima, I., Scalco, V., & Lamberts, R. (2019). Estimating the impact of urban densification on high-rise office building cooling loads in a hot and humid climate. *Energy and Buildings*, *182*, 30–44. https://doi.org/10.1016/j.enbuild.2018.10.019

Lin, P., Lau, S. S. Y., Qin, H., & Gou, Z. (2017). Effects of urban planning indicators on urban heat island: a case study of pocket parks in high-rise high-density environment. *Landscape and Urban Planning, 168*(September), 48–60. https://doi.org/10.1016/j.landurbplan.2017.09.024

Lindberg, F. and C. S. B. Grimmond (2011). "The influence of vegetation and building morphology on shadow patterns and mean radiant temperatures in urban areas: model development and evaluation." Theoretical and Applied Climatology 105(3): 311-323.

Lindberg, F., Holmer B.and Thorsson S. (2008). "SOLWEIG 1.0 – Modelling spatial variations of 3D radiant fluxes and mean radiant temperature in complex urban settings." International Journal of Biometeorology 52(7): 697–713.

Liu, J., Heidarinejad, M., Gracik, S., & Srebric, J. (2015). The impact of exterior surface convective heat transfer coefficients on the building energy consumption in urban neighborhoods with different plan area densities. *Energy and Buildings*, *86*, 449–463. https://doi.org/10.1016/j.enbuild.2014.10.062

Liu, Y., Xu, Y., Weng, F., Zhang, F., & Shu, W. (2021). Impacts of urban spatial layout and scale on local climate: A case study in Beijing. *Sustainable Cities and Society*, *68*(November 2020). https://doi.org/10.1016/j.scs.2021.102767

Lobaccaro, G., Acero, J. A., Martinez, G. S., Padro, A., Laburu, T., & Fernandez, G. (2019). Effects of orientations, aspect ratios, pavement materials and vegetation elements on thermal stress inside typical urban canyons. *International Journal of Environmental Research and Public Health*, *16*(19). https://doi.org/10.3390/ijerph16193574

Loibl, W., Vuckovic, M., Etminan, G., Ratheiser, M., Tschannett, S., & Österreicher, D. (2021). Effects of densification on urban microclimate—a case study for the city of Vienna. *Atmosphere*, *12*(4). https://doi.org/10.3390/atmos12040511

Mahdavi Adeli, M., Farahat, S., & Sarhaddi, F. (2020). Parametric analysis of a zero-energy building aiming for a reduction of CO2 emissions for warm climate. *Environmental Science and Pollution Research*, *27*(27), 34121–34134. https://doi.org/10.1007/s11356020-09467-9

Mahmoud, H., & Ragab, A. (2021). Urban geometry optimization to mitigate climate change: Towards energy-efficient buildings. *Sustainability (Switzerland)*, *13*(1), 1–21. https://doi.org/10.3390/su13010027

Mangan, S. D., Koclar Oral, G., Erdemir Kocagil, I., & Sozen, I. (2021). The impact of urban form on building energy and cost efficiency in temperate-humid zones. *Journal of Building Engineering*, *33*(June 2020), 101626. https://doi.org/10.1016/j.jobe.2020.101626

Mangkuto, R. A., Rohmah, M., & Asri, A. D. (2016). Design optimisation for window size, orientation, and wall reflectance with regard to various daylight metrics and lighting energy demand: A case study of buildings in the tropics. *Applied Energy*, *164*, 211–219. https://doi.org/10.1016/j.apenergy.2015.11.046

Marciotto, E. R., Oliveira, A. P., & Hanna, S. R. (2010). Modeling study of the aspect ratio influence on urban canopy energy fluxes with a modified wall-canyon energy budget scheme. *Building and Environment*, *45*(11), 2497-2505.

Martilli, A. (2014). An idealized study of city structure, urban climate, energy consumption , and air quality. *Urban Climate*, *10*, 430–446. https://doi.org/10.1016/j.uclim.2014.03.003

Martins, T. A. de L., Faraut, S., & Adolphe, L. (2019). Influence of context-sensitive urban and architectural design factors on the energy demand of buildings in Toulouse, France. *Energy and Buildings*, *190*, 262–278. https://doi.org/10.1016/j.enbuild.2019.02.019

Mashhoodi, B. (2019). Local and national determinants of household energy consumption in the Netherlands. *GeoJournal*, *9*. https://doi.org/10.1007/s10708-018-09967-9

Mashhoodi, B., Stead, D., & van Timmeren, A. (2020). Land surface temperature and households' energy consumption: Who is affected and where? *Applied Geography*, *114*(April 2019), 102125. https://doi.org/10.1016/j.apgeog.2019.102125

Mavrogianni, A., Davies, M., Chalabi, Z., Wilkinson, P., Kolokotroni, M., & Milner, J. (2009). Space heating demand and heatwave vulnerability: London domestic stock. *Building Research and Information*, *37*(5–6), 583–597. https://doi.org/10.1080/09613210903162597

Méndez Echenagucia, T., Capozzoli, A., Cascone, Y., & Sassone, M. (2015). The early design stage of a building envelope: Multi-objective search through heating, cooling and lighting energy performance analysis. *Applied Energy*, *154*, 577–591. https://doi.org/10.1016/j.apenergy.2015.04.090

Mingfang, T. (2002). Solar control for buildings. *Building and Environment*, *37*(7), 659–664. https://doi.org/10.1016/S0360-1323(01)00063-4

Mirkovic, M., & Alawadi, K. (2017). The effect of urban density on energy consumption and solar gains: The study of Abu Dhabi's neighborhood. *Energy Procedia*, *143*, 277–282. https://doi.org/10.1016/j.egypro.2017.12.684

Morakinyo, T. E., Lau, K. K. L., Ren, C., & Ng, E. (2018). Performance of Hong Kong's common trees species for outdoor temperature regulation, thermal comfort and energy saving. *Building and Environment*, *137*(April), 157–170. https://doi.org/10.1016/j.buildenv.2018.04.012

Morganti, M., Salvati, A., Coch, H., & Cecere, C. (2017). Urban morphology indicators for solar energy analysis. *Energy Procedia*, *134*, 807–814. https://doi.org/10.1016/j.egypro.2017.09.533

Mouzourides, P., Kyprianou, A., Neophytou, M. K. A., Ching, J., & Choudhary, R. (2019). Linking the urban-scale building energy demands with city breathability and urban form characteristics. *Sustainable Cities and Society*, *49*(February), 101460. https://doi.org/10.1016/j.scs.2019.101460

Muniz-Gäal, L. P., Pezzuto, C. C., Carvalho, M. F. H. de, & Mota, L. T. M. (2020). Urban geometry and the microclimate of street canyons in tropical climate. *Building and Environment*, *169*(July 2019). https://doi.org/10.1016/j.buildenv.2019.106547

Natanian, J. (2020). BEYOND ZERO ENERGY DISTRICTS A HOLISTIC ENERGY AND ENVIRONMENTAL QUALITY EVALUATION.

Ng, E., Chen, L., Wang, Y., & Yuan, C. (2012). A study on the cooling effects of greening in a high-density city: An experience from Hong Kong. *Building and Environment*, *47*(1), 256–271. https://doi.org/10.1016/j.buildenv.2011.07.014

Nazarian, N., & Kleissl, J. (2015). Urban Climate CFD simulation of an idealized urban environment : Thermal effects of geometrical characteristics and surface materials. *URBAN CLIMATE*, *12*, 141–159. https://doi.org/10.1016/j.uclim.2015.03.002

Nichol, J., Wong, M. S., Fung, C., & Leung, K. K. M. (2006). Assessment of urban environmental quality in a subtropical city using multispectral satellite images. *Environment and Planning B: Planning and Design*, *33*(1), 39–58. https://doi.org/10.1068/b31195

Nicholson, S. R., Shohet, R., & Fung, A. S. (2019). Modelling of a net-zero energy condo in a cold climate using an interdisciplinary design framework. *IOP Conference Series: Materials Science and Engineering*, *609*(7). https://doi.org/10.1088/1757899X/609/7/072041

Oke, T. R. (1981). Canyon geometry and the nocturnal urban heat island: comparison of scale model and field observations. *Journal of climatology*, *1*(3), 237-254

Oke, T. R. (1988). Street design and urban canopy layer climate. *Energy and buildings*, *11*(1-3), 103-113.

Oke, T. R. (1988). The urban energy balance. *Progress in Physical geography*, *12*(4), 471-508.

Oke, T. R., Johnson, G. T., Steyn, D. G., & Watson, I. D. (1991). Simulation of surface urban heat islands under "ideal" conditions at night part 2: Diagnosis of causation. *Boundary-Layer Meteorology*, *56*(4), 339–358. https://doi.org/10.1007/BF00119211

Oke, T. R., Mills, G., Christen, A., & Voogt, J. A. (2017). *Urban Climates*. Cambridge, UK: Cambridge University Press.

Oliveira, V. (2016). Urban morphology: an introduction to the study of the physical form of cities. Springer.

Onishi, A., Cao, X., Ito, T., Shi, F., & Imura, H. (2010). Evaluating the potential for urban heat-island mitigation by greening parking lots. *Urban Forestry and Urban Greening*, *9*(4), 323–332. https://doi.org/10.1016/j.ufug.2010.06.002

Ong, B.L., 2003. Green plot ratio: an ecological measure for architecture and urban planning. Landscape and Urban Planning 63, 197–211.

Ourghi, R., Al-anzi, A., & Krarti, M. (2007). *A simplified analysis method to predict the impact of shape on annual energy use for office buildings. 48*, 300–305. https://doi.org/10.1016/j.enconman.2006.04.011

Pacheco, R., Ordóñez, J., & Martínez, G. (2012). Energy efficient design of building: A review. *Renewable and Sustainable Energy Reviews*, *16*(6), 3559–3573. https://doi.org/10.1016/j.rser.2012.03.045

Pakarnseree, R., Chunkao, K., & Bualert, S. (2018). Physical characteristics of Bangkok and its urban heat island phenomenon. *Building and Environment*, *143*(February), 561–569. https://doi.org/10.1016/j.buildenv.2018.07.042

Palme, M., & Salvati, A. (Eds.). (2021). *Urban Microclimate Modelling for Comfort and Energy Studies*. Springer Nature.

Palusci, O., Monti, P., Cecere, C., Montazeri, H., & Blocken, B. (2022). Impact of morphological parameters on urban ventilation in compact cities: The case of the Tuscolano-Don Bosco district in Rome. *Science of the Total Environment*, *807*, 150490. https://doi.org/10.1016/j.scitotenv.2021.150490

Perini, K., & Magliocco, A. (2014). Effects of vegetation, urban density, building height, and atmospheric conditions on local temperatures and thermal comfort. *Urban Forestry and Urban Greening*, *13*(3), 495–506. https://doi.org/10.1016/j.ufug.2014.03.003

Pisello, A.L.; Pignatta, G.; Castaldo, V.L.; Cotana, F. (2015). The impact of local microclimate boundary conditions on building energy performance. Sustainability, 7, 9207–9230. [CrossRef]

Quan, S. J., Economou, A., Grasl, T., & Yang, P. P. J. (2020). An exploration of the relationship between density and building energy performance. *Urban Design International*, *25*(1), 92–112. https://doi.org/10.1057/s41289-020-00109-7

Quan, S. J., & Li, C. (2021). Urban form and building energy use: A systematic review of measures, mechanisms, and methodologies. *Renewable and Sustainable Energy Reviews*, *139*(January), 110662. https://doi.org/10.1016/j.rser.2020.110662

Rashdi, W. S. S. W. M., & Embi, M. R. (2016). Analysing Optimum Building form in Relation to Lower Cooling Load. *Procedia - Social and Behavioral Sciences*, *222*, 782–790. https://doi.org/10.1016/j.sbspro.2016.05.161

Ratti, C., Baker, N., & Steemers, K. (2005). Energy consumption and urban texture. *Energy and Buildings*, *37*(7), 762–776. https://doi.org/10.1016/j.enbuild.2004.10.010

Rode, P., Keim, Ch., Robazza, G., Viejo, P., & Schofield, J. (2014). Cities and energy: urban morphology and residential heat-energy demand. In *Environment and Planning B: Planning and Design* (pp. 138 – 162).

Rodríguez-Álvarez, J. (2016). Urban Energy Index for Buildings (UEIB): A new method to evaluate the effect of urban form on buildings' energy demand. *Landscape and Urban Planning*. https://doi.org/10.1016/j.landurbplan.2016.01.001

Saito, I., Ishihara, O., & Katayama, T. (1990). Study of the effect of green areas on the thermal environment in an urban area. *Energy and Buildings*, *15*(3–4), 493–498. https://doi.org/10.1016/0378-7788(90)90026-F

Salat, S. (2007). Energy and bioclimatic efficiency of urban morphologies : towards a comparative analysis of Asian and European cities. *International Conference on Sustainable Building Asia*, p. 6.

Salat, S. (2009). Energy loads, CO2 emissions and building stocks: Morphologies, typologies, energy systems and behaviour. *Building Research and Information*, *37*(5–6), 598–609. https://doi.org/10.1080/09613210903162126

Salat, S., Vialan, D., & Nowacki, C. (2010). A common metrics and set of indicators for assessing buildings and urban fabric sustainability performance. *Proceedings: CESB 2010 Prague - Central Europe towards Sustainable Building "From Theory to Practice,"* 1–12. Retrieved from http://www.scopus.com/inward/record.url?eid=2-s2.0- 84902458317&partnerID=tZOtx3y1

Salvati, A., Coch Roura, H., & Cecere, C. (2017). Assessing the urban heat island and its energy impact on residential buildings in Mediterranean climate: Barcelona case study. *Energy and Buildings*, *146*, 38–54. https://doi.org/10.1016/j.enbuild.2017.04.025

Salvati, A., Palme, M., Chiesa, G., & Kolokotroni, M. (2020). Built form, urban climate and building energy modelling: case-studies in Rome and Antofagasta. *Journal of Building Performance Simulation*, *13*(2), 209–225. https://doi.org/10.1080/19401493.2019.1707876

Salvati, Agnese, Monti, P., Coch Roura, H., & Cecere, C. (2019). Climatic performance of urban textures: Analysis tools for a Mediterranean urban context. *Energy and Buildings*, *185*, 162–179. https://doi.org/10.1016/J.ENBUILD.2018.12.024

Santamouris, M. (2014). On the energy impact of urban heat island and global warming on buildings. *Energy and Buildings*, *82*, 100–113. https://doi.org/10.1016/j.enbuild.2014.07.022

Santamouris, M. (2020). Recent progress on urban overheating and heat island research. Integrated assessment of the energy, environmental, vulnerability and health impact. Synergies with the global climate change. *Energy and Buildings*, *207*. https://doi.org/10.1016/j.enbuild.2019.109482

Santamouris, M., Cartalis, C., Synnefa, A., & Kolokotsa, D. (2015). On the impact of urban heat island and global warming on the power demand and electricity consumption of buildings - A review. *Energy and Buildings*, *98*, 119–124. https://doi.org/10.1016/j.enbuild.2014.09.052

Saroglou, T., Meir, I. A., Theodosiou, T., & Givoni, B. (2017). Towards energy efficient skyscrapers. *Energy and Buildings*, *149*, 437–449. https://doi.org/10.1016/j.enbuild.2017.05.057

Serrano, S., Ürge-Vorsatz, D., Barreneche, C., Palacios, A., & Cabeza, L. F. (2017). Heating and cooling energy trends and drivers in Europe. *Energy*, *119*, 425–434. https://doi.org/10.1016/j.energy.2016.12.080

Seto K.C., S. Dhakal, A. Bigio, H. Blanco, G.C. Delgado, D. Dewar, L. Huang, A. Inaba, A. Kansal, S. Lwasa, J.E. McMahon, D.B. Müller, J. Murakami, H. Nagendra, A. R. (2015). Human Settlements, Infrastructure, and Spatial Planning. *Climate Change 2014 Mitigation of Climate Change*, 923–1000. https://doi.org/10.1017/cbo9781107415416.018

Steadman, P., et al. (2014). "Energy and urban built form: an empirical and statistical approach." Building Research & Information **42**(1): 17-31

Shao, T., & Jin, H. (2019). The impact of rural house's orientation on heating energy consumption in severe cold regions of China. *IOP Conference Series: Earth and Environmental Science*, *257*(1). https://doi.org/10.1088/1755-1315/257/1/012035

Sharifi, E., & Lehmann, S. (2014). Comparative analysis of surface urban heat island effect in central Sydney. *Journal of Sustainable Development*, *7*(3), 23–34. https://doi.org/10.5539/jsd.v7n3p23

Shi, L., Luo, Z., Matthews, W., Wang, Z., Li, Y., & Liu, J. (2019). Impacts of urban microclimate on summertime sensible and latent energy demand for cooling in residential buildings of Hong Kong. *Energy*, *189*, 116208. https://doi.org/10.1016/j.energy.2019.116208

Shi, Z., Fonseca, J. A., & Schlueter, A. (2017). A review of simulation-based urban form generation and optimization for energy-driven urban design. *Building and Environment*, *121*, 119–129. https://doi.org/10.1016/j.buildenv.2017.05.006

Silva, M. C., Horta, I. M., Leal, V., & Oliveira, V. (2017). A spatially-explicit methodological framework based on neural networks to assess the effect of urban form on energy demand. *Applied Energy*, *202*, 386–398. https://doi.org/10.1016/j.apenergy.2017.05.113

Skelhorn, C. P., Levermore, G., & Lindley, S. J. (2016). Impacts on cooling energy consumption due to the UHI and vegetation changes in Manchester, UK. *Energy and Buildings*, *122*, 150–159. https://doi.org/10.1016/j.enbuild.2016.01.035

Steadman, P., Bruhns, H. R., Holtier, S., Gakovic, B., Rickaby, P. A., & Brown, F. E. (2000). A classification of built forms. *Environment and Planning B: Planning and Design*, *27*(1), 73–91. https://doi.org/10.1068/bst7

Steadman, P., Hamilton, I., & Evans, S. (2014). Energy and urban built form: An empirical and statistical approach. *Building Research and Information*, *42*(1), 17–31. https://doi.org/10.1080/09613218.2013.808140

Steemers, K. (2003). Energy and the city: Density, buildings and transport. *Energy and Buildings*, *35*(1), 3–14. https://doi.org/10.1016/S0378-7788(02)00075-0

Stewart, I. D., & Oke, T. R. (2012). Local climate zones for urban temperature studies. *Bulletin of the American Meteorological Society*. https://doi.org/10.1175/BAMS-D-11-00019.1

Strømann-Andersen, J., & Sattrup, P. A. (2011). The urban canyon and building energy use: Urban density versus daylight and passive solar gains. *Energy and Buildings*, *43*(8), 2011–2020. https://doi.org/10.1016/j.enbuild.2011.04.007

Sun, Yanwei, Gao, C., Li, J., Wang, R., & Liu, J. (2019). Quantifying the Effects of Urban Form on Land Surface Temperature in Subtropical High-Density Urban Areas Using Machine Learning. *Remote Sensing*, *11*(8), 959. https://doi.org/10.3390/rs11080959

Sun, Yuming, & Augenbroe, G. (2014). Urban heat island effect on energy application studies of office buildings. *Energy and Buildings*, *77*, 171–179. https://doi.org/10.1016/j.enbuild.2014.03.055

Szodrai, F., Lakatos, A., & Kalmar, F. (2016). Analysis of the change of the specific heat loss coefficient of buildings resulted by the variation of the geometry and the moisture load. *Energy*, *115*, 820–829. https://doi.org/10.1016/j.energy.2016.09.073

Taha, H. (1997). Urban climates and heat islands: Albedo, evapotranspiration, and anthropogenic heat. *Energy and Buildings*, *25*(2), 99–103. https://doi.org/10.1016/s0378-7788(96)00999-1

Taleghani, M., Tenpierik, M., Van Den Dobbelsteen, A., & De Dear, R. (2013). Energy use impact of and thermal comfort in different urban block types in the Netherlands. *Energy and Buildings*, *67*, 166–175. https://doi.org/10.1016/j.enbuild.2013.08.024

Theeuwes, N. E., Steeneveld, G. J., Ronda, R. J., Heusinkveld, B. G., van Hove, L. W. A., & Holtslag, A. A. M. (2014). Seasonal dependence of the urban heat island on the street canyon aspect ratio. *Quarterly Journal of the Royal Meteorological Society*, *140*(684), 2197–2210. https://doi.org/10.1002/qj.2289

Theodoridou, I., Papadopoulos, A. M., & Hegger, M. (2011). Statistical analysis of the Greek residential building stock. *Energy and Buildings*, *43*(9), 2422–2428. https://doi.org/10.1016/j.enbuild.2011.05.034

Tsoka, S., Tsikaloudaki, K., Theodosiou, T., & Bikas, D. (2020). Assessing the effect of the urban morphology on the ambient air temperature of urban street canyons under different meteorological conditions. Application in residential areas of Thessaloniki, Greece. *IOP Conference Series: Earth and Environmental Science*, *410*(1). https://doi.org/10.1088/1755-1315/410/1/012005

Turhan, C., Kazanasmaz, T., Erlalelitepe, I., Evren, K., & Gokcen, G. (2014). Comparative study of a building energy performance software (KEP-IYTE-ESS) and ANN-based building heat load estimation. *Energy & Buildings*, *85*, 115–125. https://doi.org/10.1016/j.enbuild.2014.09.026

Unger, J. (2004). Intra-urban relationship between surface geometry and urban heat island: Review and new approach. *Climate Research*, *27*(3), 253–264. https://doi.org/10.3354/cr027253

Ürge-Vorsatz, D., Cabeza, L. F., Serrano, S., Barreneche, C., & Petrichenko, K. (2015). Heating and cooling energy trends and drivers in buildings. *Renewable and Sustainable Energy Reviews*, *41*, 85–98. https://doi.org/10.1016/j.rser.2014.08.039

Vallati, A., Grignaffini, S., Romagna, M., Mauri, L., & Colucci, C. (2016). Influence of Street Canyon's Microclimate on the Energy Demand for Space Cooling and Heating of Buildings. *Energy Procedia*, *101*(September), 941–947. https://doi.org/10.1016/j.egypro.2016.11.119

Vallati, A., Mauri, L., & Colucci, C. (2018). Impact of shortwave multiple reflections in an urban street canyon on building thermal energy demands. *Energy and Buildings*, *174*, 77–84. https://doi.org/10.1016/j.enbuild.2018.06.037

Van Esch, M. M. E., Looman, R. H. J., & De Bruin-Hordijk, G. J. (2012). The effects of urban and building design parameters on solar access to the urban canyon and the potential for direct passive solar heating strategies. *Energy and Buildings*, *47*, 189–200. https://doi.org/10.1016/j.enbuild.2011.11.042

Vartholomaios, A. (2017). A parametric sensitivity analysis of the influence of urban form on domestic energy consumption for heating and cooling in a Mediterranean city. *Sustainable Cities and Society*, *28*, 135–145. https://doi.org/10.1016/j.scs.2016.09.006

Vasaturo, R., van Hooff, T., Kalkman, I., Blocken, B., & van Wesemael, P. (2018). Impact of passive climate adaptation measures and building orientation on the energy demand of a detached lightweight semi-portable building. *Building Simulation*, *11*(6), 1163–1177. https://doi.org/10.1007/s12273-018-0470-8

Vettorato, D. (2011). Sustainable energy performances of urban morphologies.

Wang, Y., & Akbari, H. (2016). Analysis of urban heat island phenomenon and mitigation solutions evaluation for Montreal. *Sustainable Cities and Society*, *26*, 438–446. https://doi.org/10.1016/j.scs.2016.04.015

Wang, Y., Berardi, U., & Akbari, H. (2016). Comparing the effects of urban heat island mitigation strategies for Toronto, Canada. *Energy and Buildings*, *114*, 2–19. https://doi.org/10.1016/j.enbuild.2015.06.046

Watson I.D., Johnson G.T. (1987). Graphical estimation of sky view-factors in urban environments, International Journal of Climatology 7, 193–197.

Wei, R., Song, D., Wong, N. H., & Martin, M. (2016). Impact of Urban Morphology Parameters on Microclimate. *Procedia Engineering*, *169*, 142–149. https://doi.org/10.1016/j.proeng.2016.10.017

Werner, P., & Mahdavi, A. (2003). Building Morphology, Transparence and Energy Performance. *Building Simulation 2003*, 1025–1032.

Wong, N. H., Jusuf, S. K., Syafii, N. I., & Chen, Y. (2011). Evaluation of the impact of the surrounding urban morphology on building energy consumption. *Solar Energy*, *85*(1), 57–71. https://doi.org/10.1016/j.solener.2010.11.002

Xiong, T., Fu, X., & Dong, J. (2014). Simulation analysis of building energy consumption with different surface-volume-ratio and envelop performance of rural dwellings. *Advanced Materials Research*, 1578–1583. https://doi.org/10.4028/www.scientific.net/AMR.953954.1578

Xu, Y., Ren, C., Ma, P., Ho, J., Wang, W., Lau, K. K. L., … Ng, E. (2017). Urban morphology detection and computation for urban climate research. *Landscape and Urban Planning*, *167*(July), 212–224. https://doi.org/10.1016/j.landurbplan.2017.06.018

Yan H., Wang X., Hao P., Dong L. (2012). Study on microclimatic characteristics and human comfort of park plant communities in summer, Procedia Environ. Sci. 13 (2012) 755–765.

Yang, F., & Chen, L. (2016). Developing a thermal atlas for climate-responsive urban design based on empirical modeling and urban morphological analysis. *Energy and Buildings*, *111*, 120–130. https://doi.org/10.1016/j.enbuild.2015.11.047

Yang, J., Ren, J., Sun, D., Xiao, X., Xia, J. (Cecilia), Jin, C., & Li, X. (2021). Understanding land surface temperature impact factors based on local climate zones. *Sustainable Cities and Society*, *69*(March), 102818. https://doi.org/10.1016/j.scs.2021.102818

Yannas, S. Solar Energy and Housing Design: Principles, Objectives, Guidelines, Volume 1. Architectural Association, London.1994.

Ying, X., & Li, W. (2020). Effect of floor shape optimization on energy consumption for Ushaped office buildings in the hot-summer and cold-winter area of China. *Sustainability (Switzerland)*, *12*(5). https://doi.org/10.3390/su12052079

Yu, Z., Chen, S., & Wong, N. H. (2020). Temporal variation in the impact of urban morphology on outdoor air temperature in the tropics: A campus case study. *Building and Environment*, *181*(April), 107132. https://doi.org/10.1016/j.buildenv.2020.107132

Zhang, J., Heng, C. K., Malone-Lee, L. C., Hii, D. J. C., Janssen, P., Leung, K. S., & Tan, B. K. (2012). Evaluating environmental implications of density: A comparative case study on the relationship between density, urban block typology and sky exposure. *Automation in Construction*, *22*, 90–101. https://doi.org/10.1016/j.autcon.2011.06.011

Zhang, M., & Gao, Z. (2021). Effect of urban form on microclimate and energy loads: Case study of generic residential district prototypes in Nanjing, China. *Sustainable Cities and Society*, *70*(March), 102930. https://doi.org/10.1016/j.scs.2021.102930

Zhou, S., & Teng, F. (2013). Estimation of urban residential electricity demand in China using household survey data. *Energy Policy*, *61*(2013), 394–402. https://doi.org/10.1016/j.enpol.2013.06.092

Zhou, Y., Zhuang, Z., Yang, F., Yu, Y., & Xie, X. (2017). Urban morphology on heat island and building energy consumption. *Procedia Engineering*, *205*, 2401–2406. https://doi.org/10.1016/j.proeng.2017.09.862

Zinzi, M., & Carnielo, E. (2017). Impact of urban temperatures on energy performance and thermal comfort in residential buildings. The case of Rome, Italy. *Energy and Buildings*, *157*, 20–29. https://doi.org/10.1016/j.enbuild.2017.05.021

TOC

3 A Quantitative Morphological Method for Mapping Local Climate Types

This chapter has been published as:
Maiullari, D., Pijpers-van Esch, M. M. E., & van Timmeren, A. (2021). A Quantitative Morphological Method for Mapping Local Climate Types. *Urban Planning*, *6*(3), 240-257. https://doi.org/10.17645/up.v6i3.4223

ABSTRACT Morphological characteristics of cities significantly influence urban heat island intensities and thermal responses to heat waves. Form attributes such as density, compactness, and vegetation cover are commonly used to analyse the impact of urban form on overheating processes. However, the use of abstract large-scale classifications hinders a full understanding of the thermal trade-off between single buildings and their immediate surrounding microclimate. Without analytical tools able to capture the complexity of cities with a high resolution, the microspatial dimension of urban climate phenomena cannot be properly addressed. Therefore, this study develops a new method for numerical identification of types, based on geometrical characteristics of buildings and climate-related form attributes of their surroundings in a 25m and 50m radius. The method, applied to the city of Rotterdam, combines quantitative descriptors of urban form, mapping GIS procedures, and clustering techniques. The resulting typo-morphological classification is assessed by modelling temperature, wind, and humidity during a hot summer period, in ENVI-met. Significant correlations are found between the morphotypes' characteristics and local climate phenomena, highlighting the differences in performative potential between the classified urban patterns. The study suggests that the method can be

used to provide insight into the systemic relations between buildings, their context, and the risk of overheating in different urban settings. Finally, the study highlights the relevance of advanced mapping and modelling tools to inform spatial planning and mitigation strategies to reduce the risk of urban overheating.

3.1 Introduction

Urban planning research and practice are increasingly called to confront climate-related challenges of cities. While extreme events like heatwaves are becoming more frequent (Founda et al., 2019; Smid et al., 2019), climate scenarios also prognose an overall increase in temperatures in the coming decades (Guerreiro et al., 2018; Hoegh-Guldberg et al., 2018). Furthermore, climate change is expected to exacerbate warming mechanisms in urban environments already characterised by urban heat island (UHI) phenomena (Ward et al., 2016). At the same time, a growing number of European cities have active policies of urban (re-)densification (Næss et al., 2020; Westerink et al., 2013). Following the well-known paradigm of compact and dense sustainable urban development (European Commission, 1991), this approach seems to mark a transition from a zoning-oriented planning to an infill-planning that looks at local conditions for re-development (Amer et al., 2017; Wolff et al., 2017), increasing the morphological heterogeneity of the urban fabric (Marique & Reiter, 2014) and giving rise to the so-called compact city paradox (Bibri et al., 2020). From a climate perspective, in fact, higher building densities generally increase the magnitude of UHI effects and overheating of cities (Oke, 1987).

Climate change and urban densification thus pose great challenges as well as opportunities for urban planning and design, with respect to developing new frameworks and strategies for the construction of climate-resilient cities (Terrin, 2015). Although it is demonstrated that urban form characteristics significantly influence thermal and turbulent processes in cities, contributing to the formation of UHI effect (Oke et al., 1991), a deeper understanding of these processes in increasingly complex and heterogeneous built environments appears to be needed, in order to characterise the overheating risk at a finer scale-level and to facilitate the implementation of mitigation measures more sensitive to the local spatial conditions.

In the last decades, the field of urban climatology has been studying the role of urban form in urban climate phenomena, attempting to broaden the understanding

of which spatial conditions exacerbate and reduce the risk of overheating (Zinzi & Santamouris, 2019). Two distinct morphological approaches can be recognised. The first has mainly been employed in parametric and comparative studies, focusing on the investigation of single form attributes (Ali-Toudert & Mayer, 2006; Morganti et al., 2017; Perini & Magliocco, 2014). However, methods to quantitatively identify representative samples of existing urban tissues are largely lacking. This results in the common practice of qualitative selection of homogeneous or generic form patterns (Toparlar et al., 2017) that limits its use to guide design and planning in existing cities. The second morphological approach employs qualitative and quantitative descriptions of form attributes and supervised classification techniques in order to identify zones with similar climate characteristics. A well-known representative of this approach is the local climate zone classification method (Stewart & Oke, 2012) that supports the identification of regions of uniform land cover, material, structure, and anthropogenic activities, defining characteristic temperature regimes for 17 standard local climate zones. The "urban climate maps" resulting from these classifications have, until now, been considered a crucial basis to inform design and planning decisions (Lenzholzer, 2015) and are based on the concept that different types of urban areas have typical thermal behaviours. However, while these methods cover district to city scale, their large aggregative units result in a rather coarse classification unable to describe the level of heterogeneity of the urban fabric.

Advancements in the field of mathematical urban morphology (D'Acci, 2019) over the last 50 years may help overcome the limitations of the approaches in urban climatology discussed above. This branch of urban form studies focuses on the understanding of spatial structures and characteristics of urban areas through an empirical and quantitative approach. In particular, the typo-morphology body of research—traditionally interested in identifying qualitative comparable physical characteristics (Vernez Moudon, 1997)—is increasingly showing applications of quantitative methods for measuring (Berghauser Pont & Haupt, 2010) and classifying urban forms (Serra et al., 2017). This recent typology-driven approach aims to overcome the use of traditional administrative units in the description of cities' physical context through morphological indicators (Serra et al., 2018), to support the application of typo-morphology to planning practice (Gil et al., 2012) and to facilitate the description of contemporary types that do not fall into standard classifications (Berghauser Pont et al., 2019).

Numerically defined typo-morphologies have been proposed in studies that have developed geo-computation methods for classifying forms of urban fabric and their basic physical elements: streets (Barthelemy, 2017), plots (Bobkova et al., 2019; Demetriou et al., 2013), buildings (Hecht et al., 2015; Perez et al., 2018), blocks (Peponis et al., 2007), and structural units (Haggag & Ayad, 2002). Particularly

relevant are the contributions of authors that have integrated geometrical multi-variables and inter-scalar descriptions of urban form (Bobkova, 2019; Hausleitner & Berghauser Pont, 2017; Serra et al., 2018) and have developed methodological strategies to identify potential links between contextual factors and other variables, generating context-informed samples of urban areas. A part of these multi-variables and inter-scalar studies has a strong focus on defining typologies to investigate the geographical distribution of types of urban fabric (Araldi & Fusco, 2019) and to allow comparisons between cities (Berghauser Pont et al., 2019).

Despite the high potential of applying a typo-morphology approach in climate-oriented studies, it nevertheless is still relatively unexplored. Thus, the aim of this article is to address the potentials of morpho-based classification systems as a complementary approach to those existing in urban climatology. In order to facilitate the understanding of how space at the microscale influences urban climate phenomena, this study proposes a data-driven morphological classification approach. This approach allows to address heterogeneous urban fabric by characterising buildings and their contextual conditions separately. In addition, it supports a better understanding of the impacts of form characteristics on patterns of thermal and aerodynamic behaviours.

This study focuses on the development of the approach and its application in the city of Rotterdam (the Netherlands). Section 2 of the article introduces the methodological framework (see Figure 3.1) to obtain and assess numerically defined typo-morphologies based on climate-related form attributes. In Section 3, the detailed methods to characterise urban form types are described and deployed in the Rotterdam case study. Section 4 presents the microclimate performance of the identified form types, modelled in ENVI-met. Finally, a comparison is carried out to analyse the variations in microclimate performance, dependent upon form characteristics of building types and context types, and conclusions are presented.

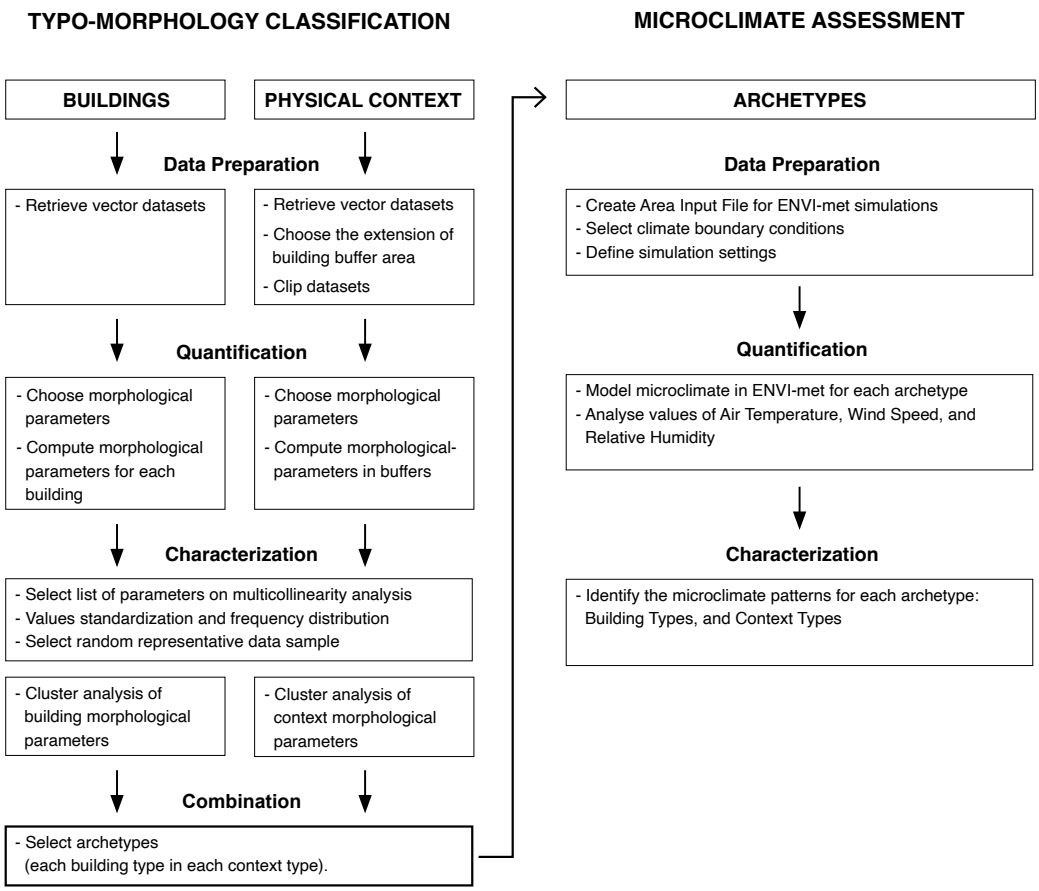


FIG. 3.1 Methodological framework.

TOC

3.2 Methodological Framework

The proposed methodological framework builds on previous studies that integrate multi-variable geometrical descriptions with inter-scalar relational descriptions of urban form. To test the application of data-driven morphological classifications in the field of urban climatology, this study carries out a performance assessment on the identified typo-morphologies, by employing microclimate modelling. The methodological framework is therefore divided in two main parts: (1) typo-morphology classification, and (2) microclimate assessment, both organised in steps of data preparation, quantification, characterisation, and linked by a step named combination.

The methodology for the typo-morphology classification follows two parallel paths to identify building types and context types. Climate-related form attributes and measuring parameters are derived from literature and computed for buildings and context areas. The latter are defined by buffer areas from the buildings' envelopes, drawn with different radii. After combined statistical analyses on the calculated parameters, an unsupervised hierarchical clustering method is employed to identify and group similar objects (buildings) and similar surrounding conditions (contexts). After evaluating the optimal number of clusters, archetypical buildings for each context type are selected for the microclimate assessment phase. This assessment is carried out through microclimate simulations in ENVI-met, a well-established urban climate model (Tsoka et al., 2018; Yang et al., 2013). Spatial vector-data of the domains under study is translated into 3D digital models and enriched with material attributes. Two hot summer days are selected as climate boundary conditions. After running the simulations, results for the selected archetypes are analysed by comparing air temperature, wind speed, and relative humidity values near building façades. Finally, microclimate patterns for the typo-morphologies and relations between building and context types are analysed.

3.2.1 Case Study Description

The methodological approach to identify and assess microclimate typo-morphologies is applied on the urban agglomeration of Rotterdam, the second largest city in the Netherlands, situated along the Nieuwe Maas river. The selection of this city allows for an analysis of the thermal performance of heterogeneous building and land cover configurations. Additionally, due to its densely built environment, Rotterdam has a significant UHI effect, as shown in previous studies (Roodenburg, 1983; Steeneveld

et al., 2011). This urban climate phenomenon has a high intensity in the inner city and varies largely among urban districts. According to van Hove et al. (2015), atmospheric UHI_{max} values in Rotterdam vary from 4.3°C to 8°C depending on local urban characteristics of different areas, while surface UHI values show a daytime magnitude of 10°C, with a maximum variation in surface temperatures between warmest and coolest districts in a range of 12°C (Klok et al., 2012).

3.3 Classification of Building and Context Types

The overall goal of this classification is to identify typo-morphologies through clustering of climate-related urban form parameters for the city of Rotterdam. Usually, in both planning research and practice, urban form parameters are measured at large predefined units (administrative or dependent upon land ownership) that are biased by a high level of aggregation (Serra et al., 2018). The proposed framework overcomes this bias by allowing for the separate identification of building and context types. This approach is expected to allow for a distinction between microclimate behaviour that depends on a building's surroundings, from that which depends on the building's own geometrical characteristics.

3.3.1 Data Preparation for Morphological Quantification

The spatial datasets used in this study were made available by the Municipality of Rotterdam, and contain information regarding buildings, street network, vegetation cover, and trees at their status in December 2018. For the building dataset, data processing was necessary to extract basic geometrical characteristics from a 3D city model. Building footprints and heights were derived from the available 3D digital model in CityGML format (Gemeente Rotterdam, 2018). The term "building" here indicates a basic unit characterised by a singular height, that can also correspond to building parts in the case of complex geometries. Regarding the context data, two extra steps of refinement were required. First, buffer areas around each building were defined, with 25 and 50m radius, calculated from the building envelope. These radii have proven adequate to observe variations in microclimate processes (Jin

et al., 2018; Takebayashi, 2017) as in these areas around the building the form characteristics of the tangent street canyons (25m) and the surrounding district structure (50m) are captured. Second, the datasets for each buffer were clipped to facilitate the computation of morphological parameters within these areas in the next phase.

3.3.2 Quantification of Morphological Attributes

In order to quantitatively describe the geometry of buildings and the form of the urban fabric, a set of eight climate-related morphological parameters was selected. The parameters chosen, based on literature, are quantitative and morphological by nature. The selection followed four main criteria; the parameters (1) describe attributes that influence the thermal behaviour of buildings and microclimate processes in their surroundings, (2) have minimal redundancy, (3) can be easily understood by planners and designers, and (4) are easily calculated.

For the building characterisation, three parameters were considered: height, footprint, and surface-to-volume ratio. Building height (B_Height) expresses the vertical dimension of a building object. From a microclimate perspective, wind speed and turbulence exponentially increase with increasing B_Height, while air temperature tends to decrease further from the ground. Building footprint (B_Footprint) describes the horizontal occupation of the buildings at the ground. The size of the footprint correlates with potential solar accessibility. Surface-to-volume ratio (B_StoV) measures the proportion between the exposed building envelope and its volume. The larger the value of B_StoV, the lower the compactness level. From a climate design perspective this parameter captures radiation accessibility and ventilation potential, mediated by the interface between outdoor and indoor environments (Vartholomaios, 2017).

In addition, five variables were used to measure urban fabric attributes of roughness, density, and green coverage, describing the morphological characteristics of the buildings' context. Mean building height (MeanH) is a primary descriptor of roughness. The roughness of the urban surface defines the friction capacity of the built environment to aerodynamic processes (Grimmond & Oke, 1999). MeanH identifies the average height of the context in a buffer of 50m radius. Floor space index (FSI) and ground space index (GSI; Berghauser Pont & Haupt, 2010) are two of the most known density indicators that describe the intensity of built space and building coverage, influencing the magnitude of overheating (Zhao et al., 2016) and solar irradiance (Morganti et al., 2017). FSI is defined as the ratio

of the gross floor area to the overall site surface, which is calculated in the larger buffer area to describe the level of fabric compactness around a building. GSI is calculated as the ratio of buildings' footprint to the overall site surface. In this study, GSI (calculated in a 25m radius buffer) is used to intercept the closeness of buildings in the immediate surrounding. Vegetation cover affects microclimate in urban environments, by influencing air temperatures through shading and evapotranspiration, and by modifying wind velocity (Duarte et al., 2015; Perini & Magliocco, 2014). Two parameters are chosen to measure greenery characteristics. Green area (GArea) measures the total green coverage of grass surfaces in the larger buffer area (50m), while tree area (TArea) measures the sum of tree crown area in the smaller buffer area (25m). The list of morphological parameters used to describe building and context form is shown in Table 3.1. The eight variables deployed were computed for over 150,000 buildings and related buffer areas through the QGIS programme.

TABLE 3.1 Summary of the selected morphological parameters.

Categories	Unit	Parameter/ Variable	Description	Sources
Building	Building parts	B_Height (m)	Measure of the B_Height	Godoy-Shimizu et al., 2018; Jurelionis & Bouris, 2016; Mangan et al., 2021; Saroglou et al., 2017; Yunhao Chen et al., 2020
		B_Footprint (m2)	Area of the B_Footprint	Allen-Dumas et al., 2020; Hecht et al., 2015; Mavrogianni et al., 2012; Yixing Chen et al., 2019
		B_StoV (m2/ m3)	Building envelope to volume ratio	Bourdic et al., 2012; Caldera et al., 2008; Mashhoodi et al., 2020; Ratti et al., 2005; Salat, 2009
Context	Buffer 25m radius	GSI	GSI	Jin et al., 2018; Lan & Zhan, 2017; Morganti et al., 2017; Salvati et al., 2019
		TArea (m2)	Tree crown area in buffer	Kong et al., 2017; Rafiee et al., 2016; Rui et al., 2018
	Buffer 50m radius	FSI	FSI	Lan & Zhan, 2017; Rodríguez-Álvarez, 2016; Wang et al., 2017; Wei et al., 2016
		MeanH (m2)	Average B_ Height in buffer	Salvati et al., 2020; Touchaei & Wang, 2015; Wang et al., 2017
		GArea (m2)	Total grass coverage area in buffer	Kong et al., 2016; Lobaccaro & Acero, 2015; Skelhorn et al., 2014; Vaz Monteiro et al., 2016; Wu et al., 2019

3.3.3 Urban Form Characterisation

All calculated morphological variables were standardised as z-scores in order to have similar scales. Since multi-collinearity should be avoided for unsupervised classification (Tan et al., 2005), a screening was performed to detect potential collinearity, confirming that the selected eight variables were not correlated.

In order to classify building and context characteristics a hierarchical cluster analysis was used. The hierarchical cluster analysis is an unsupervised classification method that groups data into homogeneous classes by proceeding stages. Beginning by defining each observation as a cluster, clusters get incrementally paired based on the minimum distance between them, until the merging of all values results in a single cluster. Although k-mean clustering has a stronger applicability to large datasets, the explorative character of the study required a certain degree of flexibility. From this perspective, hierarchical clustering would allow for the identification of the hierarchical relation between classes and provide the possibility to read the microclimate assessment results at different cutting levels of the dendrogram. Thus, to allow the applicability of a hierarchical cluster analysis despite computational restrictions, a representative 20% sample of the full data population was selected. A Kolmogorov-Smirnov test verified that the sample was statistically significant and preserved the same probability distribution of the full dataset.

The three building and five context variables calculated for the 21,047 features of the sample were separately processed using a hierarchical cluster analysis with application of Ward's minimum variance method. To select the optimal number of clusters, the resulting dendrograms for the building classification and context classification were analysed (Figure 3.2). The cutting level was selected where the linking vertical lines are long(est) and the smallest number of clusters distinguishes sufficient differences among the groups. Thus, for both building and context variables, the optimal division is a five-cluster solution. Plotting the parameter values per cluster and a visual inspection of the cluster-centroids confirmed clear differences between the five building types, as well as between the five context types.

3.3.3.1 Description of the Building and Context Types

The combination of the selected morphological characteristics produced consistent typo-morphologies. The plotting and numeric profiling of the building and context types is shown in Figure 3.3. Building types identified through clustering of B_Height, B_Footprint, and B_StoV parameters can be described based on Figure 3.4.

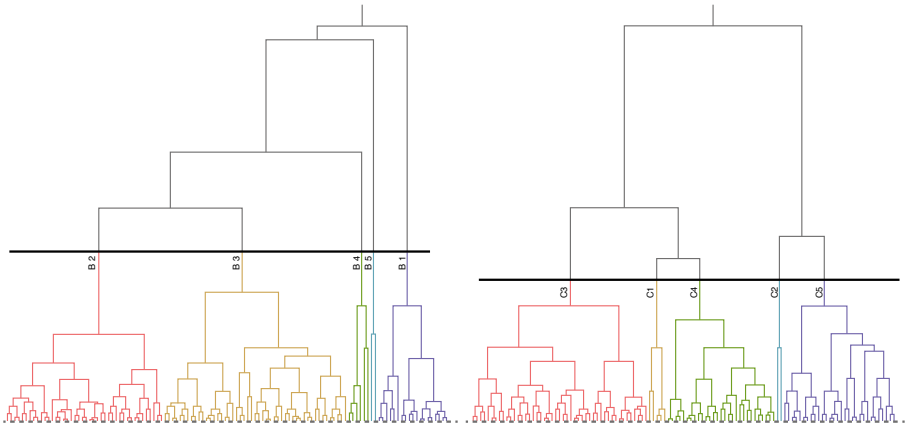


FIG. 3.2 Hierarchical classification results: Building types (left) and Context types (right).

B_Type1 and B_Type3 are low-rise buildings with a very small B_Footprint. The main difference between them is the level of compactness. Buildings of type 1 have a low compactness level (high StoV ratio), while buildings of type 3 have a high compactness level (low StoV ratio). These types predominately comprise of single houses, rowhouses, and small building parts. B_Type2 and B_Type5 consist of highly compact mid-rise buildings (low StoV). The discriminant between the two groups is the ground coverage size. While buildings in type 2 are characterised by small footprints (slabs, apartment buildings), in type 5 the B_Footprints are the largest, comprising of public facilities and industrial/commercial objects with a horizontal volume distribution. B_Type4 is composed of high-rise buildings with a medium size footprint and a high level of compactness (low StoV ratio). Towers and tall building parts on plinths belong to this group.

Context types emerged from the clustering analysis of GSI and TArea (25m buffer), and FSI, MeanH, and GArea (50m buffer). According to Figures 3 and 4, the types can be described as follows. C_Type1 consists mainly of low and mid-rise urban fabrics, with low density characteristics (low GSI and FSI). The main defining characteristic is the very large tree crown area and the medium level of grass coverage. This type of context tissue shows the ample presence of trees mainly located along street canyons. C_Type2 is characterised by mid-rise buildings, and medium density in terms of building coverage (GSI) and built-up intensity (FSI). The type has low values of grass and tree coverage area. C_Type3 and C_Type4 are urban tissues both defined by low-rise buildings and low density. The main difference between the two types is the quantity of grass surfaces, which is very low in type 3 and medium in type 4. Finally, C_Type5 can be described by highly compact conditions of the urban fabric, characterised by high-rise, high building intensity, and building coverage. In this context type, greenery level (TArea, GArea) is low.

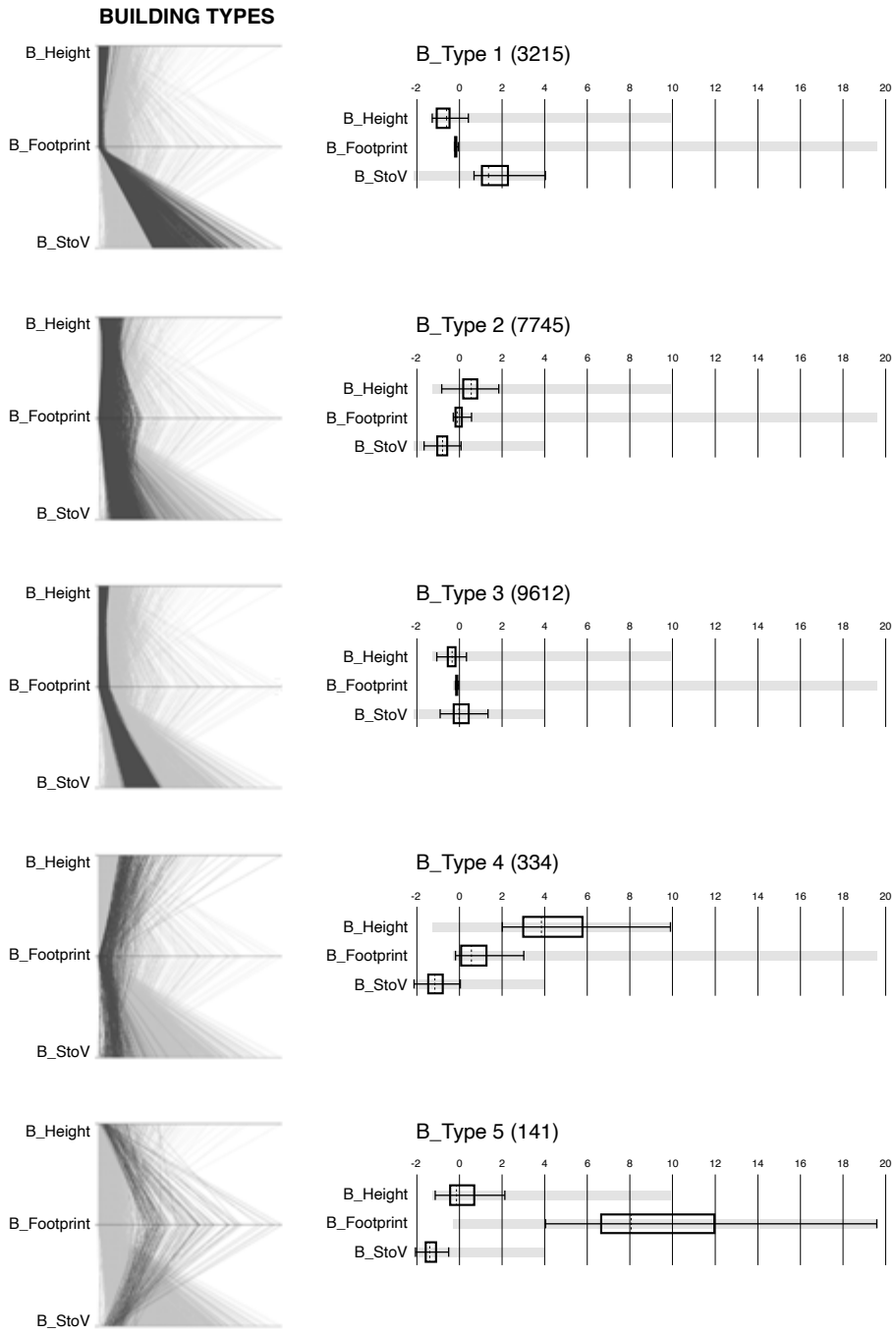
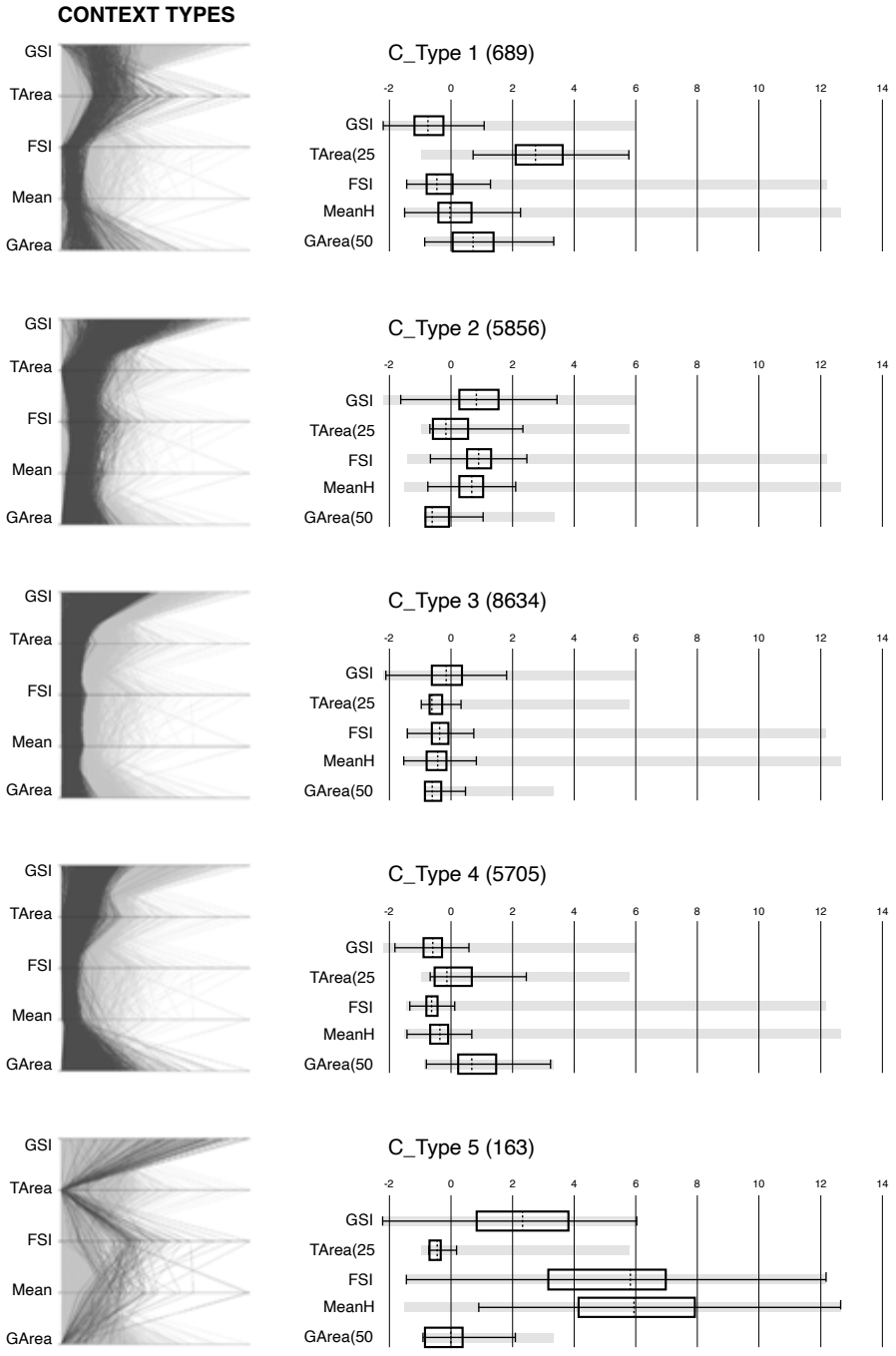


FIG. 3.3 Standardized (z-score) numerical profiles of the building types (left) and context types (right).

TOC


CONTEXT TYPES
GSI
TArea
FSI
Mean
GArea
C_Type 1 (689)
C_Type 2 (5856)
C_Type 3 (8634)
C_Type 4 (5705)
C_Type 5 (163)
-2
0
2
4
6
8
10
12
14
GSI
TArea(25
FSI
MeanH
GArea(50

TOC

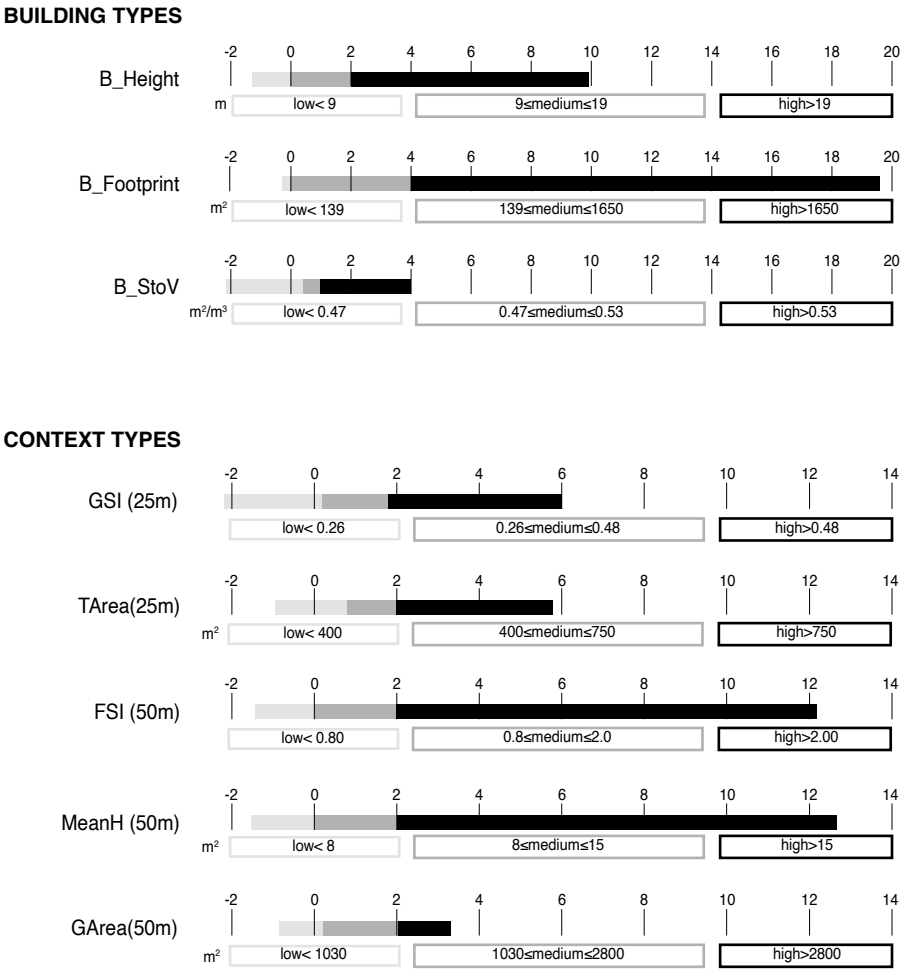


FIG. 3.4 Numerical thresholds for the description of the building types (left) and context types (right).

TOC

3.3.4 Archetype Selection

Once building types and context types were characterised and semantically described, 25 “archetypes” were selected to analyse the microclimate profile of the five building types in the five context conditions. Usually, the archetype is defined as the case that is closer to the cluster’s centroid. Therefore, five cases were selected close to the cluster’s centroid for each building type, one case for each context type (Figure 3.5).

3.4 Microclimate Assessment

Microclimate simulations of the 25 archetypes were performed with ENVI-met 4.4. ENVI-met is a three-dimensional prognostic model able to simulate the interaction between air, vegetation, and surfaces within an urban environment (Bruse & Fleer, 1998). This holistic microclimate modelling tool is widely used to compute air and surface temperatures, turbulence, radiation fluxes, humidity, and evaporation fluxes (Tsoka et al., 2018). Validation studies have confirmed its high level of accuracy in modelling microclimate processes in urban conditions (Crank et al., 2018; Salata et al., 2016), and a high sensitivity to morphological characteristics of the built environment (Forouzandeh, 2018).

3.4.1 Data Preparation for Microclimate Modelling

To perform an ENVI-met simulation three types of input are required:

1. Digital spatial model: In the area input files, the model domains were created using a grid cell unit of 3m (x) by 3m (y) by 3m (z). In these domains, the 3D models were built using the Rotterdam dataset in shape format through the ENVI-met submodule Monde. To be able to isolate the microclimate impact of morphological factors, material characteristics were kept constant in all 25 models.

2. Material database: Three surface materials (asphalt for roads, concrete bricks for other paved surfaces, and grass for unpaved areas) were derived from ENVI-met default database, and a fourth—a theoretical building wall with medium insulation properties—was created in the user database. Additionally, based on height and crown diameter, trees were classified into three categories (small, medium, large).

	BUILDING TYPE 1 Low B_Height Low B_Footprint High B_StoV	BUILDING TYPE 2 Medium B_Height Low B_Footprint Low B_StoV
CONTEXT TYPE 1 Low-Medium MeanH Low GSI Low FSI High TArea Medium GArea	B1C1 51°56'45.9"N 4°33'49.2"E	B2C1 51°57'39.9"N 4°34'03.3"E
CONTEXT TYPE 2 Medium MeanH Medium GSI Medium FSI Low TArea Low GArea	B1C2 51°54'34.9"N 4°26'43.8"E	B2C2 51°55'56.3"N 4°25'40.9"E
CONTEXT TYPE 3 Low MeanH Low GSI Low FSI Low TArea Low GArea	B1C3 51°57'14.8"N 4°29'22.2"E	B2C3 51°53'57.5"N 4°30'22.9"E
CONTEXT TYPE 4 Low MeanH Low GSI Low FSI Low TArea Medium GArea	B1C4 51°52'15.8"N 4°31'51.9"E	B2C4 51°53'54.5"N 4°34'00.3"E
CONTEXT TYPE 5 High MeanH Medium-High GSI High FSI Low TArea Low GArea	B1C5 51°53'04.8"N 4°33'10.1"E	B2C5 51°54'21.5"N 4°29'44.1"E

FIG. 3.5 Visualization of the building archetypes in the five context types.

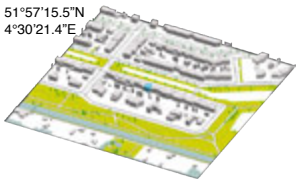
TOC

BUILDING TYPE 3

Low B_Height
Low B_Footprint
Low B_StoV

B3C1

51°57'15.5"N
4°30'21.4"E



B3C2

51°56'42.4"N
4°33'36.5"E



B3C3

51°57'20.2"N
4°31'12.7"E



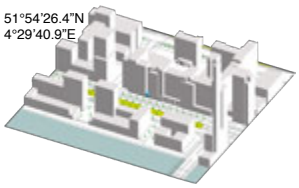
B3C4

51°53'36.8"N
4°32'57.8"E



B3C5

51°54'26.4"N
4°29'40.9"E

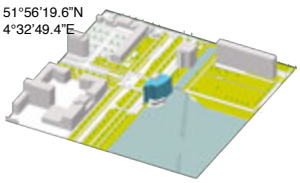


BUILDING TYPE 4

High B_Height
Medium B_Footprint
Low B_StoV

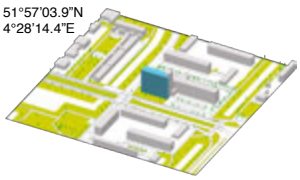
B4C1

51°56'19.6"N
4°32'49.4"E



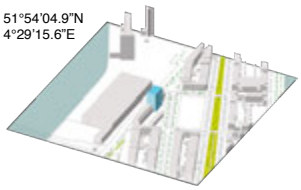
B4C2

51°57'03.9"N
4°28'14.4"E



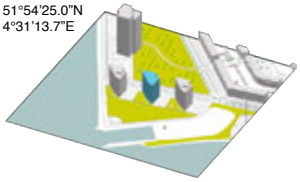
B4C3

51°54'04.9"N
4°29'15.6"E



B4C4

51°54'25.0"N
4°31'13.7"E



B4C5

51°54'05.9"N
4°29'44.0"E

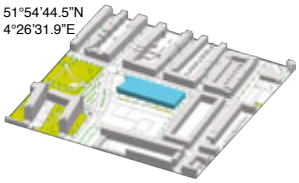


BUILDING TYPE 5

Medium B_Height
High B_Footprint
Low B_StoV

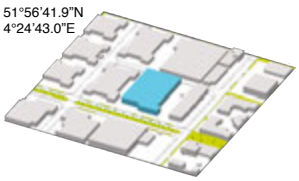
B5C1

51°54'44.5"N
4°26'31.9"E



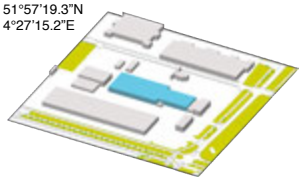
B5C2

51°56'41.9"N
4°24'43.0"E



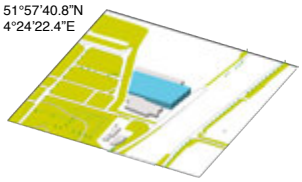
B5C3

51°57'19.3"N
4°27'15.2"E



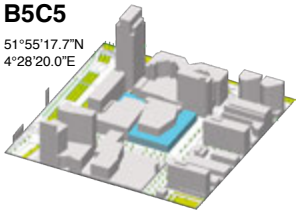
B5C4

51°57'40.8"N
4°24'22.4"E



B5C5

51°55'17.7"N
4°28'20.0"E



3 Simulation settings: ENVI-met simulations used the full forcing method, by employing KNMI data from the weather station at Rotterdam Airport. After analysing the measured data of the past 10 years, two consecutive hot days (Tmax > 24°C) were selected by filtering out days with clouds and rain. The two days identified therefore meet the required conditions for microclimate simulations. The first day (29 June 2018), a maximum air temperature of 25°C was reached, while on the second day (30 June 2018), it reached up to 28°C.

Before performing the simulations for the different archetypes a validation procedure was carried out. The existing urban areas around the urban weather stations of Delfshaven and Ommoord in Rotterdam were modelled with the material and meteorological settings described above. The ENVI-met spatial models of these two areas were built including the 50m buffer area around the building on which the sensors are positioned, in other words, with a domain size defined as for the archetypes. The comparison between model results and measured temperature values (TU Delft, 2018) showed an index of agreement (Willmott, 1983) of 0.98, confirming the good accuracy of ENVI-met and the reliability of the input data.

3.4.2 Microclimate Quantification Results and Discussions

The cumulative microclimate performance of the Rotterdam cases was analysed by comparing the rural climate conditions to the simulation results (Figure 3.6). Air temperature, wind speed and relative humidity values were retrieved in the air layer near the façades. Values were averaged for each building archetype. The comparison between simulated air temperatures and measured data at the rural KNMI weather station shows a clear UHI effect, in particular during daytime, for both days. The 25 simulated areas are generally warmer than the rural environment with an average maximum UHI effect of 1.1°C. The maximum UHI effect occurs between 12:00 and 15:00, and ranges between 0.5°C (B4C5) and 3°C (B1C4 and B3C2). The nocturnal UHI shows a smaller magnitude, reaching up to a maximum effect of 0.5°C.

Another clear effect is the decrease in wind speed. During the two days under study, wind velocity at the rural station reached 6m/s during daytime, with a significant drop during night-time. Compared to the rural hinterland conditions, the modelling results show that the overall urban wind velocity decreases strongly, down to 1m/s on average.

Relative humidity values, plotted in Figure 3.6, illustrate that during night-hours, humidity values reach a RH of 95% while during day-hours it drops below 30% for the second hot day. Compared to the values at the rural weather station, the humidity values in the urban samples from Rotterdam decrease within a maximum of 7%, which is consistent with observations in other studies (Ackerman, 1987; Liu et al., 2009). During daytime, the RH in the city is lower than in the rural hinterland, which can be correlated to the occurrence of the UHI effect.

This analysis of the simulation results also highlights the magnitude of microclimate variations for the Rotterdam sample of 25 archetypes. Since materials and settings were kept constant in the modelling process, it could be argued that the microclimate variations analysed are mainly dependent on morphological characteristics.
The observed maximum differences in air temperature, humidity, and wind among the 25 cases suggest that building geometry and urban form of the context account for up to 2.5°C change in air temperature, up to 3m/s change in wind speed, and up to 5% change in relative humidity.

As stated, the models' results indicate that, during the two days under study, the UHI intensity reaches 3°C. However, previous studies have found stronger magnitudes (between 2.3 and 8.0°C) during day- and especially night-time in Rotterdam (Steeneveld et al., 2011; van Hove et al., 2015). These studies are based on field measurements, and therefore also include anthropogenic heat and its contribution to the energy balance; ENVI-met does not. As it was the objective of this study to assess the impact of solely morphology on UHI, the omission of anthropogenic heat is justified, but is expected to lead to an underestimation of the UHI effect. Furthermore, for the same reason of isolating morphological effects, the 25 models in this study had greatly simplified building and paving material characteristics, which may also have influenced the magnitude of the modelled UHI.

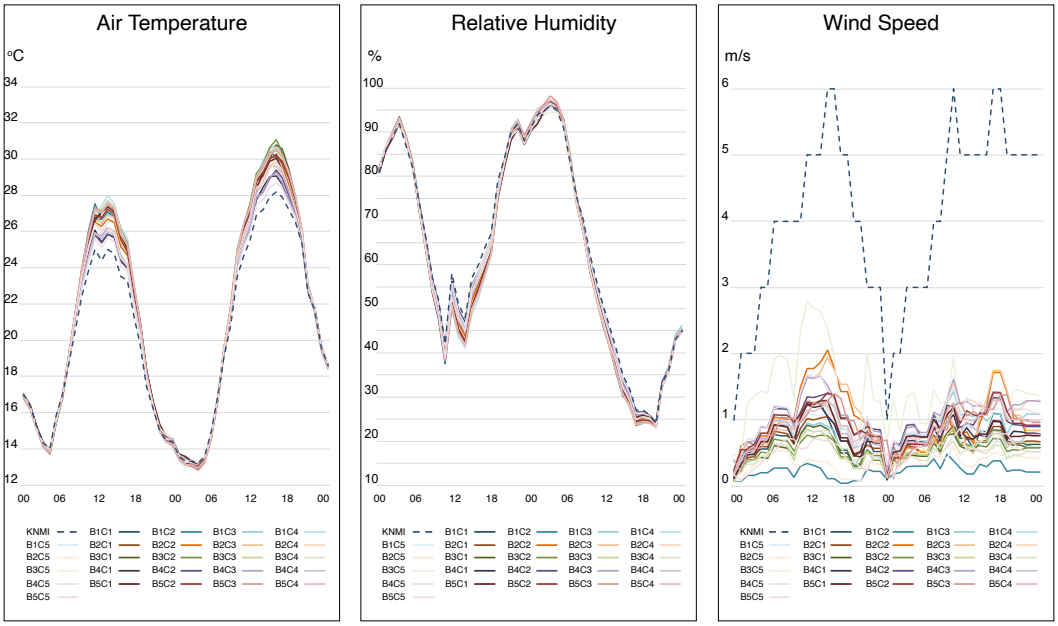


FIG. 3.6 Building average air temperature (left), relative humidity (centre), and wind speed (right) near façade.

3.4.3 Characterization of Microclimate Patterns in Types

In order to understand if the typo-morphologies have typical thermal and aerodynamic behaviour, climate patterns are analysed for each building and context type. Furthermore, the overall capability of the data-driven classification in identifying common climate conditions based on morphological characteristics is assessed. Simulation results are retrieved for indoor air temperature as well as outdoor air temperature and wind speed near the façade and averaged for each building.

TOC

3.4.3.1 Indoor Temperature Patterns for the Different Building Types

The analysis of indoor temperatures highlights common behaviour for the different building types (Figure 3.7). In particular, low-rise buildings (B Type 1 and 3) demonstrate a larger sensitivity to the influence of context. Low rise buildings in high-rise contexts (B1C5 and B3C5) yield the lowest indoor temperature among the 25 cases, due to reduced solar access at the façade. Except for these two "outliers," the cases representing each building type show similar thermal patterns. Therefore, each type can be described by the characteristic variation range between its five cases and the maximum temperature.

As shown in Table 3.2, B_Type4 has the lowest temperature variation among its cases, followed by B_Type3, 5, and 1. The highest variation is registered among B_Type2 cases. The similar behaviour among cases belonging to the same building type indicates that the context has a limited effect on the indoor temperature: The smaller the variation among cases, the lower the sensitivity of the building type to the context. Thus, high-rise buildings are the least affected by the surrounding conditions, while mid-rise buildings with low coverage are most influenced by their context.

T_{max} is higher in B_Type1 than in B_Type2, 5, and 3. High-rise buildings (B_Type4) consistently yield cooler indoor thermal conditions than the other building types. This is due to the lower contribution of radiation to the total thermal budget of the building due to the higher volumetric size, the higher exposure to cooling wind flows, and the fact that outdoor air temperatures tend to be lower when further away from the ground level.

TABLE 3.2 Patterns of indoor temperatures per building type.

Indoor Temperature	B_Type1	B_Type2	B_Type3	B_Type4	B_Type5
Variation among cases	1°C (B1C1–B1C4)	1.3°C	0.4 °C (B3C1–B3C4)	0.2°C	0.6°C
Maximum temperature	25.2°C (B1C1–B1C4)	24.6°C	24.8°C (B3C1–B3C4)	23.2°C	24.6°C
Outliers	B1C5		B3C5		

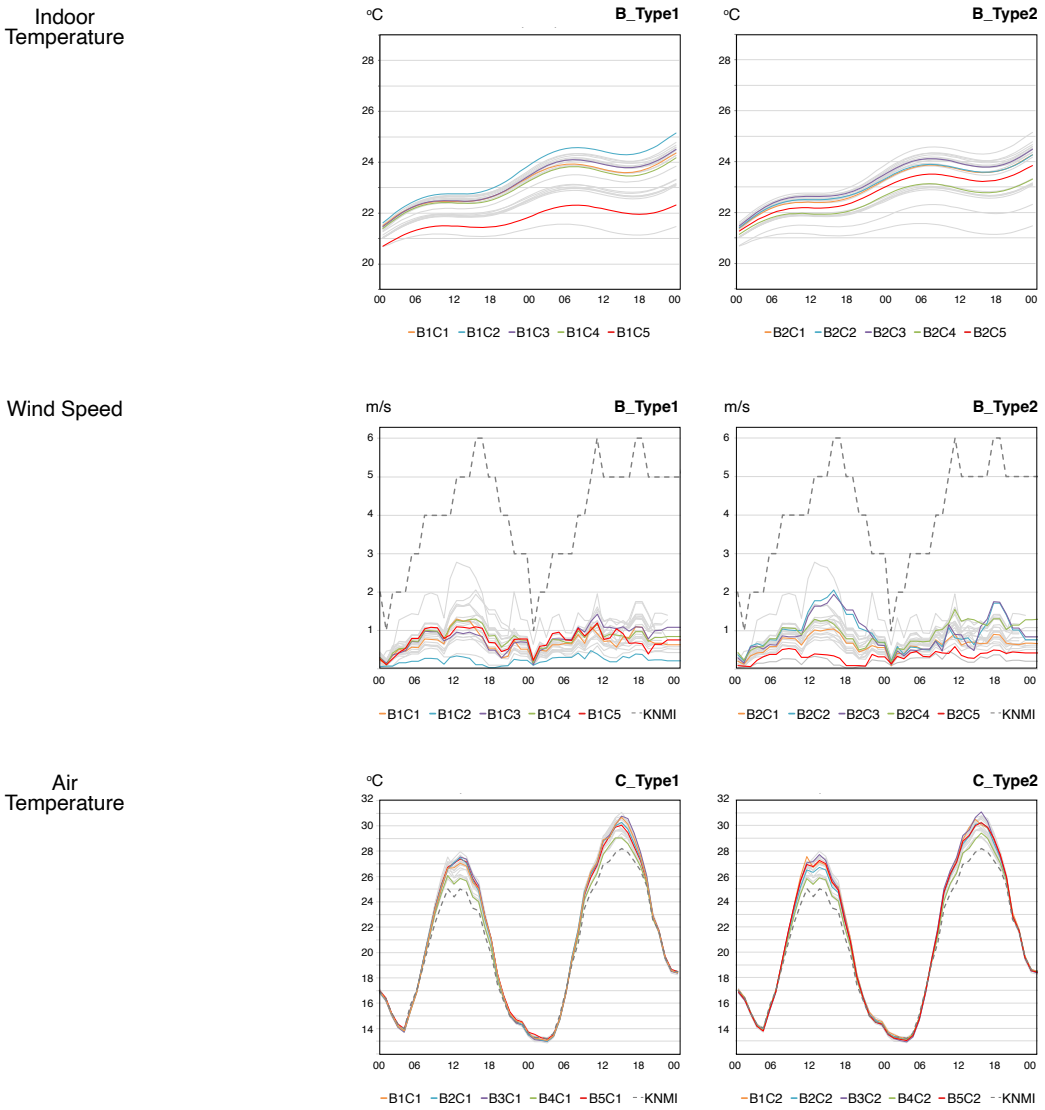
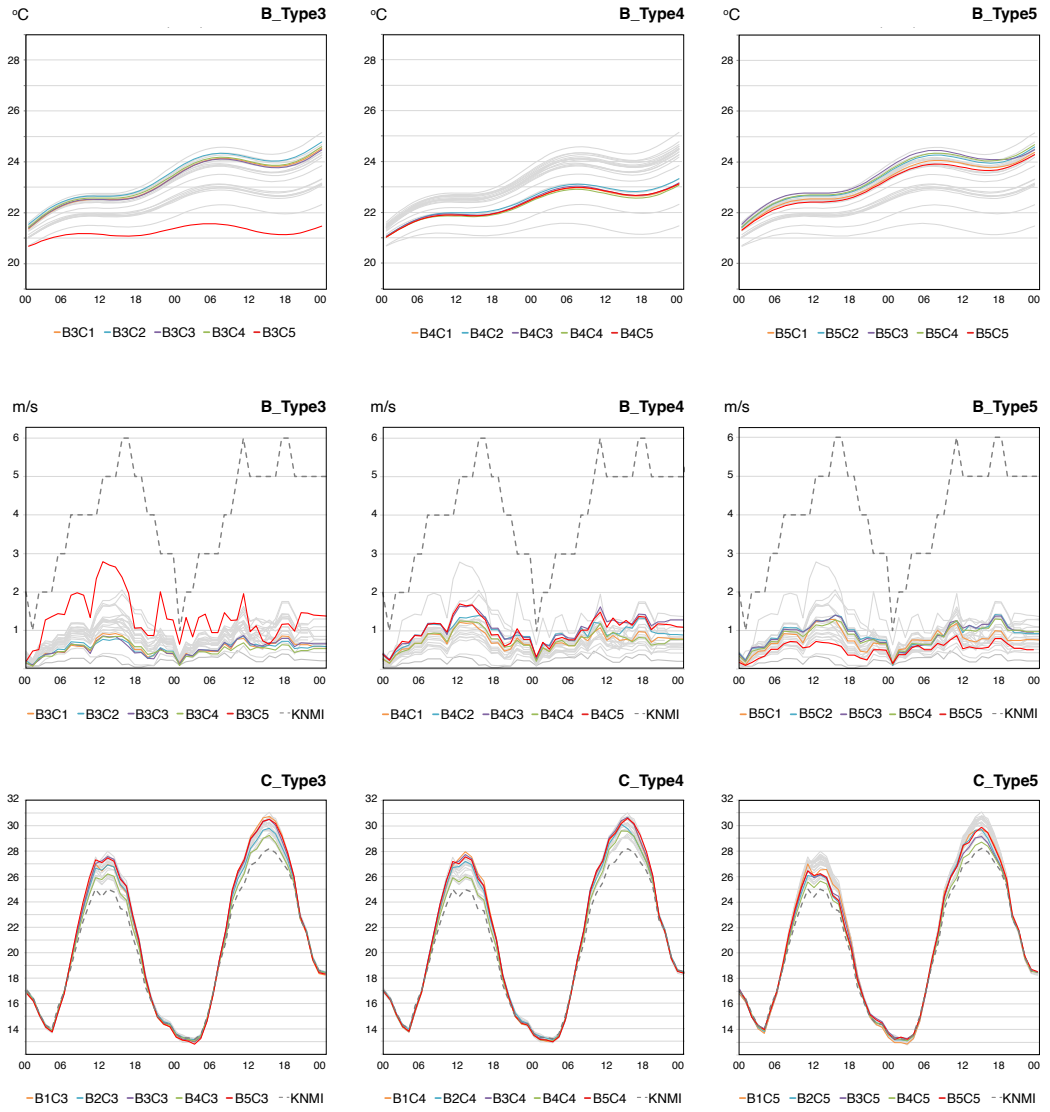


FIG. 3.7 Indoor temperature values and wind speed values for each building type; outdoor air temperature values for each context type.

TOC


°C
B_Type3
B3C1 B3C2 B3C3 B3C4 B3C5
°C
B_Type4
B4C1 B4C2 B4C3 B4C4 B4C5
°C
B_Type5
B5C1 B5C2 B5C3 B5C4 B5C5
m/s
B_Type3
B3C1 B3C2 B3C3 B3C4 B3C5 KNMI
m/s
B_Type4
B4C1 B4C2 B4C3 B4C4 B4C5 KNMI
m/s
B_Type5
B5C1 B5C2 B5C3 B5C4 B5C5 KNMI
C_Type3
B1C3 B2C3 B3C3 B4C3 B5C3 KNMI
C_Type4
B1C4 B2C4 B3C4 B4C4 B5C4 KNMI
C_Type5
B1C5 B2C5 B3C5 B4C5 B5C5 KNMI

TOC

3.4.3.2 Wind Speed Patterns for the Different Building Types

Wind velocity regulates heat dispersion from built surfaces and is strongly influenced by individual buildings and the roughness of their surroundings. As shown in Figure 3.7, the five cases of each building type experience similar wind speed behaviour near the façades. However, some exceptions can be observed for buildings in medium and highly dense contexts (B1C2, B3C5, and B5C5), which according to the size of the surrounding street canyon have very high or very low wind speed values.

All B_Type3, except for B3C5, show the lowest values of wind velocity (Table 3.3), with U_{max} below 0.8m/s and a limited maximum variation among context types (0.3 m/s). It is followed by B_Type1 (except B1C2) and B_Type 5 (except B5C5), which have a medium wind velocity near the façade (reaching an U_{max} of 1.4 m/s). The variation among cases accounts for 0.5m/s. B_Type4 is the building type that shows higher values of wind speed (U_{max} = 1.75 m/s), with a slightly higher interval among cases (0.6m/s). B_Type 2 shows quite different characteristics, as a clear pattern could not be identified. The latter type is characterised by medium height and a small footprint area and seems to be more sensitive to the size and predominant direction of the street canyons in the immediate surroundings.

TABLE 3.3 Patterns of wind speed per building type.

Wind Speed	B_Type1	B_Type2	B_Type3	B_Type4	B_Type5
Variation among cases	0.5m/s (B1C1–C3–C4–C5)	1.5m/s	0.3m/s (B3C1–B3C4)	0.6m/s	0.5m/s (B5C1–B5C4)
Maximum speed	1.4m/s	2m/s	0.8m/s	1.75m/s	1.4m/s
Outliers	B1C2		B3C5		B5C5

3.4.3.3 Air Temperature Patterns for Different Context Types

In Figure 3.7, hourly values of the five cases per context type are plotted. Data clearly show that, independently of the context, temperatures are always the lowest around high-rise buildings (B_Type4). Inversely, the other four building types all together respond in a similar way to the context conditions.

In group C_Type1, C_Type3, and C_Type4, having a low level of built-up intensity (FSI) and coverage (GSI) in common, but differing in grass and tree coverage area, T_{max} values are similar, ranging from 29.8°C to 30.6°C, the second day. T_{max} variation among cases accounts for a 0.8°C (Table 3.4). The results suggest that at the microscale, vegetation has a minor effect on heat mitigation in contexts of low building density.

In C_Type2, characterised by a mid-rise context at medium density, high air temperatures and overall larger variations are observed. The fact that more variation exists among buildings in this context indicates a stronger trade-off between building geometry and mid-rise context at medium density. This can be explained by the fact that shading caused by the surroundings increases with the incline of height and compactness. Moreover, the influence of shading from the same context has a bigger impact on low-rise buildings than on higher ones. C_Type5 is the context with the most evident influence pattern on air temperatures. The high-density and high-rise characteristics that define this context type contribute to keeping daytime temperature for all the building types below 30°C on the second day. Compared to the other contexts, here air temperatures are the lowest during daytime hours and the highest during night-time hours.

The very similar behaviours of C_Type1, 3, and 4 suggest that while the three types characterise different urban fabric conditions, from a climatic perspective they correspond to similar temperature patterns. Observing the dendrogram (Figure 3.2) and the hierarchical relations between types, it can be noted that these three groups merge at the upper level in one type.

TABLE 3.4 Patterns of outdoor air temperature per context type.

Air Temperature	C_Type1	C_Type2	C_Type3	C_Type4	C_Type5
Variation among cases	0.8 (B1C1–C2–C3–C5)	1 (B2C1–C2–C3–C5)	0.8 (B3C1–C2–C3–C5)	0.8 (B4C1–C2–C3–C5)	0.8 (B5C1–C2–C3–C5)
Maximum temperature	30.8	31.1	30.7	30.8	29.9
Outliers	B1C4	B2C4	B3C4	B4C4	B5C4

3.5 Limitations

As shown in this study, data-driven classifications offer a novel methodological approach in urban climatological mapping, able to address the complexity and heterogeneity of urban environments. The characterisation of types and microclimate assessment carried out in this study are subject to several limitations.

For the types' characterisation, climate-related morphological parameters were derived from literature. These well-established parameters describe attributes of size and compactness for single buildings, and density, roughness, and green coverage for urban fabrics. However, a more extensive list of parameters can be found in literature. Among others, characteristics of building orientation, window-to-wall ratio, sky view factor, fabric porosity, and water coverage have shown to influence thermal and aerodynamic processes. Despite the undeniable benefits of enlarging the number of variables to better characterise the types, this would result in an exponential increase of data pre-processing and multidimensional clustering computation. Therefore, the authors have chosen the parameters most relevant for the method and case study at hand.

Regarding microclimate modelling, although the heat produced by anthropogenic activities (mobility, space heating and cooling, industry) is an important component in the energy balance of urban environments, ENVI-met is not able to model the thermal contribution of these activities. Additionally, in the modelling of the archetypes, material of buildings and street surfaces are assumed to have similar characteristics for all 25 cases. Even though ENVI-met allows to define individual surface characteristics, since the study has the goal of isolating the microclimate impacts of morphological factors, all other modelling inputs—including material properties—were kept constant. In order to limit the influence of this simplification on the results, in particular for buildings, a theoretical façade and roof material was created to represent average characteristics of absorption, reflection, and insulation capacity in the context. Windows were not included, therewith also limiting indoor heating due to incoming solar radiation. Finally, due to the computational limitations of the microclimatic model, simulations for an entire summer period were not possible. Instead, two consecutive days were selected as representative of a typical hot Dutch summer day without clouds.

3.6 Conclusions

Using a novel methodological approach for a data-driven classification of local climate typo-morphologies, a characterisation of five building types and five context types were defined for the Dutch case of the city of Rotterdam. The microclimate simulations carried out in ENVI-met for the resulting 25 combined archetypes showed that the identified types are able to describe a wide range of microclimate characteristics. The overall variations in air temperature, humidity, and wind for the 25 cases suggest that the morphological characteristics considered account for up to 2.5°C change in air temperature, up to 3m/s change in wind speed, and up to 5% change in relative humidity. Among all types, high-rise buildings (B_Type4) and high-density contexts (C_Type5) provide, respectively, the lowest indoor and outdoor temperatures during the days under study, showing the ability to mitigate the overheating process during the daytime in particular.

In addition, the analysis of climate patterns has confirmed similar behaviour among the cases representing each building type. The building type classification well represents patterns of indoor temperatures and wind velocities near façades. High-rise buildings (B_Type4) are characterised by the lowest indoor temperatures, while low-compact low-rise buildings (B_Type1) reach the highest indoor temperatures.

The analysis also highlights that some building types are more (or less) sensitive to the surrounding conditions than others. Due to different context conditions, mid-rise buildings with smaller footprint area (B_Type2) show large wind speed variations near the façade and probably as a consequence larger indoor temperature variation.

Regarding the context classification, no evident relation was found between context types and climate patterns within the groups. However, the flexibility granted by the clustering method allowed for a reading of microclimate patterns based on the hierarchical relations between groups. Two distinctive thermal patterns for medium (C_Type2) and high-density contexts (C_Type5) were found. However, very similar temperatures were observed in the three context types characterised by low building intensity and low building coverage (C_Type 1,3, and 4). Here, the use of the hierarchical clustering method showed that these three types are combined at a higher aggregation level in the dendrogram scheme. Therefore, it can be concluded that three types are enough to describe the morphological configurations of the context in relation to thermal behaviour.

The framework has allowed the authors to identify and climatically characterise building and context types in a Dutch case study. The application of the methodology in other geographical regions—or even other Dutch cities—might result in different morphological types and microclimate responses. Moreover, even if similar buildings and context types to the ones identified in Rotterdam would be found, the response of microclimate patterns and the intensity of UHI would likely change according to the meso-scale climate zone of the analysed city. Ultimately, the scope of the study is not to identify types that are present worldwide, but to offer an approach able to acknowledge the climate performance in conditions of spatial heterogeneity. The method proposed, when applied to other climate and spatial contexts, will contribute to the characterisation of local climate types, by recalling the concept of "locus" with its geographical, cultural, and atmospheric significance.

In the development of climate action plans, where tools are necessary to support the implementation of guidelines and climate adaptive interventions, this approach has the potential of supporting the understanding of the local spatial conditions that increase the risk of urban overheating. In the Netherlands, for example, national policy urged all local governments to perform such a risk assessment ("stress-test") and to formulate an implementation plan for climate adaptive measures before 2021 (National Delta Programme, 2015). However, currently, only 10% of the municipalities have set such an agenda for heat (National Delta Programme, 2021), indicating that local governments struggle to formulate appropriate measures. This is partly due to the fact that the existing infrastructure, urban fabric, and buildings limit the number of possible solutions and that there is a high variability of temperatures and related problems within the city (Albers et al., 2015). The identification of "archetypes" in each urban context can facilitate the planning of local, yet structural adaptation measures. For instance, in both new and existing urban developments, planners can regulate building type characteristics, being informed on the microclimatic trade-off that the existing context is likely going to create; and define the urgency of interventions based on the patterns of outdoor and indoor temperatures of types. Moreover, the result of this study has the potential to inform designers in integrating mitigation measures in existing contexts. In fact, the morphological characteristics of the types facilitate the understanding of the starting conditions and space availability on which designers are going to operate (for example, open and green space available, compactness of the urban fabric, etc.).

Although the present approach is generally intended to support local governments in heat risk management, the conceptual instrument of climate types and the methodology presented for their definition is expected to facilitate the interaction between spatial, institutional, and technological components in a broader vision of smart sociotechnical governance (Jiang et al., 2020). From a technological

perspective this approach supports the analysis of local climate phenomena, as well as the communication of complex climate mechanisms through the use of visually and semantically explained types. Such an approach is expected to facilitate a deeper understanding of climate change challenges in urban transformation processes and constitute a common base for the elaboration of innovative strategies and novel modes of governance. In this direction, the separate identification of building types and context types can support a more targeted identification of roles and responsibilities in heat risk management, helping the collaboration between private and public actors to increase the mitigative and adaptive capacity of local communities. Additionally, from a spatial perspective, the specificity of neighbourhoods and cities inherent in the method offers a framework on which communities can elaborate the integration of other pressing social, economic and environmental needs related to sustainability goals. However, the use of such an approach in transformation processes requires testing in real life settings. Additionally, the application of a microscale typological classification needs to be further explored, in combination with a meso-scale classification, to assess its potential in informing the implementation of mitigation and adaptation measures, more attuned to the specific location and configuration of the urban fabric. Moreover, supplementary studies are necessary to explore the influence of other climate-related parameters such as surface water cover, building materials and orientation, and to further validate and assess this approach by measurements.

References

Ackerman, B. (1987). Climatology of Chicago area urban-rural differences in humidity. *Journal of Applied Meteorology and Climatology*, *26*(3), 427-430. https://doi.org/10.1175/1520-0450(1987)026<0427:COCAUR>2.0.CO;2

Albers, R. A. W., Bosch, P. R., Blocken, B., van den Dobbelsteen, A. A. J. F., van Hove, L. W. A., Spit, T. J. M., van de Ven, F., van Hooff, T., & Rovers, V. (2015). Overview of challenges and achievements in the climate adaptation of cities and in the Climate Proof Cities program. *Building and Environment*, *83*, 1–10. https://doi.org/10.1016/j.buildenv.2014.09.006

Ali-Toudert, F., & Mayer, H. (2006). Numerical study on the effects of aspect ratio and orientation of an urban street canyon on outdoor thermal comfort in hot and dry climate. *Building and Environment*, *41*(2), 94–108. https://doi.org/10.1016/j.buildenv.2005.01.013

Allen-Dumas, M. R., Rose, A. N., New, J. R., Omitaomu, O. A., Yuan, J., Branstetter, M. L., Sylvester, L. M., Seals, M. B., Carvalhaes, T. M., Adams, M. B., Bhandari, M. S., Shrestha, S. S., Sanyal, J., Berres, A. S., Kolosna, C. P., Fu, K. S., & Kahl, A. C. (2020). Impacts of the morphology of new neighborhoods on microclimate and building energy. *Renewable and Sustainable Energy Reviews*, *133*, Article 110030. https://doi.org/10.1016/j.rser.2020.110030

Amer, M., Mustafa, A., Teller, J., Attia, S., & Reiter, S. (2017). A methodology to determine the potential of urban densification through roof stacking. *Sustainable Cities and Society*, *35*, 677–691. https://doi.org/10.1016/j.scs.2017.09.021

Araldi, A., & Fusco, G. (2019). From the street to the metropolitan region: Pedestrian perspective in urban fabric analysis. *Environment and Planning B: Urban Analytics and City Science*, *46*(7), 1243–1263. https://doi.org/10.1177/2399808319832612

Barthelemy, M. (2017). From paths to blocks: New measures for street patterns. *Environment and Planning B: Urban Analytics and City Science*, *44*(2), 256–271. https://doi.org/10.1177/0265813515599982

Berghauser Pont, M., & Haupt, P. (2010). *Spacematrix: Space, density and urban form*. NAi Publishers.

Berghauser Pont, M., Stavroulaki, G., Bobkova, E., Gil, J., Marcus, L., Olsson, J., & Legeby, A. (2019). The spatial distribution and frequency of street, plot and building types across five European cities. *Environment and Planning B: Urban Analytics and City Science*, *46*(7), 1226–1242. https://doi.org/10.1177/2399808319857450

Bibri, S. E., Krogstie, J., & Kärrholm, M. (2020). Compact city planning and development: Emerging practices and strategies for achieving the goals of sustainability. *Developments in the Built Environment*, *4*, Article 100021. https://doi.org/10.1016/j.dibe.2020.100021

Bobkova, E. (2019). Towards a theory of natural occupation: Developing theoretical, methodological and empirical support for the relation between plot systems and urban processes [Doctoral dissertation, Chalmers University of Technology]. Chalmers University of Technology Repository. https://research.chalmers.se/en/publication/513622

Bobkova, E., Berghauser Pont, M., & Marcus, L. (2021). Towards analytical typologies of plot systems: Quantitative profile of five European cities. *Environment and Planning B: Urban Analytics and City Science*, 48(4), 604–620. https://doi.org/10.1177/2399808319880902

Bourdic, L., Salat, S., & Nowacki, C. (2012). Assessing cities: A new system of cross-scale spatial indicators. *Building Research and Information*, *40*(5), 592–605. https://doi.org/10.1080/09613218.2012.703488

Bruse, M., & Fleer, H. (1998). With a three dimensional numerical model. *Environmental Modelling & Software*, *13*(3/4), 373–384.

Caldera, M., Corgnati, S. P., & Filippi, M. (2008). Energy demand for space heating through a statistical approach: Application to residential buildings. *Energy and Buildings*, *40*(10), 1972–1983. https://doi.org/10.1016/j.enbuild.2008.05.005

Chen, Yixing, Hong, T., Luo, X., & Hooper, B. (2019). Development of city buildings dataset for urban building energy modeling. *Energy and Buildings*, *183*, 252–265. https://doi.org/10.1016/j.enbuild.2018.11.008

Chen, Yunhao, Wu, J., Yu, K., & Wang, D. (2020). Evaluating the impact of the building density and height on the block surface temperature. *Building and Environment*, *168*(19), Article 106493. https://doi.org/10.1016/j.buildenv.2019.106493

Crank, P. J., Sailor, D. J., Ban-Weiss, G., & Taleghani, M. (2018). Evaluating the ENVI-met microscale model for suitability in analysis of targeted urban heat mitigation strategies. *Urban Climate*, *26*, 188–197. https://doi.org/10.1016/j.uclim.2018.09.002

D'Acci, L. (2019). On urban morphology and mathematics. In L. D'Acci (Ed.), *The mathematics of urban morphology* (pp. 1–18). Birkhäuser.

Demetriou, D., See, L., & Stillwell, J. (2013). A parcel shape index for use in land consolidation planning. *Transactions in GIS*, *17*(6), 861–882. https://doi.org/10.1111/j.1467-9671.2012.01371.x

Duarte, D. H. S., Shinzato, P., dos Santos Gusson, C., & Alves, C. A. (2015). The impact of vegetation on urban microclimate to counterbalance built density in a subtropical changing climate. *Urban Climate*, *14*, 224–239. https://doi.org/10.1016/j.uclim.2015.09.006

European Commission. (1991). Green paper on the urban environment—Communication from the Commission to the Council and the Parliament.

Forouzandeh, A. (2018). Numerical modeling validation for the microclimate thermal condition of semi-closed courtyard spaces between buildings. *Sustainable Cities and Society*, *36*, 327–345. https://doi.org/10.1016/j.scs.2017.07.025

Founda, D., Pierros, F., Katavoutas, G., & Keramitsoglou, I. (2019). Observed trends in thermal stress at European cities with different background climates. *Atmosphere*, *10*(8), Article 436. https://doi.org/10.3390/atmos10080436

Gemeente Rotterdam. (2018). *Rotterdam in 3D*. https://www.rotterdam.nl/werken-leren/3d

Gil, J., Beirão, J. N., Montenegro, N., & Duarte, J. P. (2012). On the discovery of urban typologies: Data mining the many dimansions of urban form. *Urban Morphology*, *16*(1), 27–40. https://www.researchgate.net/publication/256895610_On_the_discovery_of_urban_typologies_Data_mining_the_many_dimensions_of_urban_form

Godoy-Shimizu, D., Steadman, P., Hamilton, I., Donn, M., Evans, S., Moreno, G., & Shayesteh, H. (2018). Energy use and height in office buildings. *Building Research and Information*, *46*(8), 845–863. https://doi.org/10.1080/09613218.2018.1479927

Grimmond, C. S. B., & Oke, T. R. (1999). Aerodynamic properties of urban areas derived from analysis of surface form. *Journal of Applied Meteorology*, *38*(9), 1262–1292.

Guerreiro, S. B., Dawson, R. J., Kilsby, C., Lewis, E., & Ford, A. (2018). Future heat-waves, droughts and floods in 571 European cities. *Environmental Research Letters*, *13*(3), Article 034009 . https://doi.org/10.1088/1748-9326/aaaad3

Haggag, M. A., & Ayad, H. M. (2002). The urban structural units method: A basis for evaluating environmental prospects for sustainable development. *Urban Design International*, *7*(2), 97–108. https://doi.org/10.1057/palgrave.udi.9000071

Hausleitner, B., & Berghauser Pont, M. (2017). Development of a configurational typology for micro-businesses integrating geometric and configurational variables. In *Proceedings of the 11th International Space Syntax Symposium*, (pp. 66.1-66.14). Instituto Superior Técnico.

Hecht, R., Meinel, G., & Buchroithner, M. (2015). Automatic identification of building types based on topographic databases: A comparison of different data sources. *International Journal of Cartography*, *1*(1), 18–31. https://doi.org/10.1080/23729333.2015.1055644

Hoegh-Guldberg, O., Jacob, D., Taylor, M., Bindi, M., Brown, S., Camilloni, I., Diedhiou, A., Djalante, R., Ebi, K. L., Engelbrecht, F., Guiot, J., Hijioka, Y., Mehrotra, S., Payne, A., Seneviratne, S. I., Thomas, A., Warren, R., & Zhou, G. (2018). Impacts of 1.5ºC global warming on natural and human systems. In V. Masson-Delmotte, P. Zhai, H.-O. Pörtner, D. Roberts, J. Skea, P. R. Shukla, A. Pirani, W. Moufouma-Okia, C. Péan, R. Pidcock, S. Connors, J. B. R. Matthews, Y. Chen, X. Zhou, M. I. Gomis, E. Lonnoy, T. Maycock, M. Tignor, & T. Waterfield (Eds.), *Global warming of 1.5°C. An IPCC special report on the impacts of global warming of 1.5°c above pre-industrial levels and related global greenhouse gas emission pathways, in the context of strengthening the global response to the threat of climate change, sustainable development, and efforts to eradicate poverty* (pp. 175–311).The Intergovernmental Panel on Climate Change.

Jiang, H., Geertman, S., & Witte, P. (2020). Smart urban governance: An alternative to technocratic "smartness." *GeoJournal*. https://doi.org/10.1007/s10708-020-10326-w

Jin, H., Cui, P., Wong, N., & Ignatius, M. (2018). Assessing the effects of urban morphology parameters on microclimate in Singapore to control the urban heat island effect. *Sustainability*, *10*(1), Article 206. https://doi.org/10.3390/su10010206

Jurelionis, A., & Bouris, D. G. (2016). Impact of urban morphology on infiltration-induced building energy consumption. *Energies*, *9*(3), 1–13. https://doi.org/10.3390/en9030177

Klok, L., Zwart, S., Verhagen, H., & Mauri, E. (2012). The surface heat island of Rotterdam and its relationship with urban surface characteristics. *Resources, Conservation and Recycling*, *64*, 23–29. https://doi.org/10.1016/j.resconrec.2012.01.009

Kong, F., Sun, C., Liu, F., Yin, H., Jiang, F., Pu, Y., Cavan, G., Skelhorn, C., Middel, A., & Dronova, I. (2016). Energy saving potential of fragmented green spaces due to their temperature regulating ecosystem services in the summer. *Applied Energy*, *183*, 1428–1440. https://doi.org/10.1016/j.apenergy.2016.09.070

Kong, L., Lau, K. K. L., Yuan, C., Chen, Y., Xu, Y., Ren, C., & Ng, E. (2017). Regulation of outdoor thermal comfort by trees in Hong Kong. *Sustainable Cities and Society*, *31*, 12–25. https://doi.org/10.1016/j.scs.2017.01.018

Lan, Y., & Zhan, Q. (2017). How do urban buildings impact summer air temperature? The effects of building configurations in space and time. *Building and Environment*, *125*, 88–98. https://doi.org/10.1016/j.buildenv.2017.08.046

Lenzholzer, S. (2015). Weather in the city: How design shapes urban climate. nai010.

Liu, W., You, H., & Dou, J. (2009). Urban-rural humidity and temperature differences in the Beijing area. *Theoretical and Applied Climatology*, *96*(3), 201-207. https://doi.org/10.1007/s00704-008-0024-6

Lobaccaro, G., & Acero, J. A. (2015). Comparative analysis of green actions to improve outdoor thermal comfort inside typical urban street canyons. *Urban Climate*, *14*, 251–267. https://doi.org/10.1016/j.uclim.2015.10.002

Mangan, S. D., Koclar Oral, G., Erdemir Kocagil, I., & Sozen, I. (2021). The impact of urban form on building energy and cost efficiency in temperate–humid zones. *Journal of Building Engineering*, *33*, Article 101626. https://doi.org/10.1016/j.jobe.2020.101626

Marique, A.-F., & Reiter, S. (2014). Retrofitting the suburbs: Insulation, density, urban form and location. *Environmental Management and Sustainable Development*, *3*(2), 138–153. https://doi.org/10.5296/emsd.v3i2.6589

Mashhoodi, B., Stead, D., & van Timmeren, A. (2020). Land surface temperature and households' energy consumption: Who is affected and where? *Applied Geography*, *114*, Article 102125. https://doi.org/10.1016/j.apgeog.2019.102125

Mavrogianni, A., Wilkinson, P., Davies, M., Biddulph, P., & Oikonomou, E. (2012). Building characteristics as determinants of propensity to high indoor summer temperatures in London dwellings. *Building and Environment*, *55*, 117–130. https://doi.org/10.1016/j.buildenv.2011.12.003

Morganti, M., Salvati, A., Coch, H., & Cecere, C. (2017). Urban morphology indicators for solar energy analysis. *Energy Procedia*, *134*, 807–814. https://doi.org/10.1016/j.egypro.2017.09.533

Næss, P., Saglie, I. L., & Richardson, T. (2020). Urban sustainability: Is densification sufficient? *European Planning Studies*, *28*(1), 146–165. https://doi.org/10.1080/09654313.2019.1604633

National Delta Programme. (2015). *Delta Programme 2015—Working on the delta: The decisions to keep the Netherlands safe and liveable*. https://english.deltacommissaris.nl/delta-programme/documents/publications/2014/09/16/delta-programme-2015

National Delta Programme. (2021). *Delta Programme 2021. Staying on track in climate-proofing the Netherlands* (English version). https://english.deltaprogramma.nl

Oke, T. R. (1987). *Boundary layer climates*. Routledge.

Oke, T. R., Johnson, G. T., Steyn, D. G., & Watson, I. D. (1991). Simulation of surface urban heat islands under "ideal" conditions at night part 2: Diagnosis of causation. *Boundary-Layer Meteorology*, *56*(4), 339–358. https://doi.org/10.1007/BF00119211

Peponis, J., Allen, D., French, S., Scoppa, M., & Brown, J. (2007). Street connectivity and urban density: Spatial measures and their correlation. In *Proceedings of the 6th International Space Syntax Symposium* (pp. 4.01-4.12). Istanbul Technical University.

Perez, J., Fusco, G., Araldi, A., & Fuse, T. (2018). *Building typologies for urban fabric classification: Osaka and Marseille case studies* [Conference paper]. International Conference on Spatial Analysis and Modeling, Tokyo, Japan.

Perini, K., & Magliocco, A. (2014). Effects of vegetation, urban density, building height, and atmospheric conditions on local temperatures and thermal comfort. *Urban Forestry and Urban Greening*, *13*(3), 495–506. https://doi.org/10.1016/j.ufug.2014.03.003

Rafiee, A., Dias, E., & Koomen, E. (2016). Local impact of tree volume on nocturnal urban heat island: A case study in Amsterdam. *Urban Forestry and Urban Greening*, *16*, 50–61. https://doi.org/10.1016/j.ufug.2016.01.008

Ratti, C., Baker, N., & Steemers, K. (2005). Energy consumption and urban texture. *Energy and Buildings*. https://doi.org/10.1016/j.enbuild.2004.10.010

Rodríguez-Álvarez, J. (2016). Urban energy index for buildings (UEIB): A new method to evaluate the effect of urban form on buildings' energy demand. *Landscape and Urban Planning*, *148*, 170–187. https://doi.org/10.1016/j.landurbplan.2016.01.001

Roodenburg, J. (1983). Adaptation of rural minimum temperature forecasts to an urban environment. *Archives for Meteorology, Geophysics, and Bioclimatology, Series B*, *32*(4), 395–401. https://doi.org/10.1007/BF02324659

Rui, L., Buccolieri, R., Gao, Z., Gatto, E., Rui, L., & Ding, W. (2018). Study of the effect of green quantity and structure on thermal comfort and air quality in an urban-like residential district by ENVI-met modelling. *Building Simulation*, *12*, 183–194. https://doi.org/10.1007/s12273-018-0498-9

Salat, S. (2009). Energy loads, CO_2 emissions and building stocks: Morphologies, typologies, energy systems and behaviour. *Building Research and Information*, *37*(5/6), 598–609. https://doi.org/10.1080/09613210903162126

Salata, F., Golasi, I., de Lieto Vollaro, R., & de Lieto Vollaro, A. (2016). Urban microclimate and outdoor thermal comfort: A proper procedure to fit ENVI-met simulation outputs to experimental data. *Sustainable Cities and Society*, *26*, 318–343. https://doi.org/10.1016/j.scs.2016.07.005

Salvati, A., Monti, P., Coch Roura, H., & Cecere, C. (2019). Climatic performance of urban textures: Analysis tools for a Mediterranean urban context. *Energy and Buildings*, *185*, 162–179. https://doi.org/10.1016/J.ENBUILD.2018.12.024

Salvati, A., Palme, M., Chiesa, G., & Kolokotroni, M. (2020). Built form, urban climate and building energy modelling: Case-studies in Rome and Antofagasta. *Journal of Building Performance Simulation*, *13*(2), 209–225. https://doi.org/10.1080/19401493.2019.1707876

Saroglou, T., Meir, I. A., Theodosiou, T., & Givoni, B. (2017). Towards energy efficient skyscrapers. *Energy and Buildings*, *149*, 437–449. https://doi.org/10.1016/j.enbuild.2017.05.057

Serra, M., Gil, J., & Pinho, P. (2017). Towards an understanding of morphogenesis in metropolitan street-networks. *Environment and Planning B: Urban Analytics and City Science*, *44*(2), 272–293. https://doi.org/10.1177/0265813516684136

Serra, M., Psarra, S., & O'Brien, J. (2018). Social and physical characterization of urban contexts: Techniques and methods for quantification, classification and purposive sampling. *Urban Planning*, *3*(1), 58–74. https://doi.org/10.17645/up.v3i1.1269

Skelhorn, C., Lindley, S., & Levermore, G. (2014). The impact of vegetation types on air and surface temperatures in a temperate city: A fine scale assessment in Manchester, UK. *Landscape and Urban Planning*, *121*, 129–140. https://doi.org/10.1016/j.landurbplan.2013.09.012

Smid, M., Russo, S., Costa, A. C., Granell, C., & Pebesma, E. (2019). Ranking European capitals by exposure to heat waves and cold waves. *Urban Climate*, *27*, 388–402. https://doi.org/10.1016/j.uclim.2018.12.010

Steeneveld, G. J., Koopmans, S., Heusinkveld, B. G., van Hove, L. W. A., & Holtslag, A. A. M. (2011). Quantifying urban heat island effects and human comfort for cities of variable size and urban morphology in the Netherlands. *Journal of Geophysical Research Atmospheres*, *116*(20), 1–14. https://doi.org/10.1029/2011JD015988

Stewart, I. D., & Oke, T. R. (2012). Local climate zones for urban temperature studies. *Bulletin of the American Meteorological Society*, *93*(12), 1879–1900. https://doi.org/10.1175/bams-d-11-00019.1

Takebayashi, H. (2017). Influence of urban green area on air temperature of surrounding built-up area. *Climate*, *5*(3), Article 60. https://doi.org/10.3390/cli5030060

Tan, P.-N., Steinbach, M., & Kumar, V. (2005). *Introduction to data mining*. Wesley Longman.

Terrin, J.-J. (2015). *Villes et changement climatique. Ilots de chaleur urbains* [Cities and climate change. Urban heat island]. Parentheses.

Toparlar, Y., Blocken, B., Maiheu, B., & van Heijst, G. J. F. (2017). A review on the CFD analysis of urban microclimate. *Renewable and Sustainable Energy Reviews*, *80*, 1613–1640. https://doi.org/10.1016/j.rser.2017.05.248

Touchaei, A. G., & Wang, Y. (2015). Characterizing urban heat island in Montreal (Canada)—Effect of urban morphology. *Sustainable Cities and Society*, *19*, 395–402. https://doi.org/10.1016/j.scs.2015.03.005

Tsoka, S., Tsikaloudaki, A., & Theodosiou, T. (2018). Analyzing the ENVI-met microclimate model's performance and assessing cool materials and urban vegetation applications–A review. *Sustainable Cities and Society*, *43*, 55–76. https://doi.org/10.1016/j.scs.2018.08.009

TU Delft. (2018). *Plots weather stations Rotterdam*. http://weather.tudelft.nl/plots/

van Hove, L. W. A., Jacobs, C. M. J., Heusinkveld, B. G., Elbers, J. A., Van Driel, B. L., & Holtslag, A. A. M. (2015). Temporal and spatial variability of urban heat island and thermal comfort within the Rotterdam agglomeration. *Building and Environment*, *83*, 91–103. https://doi.org/10.1016/j.buildenv.2014.08.029

Vartholomaios, A. (2017). A parametric sensitivity analysis of the influence of urban form on domestic energy consumption for heating and cooling in a Mediterranean city. *Sustainable Cities and Society*, *28*, 135–145. https://doi.org/10.1016/j.scs.2016.09.006

Vaz Monteiro, M., Doick, K. J., Handley, P., & Peace, A. (2016). The impact of greenspace size on the extent of local nocturnal air temperature cooling in London. *Urban Forestry and Urban Greening*, *16*, 160–169. https://doi.org/10.1016/j.ufug.2016.02.008

Vernez Moudon, A. (1997). Urban morphology as an emerging interdisciplinary field. *Urban Morphology*, *1*(1), 3–10. https://doi.org/1027-4278

Wang, B., Cot, L. D., Adolphe, L., Geoffroy, S., & Sun, S. (2017). Cross indicator analysis between wind energy potential and urban morphology. *Renewable Energy*, *113*, 989–1006. https://doi.org/10.1016/j.renene.2017.06.057

Ward, K., Lauf, S., Kleinschmit, B., & Endlicher, W. (2016). Heat waves and urban heat islands in Europe: A review of relevant drivers. *Science of the Total Environment*, *569/570*, 527–539. https://doi.org/10.1016/j.scitotenv.2016.06.119

Wei, R., Song, D., Wong, N. H., & Martin, M. (2016). Impact of urban morphology parameters on microclimate. *Procedia Engineering*, *169*, 142–149. https://doi.org/10.1016/j.proeng.2016.10.017

Westerink, J., Haase, D., Bauer, A., Ravetz, J., Jarrige, F., & Aalbers, C. B. E. M. (2013). Dealing with sustainability trade-offs of the compact city in peri-urban planning across European city regions. *European Planning Studies*, *21*(4), 473–497. https://doi.org/10.1080/09654313.2012.722927

Willmott, C. J. (1982). Some comments on the evaluation of model performance. *Bulletin of the American Meteorological Society*, *63*(11), 1309-1313. https://doi.org/10.1175/1520-0477(1982)063<1309:SCOTEO>2.0.CO;2

Wolff, M., Haase, A., Haase, D., & Kabisch, N. (2017). The impact of urban regrowth on the built environment. *Urban Studies*, *54*(12), 2683–2700. https://doi.org/10.1177/0042098016658231

Wu, Z., Dou, P., & Chen, L. (2019). Comparative and combinative cooling effects of different spatial arrangements of buildings and trees on microclimate. *Sustainable Cities and Society*, *51*, Article 101711. https://doi.org/10.1016/j.scs.2019.101711

Yang, X., Zhao, L., Bruse, M., & Meng, Q. (2013). Evaluation of a microclimate model for predicting the thermal behavior of different ground surfaces. *Building and Environment*, *60*, 93–104. https://doi.org/10.1016/j.buildenv.2012.11.008

Zhao, M., Cai, H., Qiao, Z., & Xu, X. (2016). Influence of urban expansion on the urban heat island effect in Shanghai. *International Journal of Geographical Information Science*, *30*(12), 2421–2441. https://doi.org/10.1080/13658816.2016.1178389

Zinzi, M., & Santamouris, M. (2019). Introducing urban overheating: Progress on mitigation science and engineering applications. *Climate*, *7*(1), Article 15. https://doi.org/10.3390/cli7010015

4 An Integrated Microclimate-Energy Demand Simulation Method for the Assessment of Urban Districts

This chapter has been published as:
Romero M., Maiullari D, Pijpers-van Esch M. and Schlueter A. (2020). An Integrated Microclimate-Energy Demand Simulation Method for the Assessment of Urban Districts. *Front. Built Environ.* 6:553946. doi: 10.3389/fbuil.2020.553946

ABSTRACT Rapid urbanization and densification processes are changing microclimatic environments in cities around the world. Even though previous studies have demonstrated the impact of urban microclimate on space cooling and heating demand, modelling tools employed to support the design process largely overlook microclimatic conditions in assessing building energy performance, making use of data from weather stations often located in rural areas. This paper presents a computational approach for the quantitative analysis of building energy demand at the district scale, including interdependent factors such as local air temperature, relative humidity and wind speed, diversity in building geometry and materials. The method, which couples the microclimate model ENVI-met and the district-scale energy simulation tool City Energy Analyst, is applied to a case study in Zurich, Switzerland, in order to analyse the energy performance of the area on a hot summer day. The study contributes to advance a coupling approach between a microclimate simulation and an energy tool at the district scale. The results

showed that the coupled assessment approach can deal with complex interactions between geometry, building materials and energy systems. The consideration of local microclimatic conditions led to a 5% increase in the space cooling demand on the selected day, while the simulated peak cooling load for each building was 8% higher on average. The variation in the space cooling demand was found to be mainly due to an increase in latent cooling demand. Moreover, the coupling method allowed a detailed analysis of energy demand variation at the building level showing that, when considering the local climate patterns, the space cooling demand of the individual buildings varied between −5% and +14% on the selected day. The proposed method represents a next step to reflect the mutual interactions between buildings and microclimate in urban districts and aims at supporting decision-making in the design process.

4.1 Introduction

In proceeding through the "Grand Transition", global energy consumption is predicted to increase by 22 to 46% by 2060 (World Energy Council, 2016). A large part of this increase is due to worldwide demographic growth in urbanized areas. European cities have also seen a faster overall rise in number of inhabitants in the last decade (Eurostat, 2016). This trend, combined with an urbanization shift from an expansive development model to a compact and concentrated one, has resulted in redevelopment projects in inner-city areas. Urban re-densification processes as well as new urban developments need to meet design objectives of sustainability and liveability generating new positive impacts on the surrounding urban environment. In order to achieve these, they need to comply with several climate and energy targets that aim to reduce greenhouse gas emissions, increase energy efficiency, and mitigate climate impacts such as heat stress.

One of the main challenges during the urban design process is predicting the effect of the urban form on the local microclimate, which influences not only outdoor thermal comfort but also the energy performance of buildings. Previous empirical and fundamental studies have shown that it is of growing importance to take the local climatic conditions into account when analysing building energy performance and its environmental impact (Magli et al., 2015; Skelhorn et al., 2016). Anthropogenic heat, urban geometry and construction materials influence local thermal and wind patterns, thus affecting the climate context in which the buildings are operated (Santamouris et al., 2001). Phenomena of urban overheating such as the Urban Heat Island (UHI) have been shown to significantly increase space

cooling demand (Hirano and Fujita, 2012; Liu et al., 2017; Guattari et al., 2018) and reduce heating consumption (Cui et al., 2017; Sun and Augenbroe, 2014) in different geographical zones. According to Li et al. (2019), UHI could result in an average increase in the electricity demand for cooling of 19% with intercity variations ranging between 10% and 120%. Moreover, as shown by the comparative analysis of Santamouris (2014) the peak electricity demand for cooling increases by 0.45 to 4.6% per degree increase in ambient temperature.

Despite the advancement of microclimate models and the growing need for more accurate energy assessment, computational models commonly used to support the understanding of building energy performance largely overlook urban microclimate phenomena. Meteorological boundary conditions adopted in Building Energy Simulations (BES) are typically based on Typical Meteorological Year (TMY) data from weather stations, which are usually smoothed and averaged over several years (Yang et al., 2012) and ignore the effect of the urban surroundings on local climate (Gobakis and Kolokotsa, 2017). As a consequence, energy assessments usually neglect the effects of urban overheating on base and peak energy demands, potentially compromising the decisions on energy strategies for future sustainable and low carbon districts.

This study aims to establish an integrated simulation method by coupling a state-of-the-art district-scale energy demand model with a microclimate simulation tool to quantitatively evaluate the effects of local climate on the energy consumption and peak power demand of individual buildings during extreme weather events. By expanding the scale from single buildings to the district level, the proposed method enables the analysis of the reciprocal influence between groups of buildings with different form, materials and orientation. The selected simulation tools are the microclimate software ENVI-met (Bruse and Fleer, 2009), which simulates small scale outdoor conditions, and the City Energy Analyst (CEA) (The CEA Team, 2018), an open-source tool for district-scale energy demand modelling and supply system optimization.

The first section of this paper provides a background on the effects of urban microclimate on energy demand and presents the state of the art in microclimate and energy demand modelling. The following section describes the simulation tools used in this paper and the coupling method, which involves extracting hourly based output data for air temperature, wind speed and relative humidity from the microclimate simulation and passing them to the energy demand simulation as the climatic boundary conditions. The method is then applied to analyse the energy performance of a case study in central Zurich (Switzerland). In order to demonstrate the approach, two consecutive hot days with clear sky were selected during the heat wave that affected Zurich in 2015. The results of simulations carried out with general weather data and with urban microclimatic data are subsequently compared,

showing the effect on space cooling demand and peak cooling power in the district. Finally, conclusions are presented regarding limitations of the method, possibilities for its improvement, as well as for its use in urban design.

4.2 Background and state of the art

Several physical phenomena that take place in the urban environment influence the thermal exchange processes of buildings. First, multiple interreflections of radiation and decreased sky view due to urban geometry, limited evapotranspiration due to sealed surfaces and scarce vegetation, and the thermal properties of construction materials used in buildings and paved areas, along with anthropogenic heat sources, lead to temperature differences between urban and rural areas. This phenomenon, known as the Urban Heat Island (UHI) effect, results in a reduction in heating demand and an increase in cooling demand in dense urban contexts (Allegrini et al., 2012). A second type of effect concerns wind patterns occurring within the canopy layer. In general, average wind speeds are lower in the urban environment (Allegrini et al., 2015); however, street network characteristics, building geometry and orientation, and the topographic location can cause significant local differences in speed as well as direction (Oke et al., 2017). These in turn affect the potential for natural ventilation and passive cooling. For example, the acceleration of air flows along street canyons increases thermal losses from building façades due to convective heat transfer, increasing heating demand during cold seasons. A third phenomenon is related to the influence of shortwave and longwave solar radiation. The compactness of the surrounding urban environment affects buildings' exposure to solar radiation, both direct and reflected, leading to differences in thermal gains and the electricity demand for lighting (Allegrini et al., 2015).

Several simulation tools have been developed to model the urban climate. The main advantage of simulations compared to using measured weather station data is that they can generate explicit information for distinct climatic parameters (Toparlar et al., 2017). Prognostic Computational Fluid Dynamics models, in particular, allow the comparison of urban areas in the design stage under numerous time and climatic frames (Blocken, 2014; Mirzaei and Haghighat, 2010). Microclimate models predict detailed spatial distributions of flow, temperatures and scalar fields at the building to district scale (Ooka, 2007). Microclimate models take into account shortwave and longwave radiation, transpiration, evaporation and sensible heat fluxes, as well as heat exchange with the soil and can be of great use to assess the energy use in city districts (Sola et al., 2018).

Although microclimate has been recognized as a relevant factor in shaping energy consumption, computational models to predict building energy performance during the design process largely overlook urban microclimate phenomena. Allegrini et al. (2015) offered a comprehensive review of existing modelling approaches and tools which address the district scale of energy systems, and argued that "it is no longer sufficient to simulate building energy use assuming isolation from the microclimate and the energy system in which they operate". Furthermore, the authors concluded that more extensive research is required into the link between thermal processes and microclimate effects, in terms of spatial and temporal detail, resolution and magnitude.

Recent advancements in computational approaches have allowed attempts to bridge this gap by coupling methods that link urban climatic variables to the thermal performance of buildings. A series of studies have presented coupling procedures between BEM and CFD in order to investigate the influence of urban climate on energy demand (Sánchez de la Flor and Álvarez Domínguez, 2004; He et al., 2008; Kolokotroni et al., 2010; Gros et al., 2016), to assess the influence of geometry and materials on urban temperatures and energy consumption (Gros et al., 2014; Toparlar et al., 2018), or to compare the performance of design measures to decrease heating and cooling loads (Skelhorn et al., 2016). However, previous work in this field has so far focused mainly on single buildings (e.g., Gobakis and Kolokotsa, 2017) and explorations of generic typologies employing homogeneous urban patterns that are not representative of the complexity of cities (e.g., He et al., 2008; Yang et al., 2012; Liu et al., 2015). On the other hand, attempts to couple district-scale energy demand simulations to urban climate models usually rely on simplified geometries and lower resolution mesoscale models (e.g., Rasheed et al., 2011; Mauree et al., 2016).

Planning energy systems at the district scale requires a detailed characterization of the energy needs of urban areas. In order to accurately account for the distribution of cooling loads in a district, it is necessary to explicitly simulate each building and their surrounding urban climate at the micro scale. However, the coupling at such a scale has as of yet not been carried out (Frayssinet et al., 2018). The main reason can be found in computational limitations, since the analysis of a large area such as a district in some cases surpasses the capability of energy simulation tools developed for single buildings, whereas urban building energy models (UBEM) have only been introduced relatively recently (Reinhart and Cerezo Davila, 2016).

4.3 Methodology

The proposed coupling approach, shown schematically in Figure 4.1, is based on passing simulated microclimate data from ENVI-met to the City Energy Analyst (CEA) to act as boundary conditions for building energy simulation. ENVI- met is a three-dimensional prognostic model designed to simulate heat, evapotranspiration and air flow processes between buildings, surfaces, and plants in urban environments, while CEA is an open-source tool for the analysis and optimization of energy systems in neighbourhoods and city districts. The aim of the coupling method is to model the energy demand of a number of buildings at the district scale taking into account the various factors that influence energy performance, namely the microclimatic environment, locus and topographic context, and the building geometry and materials.

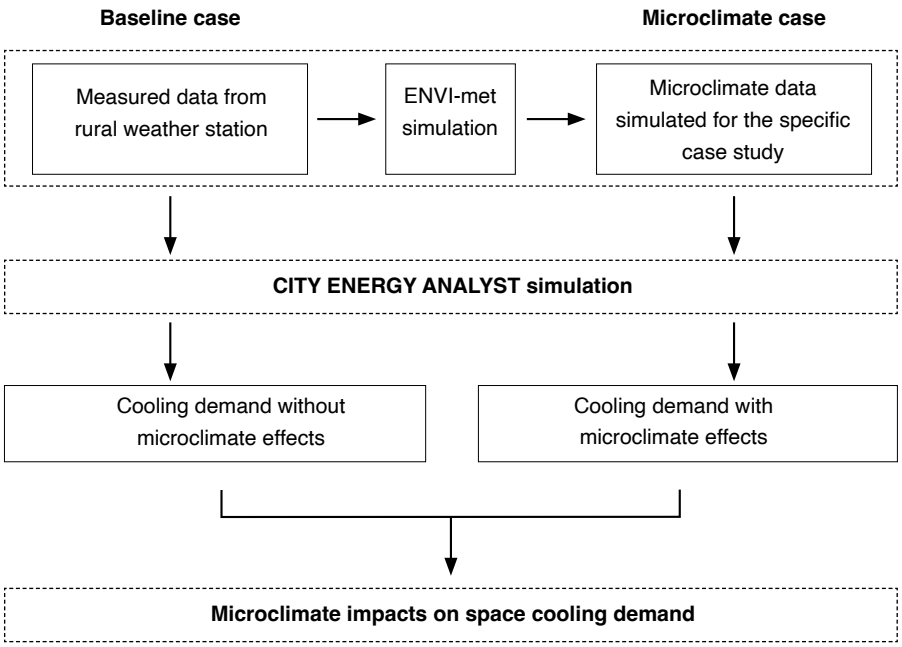


FIG. 4.1 Diagram showing the proposed integration method between ENVI-met and CEA for each of the climatic cases considered.

TOC

In order to compare the effects of local microclimate on the predicted energy demands of the area, two climate datasets are prepared. The first consists of measured data from an offsite weather station, used as an input to the ENVI-met simulations as well as to CEA, where it provides a Baseline case. The second dataset, derived from ENVI-met simulations, reports the specific microclimate conditions within the area and is used to run a second energy demand simulation in the Microclimate case.

In the first step, the Baseline climate dataset for the offsite weather station is derived for a selected day. The model for the selected case study is built in ENVI-met 4.4 and validated against temperature data measured on location. The simulation results from ENVI-met for air temperature, wind speed and relative humidity for each façade are then averaged to obtain hourly values for each building in the area. Finally, the microclimate simulation results are passed to the City Energy Analyst (CEA) in order to carry out energy demand simulations. The software includes a dynamic model for building energy performance simulation, as well as tools for the assessment of local energy potentials, conversion and storage technology simulation, and energy system optimization. The method presented here was developed and tested in a district in Zurich. For the application two consecutive hot days with clear sky were selected during the heat wave that affected Zurich in 2015. A detailed description of the case study and simulation settings are reported in section “Case Study Description”.

4.3.1 Step 1: Microclimate Modeling in ENVI-met

ENVI-met is a three-dimensional prognostic microclimate model designed to simulate the interaction between surfaces, plants and air in an urban environment (Bruse and Fleer, 2009). ENVI- met relies on Reynolds-Averaged Navier–Stokes equations to resolve heat transfer and fluid flows in urban settings. This approach reduces computational cost of the Computational Fluid Dynamics (CFD) model compared to large eddy simulation while achieving reasonable accuracy (Mirzaei and Haghighat, 2010). Moreover, ENVI-met has a typical resolution of 0.5 to 10 meters in space and a typical time frame of 24 to 48 h with a time step of 1 to 5 s. It consists of four models: an atmospheric model, a soil model, a vegetation model and a building model. The structure and equations that govern these sub-models are described in detail by Huttner (2012). The atmospheric model computes mean air flow, turbulence, fluxes of direct, diffuse and reflected short-wave and long-wave radiation, and air temperature and humidity. The soil model computes surface and soil temperatures and soil water fluxes and is coupled with the vegetation model, which calculates evaporation rates, foliage temperatures and exchanges

of vegetation with the environment (heat, evaporation and transpiration fluxes). The building model computes fluxes of momentum, heat and vapor at and inside building walls and roofs taking into account material properties. The tool is well established to estimate and assess outdoor thermal comfort (Ali-Toudert and Mayer, 2006, 2007; Taleghani et al., 2015). In fewer cases it has also been used to estimate the impact of the urban microclimate on building energy demand, as is done in this study. Such studies have, however, only looked at the energy demand of single buildings, either theoretical typologies (Yang et al., 2012; Carnielo and Zinzi, 2013; Skelhorn et al., 2016) or existing case studies (Gobakis and Kolokotsa, 2017).

To perform an ENVI-met simulation, model input parameters must be provided for the Area Input file, Database, and Configuration file. The Area Input file (.INX) stores data regarding size and resolution of the domain, as well as spatial characteristics of the calculation mesh, by using an orthogonal 3D grid (either equidistant or telescoping), whose sizes in the x-, y- and z-directions can be defined by the user. Links with the Database ensure that descriptive parameters (such as thermal conductivity, albedo, water content, etc.) for soil, vegetation and surface materials can be used to solve equations of the mathematical model. Finally, the Configuration file (.SIMX) stores the simulation settings including weather boundary conditions. For the selected case study, section “Microclimate Dataset: Envi- met Model Construction and Parameters” describes data sources and input settings for the mentioned ENVI-met modules.

On the simulated results a mesh sensitivity analysis is performed and a validation procedure against measured temperature data is carried out. The validated model with the highest level of accuracy is selected for coupling with the energy model. The ENVI-met results consist of hourly values of a variety of climate parameters reported in a three-dimensional grid that can be exported in different formats. Atmospheric outputs report the values of various climate parameters, including: wind speed and direction; air temperature; mean radiant temperature; specific and relative humidity; turbulence kinetic energy; dissipation; vertical exchange coefficient; diffuse/ reflected solar radiation; temperature and vapor flux; and CO_2 concentration. Given the simplified nature of the energy demand model used in CEA, only a few of these parameters are relevant for the energy demand simulation, namely air temperature, relative humidity, and wind speed. In the next section, the use of these values in CEA is described. Version 4.4 of ENVI-met allows users to export climate hourly results for each building. These are used in order to generate building-scale average hourly values of these climatic parameters, which are then passed as weather boundary conditions to CEA.

4.3.2 Step 2: Energy Demand Modelling in CEA and Main Environmental Parameters

The CEA thermal load model comprises two main sub-models, one for sensible loads and one for latent loads. The main environmental parameters that affect this model are the solar irradiation, relative humidity, outdoor temperature, and wind speed. The CEA urban solar radiation model is used to calculate the incident solar radiation in buildings accounting for both vertical and horizontal surfaces, material properties, shading, terrain topography and reflections. The tool first creates 3D representations of the geometry of buildings out of meta information about the size of windows, height, and number of floors in buildings. Each surface in the 3D representation is subdivided in a grid, and the calculation is performed at the centroid of every subdivision for every hour of the year. The calculation engine is based on the open-source software DAYSIM (Reinhart, 2013), a validated radiation model for daylighting analysis. While fine-grained solar irradiation results for individual building surfaces can be obtained from DAYSIM, hourly values of air temperature, wind speed and relative humidity are usually obtained from weather stations in the form of Typical Meteorological Year data, which may not be representative of a district's local climate. Therefore, these three parameters were selected for the study of the microclimate effects on space cooling demand.

4.3.2.1 Outdoor Air Temperature and Sensible Loads

The sensible load calculation implemented in CEA is based on a simplified resistance-capacitance model as described in Swiss norm (SIA Merkblatt 2044), which itself is an adaptation of ISO 13790 (2008). Each building in the area is represented by a single thermal zone, meaning that the building interior is assumed to be well-mixed with no effects from occupant distribution within the building or localized temperature differences.

The building material properties, solar gains, and internal gains caused by occupants as well as the use of lighting and appliances are then represented as resistances and capacitances in an electrical circuit, as shown in Figure 4.2. This system is composed of four nodes representing outdoor air, indoor air, a surface node, and a node in the building's thermal mass.

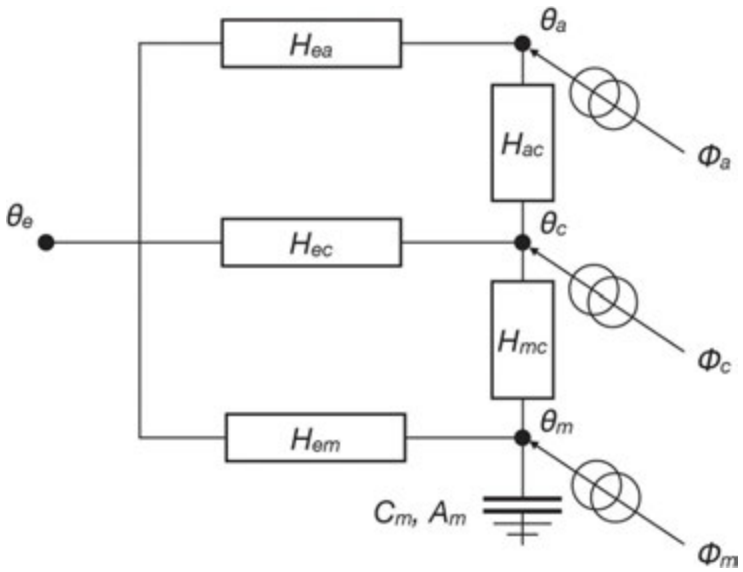


FIG. 4.2 Resistance-capacitance (RC) model used in CEA (adapted from SIA Merkblatt 2044).

θe, θa, θc, and θm are the temperatures of the exterior air, indoor air, surface node, and building thermal mass, respectively. Hea is the air heat flow coefficient of the ventilation systems, whereas Hec and Hem are the transmission heat coefficients lightweight and heavyweight building materials, respectively, and the heat transfer coefficients between the air and surface node, and between the surface node and the thermal mass are Hac and Hmc, respectively. The internal and solar gains in the air, surface and thermal mass nodes are <Da, <Dc and <Dm, respectively. Finally, Cm and Am are the internal heat capacity and effective mass area of the building

These nodes are connected by resistances representing building materials and systems, whose heat transfer coefficients are shown and described in Figure 4.2. The solar gains and the internal gains, which arise from building occupants and lighting and appliances in the building, are distributed among the three indoor nodes. The building also has an effective mass area and an internal heat capacity, which represents the thermal inertia in the building thermal mass. The derivation of these parameters is beyond the scope of this paper and can be found in the aforementioned standards. The goal of this model is to calculate, given the boundary conditions provided by the physical properties of the building and outdoor weather conditions, the heating or cooling required ($<D_{HC}$) in order to satisfy the building's set point temperature.

TOC

4.3.2.2 Latent Load Calculation and Relative Humidity

In addition to these sensible loads, buildings with mechanical ventilation systems and air-based cooling systems also have latent loads, *i.e.*, the loads for humidifying or dehumidifying the air supplied in buildings. For buildings with natural ventilation, the minimum ventilation rate for each building is assumed to be provided from the windows with no dehumidification. Otherwise, when mechanical ventilation or air-based cooling systems are activated the latent load calculation in CEA is carried out following ISO Standard 52016-1 (ISO 52016-1, 2017). The latent and sensible heat loads in the air handling unit for the required ventilation rate in the building are calculated as follows:

$$Q_{cs,sen} = m_{ve,mech} \cdot c_{p,air} \cdot \left(T_{sup,ahu} - T_{ve,mech}\right) \quad (1)$$

$$Q_{cs,lat} = m_{ve,mech} \cdot \left(x_{sup,ahu} - x_{ve,mech}\right) \cdot h_{we} \quad (2)$$

where $m_{ve,mech}$ is the mechanical ventilation mass flow rate, h_{we} is the latent heat of vaporization of water and $x_{sup,ahu}$ is the supply moisture content, which is the lowest value of the moisture content of outdoor air or the moisture content in saturated air at the supply temperature of the coil in the air handling unit. $x_{ve,mech}$ is the moisture content in the ventilation airflows, which is equal to the moisture content in outdoor air, and is either obtained from the relative humidity from the weather file or, in this study, from the microclimate simulation results. Thus, this difference in moisture content is equal to the amount of moisture that needs to be added or removed from the outdoor air supplied to the building.

4.3.2.3 Wind Speed Effects on Air Infiltration

In its present implementation, wind speed does not affect the CEA sensible load model directly. However, it does affect the infiltration in the building, and hence the air heat flow coefficient of the ventilation systems H_{ea}, as shown in Figure 4.2, calculated as follows:

$$H_{ea} = \left(\dot{m}_{ve,mech} + \dot{m}_{ve,w} + \dot{m}_{ve,inf}\right) \cdot c_{p,air} \quad (3)$$

where $\dot{m}_{ve,mech}$, $\dot{m}_{ve,w}$ and $\dot{m}_{ve,inf}$ are, respectively, the mass flow rates of air from mechanical ventilation, from window openings and from infiltration through the building envelope, and $c_{p,air}$ is the specific heat capacity of air. The total amount of

air to be supplied is calculated based on the number of people in the area and the amount of air required per person, defined as an input to the demand model. The amount of air that needs to be supplied by either mechanical or natural ventilation is then calculated as the difference between the required ventilation and the infiltration rate $\dot{m}_{ve,inf}$.

The CEA dynamic calculation procedure for air infiltration is based on the formulation of all air volume flows into and out of a zone as a function of the unknown zone reference pressure and calculating air flows through leakage (Happle et al., 2017). The method, derived from standards (DIN EN 16798-7, 2015; ISO 9972:2015, 2015), is based on defining standard air leakage paths for each building in the area and calculating air flow through these paths based on a standard total leakage coefficient, C_{lea}, which is then assigned to individual leakage paths on the façade and roof. The volumetric flow rate through each path is then calculated as follows:

$$\dot{V}_{lea,i} = C_{lea,i} \cdot sign\left(\Delta p_{lea,i}\right) \cdot \left|\Delta p_{lea,i}\right|^{2/3} \tag{4}$$

where $\Delta p_{lea,I}$ is the indoor-outdoor pressure difference at air path i, and is a function of the outdoor wind speed u_{wind}:

$$\Delta p_{lea,i}(t) = \rho_{e,ref} \cdot \left(0.5 \cdot C_{p,i} \cdot [u_{wind}(t)]^2 - h_{path,i} \cdot g \cdot \frac{\theta_{e,ref}}{\theta_e(t)}\right) - \cdot \left(p_{zone,ref} - \rho_{e,ref} \cdot h_{path,i} \cdot g \cdot \frac{\theta_{e,ref}}{\theta_a(t)}\right) \tag{5}$$

where $\theta_{e,ref}$ and $\rho_{e,ref}$ are the reference outdoor temperature and pressure (283 K and 1.23 kg/m^3, respectively), g is the acceleration of gravity (9.81 m/s^2), $h_{path,i}$ is the height of the leakage path as defined above, and θ_e and θ_a correspond to the temperatures defined in the RC model shown in Figure 4.2. $C_{p,i}$ is the wind pressure coefficient of path i and is equal to 0.05 if the path faces the direction of the wind, -0.05 if it faces the opposite direction, and 0 if the path is in the roof. The zone reference pressure $p_{zone,ref}$ is unknown and needs to be calculated iteratively by minimizing the absolute value of the mass flows in and out of the building ($\dot{m}_{in}$ and $\dot{m}_{out}$). Once the reference pressure has been found, the infiltration into the building is given by:

$$\dot{m}_{ve,inf} = \dot{m}_{in}\left(p_{zone,ref}\right) \tag{6}$$

4.3.2.4 Wind speed effects on convective heat transfer at exterior building surfaces

By default, CEA assumes a constant thermal resistance of external surfaces, equal to 0.04 Km^2/W as suggested in ISO 6946 (ISO 6946, 2007). The use of this constant value however neglects the effects of wind on convective heat transfer at the building surface. Furthermore, the resistance given in the ISO standard was calculated for a wind speed of 4 m/s, whereas according to typical meteorological year (TMY) data for the case study under consideration the local wind speed is lower than that 97.5% of the time. Thus, the full procedure to calculate the thermal resistance of external surfaces R_{SE} according to ISO 6946 was implemented:

$$R_{SE}(t) = \frac{1}{h_{c,e}(t) + h_{r,e}(t)} \tag{7}$$

where $h_{c,e}$ and $h_{r,e}$ are the convective and radiative heat transfer coefficients, respectively.

The convective heat transfer is given by:

$$h_{c,e}(t) = 4 + 4 \cdot u_{wind}(t) \tag{8}$$

The radiative heat transfer coefficient, on the other hand, is calculated as follows (ISO 13790, 2008):

$$h_{r,e}(t) = 4 \cdot \varepsilon \cdot \sigma \cdot [\theta_{ss}(t)]^3 \tag{9}$$

where ε is the emissivity of the façade material, σ is the Stefan-Boltzmann constant and θ_{ss} is the arithmetic average of the surface temperature and the sky temperature. Since only the dynamic model can account for the effect of local variations in wind patterns, the effects of microclimate on buildings' space cooling demand was investigated using the dynamic heat transfer model.

4.4 Case Study Description

The coupling method was applied to assess the energy performance of a district in Zurich, Switzerland. The *Hochschulquartier* is a dense and central area comprising two universities (ETH Zurich and the University of Zurich) and the University Hospital, as well as a number of secondary functions. The area is undergoing a transformation with the goal of increasing the usable floor space by 40% (Baudirektion Kanton Zürich, 2014). In order to demonstrate the integration approach, we focused on an existing area within the case study district, as shown in Figure 4.3. The city of Zurich is situated at the border between an oceanic climate (Köppen–Geiger climate classification Cfb) and a humid continental climate (Köppen climate classification Dfb), with an average of 30 summer days (maximum temperature equal to or above 25°C) and 5.8 so-called heat days (maximum temperature equal to or above 30°C) per year (Mussetti et al., 2019).

The importance of the climatic environment in relation to energy-efficient solutions is expected to increase in view of climate change. During a heat wave in 2015, a difference of up to 5 K was observed between urban and rural weather stations in Zurich, and even a slightly positive UHI during the daytime was found (Mussetti et al., 2019). Several studies have estimated the impact of increased temperatures on Swiss energy demand (Frank, 2005; OcCC and ProClim, 2007; Gonseth et al., 2017), stating that while the number of heating days is expected to decline, the number of cooling days will grow significantly, with a consequent increase in energy demand for space cooling. In the Swiss central plateau where Zurich is located, annual cooling energy consumption for office buildings in the scenarios analysed by Frank (Frank, 2005) is calculated to rise by 223–1050%, while annual heating energy consumption is expected to fall by 36–58%. In order to assess the effects of such extreme weather events on the district's energy demands, we selected two consecutive hot days with clear sky during the heat wave that affected Zurich in 2015 (2–3 July 2015). For the selected period, two climate datasets were prepared. The Baseline climate dataset was obtained from Meteonorm (Meteotest, 2014) and uses data from the offsite weather station SMA. The Microclimate dataset was obtained through ENVI-met simulations and was validated by comparing the simulated air temperature to measured data from a roof sensor within the case study area. Spatial data for the case study area, comprising the topography, building footprints and number of floors, were retrieved from local GIS data and the from the Federal Register of Buildings and Dwellings (Bundesamt für Statistik, 2010).

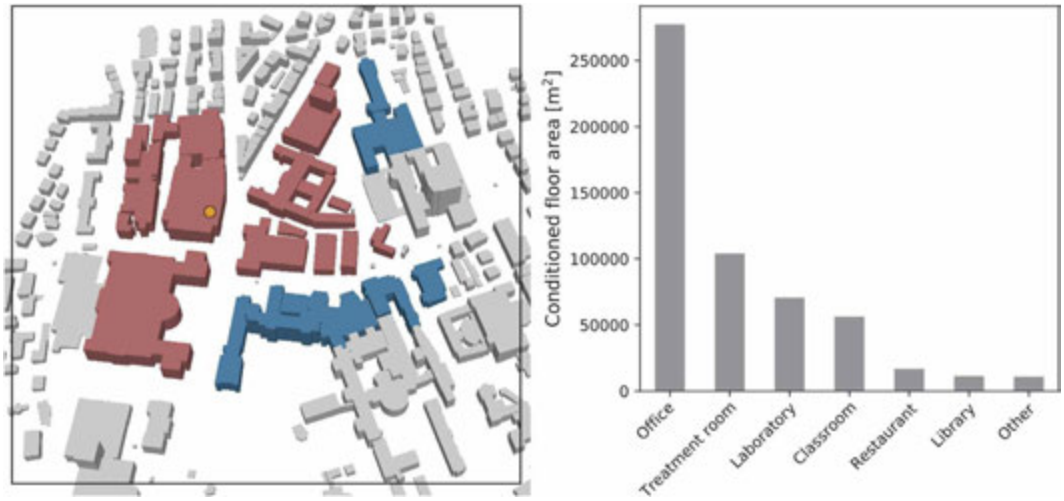


FIG. 4.3 Aerial representation of the case study area and functional distribution of the buildings under consideration. The functions shown as "Office" include both research and hospital spaces. The buildings selected for this study are colored red for university buildings and blue correspond to the hospital. The yellow circle marks the location of the temperature sensor in the case study area.

4.4.1 Baseline Climate Dataset

The Baseline climate dataset is derived from measured data from the national weather station SMA, located in Zurich Fluntern, 1.35 km uphill from the area. This dataset is employed both as an input to the ENVI-met simulation and as climatic boundary conditions to model energy demand in CEA for the Baseline case. The selected days (2–3 July 2015), during which Zurich was affected by a heat wave event, are selected as representative extreme hot days. As shown in Figure 4.4, the two days reach temperatures higher than 30°C and humidity values above 70%. During both days, the maximum diurnal temperature is registered at around 33°C, while the night temperature is lower at around 20°C for the first day and 22°C during the second day. As clear sky and no rain were filtering parameters for the selection of the period, the daily humidity pattern appears similar during the two days, ranging between 35% and 80%. Wind velocity reaches a maximum speed of 3.3 m/s and wind speed below 1 m/s is registered generally between sunset and sunrise.

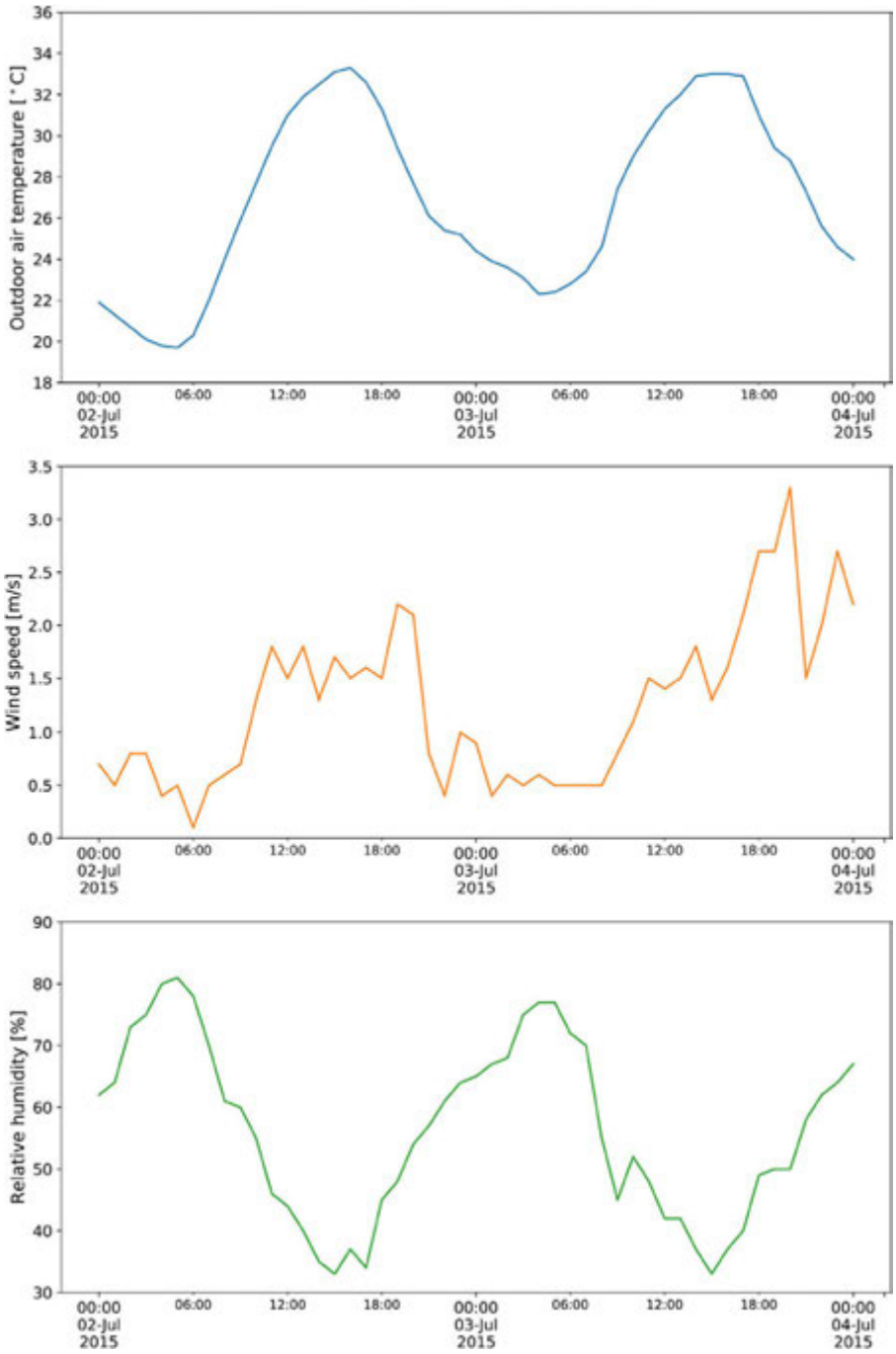


FIG. 4.4 Data from the weather station SMA for the time period under analysis.

TOC

4.4.2 Microclimate Dataset: ENVI-met Model Construction and Parameters

The second dataset is obtained by validated ENVI-met simulations and reports the specific thermodynamic characteristics of the Hochschulquartier district. After an iterative calibration process of building and paving materials, two simulations were performed with different grid resolutions. The following section reports ENVI-met inputs and simulation settings. Table 4.1 summarizes the input parameters used for the ENVI- met model subdivided into the categories of Area Input file and Configuration file. To obtain reliable simulation results for the area of interest it is necessary to model a larger area. This is because the urban surrounding influences the microclimate in the area of interest, but also because microclimate models do not work reliably at the model borders. In this case study, a first boundary has been drawn around the area of interest including adjacent street canyons and adjoining building façades. From this border an offset area of 100 m was taken as the area of influence (as seen in Figure 4.3) as a conservative assumption (Wong et al., 2012).

As the process of validation was complemented by a mesh sensitivity analysis, two Area Input Files were created using a grid cell unit of 6 m (x) by 6 m (y) by 6 m (z) -Model A-, and 6 m (x) by 6 m (y) by 3 m (z) -Model B-, respectively. On the horizontal plane, to cover the area of study plus the area of influence, 87 cells were set for the x axes and 83 cells for the y axes. Regarding the z axis, the height of the model was calculated as the sum of maximum topographic elevation and the height of the tallest building in the district (55 m). In order to avoid computational instability due to proximity of objects to the upper domain limit, the height of the domain was doubled. As the mesh sensitivity explores the variation in vertical resolution the number of z cells was therefore set to 22 for Model A, and 40 for Model B, using a telescopic factor of 20% (from 90 m upward).

TABLE 4.1 ENVI-met model settings.

		Model A	Model B
Area Input File	Domain	522m(x), 498m(y), 172m(z)	522m(x), 498m(y), 174m(z)
	Grid size	87 (x) x 83(y) x 22 (z)	87 (x) x 83(y) x 40 (z)
	Grid Resolution	dx = dy = 6m, dz = 6m	dx = dy = 6m, dz = 3m
Configuration File	Simulation days	02–03.07.2015 (DD.MM.YYYY)	
	Simulation time (h)	48 (data analyzed for the last 24 h)	
	Location	Zurich	
	Include nesting Grid	No	
	Output interval main files	60 min	

Once the domain was defined, the 3D model of the Hochschulquartier was built. Detailed spatial data, collected by survey, was used to build a database in the appropriate formats required by the tool. The database includes topographical information, building geometry and materials, tree position and height, and surface cover. For some of the retrieved data, a process of classification allowed to reduce complexity while preserving the main characteristics of the district, i.e., building materials were classified in four categories according to the building's construction year and construction type, while trees were classified on the basis of height and leaf area density (Table 4.2). Moreover, two surface/soil materials, one for impervious (asphalt) and one for pervious surfaces (loamy soil), were used from the ENVI-met default Database (Table 4.3).

Table 4.4 shows the characteristics of the materials employed for the simulations in detail. ENVI-met simulations are performed using the full forcing method and employing weather data for the selected days from the SMA weather station. Hourly data of dry bulb temperature and relative humidity (shown in Figure 4.4) as well as the hourly average wind speed and predominant wind direction were used as forcing climate variables. The day under analysis was 3 July 2015, a hot day with clear sky. Taking into account initialization time, the simulation started at 00:00:01 on July 2 and had a duration of 48 h. Only the values of the last 24 h were then selected for the analysis. Simulations were carried out for Model A and B with the described settings. The validated model with higher level of accuracy will be selected and passed to CEA for the building energy demand simulation in the Microclimate case.

TABLE 4.2 Physical properties of the vegetation used in the ENVI-met model.

Physical properties	Deciduous Trees		
	Small	Medium	Large
Height (m)	5	15	25
Foliage Shortwave Albedo	0.18	0.18	0.18
Foliage Shortwave Transmittance	0.30	0.30	0.30

TABLE 4.3 Physical properties of the soil materials used in the ENVI-met model.

Physical properties	Soil Materials	
	Asphalt	Loamy Soil
Roughness	0.01	0.015
Albedo	0.2	0.2
Emissivity	0.9	0.98

4.4.3 CEA Database and Model Construction

The inputs to the CEA energy demand model comprise a set of primary and secondary inputs. The primary inputs to the simulation must be provided by the user as an input and correspond to the geometry, functional mix, and construction and renovation years for each building in the district. As previously mentioned, the spatial data for the Hochschulquartier case study area, such as the topography and building footprints, were retrieved from local GIS data. The number of floors and the construction year of each building were obtained from the Federal Register of Buildings and Dwellings (Bundesamt für Statistik, 2010). Each building's functional mix was derived from building catalogues obtained from the institutions that operate them, namely ETH Zürich and the University Hospital Zürich, as shown in Figure 4.3.

TABLE 4.4 Physical properties of the wall materials used in the ENVI-met model.

Physical properties	Material 1	Material 2	Material 3	Material 4
	Exposed concrete block, medium construction, old building	Exposed concrete block, heavy construction, old building	Exposed concrete block, medium construction, new building	Exposed concrete block, heavy construction, new building
Thickness (m)	0.30	0.30	0.30	0.30
Absorption	0.6	0.6	0.6	0.6
Transmission	0	0	0	0
Reflection	0.4	0.4	0.4	0.4
Emissivity	0.95	0.95	0.95	0.95
Specific Heat (J/kg·K)	840	840	840	840
Thermal conductivity (W/m·K)	0.225	0.225	0.06	0.06
Density (kg/m3)	665	1190	665	1190
U-value (W/m2·K)	0.75	0.75	0.2	0.2
Heat Capacity (kJ/m2·K)	165	300	165	300

In order to reduce the amount of data that needs to be collected for individual buildings, the secondary inputs to CEA may be supplied by the user where available, or otherwise derived from the CEA archetype database (Fonseca and Schlueter, 2015), which contains typical construction properties for a variety of building functions and construction years. These inputs include the thermal properties of the building envelope, building systems and controls, occupancy schedules, internal gains from occupant activities and electricity use, as well as the indoor comfort setpoints. For the present study, window-to-wall ratios were estimated based on the actual characteristics of the buildings, while construction materials from the CEA archetype database were adapted in order to match the

inputs required for the ENVI-met simulation (Table 4.4) and assigned to individual buildings based on their construction year. All other inputs were derived from the CEA archetype database for the corresponding construction years and building functions. The most relevant secondary input parameters used in the model of the Hochschulquartier are summarized in Table 4.5.

While CEA includes a stochastic occupancy model (Mosteiro- Romero et al., 2020), the simpler standard-based deterministic schedules of occupant presence and electricity consumption were used in this study in order to isolate the effects of microclimate from changes in occupancy patterns. As discussed in section "Wind Speed Effects on Air Infiltration," the CEA dynamic infiltration model was used and a dynamic convective heat transfer model was added to the software in order to fully capture the effects of wind speed on the predicted demands of the district.

TABLE 4.5 CEA model settings used in the case study.

Input parameter		Range of values (number of buildings)			
U-values (W/m2·K)	**Roof**	0.15 (2)	0.2 (24)	0.3 (8)	0.6 (2)
	Walls	0.15 (25)	0.75 (11)		
	Basement	0.25 (25)	2.9 (11)		
	Windows	0.99 (2)	1.3 (23)	3.1 (10)	
Window-to-wall ratios		< 25% (8)	25–34% (13)	35–49% (8)	≥ 50% (7)
Type of construction		Light (1)	Medium (18)	Heavy (17)	
Cooling systems		Air-based: 6°C supply/15°C return (all buildings)			

4.5 Results

The following sections describe the results from the microclimate simulation and its consequent effects on the predicted space cooling demand for the case study area. In the first section, ENVI-met results are validated by comparing the simulated air temperature on the roof of a building in the case study area to measured data from a sensor on the roof of that building. The local microclimate is then characterized by comparison to the data from the off-site weather station SMA. The CEA simulation results for space cooling demand for the Baseline case using weather station data are compared to the Microclimate case using ENVI-met results as an input.

4.5.1 Validation of the ENVI-met Model

In order to validate the results of the microclimate model obtained through ENVI-met, the simulated results are compared to field measurements. This process allows to evaluate the model accuracy and the reliability of the input data. A temperature sensor positioned on the roof of the *Maschinenlaboratorium* (ML) building, located within the case study area (Figure 4.3) provides measured data for the period studied with a time interval of 15 min.

A mesh sensitivity analysis is performed to estimate the accuracy of ENVI-met while changing the height resolution. This analysis consists of the comparison of the simulation results between two models with a respective resolution of 6 m(x) x 6 m(y) x 6 m (z) (Model A) and 6 m(x) x 6 m(y) x 3 m(z) (Model B) for 2–3 July. Simulation data for the comparison is extracted at the same height as the actual temperature sensor.

Figure 4.5 compares the hourly evolution of measured temperature with ENVI-met modelled temperatures. Results show a similar pattern between simulated and monitored data and good stability of ENVI-met concerning the sensitivity to cell height resolution. However, for both models, the simulated air temperature is higher than the measured air temperatures during daytime hours with an absolute maximum divergence of 1.9°C (Model B) and 2.3(°C (Model A). As the change in mesh resolution shows minor variations in the computation of air temperature values, a comparison of the Mean Absolute Error (MAE) is employed to estimate the average of the absolute residual values. As Model B presents slightly lower MAE value (0.80) than Model A (0.91), the simulation results from Model B are used as boundary climate conditions for the Microclimate Case in CEA.

Before passing the data to CEA, the accuracy of the ENVI- met model performance is examined through few parameters, usually applied to ensure the reliability of the simulations' outputs (Tsoka et al., 2018). For this purpose, a linear covariance correlation (R2) is carried out. As statistically significant values of R2 are often unrelated to the magnitude of differences between observations and predictions (Willmott, 1983), the Root Mean Square Error (RMSE), which describes the magnitude of mean differences between observed and predicted values, and the index of agreement (d), which indicates the degree of model prediction error, were determined additionally.

The model is considered reliable when $R2$ and d both tend to 1 and RMSE tends to 0. The measured parameters show that the simulation results are highly accurate, with a $R2$ of 0.97, d index of 0.98 and a RMSE of 1.02°C. Thus, the comparison confirms

that ENVI-met has simulated atmospheric temperature in the studied area with good accuracy. However, the model tends to overestimate daytime temperature up to 2°C and a divergence of this magnitude might have repercussions on energy demand estimation.

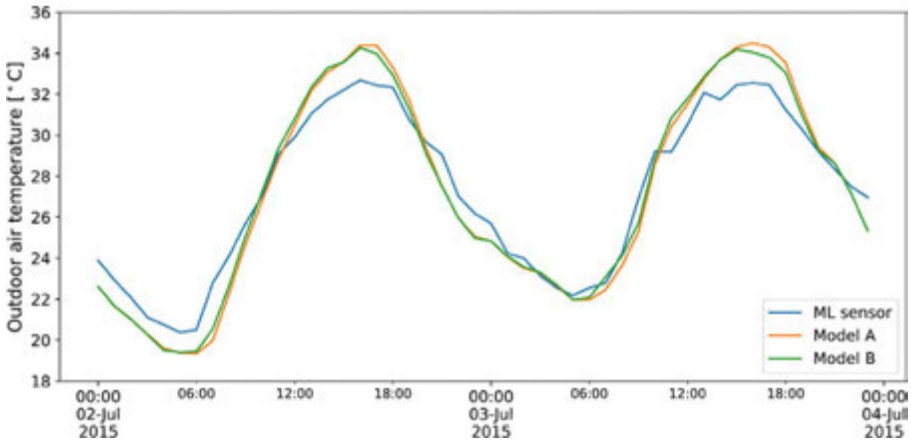


FIG. 4.5 Outdoor air temperature results from the microclimate simulations for Model A and Model B compared to measured data from the sensor on the ML building.

4.5.2 Microclimate Characteristics of the Hochschulquartier

The radiative, aerodynamic and thermal properties of urban materials lead to microclimatic processes that are reflected in the distinct formulation of the Surface Energy Balance (SEB) for rural and urban systems. In particular, the SEB of cities is influenced by the larger heat storage capacity of urban materials, and thermal exchanges between built surfaces and the atmosphere. Urban materials and geometric characteristics contribute to the local climate performance of the district by influencing solar access, radiative absorption and friction to wind flows. Such a performance is examined here based on the ENVI-met results of air temperature, relative humidity, and wind speed. The overall microclimate profile of the Hochschulquartier is observed by analysing averaged hourly values for the full district, while a more detailed spatial analysis allows the understanding of microclimate patterns and the local climate context of each building in the district.

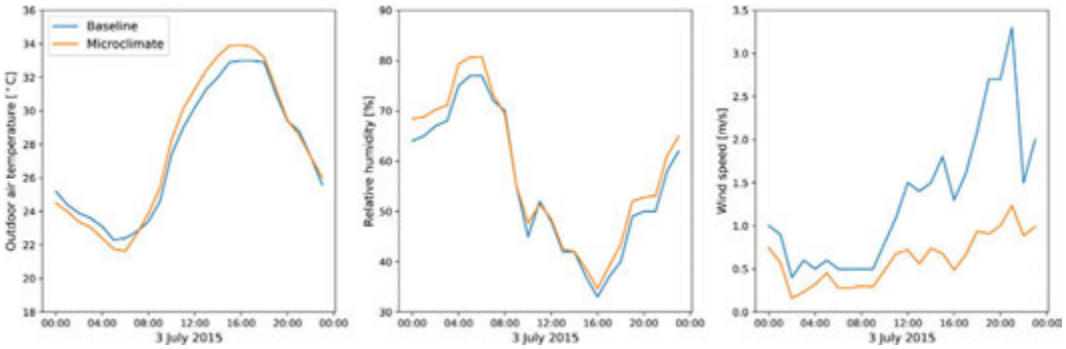


FIG. 4.6 Simulated mean air temperature, relative humidity and wind speed in the area compared to data from Baseline climate values.

For the analysis of the Hochschulquartier microclimate profile, values around building envelopes are obtained from ENVI-met results for air temperature, wind speed and relative humidity. Aggregated district data reporting average values are then compared to the Baseline climate values, used as boundary conditions for the simulation. Figure 4.6 shows that local temperatures are generally around 0.7°C lower during night- time and 1.2°C higher during daytime compared to Baseline temperatures. The maximum variation is reached during the warmest hours when the local temperature increases till 34°C.

The simulation results show slightly higher values than the Baseline regarding relative humidity, however, minor variations are observed during the warmest hours of the day. As processes of evapotranspiration and evaporation are usually enhanced by solar radiation, this pattern suggests that the presence of unpaved surfaces and greening gives a minor contribution to the moisture level of the Hochschulquartier. Thus, higher values of local relative humidity during night hours might be influenced by lower temperatures and by lower wind velocity in the district that prevent humidity dispersion. Additionally, the average wind speed around the buildings compared to the Baseline shows a relevant decrease in velocity during the second half of the day. This suggests that the roughness elements such as buildings and trees generally contribute to lowering the wind velocity; wind speeds are below 1.3 m/s in the Hochschulquartier while the meso-scale wind velocity reaches 3 m/s.

Moreover, the observation of the Hochschulquartier results, visualized through the ENVI-met visualization tool Leonardo, highlights daily microclimate patterns on the horizontal dimension. To better describe the distribution of thermal and ventilation effects, three representative hours for the morning, afternoon and night patterns are selected. Figure 4.7 shows the distribution of ambient temperature values in the district. Relevant variations, in the range of 4°C, are observed during daytime.

While during morning hours higher values are registered in the central part of the district, during afternoon hours the west part results to be consistently warmer, reaching 38°C. The west part also has a lower absorption capacity than the east part since during night hours temperature values quickly decrease inverting the daytime pattern. However, the difference in temperature during the night-time is lower, at around 1°C.

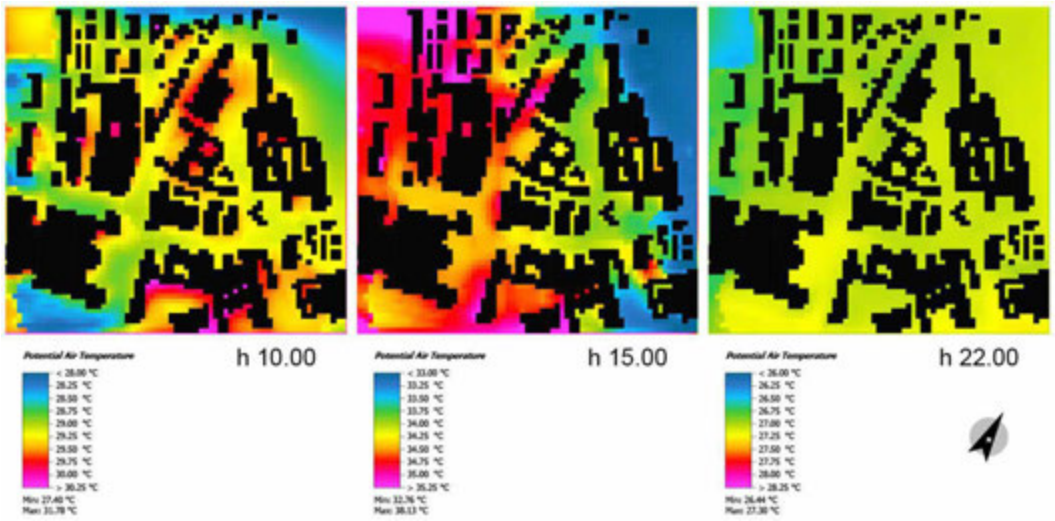


FIG. 4.7 Spatial distribution of air temperature at 2 m height.

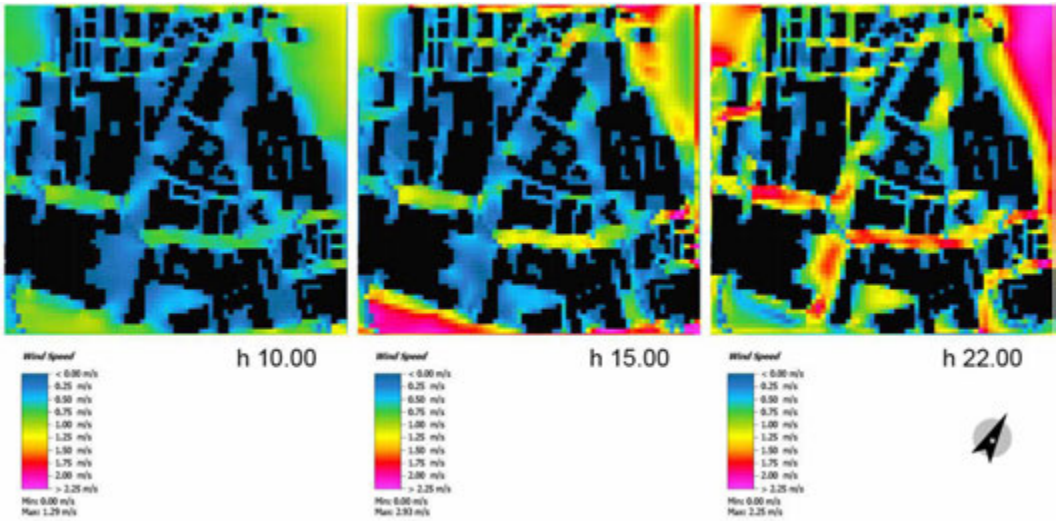


FIG. 4.8 Spatial distribution of wind speed at 2 m height.

TOC

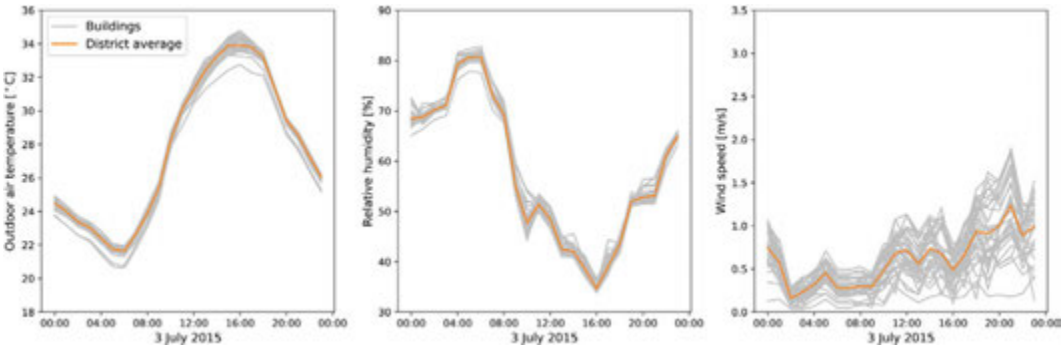


FIG. 4.9 Simulated mean air temperature, relative humidity and wind speed around buildings.

Figure 4.8 shows wind velocity results for three hours that were found to be representative of the wind flow distribution in the area. Generally, the spatial visualization confirms the overall microclimate profile indicating that the roughness level of the district significantly lowers wind velocity. However, some variations can be observed concerning the southern part of the area. Here the main street canyons generally show higher wind velocities than the rest of the district during day and night hours. In particular, the street with direction east-west sees an increase in flow velocity from 0.75 m/s in the morning to 2 m/s in the night. This pattern seems to be a function of the meso-scale input, suggesting that the southern street canyons are most influenced by changes in meso-scale wind flows.

Finally, Figure 4.9 shows the hourly results for air temperature, relative humidity and wind speed around each building under analysis. These values have been used as boundary climate conditions in the CEA simulation for the Microclimate case. The differences observed between buildings confirm the previous spatial analysis that showed significant variations within the area and distribution patterns during day and night-time, in particular regarding wind speed.

4.5.3 Comparison of the Space Cooling Demand for Each Weather Case

The district's space cooling demand was simulated in CEA using the Baseline climate dataset and the microclimate simulation results from ENVI-met for the day being analysed (3 July 2015). The distribution of the predicted space cooling demand for each building on the selected day is shown in Figure 4.10. The results show that the cooling demands in the area are dominated by sensible cooling, meaning that

air dehumidification contributes a comparatively lower share of the total cooling demand in the district. Accounting for local microclimate in the simulations leads to an increase in the daily and peak demands for both latent and sensible cooling. The results for the peak latent cooling show a smaller spread for the Microclimate case, with a higher average value but a lower maximum.

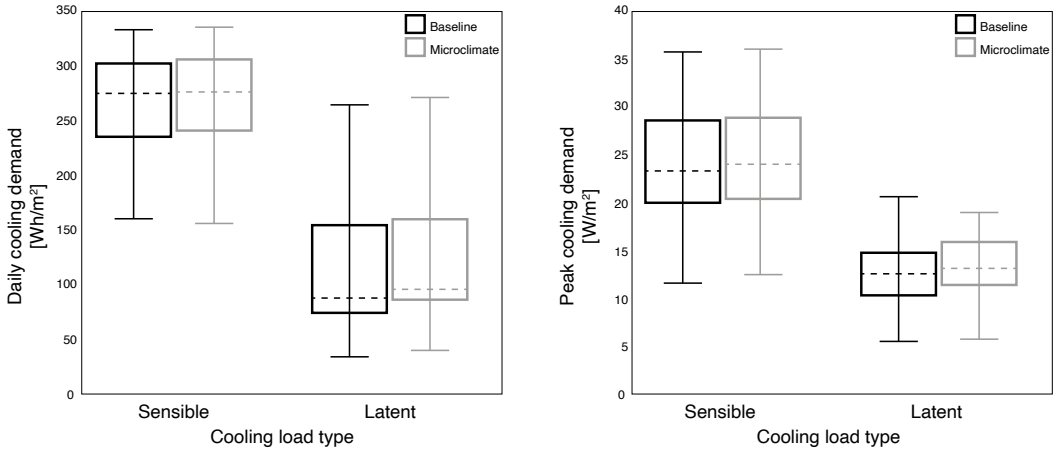


FIG. 4.10 Box plots showing the space cooling demand and peak cooling power on the selected day when using weather station data compared to using local microclimate simulations. The total space cooling demand comprises the sensible and latent demands.

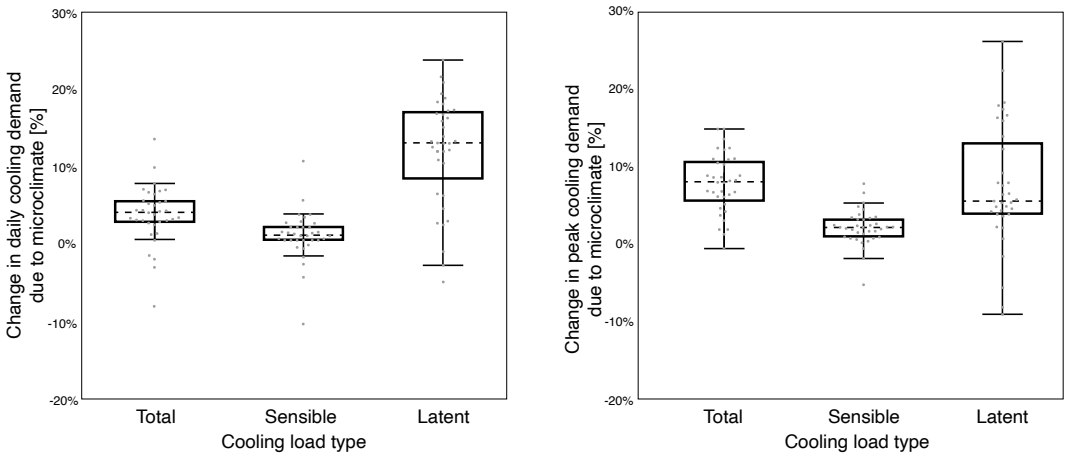


FIG. 4.11 Box plots showing the change in space cooling demand and peak cooling power on the selected day when replacing the weather station data with simulated local microclimate results. The total space cooling demand comprises the sensible and latent demands.

TOC

In relative terms, as shown in Figure 4.11, accounting for local microclimate leads to a 5% increase in the district's space cooling demand on this day, with a maximum increase of 14% for one of the buildings. The effects are even more visible on the peak demands, where the use of simulated microclimate data leads to an average increase of 8% in the peak cooling power required by the buildings in the district. The peak cooling demand is increases by up to 15%. The increase in space cooling demand is mainly caused by latent cooling, which increases by 11% for the entire district. This is due to both the increase in relative humidity when accounting for microclimate as well as the overall lower wind speeds in the area. Since wind speed affects the infiltration rate in individual buildings, the required ventilation rate is also affected by local low wind velocity, as discussed in section "Wind Speed Effects on Air Infiltration." The overall lower wind speeds in the district lead to lower air infiltration, which in the CEA calculation leads to increased ventilation rates and thus the amount of air that needs to be dehumidified also increases. This is further demonstrated by the large spread in the variation in latent cooling demand, and particularly for the peak latent cooling load. The large variations in wind speed around individual buildings observed in Figure 4.9, leads to varying ventilation rates in different buildings, and hence the latent cooling loads vary from building to building.

However, a few outliers for which the cooling demand actually decreases when including microclimate are also encountered. This effect can be explained by analysing the hourly results, shown in Figure 4.12. The area has a distinct cooling load pattern that closely follows the occupancy and lighting schedules in the buildings, with two peaks and a valley during the middle of the day as building occupants leave their work spaces for lunch. When accounting for the effects of urban microclimate, the overall cooling demand is higher during the second peak due to the increased outdoor air temperatures, leading to an overall higher cooling peak for the district. However, the cooling demand is lower in the morning peak due to the lower latent cooling in the morning hours. At least one of the buildings has its peak cooling demand at 10 in the morning in the Baseline case. At this time, however, the distribution in the cooling loads for the buildings in the area is drastically smaller in the Microclimate case. Hence, some buildings have lower peak cooling demands on the selected day due to the lower morning peak.

The deviation for individual buildings is shown spatially in Figure 4.13. The results show that the change in daily space cooling demand is greatest for a large historical building in the area. This building includes sports facilities, and therefore require a significant amount of cooling and dehumidification. Furthermore, as an older building the infiltration rate is large, thus the aforementioned variation in wind speed has a particularly large effect for this building. The increase in the peak cooling demand,

on the other hand, is greatest for hospital buildings, concentrated on the eastern part of the district. Relative decreases in space cooling demand are comparatively smaller and mostly correspond to smaller buildings.

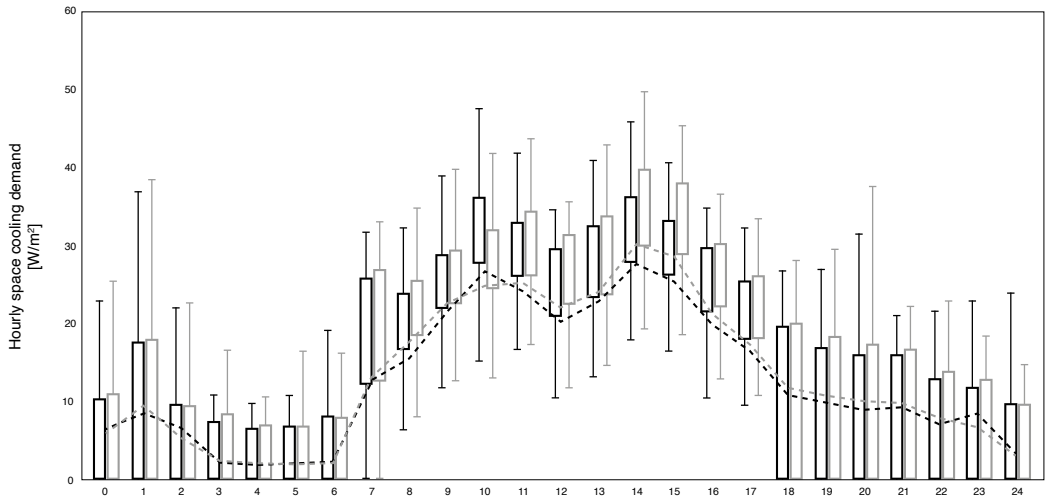


FIG. 4.12 Hourly space cooling demand in the district on the selected day for each of the climate cases. The boxplots at each hour show the distribution in the space cooling demand per conditioned floor area for all buildings in the area, whereas the lines show the entire district's demand per square meter for each case.

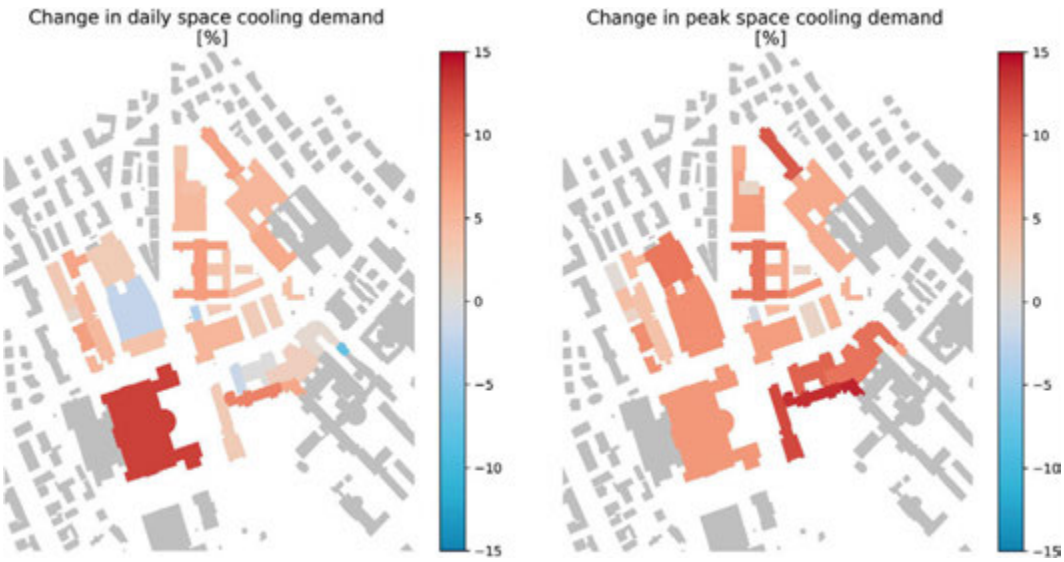


FIG. 4.13 Change in total and peak cooling demand on the selected day due to the effect of microclimate for each building in the area.

TOC

4.6 Limitations

The proposed method represents a promising new approach to analyse the mutual interactions between buildings and microclimate in urban districts. Regarding the application of the method on the Hochschulquartier district, the study has shown significant variations in cooling demand between a Baseline and a Microclimate case, confirming the findings of previous studies regarding the increase of cooling loads when local climate phenomena are taken into account in the energy assessment (Santamouris, 2014; Li et al., 2019). However, in the energy simulations the microclimate profile of the area was compared to the Baseline climate data derived from an offsite weather station in Zurich Fluntern. Since the weather station is located in a suburban area the magnitude of the UHI phenomena is not fully captured. Thus, the use of rural weather data for the Baseline energy scenario would likely result in higher variations of cooling loads between the two cases.

The applicability of the method is furthermore somewhat limited by the extremely high computational costs, in particular for running ENVI-met simulations. In the present work, a one-way integration method was investigated, whereby urban microclimate affected energy performance, but buildings' energy consumption did not affect microclimate. However, given the feedback loop created between urban microclimate, buildings' energy performance, building surface temperatures and heat emissions from cooling systems, an iterative simulation method would be required to fully capture these mutual effects, however, this would further explode the computational expense of the method.

While the method permits the exploration of different coexisting geometries, materials, energy systems and the analysis of their effects during extreme weather events, planning energetic interventions based on analysing patterns observed during a single day is not recommended. The implementation of this methodology during the design process might thus hinge on the further development of less computationally expensive methods to provide high-resolution simulations of local climate in urban areas. Further work needs to be carried out to expand the time scale of urban microclimate simulations without losing spatial resolution in order to support design assessment and energy demand simulations.

4.7 Conclusions

The study outlines a method for quantitative analysis of district- scale energy consumption taking into account the microclimatic effects created by the design of open and built space. The study constitutes a first attempt at coupling microclimate and building energy modelling tools at the district scale. The method applied to a case study in Zurich, Switzerland showed that the coupled tools can deal with complex geometrical, material and behavioural features. Validated ENVI-met results were used to analyse microclimate patterns in the case study for a hot summer day during a heat wave. The space cooling demand for the buildings in the area was modelled in the City Energy Analyst (CEA) in order to assess the district's energy performance when accounting for the local microclimate. Results were compared to a second energy demand simulation using measured data from an offsite weather station.

For the exemplary case study, the urban microclimate model showed good agreement with the measured data available in the district analysed. The comparison between Microclimate and Baseline climate values showed that mean local air temperature was generally higher during daytime in a range of 1.2°C, while humidity was higher during night hours. However, when analysing more in detail the spatial distribution of microclimate variables it is possible to observe that during the daytime the west part of the district was significantly warmer than the east part and temperature rapidly decreased during night-time. This thermal pattern suggests a relatively low absorption capacity of the western part of the district, influenced by material characteristics and urban form. In addition, the roughness level of the district contributes to lower local mean wind velocity, which was below 1.3 m/s throughout the day, while a relative increase in wind speed and turbulence is observed along the street canyons in the south part of the district.

While the increased air temperatures due to local microclimate led to an increase in the sensible cooling demand in the case study area, the increased relative humidity and the high variance in the local wind speed led to an even greater change in the latent cooling demand. Overall, the district's space cooling demand on the selected day was found to increase by 5% when considering local microclimate, with an average increase in the peak cooling demand of 8%. Moreover, the coupling method allowed a detailed analysis of the different effects microclimate can have on buildings' energy, showing that, when considering the local climate patterns, space cooling demand on the selected day varied between 5% and +14%.

The results indicate the capacity of the integrated method to depict the influence of microclimatic conditions on the cooling demand in an urban district. By expanding the scope from the single-building to the district scale, the method can be used to explore the mutual thermal and aerodynamic influence between buildings, and the consequent impact on the cooling loads at both the building and the district scale. In particular, the fine resolution of the results allows a deep understanding of the variation in performance of single buildings depending on local climate patterns of ambient temperature, relative humidity and wind velocity. Therefore, the method can support the challenge of improving building energy efficiency by offering an assessment instrument that integrates form configuration, materials and consequent microclimate factors.

Further consideration should be given to the possible employment of this method during the design process and not only as an assessment instrument. In the current study, an existing district was modelled in order to validate the microclimate simulations against measured data. Future studies could use the proposed methodology to further explore the effects of design decisions on future districts' performance as well as to test the potential for urban form interventions to mitigate the urban heat island and reduce cooling demand.

Author contributions

Maiullari and Mosteiro-Romero contributed equally to this work and are co-main authors of this article.

Funding

This research was developed as part of the project SPACERGY, within the JPI Urban Europe research framework. The work presented in this paper was financed by the Swiss Federal Office of Energy (SI/501404-01) and the Netherlands Organisation for Scientific Research (NWO 438.15.413).

References

Ali-Toudert, F., and Mayer, H. (2006). Numerical study on the effects of aspect ratio and orientation of an urban street canyon on outdoor thermal comfort in hot and dry climate. Build. Environ. 41, 94–108. doi: 10.1016/J.BUILDENV.2005. 01.013

Ali-Toudert, F., and Mayer, H. (2007). Effects of asymmetry, galleries, overhanging façades and vegetation on thermal comfort in urban street canyons. *Solar Energy* 81, 742–754. doi: 10.1016/j.solener.2006. 10.007

Allegrini, J., Dorer, V., and Carmeliet, J. (2012). Influence of the urban microclimate in street canyons on the energy demand for space cooling and heating of buildings. *Energy Build.* 55, 823–832. doi: 10.1016/j.enbuild.2012.10. 013

Allegrini, J., Orehounig, K., Mavromatidis, G., Ruesch, F., Dorer, V., and Evins, R. (2015). A review of modelling approaches and tools for the simulation of district-scale energy systems. *Renew. Sustain. Energy Rev.* 52, 1391–1404. doi: 10.1016/j.rser.2015.07.123

Baudirektion Kanton Zürich (2014). Masterplan Hochschulgebiet Zürich-Zentrum. Zurich: Zentrum University.

Blocken, B. (2014). 50 years of computational wind engineering: past, present and future. *J. Wind Eng. Indust. Aerodyn.* 129, 69–102. doi: 10.1016/j.jweia.2014.03. 008

Bruse, M., and Fleer, H. (1998). Simulating surface-plant-air interactions inside urban environments with a three dimensional numerical model. *Environ. Model. Softw.* 13, 373–384. doi: 10.1016/S1364-8152(98)00042-5

Bundesamt für Statistik (2010). *Eidgenössisches Gebäude- und Wohnungsregister*. Neuchâtel: Bundesamt für Statistik (BFS).

Carnielo, E., and Zinzi, M. (2013). Optical and thermal characterisation of cool asphalts to mitigate urban temperatures and building cooling demand. *Build. Environ.* 60, 56–65. doi: 10.1016/J.BUILDENV.2012. 11.004

The CEA Team (2018). *City Energy Analyst v2.9.0*. Zenodo. doi: 10.5281/zenodo.1487867

Cui, Y., Yan, D., Hong, T., and Ma, J. (2017). Temporal and spatial characteristics of the urban heat island in Beijing and the impact on building design and energy performance. *Energy* 130, 286–297. doi: 10.1016/j.energy.2017.04.053

DIN EN 16798-7 (2015). Energieeffizienz von Gebäuden – Berechnungsmethoden zur Bestimmung der Luftvolumenströme in Gebäuden inklusive Infiltration. Berlin: Deutsches Institut für Normung.

Eurostat (2016). Urban Europe – Statistics on Cities, Towns and Suburbs. Luxembourg: European Union.

Fonseca, J., and Schlueter, A. (2015). Integrated model for characterization of spatiotemporal building energy consumption patterns in neighborhoods and city districts. *Appl. Energy* 142, 247–265. doi: 10.1016/j.apenergy.2014.12.068

Frank, T. (2005). Climate change impacts on building heating and cooling energy demand in Switzerland. *Energy Build.* 37, 1175–1185. doi: 10.1016/J.ENBUILD. 2005.06.019

Frayssinet, L., Merlier, L., Kuznik, F., Hubert, J., Milliez, M., and Roux, J. (2018). Modeling the heating and cooling energy demand of urban buildings at city scale. *Renew. Sustain. Energy Rev.* 81, 2318–2327. doi: 10.1016/j.rser.2017.06. 040

Gobakis, K., and Kolokotsa, D. (2017). Coupling building energy simulation software with microclimatic simulation for the evaluation of the impact of urban outdoor conditions on the energy consumption and indoor environmental quality. *Energy Build.* 157, 101–115. doi: 10.1016/j.enbuild.2017. 02.020

Gonseth, C., Thalmann, P., and Vielle, M. (2017). Impacts of global warming on energy use for heating and cooling with full rebound effects in Switzerland. *Swiss J. Econ. Statist.* 153, 341–369. doi: 10.1007/BF03399511

Gros, A., Bozonnet, E., and Inard, C. (2014). Cool materials impact at district scale – coupling building energy and microclimate models. *Sustain. Cit. Soc.* 13, 254–266. doi: 10.1016/j.scs.2014.02.002

Gros, A., Bozonnet, E., Inard, C., and Musy, M. (2016). Simulation tools to assess microclimate and building energy – A case study on the design of a new district. *Energy Build.* 114, 112–122. doi: 10.1016/j.enbuild.2015. 06.032

Guattari, C., Evangelisti, L., and Balaras, C. (2018). On the assessment of urban heat island phenomenon and its effects on building energy performance: a case study of Rome (Italy). *Energy Build.* 158, 605–615. doi: 10.1016/j.enbuild.2017. 10.050

Happle, G., Fonseca, J., and Schlueter, A. (2017). Effects of air infiltration modeling approaches in urban building energy demand forecasts. *Energy Proc.* 122, 283–288. doi: 10.1016/j.egypro.2017.07.323

He, J., Hoyano, A., and Asawa, T. (2008). A numerical simulation tool for predicting the impact of outdoor thermal environment on building energy performance. *Appl. Energy* 86, 1596–1605. doi: 10.1016/j.apenergy.2008.12.034 Hirano, Y., and Fujita, T. (2012). Evaluation of the impact of the urban heat island on residential and commercial energy consumption in Tokyo. *Energy* 37, 371–383. doi: 10.1016/j.energy.2011.11.018

Huttner, S. (2012). Further Development and Application of the 3D Microclimate Simulation ENVI-Met. Mainz: University of Mainz.

ISO 52016-1 (2017). Energy Performance of Buildings – Energy Needs for Heating and Cooling, Internal Temperatures and Sensible and Latent Heat Loads - Part 1: Calculation Procedures. Geneva: International Organization for Standardization.

ISO 13790 (2008). Energy Performance of Buildings –Calculation of Energy Use for Space Heating and Cooling. Geneva: International Organization for Standardization.

ISO 6946 (2007). Building Components and Building Elements — Thermal Resistance and Thermal Transmittance — Calculation Method. Geneva: International Organization for Standardization.

ISO 9972:2015 (2015). Thermal Performance of Buildings – Determination of Air Permeability of Buildings – Fan Pressurization Method (ISO 9972:2015). Berlin: DIN Deutsches Institut für Normung.

Kolokotroni, M., Davies, M., Croxford, B., Bhuiyan, S., and Mavrogianni, A. (2010). A validated methodology for the prediction of heating and cooling energy demand for buildings within the Urban Heat Island: case-study of London. Solar Energy 84, 2246–2255. doi: 10.1016/j.solener.2010.08.002

Li, X., Zhou, Y., Yu, S., Jia, G., Li, H., and Li, W. (2019). Urban heat island impacts on building energy consumption: a review of approaches and findings. *Energy* 174, 407–419. doi: 10.1016/j.energy.2019.02.183

Liu, J., Heidarinejad, M., Guo, M., and Srebric, J. (2015). Numerical evaluation of the local weather data impacts on cooling energy use of buildings in an urban area. *Proc. Eng.* 121, 381–388. doi: 10.1016/j.proeng.2015.08. 1082

Liu, Y., Stouffs, R., Tablada, A., Wong, N. H., and Zhang, J. (2017). Comparing micro-scale weather data to building energy consumption in Singapore. *Energy Build.* 152, 776–791. doi: 10.1016/j.enbuild.2016.11.019

Magli, S., Lodi, C., Lombroso, L., Muscio, A., and Teggi, S. (2015). Analysis of the urban heat island effects on building energy consumption. *Intern. J. Energy Environ. Eng.* 6, 91–99. doi: 10.1007/s40095-014-0154-9

Mauree, D., Coccolo, S., Monna, S., Kämpf, J., and Scartezzini, J. (2016). "On the impact of local climatic conditions on urban energy use: a case study," in *Proceedings of the PLEA 2016 Los Angeles - 36th International Conference on Passive and Low Energy Architecture*, Los Angeles.

Meteotest (2014). Meteonorm Version 7.1. Bern: Meteotest.

Mirzaei, P., and Haghighat, F. (2010). Approaches to study urban heat island – Abilities and limitations. *Build. Environ.* 45, 2192–2201. doi: 10.1016/j.buildenv. 2010.04.001

Mosteiro-Romero, M., Hischier, I., Fonseca, J. A., and Schlueter, A. (2020). A novel population-based occupancy modeling approach for district-scale simulations compared to standard-based methods. *Build. Environ.* 181:107084. doi: 10. 1016/j.buildenv.2020.107084

Mussetti, G., Brunner, D., Allegrini, J., Wicki, A., Schubert, S., and Carmeliet, J. (2019). Simulating urban climate at sub-kilometre scale for representing the intra-urban variability of Zurich, Switzerland. *Intern. J. Climatol.* 40, 458–476. doi: 10.1002/joc.6221

OcCC and ProClim (2007). Climate Change and Switzerland 2050: Expected Impacts on Environment, Society and Economy. Bern: Advisory Body on Climate Change (OcCC)-ProClim.

Oke, T., Mills, G., Christen, A., and Voogt, J. (2017). *Urban Climates*. Cambridge: Cambridge University Press.

Ooka, R. (2007). Recent development of assessment tools for urban climate and heat-island investigation especially based on experiences in Japan. *Intern. J. Climatol.* 27, 1919–1930. doi: 10.1002/joc.1630

Rasheed, A., Robinson, D., Clappier, A., Narayanan, C., and Lakehal, D. (2011). Representing complex urban geometries in mesoscale modeling. *Intern. J. Climatol.* 31, 289–301. doi: 10.1002/joc.2240

Reinhart, C. (2013). *DAYSIM Version 4.0*.

Reinhart, C., and Cerezo Davila, C. (2016). Urban building energy modeling – A review of a nascent field. *Build. Environ.* 97, 196–202. doi: 10.1016/j.buildenv. 2015.12.001

Sánchez de la Flor, F., and Álvarez Domínguez, S. (2004). Modelling microclimate in urban environments and assessing its influence on the performance of surrounding buildings. *Energy Build.* 36, 403–413. doi: 10.1016/j.enbuild.2004. 01.050

Santamouris, M. (2014). On the energy impact of urban heat island and global warming on buildings. *Energy Build.* 82, 100–113. doi: 10.1016/j.enbuild.2014. 07.022

Santamouris, M., Papanikolaou, N., Livada, I., Koronakis, I., Georgakis, C., Argiriou, A., et al. (2001). On the impact of urban climate on the energy consumption of buildings. *Solar Energy* 70, 201–216. doi: 10.1016/S0038- 092X(00)00095-5

SIA Merkblatt 2044 (2011). *Klimatisierte Gebäude – Standard- Berechnungsverfahren für den Leistungs- und Energiebedarf.* Zürich: Schweizerischer Ingenieur- und Architektenverein (SIA).

Skelhorn, C., Levermore, G., and Lindley, S. (2016). Impacts on cooling energy consumption due to the UHI and vegetation changes in manchester, UK. *Energy Build.* 122, 150–159. doi: 10.1016/j.enbuild.2016. 01.035

Sola, A., Corchero, C., Salom, J., and Sanmarti, M. (2018). Simulation tools to build urban-scale energy models: a review. *Energies* 11:3269. doi: 10.3390/ en11123269

Sun, Y., and Augenbroe, G. (2014). Urban heat island effect on energy application studies of office buildings. *Energy Build.* 77, 171–179. doi: 10.1016/j.enbuild. 2014.03.055

Taleghani, M., Kleerekoper, L., Tenpierik, M., and van den Dobbelsteen, A. (2015). Outdoor thermal comfort within five different urban forms in the Netherlands. *Build. Environ.* 83, 65–78. doi: 10.1016/j.buildenv.2014. 03.014

Toparlar, Y., Blocken, B., Maiheu, B., and van Heijst, G. (2017). A review on the CFD analysis of urban microclimate. *Renew. Sustain. Energy Rev.* 80, 1613–1640. doi: 10.1016/j.rser.2017.05.248

Toparlar, Y., Blocken, B., Maiheu, B., and van Heijstd, B. (2018). Impact of urban microclimate on summertime building cooling demand: a parametric analysis for Antwerp, Belgium. *Appl. Energy* 228, 852–872. doi: 10.1016/j.apenergy.2018. 06.110

Tsoka, S., Tsikaloudaki, A., and Theodosiou, T. (2018). Analyzing the ENVI-met microclimate model's performance and assessing cool materials and urban vegetation applications–A review. *Sustain. Citi. Soc.* 43, 55–76. doi: 10.1016/j. scs.2018.08.009

Willmott, C. J. (1983). Some comments on the evaluation of model performance. *Exper. Techn.* 7, 20–21. doi: 10.1111/j.1747-1567.1983.tb0 1755.x

Wong, N. H., Ignatius, M., Eliza, A., Jusuf, S. K., and Samsudin, R. (2012). Comparison of STEVE and ENVI-met as temperature prediction models for Singapore context. *Intern. J. Sustain. Build. Technol. Urban Dev.* 3, 197–209. doi: 10.1080/2093761X.2012.720224

World Energy Council (2016). *World Energy Scenarios 2016 – The Grand Transition.* London: World Energy Council.

Yang, X., Zhao, L., Bruse, M., and Meng, Q. (2012). An integrated simulation method for building energy performance assessment in urban environments. *Energy Build.* 54, 243–251. doi: 10.1016/j.enbuild.2012.07.042

5 Energy Performance in Local Climate Types

Application of an Integrated Microclimate-Energy Demand Simulation Method in a Dutch Context

ABSTRACT Urban Heat Islands significantly influence the energy demand of the built environment. To aid the assessment of district and building energy demand, coupling attempts between climate models and energy models have been made, allowing for a better understanding of the local climate influence on building energy loads. However, these modelling studies typically focus on the analysis of generalized building types and homogeneous urban patterns, overlooking the complexity of urban environments. Additionally, the majority of the energy assessments do not distinguish between the energy impacts of buildings and context form characteristics. In order to investigate the influence of urban form characteristics on cooling loads in urban climates, this study uses microclimate simulation results (ENVI-met) as input to a district-scale energy demand model (City Energy Analyst; CEA) to assess different urban types in the city of Rotterdam, The Netherlands. The study identifies local climate types (LCTs) based on building and context form characteristics, through an unsupervised classification technique. For the selected 25 types, energy simulations in CEA are carried out for two scenarios: a Baseline scenario, employing rural climate data, and a Microclimate scenario,

employing microclimate results from the ENVImet modelling. The microclimate simulations for two consecutive representative hot days show that in the urban environment air temperatures are higher than in the rural environment, within a range of 3°C, leading to an average cooling demand increase between 24% and 32% in the city of Rotterdam. However, it is observed that cooling loads increase when the sensitivity of building type to urban overheating increases. Taking into account microclimate conditions, low-rise buildings are found to have the highest cooling demand increase between 31% and 58%. On average, mid-rise buildings increase their energy load between 20% and 34% while high-rise buildings' energy loads increase between 9% and 13%. Additionally, dense and high-rise contexts decrease the impact of day-time urban temperatures on energy demand for all the building types under study.

5.1 Introduction

Urban form factors have been found to play a crucial role in shaping the energy demand of buildings (Quan & Li, 2021; Silva et al., 2017; Sanaieian et al., 2014). Quantitative morphological studies have shown significant correlations between energy loads and parameters measuring building characteristics such as compactness (Depecker et al., 2001; Rode Philipp et al., 2014), orientation (Ascione et al., 2019; Mangan et al., 2021) and size (Martins et al., 2019; Steadman et al., 2014). Other studies have also highlighted that form attributes of the urban fabric such as density (Ahmadian et al., 2021; Javanroodi & Nik, 2019), roughness (Salvati et al., 2019; Gracik et al., 2015) and greenery (Aboelata & Sodoudi, 2019; Wong et al., 2011) affect energy consumption by modifying the local thermal conditions of urban environments. Urban form is in fact one of the factors responsible for warming mechanisms, such as the Urban Heat Island (UHI) effect, which contributes to increasing cooling energy consumption in cities (Hirano & Fujita, 2012; Liu et al., 2017; Guattari et al., 2018; Santamouris, 2020). UHIs are caused by anthropogenic activities, material and geometrical properties of urban environments, which influence the thermal exchange between buildings, surfaces and local environment, modifying air temperatures and wind patterns in which buildings operate. Higher radiation storage and lower wind speed, heat dispersion capacity and evapotranspiration result in higher air and surface temperatures in cities than in rural areas (Oke et al., 2017). As a consequence, both average electricity consumption and peak electricity demand for cooling purposes are significantly higher in cities due to the UHI effect (Santamouris, 2014; Li et al., 2019).

Although a few studies have acknowledged that it is fundamental to take urban climate conditions into consideration to estimate building energy demand with more accuracy (Magli et al., 2015; Skelhorn et al., 2016; Allegrini et al., 2012), further research is necessary to understand to what extent urban climate and morphological patterns affect building cooling demand and how the combination of building and context form characteristics influences the variations.

The two main approaches currently employed for assessing the effect of UHI on energy consumption present some limitations in addressing the morphological components. The first approach relies on rural and urban temperature data as boundary climate conditions for energy modelling (Hassid et al., 2000; Hong et al., 2021; Zinzi & Carnielo, 2017). In these studies, modelling techniques are usually applied to compare the energy needs of a reference building in rural and urban environments on a seasonal or annual base. While offering a first indication of the magnitude of demand variation caused by urban climate (at the mesoscale), the approach does not allow for the understanding of the complex trade-off between building types and contextual conditions at the micro-scale, because of the single building focus and the spatially unspecified setting. The second approach enlarges the scale of study to a district level and relies on advanced modelling techniques to simulate the complex microclimate conditions (Gros et al., 2016; He et al., 2009; Liu et al., 2015; Salvati et al., 2020). Coupling methods are then employed to use the results of the microclimate simulations as climate boundary conditions for energy demand estimations. However, again, morphology is simplified either through the selection of homogeneous urban fabrics from a real environment or through the generation of generic urban patterns on a grid structure. This second approach starts from the assumption that the building under analysis and its context have similar geometrical characteristics, and the behaviour found for the building type is transferable to all the buildings in the area. As a consequence, it becomes difficult to understand to what extent the variation of form characteristics and urban microclimate influence energy consumption by using the existing methodologies.

Thus, by focusing on the described limitations, this study explores the use of advanced morphological classifications to support a more comprehensive analysis of the spatial components related to climate and energy performance of the built environment. Specifically, it addresses the question: How and to what extent do urban microclimate and urban form impact building cooling demand in the Rotterdam case?. By employing a data-driven classification of local climate types (LCTs) and a coupling modelling between ENVI-met and City Energy Analyst (CEA), the study analyses the effect of local climate conditions on energy consumption during two hot summer days, in the city of Rotterdam, selected as case study in this thesis.

Section 5.2 describes the methodological framework, its application on the case study of Rotterdam, and the methods employed to assess microclimate and energy performance through model coupling. In section 5.3, the results of energy simulations carried out for the case study, with general weather data and urban microclimate data, are compared to observe related demand variation caused by the urban climate. Next, a sensitivity analysis is carried out to identify the influence of form variables on the types' energy performance. Finally, conclusions are presented regarding the limitation of the framework and the relevance of the results from an energy transition perspective.

5.2 Methodological Framework

Differing from previous qualitative selections of representative homogeneous form patterns, in this study, the Local Climate Type method (Maiullari et al.,2021) was employed to identify urban archetypes through a data-driven morphological classification of the Rotterdam urban fabric. The 25 archetypes, emerging through clustering analysis of form characteristics, consist of a combination of five different building types and five different contextual conditions, allowing to capture Rotterdam's urban tissue heterogeneity.

Building energy demand simulations were carried out for these different archetypes Figure 5.1. To assess the effects of urban climate on modelled energy demand, two scenarios employing rural (Baseline) and urban (Microclimate) datasets were used as climate boundary conditions. The first dataset was derived from the Rotterdam Airport KNMI weather station, representative of a rural climate, while the second dataset represents urban climate conditions and was created through microclimate simulations with ENVI-met 4.4. ENVI-met is a three-dimensional prognostic microclimate model designed to simulate the interaction between surfaces, plants, and air in an urban environment (Bruse & Fleer, 2009). It is widely used to estimate and assess urban climate processes, and it has previously been employed for couplings with energy models (Gobakis & Kolokotsa, 2017; Natanian et al., 2019). With the simulation tool, hourly values for air temperature, wind speed and relative humidity were obtained for each building under analysis. The energy simulations for the Baseline and the Microclimate scenarios were then performed with City Energy Analyst (CEA) (The CEA Team, 2018), an open-source tool for the analysis and

optimization of energy systems in neighbourhoods and city districts and were based on the method developed and tested in Mosteiro-Romero et al. (2020).

In this application on the Rotterdam case, two consecutive hot days with clear sky were selected (June 29th, 30th 2018). Once the energy simulations of the 25 archetypes were performed, data comparison between the two scenarios allowed for an analysis of the impact of urban microclimate on building cooling demand. Additionally, a sensitivity analysis highlighted significance and relevance of morphological factors in shaping thermal behaviour and projected energy consumption. A detailed description of the archetypes and simulation settings is reported in the following section.

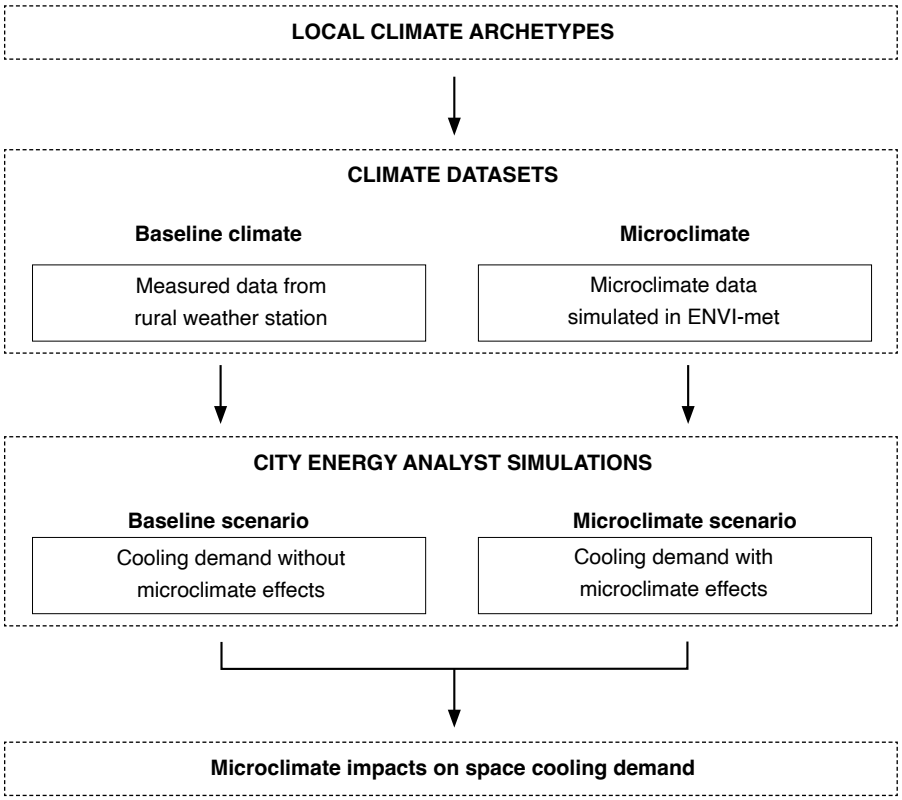


FIG. 5.1 Scheme of the methodological framework

TOC

5.2.1 Building and context types' description

A data-driven classification was employed to identify LCTs based on morphological characteristics of both buildings and context. Spatial datasets containing geometrical features and attributes of buildings, street networks, vegetation cover, and trees were provided by the Rotterdam Municipality. By using these datasets, 8 quantitative morphological parameters were calculated and processed through a hierarchical cluster analysis. The selected parameters allow for the quantitative description of building geometry as well as roughness, built density, and vegetation coverage of the buildings' context. For the latter, data was selected in buffer areas with a 25 and 50 meter radius from the building envelope.

Five building types (B_Type) were identified through the clustering of values for (i) building height, (ii) footprint, and (iii) surface-to-volume ratio; and five context types (C_Type) through the clustering of values of (i) mean building height (50m buffer), (ii) Ground Space Index (25m buffer), (iii) Floor Space Index (50m buffer), (iv) tree crown area (25m buffer), and (v) grass cover (50m buffer).

The resulting building types can be described as follows. B_Type1 and B_Type3 are low-rise buildings (B_Height<9 m) with small footprints (B_Footprint<139 m^2). Buildings of type 1 have a low compactness level (StoV>0.53), while buildings of type 3 have a high compactness level (StoV<0.47). B_Type2 and B_Type5 consist of highly compact mid-rise buildings (B_Height= 9-19 m). While buildings in type 2 are characterised by small footprints (slabs, apartment buildings), in type 5 the footprints are the largest (B_Footprint>1650 m^2), comprising public facilities and industrial/commercial objects with a horizontal volume distribution. B_Type4 is composed of high-rise buildings (B_Height>19 m). Regarding context types, C_Type1 consists mainly of low and mid-rise urban fabrics (MeanH<15 m), with low-density characteristics (GSI<0.26 and FSI<0.80), large tree crown area (TArea>755 m^2) and a medium-level of grass coverage area (GArea=1030-2800 m^2). C_Type3 and C_Type4 are urban tissues defined by low-rise buildings (MeanH<8 m), and low density (GSI<0.26 and FSI<0.80). The main difference between the two types is the quantity of grass surfaces, which is very low in type 3 (GArea<1030) and medium in type 4 (GArea=1030-2800 m^2). C_Type2 is characterised by mid-rise buildings (MeanH=8-15 m), medium building coverage (GSI= 0.26-0.48) and built-up intensity (FSI=0.8-2.0), and has low values of tree and grass coverage area (TArea<400 m^2; GArea<1030 m^2). C_Type5 can be described by highly compact conditions of the urban fabric, characterised by high mean height (MeanH>15 m), high building intensity, and building coverage (GSI>0.48; FSI>2) and a low level of greenery (TArea<400 m^2; GArea<1030 m^2).

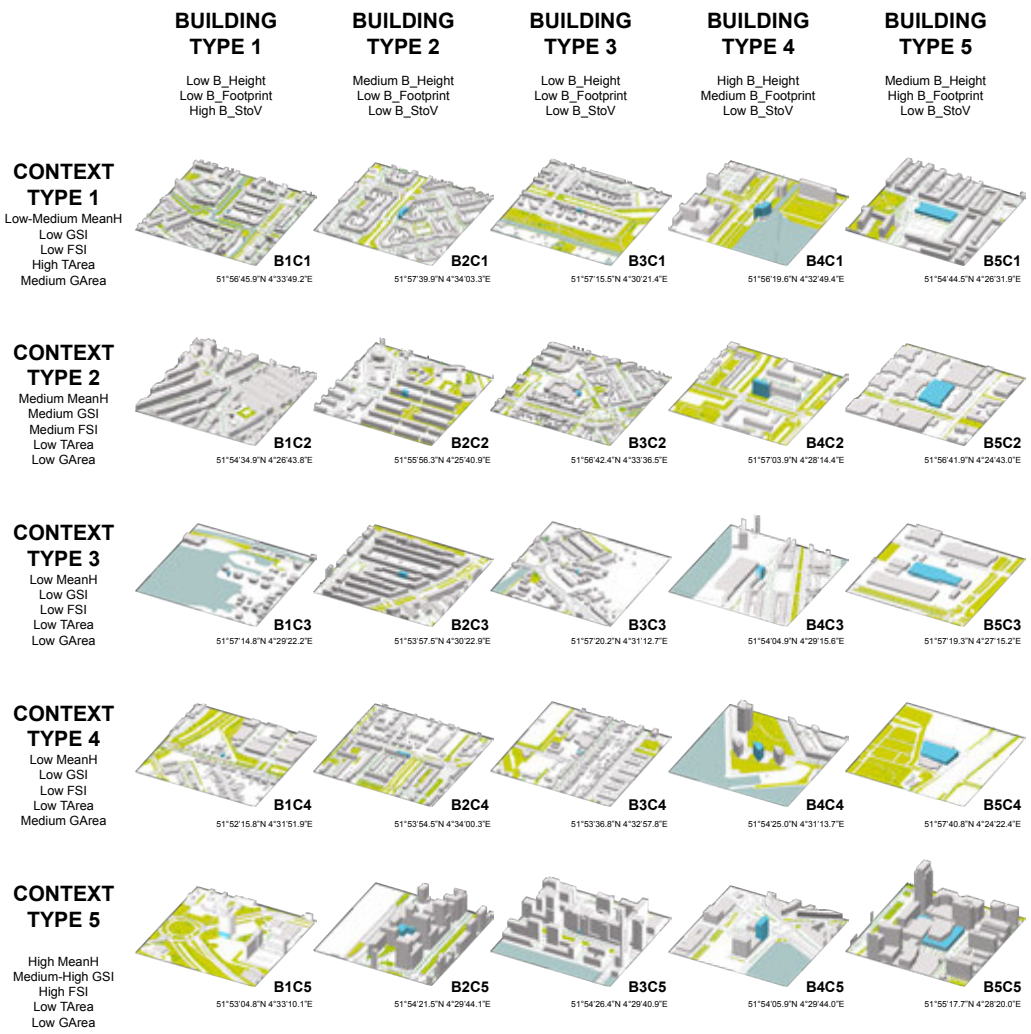


FIG. 5.2 Visualization of the 25 archetypes based on the five building types and the five context types.

Figure 5.1 reports the numerical and semantic description of the types, while more details about the clustering method can be found in (Maiullari et al., 2021). Finally, as shown in Figure 5.2, a matrix of archetypes was built by selecting 25 cases; one building type in each context type.

TOC

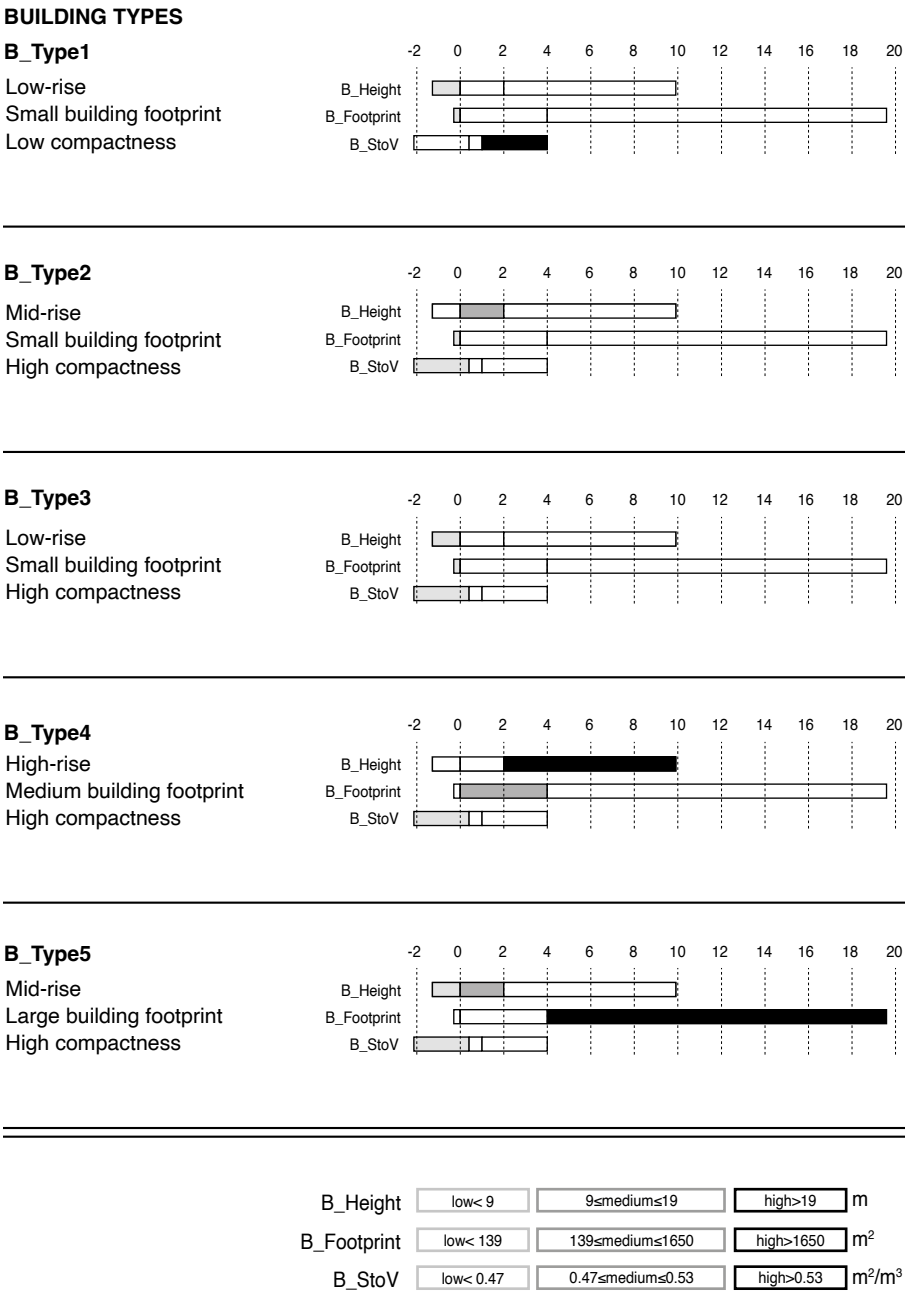


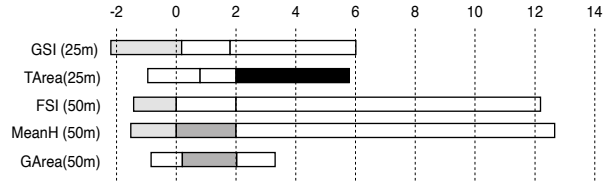
FIG. 5.3 Standardized (z-score) numerical profiles of building types (left) and context types (right).

TOC

CONTEXT TYPES

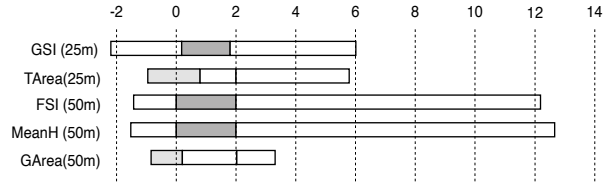
C_Type1

Low Ground Space Index
High tree crown area
Low Floor Space Index
Low-Medium mean b. height
Medium grass coverage



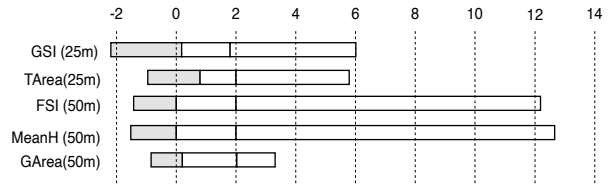
C_Type2

Mid Ground Space Index
Low tree crown area
Medium Floor Space Index
Medium mean b. height
Low grass coverage



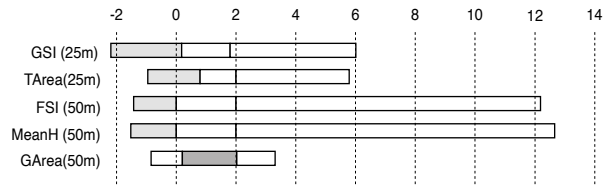
C_Type3

Low Ground Space Index
Low tree crown area
Low Floor Space Index
Low mean b. height
Low grass coverage



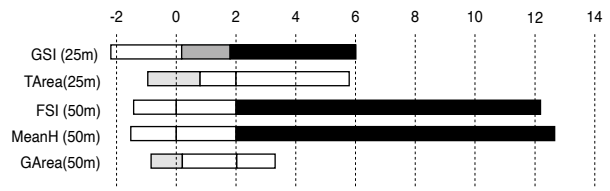
C_Type4

Low Ground Space Index
Low tree crown area
Low Floor Space Index
Low mean b. height
Medium grass coverage



C_Type5

Mid-High Ground Space Index
Low tree crown area
High Floor Space Index
High mean b. height
Low grass coverage



GSI (25m)	low< 0.26	0.26≤medium≤0.48	high>0.48	
TArea(25m)	low< 400	400≤medium≤750	high>750	m^2
FSI (50m)	low< 0.80	0.8≤medium≤2.0	high>2.00	
MeanH (50m)	low< 8	8≤medium≤15	high>15	m^2
GArea(50m)	low< 1030	1030≤medium≤2800	high>2800	m^2

TOC

5.2.2 Baseline and Microclimate Datasets

In this study a Baseline and a Microclimate dataset constitute the climate inputs of the energy model. For the energy modelling of the Baseline scenario (rural climate), the climate dataset was derived from the KNMI weather station at Rotterdam Airport. During the two selected days, air temperature values reach 25°C (June 29th) and 28°C (June 30th) respectively. Additionally, as shown in Figure 5.4, relative humidity decreases during diurnal hours, dropping to around 40% on the first day and 25% on the second day. The plotting of wind speed shows high values during daytime and a significant decay during the night. Overall, during the two days, wind velocity reaches a maximum of 6 m/s. Next, this dataset was employed both as input to model energy demand in CEA for the Baseline case, and as climate boundary conditions in the ENVI-met simulations.



FIG. 5.4 Plotting of hourly air temperature, relative humidity and wind speed values at KNMI weather station at Rotterdam airport (June 29th-30th 2018)

For the energy modelling of the Microclimate scenario, the climate dataset was obtained through ENVI-met simulations and represents the local climate characteristics of the 25 archetypes. ENVI-met is a numerical microclimatic tool with a high spatial (0,5-10m) and temporal (timestep 1-5s) resolution, that relies on Reynolds-Averaged Navier–Stokes equations to resolve heat transfer and fluid flows in urban environments (Bruse & Fleer, 2009). By computing multiple climate parameters in four main sub-models - atmospheric, soil, vegetation, and building model - (Huttner, 2012), it allows for the exploration of the impacts of vegetation (Morakinyo et al., 2020), materials (Yang et al., 2013) and urban geometry (Sharmin et al., 2017; Wang et al., 2016) on the microclimate. ENVI-met has been used in various studies focusing on UHI phenomena (Conry et al., 2015; Chen et al., 2020), human thermal comfort (Taleghani et al., 2015; Qaid et al., 2016),

TOC

and the assessment of heat mitigation strategies (Ambrosini et al., 2014; Crank et al., 2018) at different spatial scales. The majority of these studies have also evaluated and confirmed the accuracy of the model by comparing results against data measurements (Tsoka et al., 2018).

Based on the geometrical and material characteristics of the Rotterdam case, model domains and spatial models were created through the ENVI-met submodule Monde. A grid cell resolution of 3 m (x) by 3 m (y) by 3 m (z) was employed for all 25 archetypes, and vertical and horizontal domain sizes were defined, based on the maximum height of the buildings and buffer extension respectively. All 25 models were modelled with the same building materials, pavement, vegetation type in order to be able to isolate the influence of urban form on climate and energy behaviour. The ENVI-met default Database was employed to assign physical and thermal characteristics to surface materials (asphalt for roads, concrete bricks for sidewalks, grass and, deciduous trees), while for building walls, a theoretical material with medium insulation properties was created (Table 5.1). Simulations were performed applying the ENVI-met full forcing method which allows for hourly inputs as climate boundary conditions. Including initialization time, the simulations had a duration of 72 hours starting on the 28th of June. Values for the final 48 hours (June 29th and 30th) were then selected for the energy simulations of the Microclimate scenario. Hourly results for air temperature, wind speed and relative humidity averaged at building level are used as climatic boundary conditions in the CEA energy tool.

TABLE 5.1 Rotterdam Material Database

	User Defined Wall Medium insulation		Dark Asphalt	Grey Concrete
Transmission	0	Emissivity	0.9	0.9
Reflection	0.4			
Emissivity	0.95			
Specific Heat (J/kgK)	840			
Thermal Conductivity (W/mK)	0.140			
Density (kg/m3)	1190			

5.2.3 City Energy Analyst: modelling and settings

As previously mentioned, energy demand simulations were carried out using CEA. This tool uses a combination of simplified physical models and building archetypes to simulate the demand and energy production potential of urban districts. While many energy models are able to estimate energy demand for buildings, only few are able to address the district scale due to the computational limitations of the energy simulation tools. CEA has shown in multiple studies to be reliable and able to deal with large scale modelling. In CEA, sensible load calculation is based on a resistance-capacitance model (ISO 13790, 2008) that considers each building to be a single thermal zone in which gains and losses are homogeneously distributed. In addition to the sensible loads, CEA calculates latent loads based on the moisture level difference between outdoors and indoors (ISO 52016-1, 2017). Furthermore, the thermal resistance of external surfaces is calculated as a function of wind speed.

The comfort requirements in this thermal load model are limited to specifying heating and cooling set point temperatures, minimum ventilation rates, and minimum and maximum humidity within a space. For each hour of the year, the indoor temperature in a space without any heating or cooling is calculated as a function of the internal gains (from occupants, electrical devices, etc.), solar heat gains, ventilation rate, outdoor temperature. If the indoor temperature is higher than the cooling set point temperature and the hour lies within the predefined cooling season, the cooling demand is calculated until the indoor temperature reaches the intended cooling set point temperature.

TABLE 5.2 CEA inputs from Dutch standards

Inputs		Source
Occupant density [m2/p]	30	NTA 8800_2018
Electricity for lighting [W/m2]	1.7	
Domestic hot water [l/p/d]	40.3	
Ventilation rate [l/p/s]	7.0	Praktijkboek bouwbesluit
Minimum relative humidity [%]	25.0	NEN-EN15251 (class II)
Maximum relative humidity [%]	60.0	

The main environmental parameters that affect CEA's thermal load model are (i) relative humidity, (ii) outdoor air temperature, (iii) wind speed, and (iv) solar irradiation. The urban solar radiation model used to calculate the incident solar radiation on buildings is based on the open-source software DAYSIM (Reinhart, 2013), while hourly values of air temperature, wind speed, and relative humidity are usually obtained from weather stations. Therefore, these

three parameters were selected here to study the microclimate effects on space cooling demand.

The primary inputs to CEA comprise (i) building geometry, (ii) construction typology (envelope characteristics), and (iii) use types. Building form characteristics were retrieved from the Rotterdam dataset and include building footprint and height. Similar to the microclimate modelling, other parameters were kept constant in order to identify the morphological impact on energy demand: residential use was assumed as building function for all the archetypes, window-to-wall ratio was assumed to be 21%, and thermal properties of the envelope matched the construction material used in the ENVI-met models. Regarding the cooling energy systems, mini-split AC installations were assumed.

Secondary inputs - usually derived from the CEA database (Fonseca & Schlueter, 2015) - were modified based on Dutch standards as shown in Table 5.2. The occupancy schedule was derived from ASHRAE 90.1 (2016) and used as standard based deterministic schedule (Table 5.3). Additionally, the set-point temperature was set at 22°C in both the Baseline and Microclimate scenario.

TABLE 5.3 Occupancy schedule

Hours	1	2 4	5	6	7	8	9	10 15	16	17	18	19	20 21	22	23	24
Occupancy	1	1	1	1	1	0.9	0.4	0.25	0.25	0.3	0.5	0.9	0.9	1	1	1
Appliances	0.5	0.4	0.4	0.4	0.5	0.7	0.7	0.7	0.7	0.8	1	1	0.9	0.8	0.7	0.6
Lighting	0.1	0.1	0.2	0.4	0.4	0.4	0.2	0.1	0.2	0.4	0.6	0.8	1	0.7	0.4	0.2

5.3 Results

The following sections describe the Microclimate dataset resulting from the ENVI-met simulations and compare modelled space cooling demand of the 25 archetypes in the Baseline and Microclimate scenarios. In Section 5.3.1, ENVI-met results for air temperature, relative humidity and wind speed retrieved in the air layer near facades are analyzed. Maximum UHI magnitude and average indoor temperature in the type groups are compared for the two days under analysis. In Section 5.3.2, the CEA simulation results for space cooling demand of the two scenarios are presented.

5.3.1 Outdoor and indoor conditions of Rotterdam archetypes

Figure 5.5 shows hourly average outdoor air temperature, relative humidity and wind speed for each of the 25 Rotterdam archetypes simulated in ENVI-met. The comparison against rural measured data at the KNMI weather station shows the effects of urban environments on thermal, aerodynamic, and evaporative processes during the selected days. Overall, air temperature is generally higher than in the rural environment in a range between 0,5 °C and 3 °C during daytime. Wind velocity drops, showing that urban form accounts for a decrease in wind speed up to 3 m/s. The large presence of impervious and paved areas also contributes to lower relative humidity up to 5%.

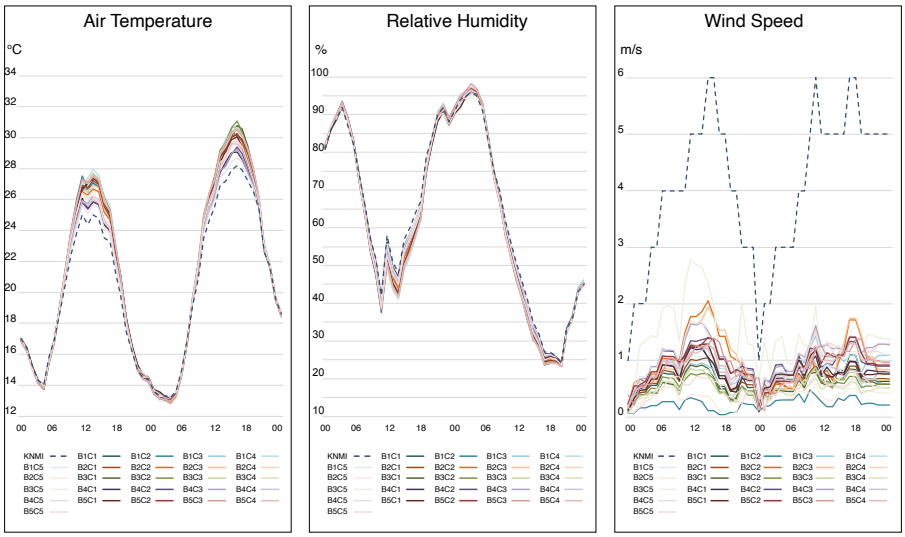


FIG. 5.5 Building average air temperature (left), relative humidity (center), wind speed (right) near façade

The maximum UHI intensity ($UHI_{max)}$ is also analysed through a comparison of the morphological types for the first milder day, that reached 25 °C, as well as for the second warmer day, which reached 28 °C at the KNMI station. Results show that despite building and context characteristics determine a UHI_{max} up to 3 °C, different patterns of magnitude can be recognised by grouping the values of the 5 cases representing each type. For example, for building types, Figure 5.5 (left) shows that the lowest UHI_{max} is measured around high-rise buildings (B_Type4 cases), followed by mid-rise, (B_Type2, 5) and low-rise types (B_Type1, B_Type3). However, during

TOC

the second, warmer day, high-rise buildings see an increase in the range of UHI_{max} values while mid-rise types see a reduction of both UHI_{max} and the range of values.

Patterns appear more similar when observing UHI magnitude for context types Figure 5.6 (right). The lowest UHI_{max} variability is observed in C_Type5, characterised by high built density and high mean height (respectively between UHI_{max} =0,7 - 2 °C the first day, and UHI_{max} =0,6 - 1.7 °C the second day. Differently, in low-density contexts (C_Type1,3,4) and medium-density context (C_Type 2) UHI_{max} is higher than 2°C and values are distributed in a larger range.

These results suggest that high-rise buildings are less affected than other types by urban overheating mechanisms and that high-density surroundings contribute to decreasing UHI magnitude at the micro-scale, probably due to the increase of shading. Additionally, the analysis for the two hot days indicates that the role of morphological characteristics in UHI mechanisms varies with the change of temperature level. In other words, buildings and context types might have different impact magnitudes on urban temperatures during hotter summer days.

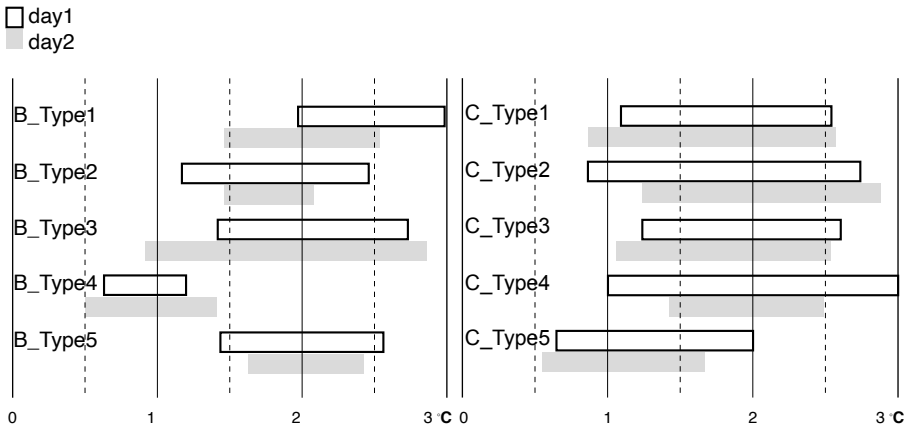


FIG. 5.6 Urban Heat Island maximum intensity for building types (left), and for context types (right)

By analysing the five cases representing each building type, distinct thermal patterns can be observed also regarding average diurnal indoor temperature. As shown in Figure 5.7 the largest spread of indoor temperature values (1.4°C during day one, 3.2 °C during day 2) is noticed for the low-rise buildings (B_Type1, B_Type3), suggesting that for these building types indoor thermal conditions are highly influenced by the urban context characteristics. In particular when surrounded

TOC

by highly dense contexts, indoor temperature drops below 22.5°C. Differences in average temperature values for mid-rise buildings characterised by small footprints (B_Type2) follow, varying up to 0.7°C (during day1) and 1 °C (during day2). Differently, large building footprints in B_Type5 lead to similar temperature values among the five cases (0.4 °C during day1, 0.5 °C during day2), suggesting that contextual conditions hardly affect the balance between thermal gains and losses. Finally, high-rise buildings (B_Type4) show lower indoor temperature values and minor differences between cases (0.2°C during day1, 0.3 °C during day2). Thus, these observations indicate that indoor temperature of towers and skyscrapers is less influenced by the urban form of their surroundings.

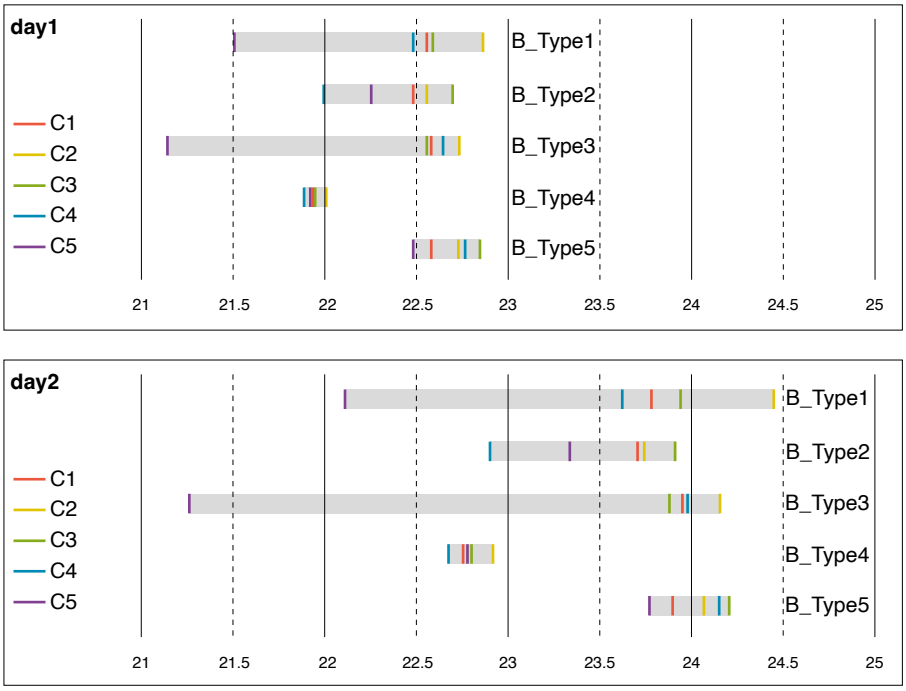


FIG. 5.7 Average daytime Indoor temperature in building types cases

5.3.1.1 Correlations between morphological characteristics and temperatures

A multiple linear regression analysis, applied to the ENVI-met simulation results, allowed to examine the statistical relation between average indoor temperature

TOC

values, maximum outdoor temperature values, and the urban form variables employed in this study. During diurnal hours, building height and Floor Area Ratio (FSI) are highly correlated to outdoor temperature, together explaining between 85% (day 1) to 77% (day2) of the temperature variation. The negative sign of the correlation confirms that decreasing built intensity and building height leads to a warmer urban environment, probably due to the reduced shading. During night-hours, a significant relationship is found between outdoor air temperature and the morphological variables of tree crown area and Ground Space Index (GSI) that together explain 39% of urban temperatures. The positive sign of the correlation indicates that high building and tree coverage leads to an increase in air temperature during night-time. The possible reason is that compactness and roughness elements inhibit radiative heat loss and ventilation. Finally, a consistent strong correlation (R^2= 0.50) is found between indoor air temperature and two morphological variables: building footprint (same as roof area) and mean building height of the context, suggesting that these are the main factors governing solar gains and (convective) heat loss respectively, at the building envelope.

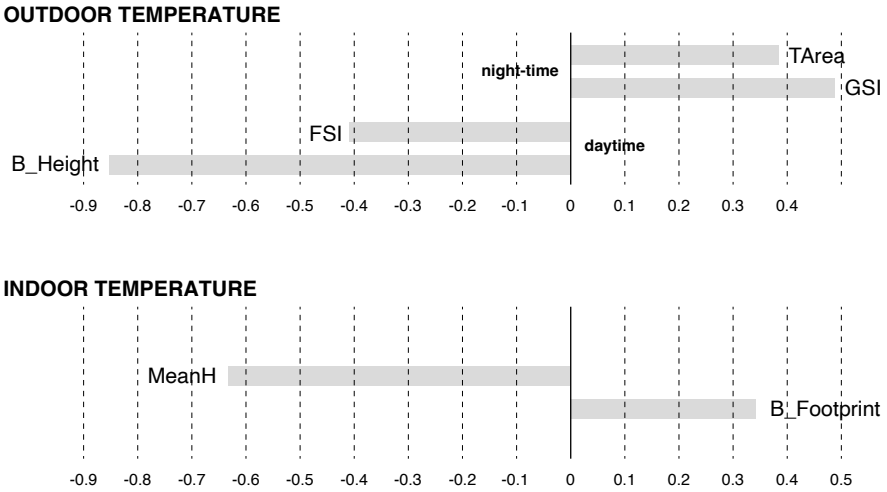


FIG. 5.8 Standardized coefficient of the relation between temperatures and form parameters.

TOC

5.3.2 Space cooling demand in Baseline and Microclimate scenarios

The district's space cooling demand was simulated in CEA for the two days (29-30 June 2018) using the Baseline climate dataset and the Microclimate dataset resulting from ENVI-met modelling. The results show that average cooling demand for the 25 archetypes is around 64 Wh/m^2 (day 1), and 85 Wh/m^2 (day 2) in the Baseline Scenario, and for around 94 Wh/m^2 (day 1), and 111 Wh/m^2 (day 2) in the Microclimate Scenario. During the second day, cooling demand increases in both scenarios due to higher overall temperatures. However, the impact of microclimatic conditions is smaller on this second day. In fact, urban climate conditions lead to an average cooling demand increase (cooling penalty) of about 32% the first day and 24% the second day. Additionally, observing the differences between Baseline and Microclimate scenarios in all 25 archetypes, a change of range in building cooling demand can be noticed: between 5% and 100% during the first mild day, and between 3.5% and 39% during the second warmer day.

5.3.2.1 Average daily cooling demand in building types

Results, analysed by comparing the simulation results of the 25 archetypes, suggest that space cooling demand for a specific building type follows a similar pattern in both days. Figure 5.9 (left) shows the absolute daily demand of the five cases simulated per building type (one in each context type), as well as the average demand in the Baseline (blue line) and Microclimate scenario (orange line) for each building type. B_Type5, consisting of mid-rise buildings with a large footprint, has the greatest average cooling load among types: in the Baseline scenario 107 Wh/m^2 (day 1) and 108 Wh/m^2 (day 2), in the Microclimate scenario 135 Wh/m^2 (both day 1 and 2). The increase of overall temperatures during the second day has a limited impact on the energy demand of these buildings, probably because solar irradiation of the large roofs and well-exposed facades are the major factors influencing their performance. Among the cases in this group, B5C5 has the lowest cooling demand (below 65 Wh/m^2), suggesting that a highly compact and dense context can help to drastically reduce solar gains and consequentially cooling demand. For mid-rise buildings with a smaller footprint (B_Type2), average cooling demand rises from 49 Wh/m^2 the first day to 75 Wh/m^2 the second day in the Baseline scenario, and from 74 Wh/m^2 the first day to 96 Wh/m^2 the second day in the Microclimate scenario. High-rise buildings (B_Type4) have average cooling loads very similar to B_Type2 in the Microclimate scenario: 82 Wh/m^2 (day 1) and 96 Wh/m^2 (day 2). However, for the high-rise type, the second highest demand is observed

when rural data is taken into account, being the average Baseline demand 72 Wh/m^2 (day 1) and 87 Wh/m^2 (day 2). The two low-rise building types largely increase their cooling loads in the second warmer day. Here, B_Type3, characterised by high compactness and small footprints, has the lowest Baseline average demand among types: 29 Wh/m^2 (day 1) increasing up to 61 Wh/m^2 (day 2). When local climate conditions are taken into account, the cooling load notably increases up to 69 Wh/m^2 (day 1) and 97 Wh/m^2 (day 2). Contrastingly, B_Type1 buildings, being less compact, have higher cooling loads in the Baseline scenario (64 Wh/m^2 in day 1 and 92 Wh/m^2 in day 2). Considering microclimate conditions increases the energy demand for this type up to 110 Wh/m^2 (day 1) and up to 133 Wh/m^2 (day 2). Thus, among all types, B_Type1 has the second highest average cooling demand in the Microclimate scenario, after B_Type5.

5.3.2.2 Sensitivity of cooling demand to microclimate

Accounting for microclimate leads to a daily cooling demand increase for all types. The largest relative difference between the Baseline and the Microclimate demand is observed for low-rise types (B_Type3, 1) followed by mid-rise (B_Type2, 5) and high-rise buildings (B_Type4). During the first day, when accounting for microclimate, B_Type3 sees a cooling demand increase up to 58% and B_Type1 up to 42%, suggesting that cooling loads of low-rise buildings are the most sensitive to urban overheating. Additionally, the size variation of the impact can be associated with the difference in building compactness since building surface-to-volume ratio is lower in the first case. More compact buildings (lower StoV) have a lower proportion of envelope exposed to convective processes and thus building surfaces release heat accumulated through absorption of short-wave radiation less rapidly. When analysing the difference between Baseline and Microclimate scenarios for mid-rises, cooling loads increase due to urban overheating by 34% in B_Type2, and by 21% in B_Type5. The use of simulated microclimate data leads to an average cooling load increase of 12% in B_Type4. The cooling demand in high-rise buildings is thus the least sensitive to urban overheating, probably due to higher wind velocities and lower temperatures in the upper part of the canopy layer. During the second day the cooling load in the Microclimate scenarios shows a smaller increase, reaching to 37% in B_Type3, 31% in B_Type1, 22% in B_Type2, 20% in B_Type5, and 9% in B_Type4. This result suggests that overall higher air temperatures decrease the impact of urban climate on space cooling demand.

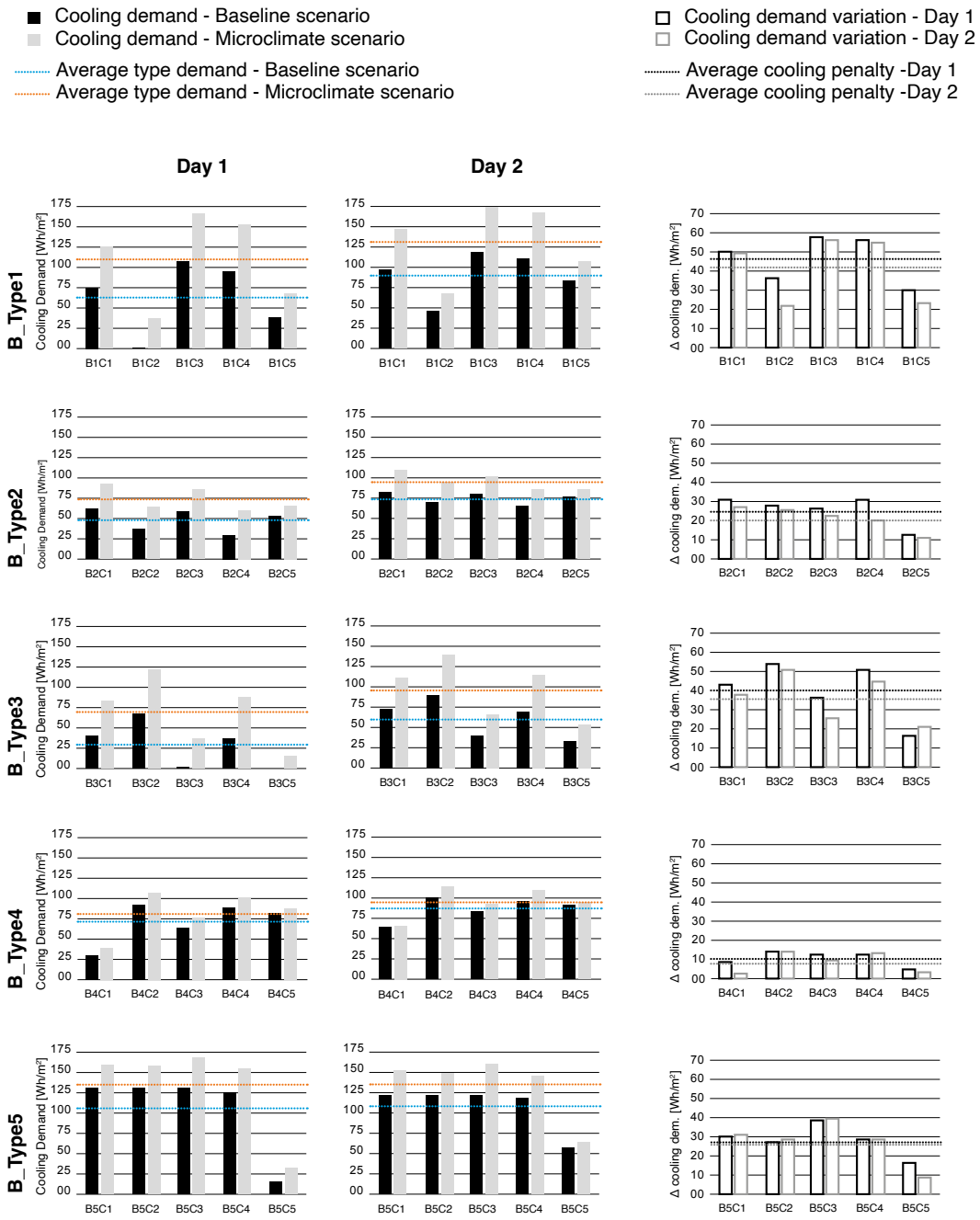


FIG. 5.9 Daily cooling demand in Baseline and Microclimate scenarios grouped for building type (left) and cooling demand variation between Baseline and Microclimate scenarios (right).

TOC



FIG. 5.10 Average and total cooling demand of each building type; cooling demand variation between Baseline and Microclimate scenarios for the two days analyzed.

TOC

5.3.2.3 Sensitivity of cooling demand to Context Types

Analysing the results for the five cases in each building type (Figure 5.9) allows observing to what extent absolute demand per square meter changes at the change of the surrounding urban fabric conditions. In other words, how sensitive a building type's cooling load is to contextual morphological characteristics. The plotting indicates that the five buildings in mid-rise (B_Type2) and high-rise types (B_Type4) have generally similar loads; thus, variations are less determined by the change in context conditions. Differently, in low-rise types (B_Type1,3), the demand is dissimilar among buildings, suggesting that this type is more responsive to surrounding morphological conditions.

Other patterns can be observed when analysing the absolute cooling difference between Baseline and Microclimate scenarios in Figure 5.9 (right). Notably for all the building types, high-density and high-rise contexts (C_Type5) determine a smaller cooling demand increase when considering local climate conditions. In line with the findings on the UHI mitigative effect of this context type during daytime, this result confirms the benefit in terms of reduced cooling penalty. The explanation can be found in the fact that highly compact urban fabrics reduce solar access and therewith thermal gains through building envelopes during diurnal hours. Therefore, all the building types performing in this context have a similar lower increase in microclimate-related energy demand. When compared to the average of each building type, cooling penalty is 35% to 60% lower for low-rise buildings, 43% to 68% lower for mid-rise buildings, and 54% to 59% lower for high-rise buildings, in a high-density high-rise context.

5.3.2.4 Hourly cooling demand

Finally, daily patterns of cooling demand are shown for the 25 archetypes in Figure 5.11. The plotting of hourly demand values indicates that cooling demand peaks are generally the highest in low-rise building were the curves see an exponential rise during afternoon hours. Building orientation seems to influence the cooling systems activation time more than in other types. Mid-rise and high-rise buildings reach high cooling loads already during morning hours and maintain a relatively constant load till sunset. Differently from other types, B_Type5 and B_Type4 reach the set-point temperature generally before 8:00 in the morning thus requiring space cooling for a longer period of the day.

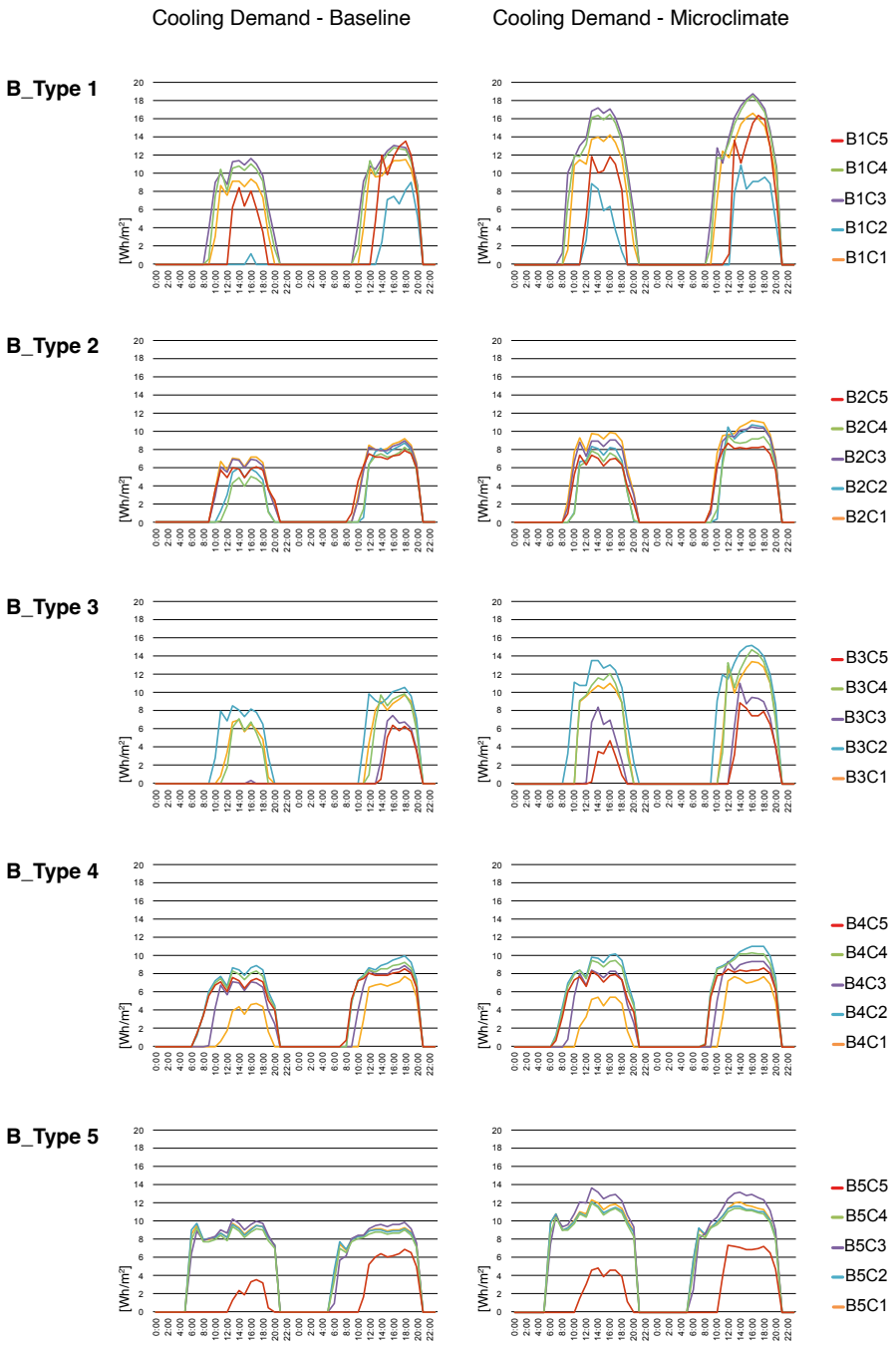


FIG. 5.11 Daily patterns of cooling demand in Baseline and Microclimate scenarios

TOC

5.3.3 Analysis of the correlation between diurnal cooling demand, morphological and climate variables.

In order to understand to what extent morphological and local climate parameters influence space cooling demand in the urban climate context of Rotterdam, a multiple linear regression analysis is carried out. Modelled diurnal cooling demand of the Microclimate scenario is set as a dependent variable while urban form and microclimate parameters are set as independent variables. Average wind speed, relative humidity and outdoor air temperatures are calculated for daytime hours (7am to 8pm). The found R^2 values are 0,79 and 0,76, meaning that the 79% and 76% of the variance in daytime cooling demand is explained by the morphological and climate variables, for the first and second day of focus respectively.

During the first day with milder temperatures, two climate variables and five morphological variables are statistically significant predictors of cooling demand. The standardized coefficients (Table 5.4) show that the most important predictors are local air temperature and building height, followed by FSI and relative humidity. Mean building height of the context is the fifth predictor for importance followed by building footprint and GSI. Additionally, GSI and mean building height have a negative correlation sign, meaning that the lower their values, the greater the cooling demand.

TABLE 5.4 Results of the linear regression analysis on Microclimate energy estimation in order of significance.

Day 1	
Variables	Standardized Coefficients
AVGday Air Temperature (ENVI-met)	2.84
Building height	1.86
Floor Space Index	1.68
AVGday Relative Humidity (ENVI-met)	1.45
Mean building height	-1.05
Building footprint	0.67
Ground Space Index	-0.57
Surface-to-Volume	Not Sign.
Grass Coverage Area	Not Sign.
Tree Crown Area	Not Sign.
AVGday Wind Speed (ENVI-met)	Not Sign.

Day 2	
Variables	Standardized Coefficients
AVGday Air Temperature (ENVI-met)	1.31
Building height	0.99
AVGday Wind Speed (ENVI-met)	0.67
Surface-to-Volume	0.60
Mean building height	Not Sign.
Building footprint	Not Sign.
Ground Space Index	Not Sign.
Floor Space Index	Not Sign.
Grass Coverage Area	Not Sign.
Tree Crown Area	Not Sign.
AVGday Relative Humidity (ENVI-met)	Not Sign.

During the second day only four variables are statistically significant. The most important predictors are average daily local temperatures and building height (similarly to the first day). However, the size of their coefficients is generally smaller than for the first day, showing that when overall temperatures are generally higher, local climate factors and urban form are less capable of explaining cooling demand variance. Following in importance, wind speed and surface-to-volume ratio appear equally important.

5.4 Limitations

The study employs a morphological parametric approach to analyse the impacts of urban form on cooling demand in urban climate conditions. The performed microclimate and energy assessments are however subjected to a few limitations. All buildings and street surfaces are assumed to have identical materials, both in the ENVI-met and CEA model, to be able to isolate the influence of morphological components as much as possible. For the same reason, the residential function and related occupants' schedules are kept constant in CEA. Differently, trees modelled in ENVI-met to estimate air temperature, relative humidity and wind speed, were not modelled in CEA since the tool doesn't allow for those to be taken into account in the radiation module. Thus, the beneficial effect of their shadow on building surfaces is neglected. Additionally, this study analyses only two representative hot days. To analyse the impacts of urban form on the net building energy demand, an annual study should be conducted. However, while CEA can simulate annual energy loads, ENVI-met simulations for such a period are not feasible due to the large computational costs of CFD modelling. Furthermore, in this study UHI_{max} is observed during daytime. Results indicate that high-rise urban patterns contribute to lower temperatures, and pinpoint the beneficial effect of shading in reducing incoming radiation. Despite this finding confirms previous results (Yang et al., 2020; Loibl et al., 2021), it is also well established in literature that compact and dense environments have a lower capacity to release heat during night-hours, increasing nocturnal UHI (Oke et al., 2017).

5.5 Conclusions

In the Rotterdam context five building types and five context types were classified based on building geometry and the urban form characteristics of their surroundings. The type classification was performed through an unsupervised classification method and allowed for an identification of 25 archetypes on which energy modelling was performed. To understand cooling load variance including local microclimate, a coupling modelling method has been employed to use ENVI-met simulation results as boundary climate conditions for energy demand estimation in City Energy Analyst. Results were compared to energy demand simulations using measured data from a rural weather station for two representative consecutive hot days (29-30 June 2018).

The simulated hourly temperatures around buildings (microclimate dataset), were compared to rural weather data from the closest KNMI weather station at Rotterdam airport. Variations in urban form for the 25 cases determine a diurnal UHI_{max} intensity up to 3 °C. The geometrical attributes of buildings substantially influence the degree of sensitivity to urban overheating. Among the building types studied, the high-rise type is the least sensitive to urban temperatures, followed by mid-rise and low-rise buildings. Additionally, the context in which the building stands affects the UHI variability. A surrounding characterised by high-rise and high density in particular can reduce daytime urban warming up to 1.3 °C at the building façade. The analysis of two days with different thermal profiles also indicates that both the sensitivity of buildings to (local) outdoor air temperatures and the impact of context characteristics on urban climate phenomena vary in size related to overall temperatures. This observation confirms the complexity of the relationship between form and climate phenomena, which needs to be further addressed in future studies by exploring trade-offs related to thermal thresholds.

This study also confirmed that the difference in temperature between the rural and the urban environment leads to substantial differences in cooling demand. Here, cooling demand was estimated in CEA for the 25 Rotterdam archetypes in a Baseline and Microclimate scenario. Overall, the average daily space cooling demand was found to increase between 24% and 32% when considering microclimate conditions. However, low-rise buildings are more sensitive to urban overheating than other building types. Compared to the same building type in a rural area, in an urban context, low-rise buildings (B_Type1, B_Type3) are found to have a 31% to 58% higher cooling demand, mid-rise buildings (B_Type2, B_Type5) between 20% and 34%, and high-rise buildings (B_Type4) between 9% and 13%. In the high-density and high-rise context type (C_Type5), the cooling penalty dependent on urban overheating tends to drastically decrease.

Generally, lower variations in cooling demand between the two scenarios were found during the second day analysed. This day reached higher temperatures than the first one in both the rural and urban environment. This observation suggests that higher mesoscale weather temperatures decrease the impact of urban climate on space cooling demand. Additionally, a sensitivity analysis showed that different variables are significantly correlated with cooling loads for the two days. During the first day, average daytime temperature, relative humidity, building height and footprint, density, and mean height of the context explain 79% of cooling demand variance. However, during the second warmer day, 76% of the cooling demand is explained by only four variables: average daytime temperature, wind speed, building height, and surface-to-volume ratio. Such a difference indicates that the role of form characteristics might change accordingly to temperature thresholds, demonstrating the high complexity of the trade-off between urban form and energy cooling in urban climate environments.

Finally, this study demonstrates the importance of form characteristics in shaping cooling loads of buildings in urban climate conditions and points out that some building types are more sensitive than others to temperature variations. Future studies should investigate this relationship further using different temperature scenarios, preferably by employing measured urban climate and energy consumption data. Design and planning guidelines for a low carbon transition should further explore strategies to achieve energy demand reduction through UHI mitigation measures.

References

Aboelata, A., & Sodoudi, S. (2019). Evaluating urban vegetation scenarios to mitigate urban heat island and reduce buildings' energy in dense built-up areas in Cairo. *Building and Environment*, *166*(August), 106407. https://doi.org/10.1016/j.buildenv.2019.106407

Ahmadian, E., Sodagar, B., Bingham, C., Elnokaly, A., & Mills, G. (2021). Effect of urban built form and density on building energy performance in temperate climates. *Energy and Buildings*, *236*, 110762. https://doi.org/10.1016/j.enbuild.2021.110762

Allegrini, J., Dorer, V., & Carmeliet, J. (2012). Influence of the urban microclimate in street canyons on the energy demand for space cooling and heating of buildings. *Energy and Buildings, 55*, 823–832. https://doi.org/10.1016/j.enbuild.2012.10.013.

Ambrosini, D., Galli, G., Mancini, B., Nardi, I., & Sfarra, S. (2014). Evaluating mitigation effects of urban heat islands in a historical small center with the ENVI-Met® climate model. *Sustainability (Switzerland)*, *6*(10), 7013–7029. https://doi.org/10.3390/su6107013

Ascione, F., Bianco, N., Maria Mauro, G., & Napolitano, D. F. (2019). Building envelope design: Multi-objective optimization to minimize energy consumption, global cost and thermal discomfort. Application to different Italian climatic zones. *Energy*, *174*, 359–374. https://doi.org/10.1016/j.energy.2019.02.182

ASHRAE Standard 90.1. (2016). *Energy Standard for Buildings Except Low-rise Residential Buildings.* American Society of Heating, Refrigerating and Air-Conditioning Engineers. Atlanta, GA, USA, 2016.

Bruse, M., & Fleer, H. (2009). *ENVI-met*. http://www.envi-met.com
CEA type 4 The CEA Team (2020) CityEnergyAnalyst v3.10.0. Zenodo.http://doi.org/10.5281/zenodo.4032169
Chen, Y., Wu, J., Yu, K., & Wang, D. (2020). Evaluating the impact of the building density and height on the block surface temperature. *Building and Environment*, *168*(19). https://doi.org/10.1016/j.buildenv.2019.106493
Conry, P., Sharma, A., Potosnak, M. J., Leo, L. S., Bensman, E., Hellmann, J. J., & Fernando, H. J. S. (2015). Chicago's heat island and climate change: Bridging the scales via dynamical downscaling. *Journal of Applied Meteorology and Climatology*, *54*(7), 1430–1448. https://doi.org/10.1175/JAMC-D-14-0241.1
Crank, P. J., Sailor, D. J., Ban-Weiss, G., & Taleghani, M. (2018). Evaluating the ENVI-met microscale model for suitability in analysis of targeted urban heat mitigation strategies. *Urban Climate*, *26*(April), 188–197. https://doi.org/10.1016/j.uclim.2018.09.002
Depecker, P., Menezo, C., Virgone, J., & Lepers, S. (2001). Design of buildings shape and energetic consumption. *Building and Environment*, *36*, 627–635.
Fonseca, J., & Schlueter, A. (2015)). Integrated model for characterization of spatiotemporal building energy consumption patterns in neighborhoods and city districts. *Applied Energy, 142*, 247–265.
Gobakis, K., & Kolokotsa, D. (2017). Coupling building energy simulation software with microclimatic simulation for the evaluation of the impact of urban outdoor conditions on the energy consumption and indoor environmental quality. *Energy and Buildings, 157*, 101–115.
https://doi.org/10.1016/j.enbuild.2017.02.020.
Gracik, S., Heidarinejad, M., Liu, J., & Srebric, J. (2015). Effect of urban neighborhoods on the performance of building cooling systems. *Building and Environment*, *90*, 15–29. https://doi.org/10.1016/j.buildenv.2015.02.037
Gros, A., Bozonnet, E., Inard, C., & Musy, M. (2016). Simulation tools to assess microclimate and building energy – A case study on the design of a new district. *Energy and Buildings, 114*, 112–122. https://doi.org/10.1016/j.enbuild.2015.06.032.
Guattari, C., Evangelisti, L., & Balaras, C. (2018). On the assessment of urban heat island phenomenon and its effects on building energy performance: a case study of Rome (Italy). Energy Build 2018;158:605e15. *Energy and Buildings, 158*, 605–615. https://doi.org/10.1016/j.enbuild.2017.10.050.
Hassid, S., Santamouris, M., Papanikolaou, N., Linardi, A., Klitsikas, N., Georgakis, C., & Assimakopoulos, D. N. (2000). Effect of the Athens heat island on air conditioning load. *Energy and Buildings*, *32*(2), 131–141. https://doi.org/10.1016/S0378-7788(99)00045-6
He, J., Hoyano, A., & Asawa, T. (2009). A numerical simulation tool for predicting the impact of outdoor thermal environment on building energy performance. *Applied Energy, 86*, 1596– 1605. https://doi.org/10.1016/j.apenergy.2008.12.034.
Hirano, Y., & Fujita, T. (2012). Evaluation of the impact of the urban heat island on residential and commercial energy consumption in Tokyo. *Energy, 37*(1), 371–383. https://doi.org/10.1016/j.energy.2011.11.018.
Hong, T., Xu, Y., Sun, K., Zhang, W., Luo, X., & Hooper, B. (2021). Urban microclimate and its impact on building performance: A case study of San Francisco. *Urban Climate*, *38*(March), 100871. https://doi.org/10.1016/j.uclim.2021.100871
Huttner, S. (2012). Further development and application of the 3D microclimate simulation ENVI-met. University of Mainz.
ISO 13790. (2008). Energy performance of buildings –calculation of energy use for space heating and cooling. International Organization for Standardization, ISO.
ISO 52016-1. (2017). Energy performance of buildings – Energy needs for heating and cooling, internal temperatures and sensible and latent heat loads - Part 1: Calculation procedures. International Organization for Standardization, ISO.
Javanroodi, K., & Nik, V. M. (2019). Impacts of microclimate conditions on the energy performance of buildings in urban areas. *Buildings*, *9*(8). https://doi.org/10.3390/buildings9080189
Li, X., Zhou, Y., Yu, S., Jia, G., Li, H., & Li, W. (2019). Urban heat island impacts on building energy consumption: A review of approaches and findings. *Energy, 174*, 407–419. https://doi.org/10.1016/j.energy.2019.02.183.
Liu, J., Heidarinejad, M., Guo, M., & Srebric, J. (2015). Numerical evaluation of the local weather data impacts on cooling energy use of buildings in an urban area. *Procedia Engineering, 121*, 381–388. https://doi.org/10.1016/j.proeng.2015.08.1082.

Liu, Y., Stouffs, R., Tablada, A., Wong, N., & Zhang, J. (2017). Comparing micro-scale weather data to building energy consumption in Singapore. *Energy and Buildings, 152*, 776–791. https://doi.org/10.1016/j.enbuild.2016.11.019.

Loibl, W., Vuckovic, M., Etminan, G., Ratheiser, M., Tschannett, S., & Österreicher, D. (2021). Effects of densification on urban microclimate— a case study for the city of Vienna. *Atmosphere*, *12*(4). https://doi.org/10.3390/atmos12040511

Magli, S., Lodi, C., Lombroso, L., Muscio, A., & Teggi, S. (2015). Analysis of the urban heat island effects on building energy consumption. *International Journal of Energy and Environmental Engineering, 6*(1), 91–99. https://doi.org/10.1007/s40095-014-0154-9.

Maiullari, D., Pijpers-Van Esch, M., & van Timmeren, A. (2021). A quantitative morphological method for mapping local climate types. *Urban Planning, 6*(3), 240–257. https://doi.org/10.17645/up.v6i3.4223

Mangan, S. D., Koclar Oral, G., Erdemir Kocagil, I., & Sozen, I. (2021). The impact of urban form on building energy and cost efficiency in temperate-humid zones. *Journal of Building Engineering*, *33*(June 2020), 101626. https://doi.org/10.1016/j.jobe.2020.101626

Martins, T. A. de L., Faraut, S., & Adolphe, L. (2019). Influence of context-sensitive urban and architectural design factors on the energy demand of buildings in Toulouse, France. *Energy and Buildings*, *190*, 262–278. https://doi.org/10.1016/j.enbuild.2019.02.019

Morakinyo, T. E., Ouyang, W., Lau, K. K. L., Ren, C., & Ng, E. (2020). Right tree, right place (urban canyon): Tree species selection approach for optimum urban heat mitigation - development and evaluation. *Science of the Total Environment, 719*, 137461. https://doi.org/10.1016/j.scitotenv.2020.137461

Mosteiro-Romero, M., Maiullari, D., Pijpers-van Esch, M., & Schlueter, A. (2020). An Integrated Microclimate-Energy Demand Simulation

Method for the Assessment of Urban Districts. *Frontiers in Built Environment*, Vol. 6, p. 165. https://www.frontiersin.org/article/10.3389/fbuil.2020.553946

Natanian, J., Maiullari, D., Yezioro, A., & Auer, T. (2019). Synergetic urban microclimate and energy simulation parametric workflow Synergetic urban microclimate and energy simulation parametric workflow. *Journal of Physics: Conference Series*, *1343*. https://doi.org/10.1088/1742-6596/1343/1/012006

Oke, T., Mills, G., Christen, A., & Voogt, J. (2017). *Urban Climates*. Cambridge University Press.

Qaid, A., Bin Lamit, H., Ossen, D. R., & Raja Shahminan, R. N. (2016). Urban heat island and thermal comfort conditions at micro-climate scale in a tropical planned city. *Energy and Buildings*, *133*, 577–595. https://doi.org/10.1016/j.enbuild.2016.10.006

Quan, S. J., & Li, C. (2021). Urban form and building energy use: A systematic review of measures, mechanisms, and methodologies. *Renewable and Sustainable Energy Reviews, 139*(January), 110662. https://doi.org/10.1016/j.rser.2020.110662

Reinhart, C. (2013). *DAYSIM Version 4.0*. http://daysim.ning.com

Rode Philipp, Christian Keim, Guido Robazza, Pablo Viejo, & James Schofield. (2014). Cities and energy: urban morphology and residential heat-energy demand. *Environment and Planning B: Planning and Design,* 138-162.

Salvati, A., Palme, M., Chiesa, G., & Kolokotroni, M. (2020). Built form, urban climate and building energy modelling: case-studies in Rome and Antofagasta. *Journal of Building Performance Simulation*, *13*(2), 209–225. https://doi.org/10.1080/19401493.2019.1707876

Salvati, Agnese, Monti, P., Coch Roura, H., & Cecere, C. (2019). Climatic performance of urban textures: Analysis tools for a Mediterranean urban context. *Energy and Buildings*, *185*, 162–179. https://doi.org/10.1016/j.enbuild.2018.12.024

Sanaieian, H., Tenpierik, M., Linden, K. Van Den, Mehdizadeh Seraj, F., & Mofidi Shemrani, S. M. (2014). Review of the impact of urban block form on thermal performance, solar access and ventilation. *Renewable and Sustainable Energy Reviews*, *38*, 551–560. https://doi.org/10.1016/j.rser.2014.06.007

Santamouris, M. (2014). On the energy impact of urban heat island and global warming on buildings. *Energy and Buildings, 82*, 100-113. https://doi.org/10.1016/j.enbuild.2014.07.022.

Santamouris, M. (2020). Recent progress on urban overheating and heat island research. Integrated assessment of the energy, environmental, vulnerability and health impact. Synergies with the global climate change. *Energy and Buildings*, *207*. https://doi.org/10.1016/j.enbuild.2019.109482

Sharmin, T., Steemers, K., & Matzarakis, A. (2017). Microclimatic modelling in assessing the impact of urban geometry on urban thermal environment. *Sustainable Cities and Society*, *34*(February), 293–308. https://doi.org/10.1016/j.scs.2017.07.006

Silva, M., Oliveira, V., & Leal, V. (2017). Urban Form and Energy Demand: A Review of Energy-relevant Urban Attributes. *Journal of Planning Literature*, *32*(4), 346–365. https://doi.org/10.1177/0885412217706900

Skelhorn, C., Levermore, G., & Lindley, S. (2016). Impacts on Cooling Energy Consumption Due to the UHI and Vegetation Changes in Manchester, UK. *Energy and Buildings, 122*, 150–159. https://doi.org/10.1016/j.enbuild.2016.01.035.

Steadman, P., Hamilton, I., & Evans, S. (2014). Energy and urban built form: An empirical and statistical approach. *Building Research and Information*, *42*(1), 17–31. https://doi.org/10.1080/09613218.2013.808140

Taleghani, M., Kleerekoper, L., Tenpierik, M., & Van Den Dobbelsteen, A. (2015). Outdoor thermal comfort within five different urban forms in the Netherlands. *Building and Environment*, *83*, 65–78. https://doi.org/10.1016/j.buildenv.2014.03.014

The CEA Team. (2018). City Energy Analyst v2.9.0. https://doi.org/10.5281/zenodo.1487867

The CEA Team (2020) City Energy Analyst v3.10.0. Zenodo. http://doi.org/10.5281/zenodo.4032169

Tsoka, S., Tsikaloudaki, A., & Theodosiou, T. (2018). Analyzing the ENVI-met microclimate model's performance and assessing cool materials and urban vegetation applications–A review. Sustainable Cities and Society, 43(July), 55–76. https://doi.org/10.1016/j.scs.2018.08.009

Wang, Y., Berardi, U., & Akbari, H. (2016). Comparing the effects of urban heat island mitigation strategies for Toronto, Canada. Energy and Buildings, 114, 2–19. https://doi.org/10.1016/j.enbuild.2015.06.046

Wong, N. H., Jusuf, S. K., Syafii, N. I., & Chen, Y. (2011). Evaluation of the impact of the surrounding urban morphology on building energy consumption. Solar Energy, 85(1), 57–71. https://doi.org/10.1016/j.solener.2010.11.002

Yang, X., Peng, L. L. H., Jiang, Z., Chen, Y., Yao, L., He, Y., & Xu, T. (2020). Impact of urban heat island on energy demand in buildings: Local climate zones in Nanjing. Applied Energy, 260(30), 114279. https://doi.org/10.1016/j.apenergy.2019.114279

Yang, X., Zhao, L., Bruse, M., & Meng, Q. (2013). Evaluation of a microclimate model for predicting the thermal behavior of different ground surfaces. Building and Environment, 60, 93–104. https://doi.org/10.1016/j.buildenv.2012.11.008

Zinzi, M., & Carnielo, E. (2017). Impact of urban temperatures on energy performance and thermal comfort in residential buildings. The case of Rome, Italy. *Energy and Buildings*, *157*, 20–29. https://doi.org/10.1016/j.enbuild.2017.05.021

6 Discussion

The aim of this thesis was to achieve a greater understanding of the complex relationship between urban form characteristics and building cooling demand in urban climate conditions. It acknowledged the need for a new methodological framework to analyse, classify and assess this relationship. While the previous chapters described the research process and findings, this chapter elaborates on the thesis's methodological limitations and discusses the results by reflecting on their meaning and contextualization.

6.1 Local Climate Type Classification

The study presented in Chapter 3 demonstrated that urban form has a significant impact on both indoor and outdoor air temperature. As shown, the developed local climate type (LCT) classification method enables the quantitative identification of building and context types, advancing the use of morphological methods to individually analyse thermal patterns dependent upon buildings' form characteristics and surroundings. In contrast to traditional typological micro and local climate approaches, which focus on homogeneous and often generic urban form patterns, the LCT classification method acknowledges the re-development and densification processes that drive diversity and heterogeneity in the urban fabric. Thus, this methodological approach confronts the challenge of describing urban heterogeneity, building on previous studies that have called for an investigation of urban diversity (e.g., Barlow, 2014; Leng et al., 2020; Ratti, Baker & Steemers, 2005) and highlighted the benefits of understanding microclimate processes in existing urban settings (e.g., Steemers, Ramos & Sinou, 2004). Additionally, the LCT classification method allows a multi-variable and multi-scalar description in proximity units. These three properties are not new in the field of urban climatology. The local climate zones (LCZs) framework (Stewart & Oke, 2012) has long identified and described spatial components of climate phenomena based on multiple form and land- cover variables. Furthermore, several climatological studies on the influence of urban form on climate have employed different scales of proximity and buffer units of analysis (e.g.,

Gunawardena, Kershaw & Steemers, 2019; Jin, Cui, Wong & Ignatius, 2018; Leng et al., 2020; Takebayashi, 2017). However, the novelty of the LCT method lies in the systematisation of the three aforementioned properties, which in turn facilitates the description of heterogeneity in the urban fabric. In fact, the eight form parameters in this study were used to independently classify building and context types; for the latter, buffer areas with different radii were employed as units of proximity. This methodological approach acknowledges the possibility that a building may be different from those around it, establishing the concept of building-relative context. In other words, form characteristics (e.g., density, roughness, green coverage) are gauged immediately around a building (via a circular buffer area) rather than in the land unit (e.g., block, plot) to which they belong.

As shown in Chapter 5, the testing of the method on the Rotterdam case study and its sensitivity analysis highlighted that, for the period under study, not all eight of the form parameters are related to outdoor air temperature. This result finding is discussed in greater detail in Section 5.3. However, regarding the context type classification, it should be noted that the statistical significance of such relationships may depend on the radius of the considered buffer area. For example, the heat mitigation effect of vegetation coverage may be more visible in larger units of analysis. This observation suggests that buffer radii (used to trace the context boundaries) should be tested and validated, as they can impact the results. In this direction, recent studies have shown that measured data can aid in cross-scale analysis and systemic proximity buffer analysis. For example, Du et al. (2020), by comparing significant morphological predictors of air temperature at the spatial microscale and mesoscale, found that form parameters vary their explanatory power according to scale. Similarly, Alonso and Renard (2020) analysed the correlation between air temperature and various parameters as a function of scale to determine the most appropriate radius for each variable. This proximity buffer analysis revealed that the explanatory zone for form parameters (the scale with the highest correlation between air temperature and form) ranges in radius from 5m to 1000m. Thus, these studies indicate that contextual buffer areas with a radius larger than 25m and 50m radius should be explored to improve the LCT method.

While the LCT method facilitates type classification, it has limited applicability for city mapping purposes. Hwang, Lin and Lin (2020) demonstrated that mapping overheating risks at the city-wide scale can guide the evaluation of energy performance in urban areas by detailing the distribution of air and surface temperatures. In this thesis, despite the cluster analysis with a hierarchical clustering method supports the exploration of structural connections among different types, it is computationally limited in processing large datasets. Therefore, city mapping that could offer insights into types spatial distribution appears difficult

to achieve by using this specific statistical method. Thus, other unsupervised classification techniques should be tested for LCT mapping to advance the analysis of urban climate patterns and their effects on building energy performance. This is also necessary in the perspective of using LCT classification for other purposes, such as heat vulnerability analysis. As observed by Ellena, Breil and Soriani (2020), heat vulnerability is not simply related to air temperature alone. Therefore, more research and tools are required to connect heat exposure and health impacts to urban form characteristics. The evolution of LCT from a classification instrument to a mapping instrument has the potential to fulfil this need by promoting a greater understanding of urban overheating patterns and their consequences. Furthermore, it could facilitate the evaluation of urban-planning policies (Hwang et al., 2020) and decision- making, as described in Chapter 7.

6.2 Microclimate assessment

To explore the role of urban form on energy demand, urban microclimate was modelled in Chapter 3, 4 and 5 by using the microclimate tool ENVI-met. Modelling was chosen over an observational approach based on urban climate measurements because the required measurements would include contributions of anthropogenic heat, and materials' thermal characteristics, making difficult to separate the form impacts on the urban microclimate from the others . However, it's important to note that urban climate models also have some limitations (Mirzaei, 2021). Their most prominent limitation is the substantial computational power necessary to solve fluid dynamics and thermodynamics equations, which challenges the balance between tempo-spatial resolution, the extension of the spatial domain and the time-period of the analysis. For this reason, this thesis considers limited time frames, looking only at representative (consecutive) hot days. Additionally, the Rotterdam case study did not explore buffer areas with a radius larger than 50m to avoid needing to reduce the grid-cell resolution for the simulations; in fact increasing cell size to anything above 3mx3mx3m would likely reduce the accuracy of the results.

Previous studies have already established, by comparing model results against field observations across different geographical contexts, that ENVI-met is capable of performing accurate urban climate simulations (e.g., Conry et al., 2015; Middel, Häb, Brazel, Martin & Guhathakurta, 2014; Salata, Golasi, de Lieto Vollaro & de Lieto Vollaro, 2016; Salata et al., 2017; Skelhorn, Lindley & Levermore, 2014;

Taleghani, Kleerekoper, Tenpierik & Van Den Dobbelsteen, 2015; Yang, Zhao, Bruse & Meng, 2013). Still, the accuracy of the model was confirmed in this thesis by performing a validation of the ENVI- met simulations' results. In the Rotterdam case, the Willmott index of agreement (Willmott, 1982) between measured and modelled air temperature was found to be equal to 0.98, confirming a high level of accuracy. . However, the comparison between simulated and measured temperatures indicates that the level of accuracy is higher during daytime hours than during night-time hours. This finding suggests that the model underestimates night-time temperatures, adding to the debate over ENVI-met's ability to compute nocturnal UHI effects (S. Tsoka, Theodosiou, Tsikaloudaki & Flourentzou, 2018). One simple explanation for the mismatch between simulated and measured temperature values at night is that the measurements include anthropogenic heat, while the simulated values do not. In cities, solar radiation and anthropogenic heat are absorbed by pavement and other built surfaces during the daytime, resulting in the warming of the urban atmosphere. UHI intensity is generally higher at night, when the energy absorbed during the day is released, increasing urban air temperatures. In this thesis the microclimate assessment of LCTs neglects anthropogenic heat, as ENVI-met does not have a computational module to assess it. According to Middel et al. (2014), the underestimation of night-time temperature may also stem from the model's systematic underestimation of sensible heat flux. However, more detailed measurements would be necessary to verify this.

ENVI-met was selected for this study over other tools due to its holistic ability to simulate heat exchange on different surfaces (e.g., building, soil), sensible heat flux from urban elements to the air, airflow between roughness elements, and evapotranspiration processes for vegetation and surface water. It was found to be accurate in its estimation of diurnal urban climate variables, though its aforementioned limitations prevented the author from analysing the night-time relationship between urban form and climate processes. Finally, the low accuracy of modelled night-time air temperatures in this study and others like it prompts new questions regarding the validation of sensible heat flux in ENVI-met as well as the weight of anthropogenic heat in the Rotterdam-specific energy balance.

6.3 Relationship between form and microclimate

In Chapter 3, the climate assessment of Rotterdam's LCTs revealed that high-density, high-rise urban fabrics generally lead to lower UHI. However, this effect is only observed on a diurnal basis, and these morphological characteristics may result in higher night-time UHI intensity. Higher-density environments entail more shaded areas and, in turn, reduced daytime solar radiation absorption; while, they exhibit lower long-wave radiative losses and ventilation, resulting in air temperature increases at night (Loibl et al., 2021; Salvati, Palme, Chiesa & Kolokotroni, 2020). Among others, Boccalatte, Fossa, Gaillard and Menezo (2020) recently studied the overall climate performance of high-density and high-rise urban fabrics, demonstrating that monthly average UHI intensity rises proportionally alongside increases in density and height. This may be linked to the influence on UHI at night. More specifically, they attribute the trapping of radiation and hot air to the high compactness of the urban fabric and the low ratio between street canyons' width and height, and they attribute the hindered night-temperature mitigation to high roughness, which lowers wind velocity.

Additionally, this thesis employed a multiple regression analysis on the 25 Rotterdam archetypes selected through the LCT method. In Chapter 5 the statistical analysis of the relationship between form parameters and outdoor air temperature highlighted the fact that FSI and building height are significant predictors of average diurnal air temperature. The negative correlation between diurnal outdoor air temperature and building height is consistent with previous research. Gui et al. (2021) found that, as height increases, temperature decreases linearly during both summer and winter days. Zhang and Gao (2021) revealed a negative correlation between FSI and direct shortwave radiation. Notably, this study did not detect a significant correlation between diurnal air temperature and any form factors aside from FSI and building height. This may stem from the fact that the 25 samples, which varied in urban form type, were analysed collectively. Among others, Du et al. (2020) and Agnese Salvati, Monti, Coch Roura and Cecere (2019) have argued that the correlation between morphological and climate variables changes across different spatial patterns. Du et al. (2020), for example, found that despite GSI being one of the parameters most frequently correlated with air temperature, both the size and sign of this correlation vary based on urban pattern. While a regression analysis of each group of buildings or context types in the Rotterdam case study may have revealed other relevant relationships, the use of only five cases for each type was statistically insufficient.

One correlation that was expected but not detected in this study is that between descriptors of vegetation coverage and diurnal air temperature. As Saaroni, Amorim, Hiemstra and Pearlmutter (2018) pointed out, the relationship between green coverage and heat mitigation is still controversial. City-scale scenarios considered by Houmani et al. (2019) across several European cities highlighted a potential decrease in annual average air temperature up to 10% due to increases in green coverage alone. Additionally, Ouyang, Morakinyo, Ren and Ng (2020) argued that a negative logarithmic correlation exists between tree coverage and temperature mitigation. The study found that, in the subtropical climate of Hong Kong, the optimal outdoor cooling efficiency of trees is achieved at a surface coverage of 30% regardless of building density. However, the correlation between green coverage and air temperature may simply be a function of the areal unit in which the coverage is calculated, as demonstrated by Heusinkveld, Steeneveld, Hove, Jacobs and Holtslag (2014).

6.4 Energy assessment

Chapter 4 presented a coupling method between ENVI-met and CEA to model building cooling demand with urban climate boundary conditions. This method enables the extraction of microclimate simulation outputs (e.g., air temperature, wind speed, relative humidity) and their use as inputs in CEA, an energy-modelling tool. The aggregation of climate values aligns with recommendations by Toparlar, Blocken, Maiheu and van Heijst, (2018) and thus, hourly microclimate values are calculated as an average of the values detected in the air layer around each building envelope; this approach avoids basing energy simulations on location-specific climate variables gathered at one specific point.

The developed coupling method was first tested on a district in Zurich (CH) and then on 25 archetypes across Rotterdam (NL). These studies, presented in Chapter 4 and Chapter 5, respectively, wield similar methodologies, both comparing cooling demand between a Baseline and a Microclimate scenario. As the Baseline scenario uses rural weather data in CEA simulations while the Microclimate scenario uses the coupling ENVI-met/CEA, the difference between them in cooling demand can be interpreted as the cooling penalty caused by urban microclimate conditions. However, the cooling penalty found in the Zurich and Rotterdam cases is not directly comparable, as their model inputs are substantially different. Building

characteristics, energy systems, national standards and climate boundary conditions are specific to each case study. In Zurich, for example, the two days analysed reached outdoor temperatures higher than 33°C (at a rural weather station); and the results indicate that the average increase in cooling demand due to microclimate conditions accounts for 5% at the district scale and between -5% and +14% at the level of individual buildings. The Rotterdam simulations were performed across two consecutive hot days with clear skies, reaching air temperatures at the rural weather station of 25°C and 28°C, respectively. The average cooling penalty due to microclimate conditions reached 32% on the first day and 24% on the second day.

In general, both cases point to urban microclimate conditions increasing cooling loads. However, the size of the increase may be influenced by weather conditions (at rural weather stations). The pattern observed in the Rotterdam case suggests that microclimate-cooling penalties decrease as overall rural air temperatures increase. This trend may partially explain why, in the Zurich case, higher temperatures are linked to lower average cooling penalties. Additionally, the buildings in the Zurich case predominantly serve office functions, while the Rotterdam case study assumed residential use. As shown by Toparlar et al. (2018) and Yang et al. (2020), residential buildings are more sensitive than office buildings to microclimate changes. The results in both cases point to the capacity of the integrated modelling method to depict the influence of microclimatic conditions on cooling demand in urban environments. In particular, the fine resolution of the results offers a deep understanding of performance variation across individual buildings based on microclimatic ambient temperature, relative humidity and wind velocity. Therefore, this method's acknowledgement of the trade-off between form configuration, materials and microclimate factors can be of great support in design and planning for improving buildings' energy efficiency. However, as stated by Lauzet et al. (2019), coupling strategies should facilitate feedback loops, with Urban Climate Models and Building Energy Simulations running simultaneously or iteratively. This is not the case with the method developed in this thesis which according to the definitions in Lauzet et al. (2019) is more akin to a chaining method than a coupling method. Further enhancement should be directed towards the implementation of simultaneous and iterative computation between ENVI-met and CEA models.

6.5 Cooling energy demand among Rotterdam LCTs

The results presented in Chapter 5 on the 25 archetypes in Rotterdam show that building cooling demand in the Microclimate scenario was 3.6–100% higher than that in the Baseline scenario. This large range is primarily driven by urban climate and morphological characteristics, as all of the other modelling inputs (e.g., window-to-wall ratio, energy systems, building and pavement materials) are identical across the 25 archetypes. Previous studies comparing cooling demand in rural and urban areas have also found that urban climate conditions contribute to higher cooling loads. Recent literature review studies indicate that UHI accounts for increases in average cooling energy consumption of 12% (Santamouris, 2020), 19% (Li et al., 2019) and 10–16% (Tian, Li, Lu & Wang, 2021). However, as shown in Table 6.1, the impact of UHI on cooling demand can vary drastically in magnitude, confirming the wide range of values uncovered in Rotterdam.

A few studies point to a cooling penalty of up to 30%. Afshari and Liu (2017) were able to isolate weather-driven cooling loads by analysing energy consumption in Abu Dhabi, uncovering a cooling penalty of around 15%. J. Huang et al. (2020) predicted a similar penalty in Hong Kong for a representative summer day. Zhang and Gao (2021) found variation in cooling demand between 9.2% and 16.4% driven by different morphological conditions, when considering the UHI effect. By modelling typical buildings in LCZs, Yang et al. (2020) found that local climate conditions led to increases in annual cooling demand of 12–24% for residential buildings and 9–14% for office buildings, resulting in an annual total demand increase up to 6%. Parametric studies by Boccalatte et al. (2020) and Gunawardena et al. (2019) estimated increases in cooling demand of up to 30% during summers in Rome and London, respectively. Others have found much higher cooling penalties. M. Kolokotroni, Davies, Croxford, Bhuiyan and Mavrogianni (2010) found that the urban climate in London can result in annual differences of up to 42% in cooling energy usage, while Hassid et al. (2000) uncovered a figure of 50% in Athens, and Hong et al. (2021) found one of 65% in San Francisco. Similarly, in comparing 17 European capitals, Krafess et al. (2019), concluded that UHI can lead to increases of up to 60% in cooling demand; however, they noted that this pattern is more prominent in southern cities.

TABLE 6.1 Key studies on urban climate related cooling penalty

City	Period of analysis	Climate method	Energy method	Type of building	Change in cooling (%)	Reference
Athens	1 year	Observation	DOE2.1.E	Typical building across 3 urban zones	-20, +15, +50%	(Hassid et al., 2000)
Rome	Summer	UWG	TRNSYS	Apartment block (residential) Detached building (residential) across 5 urban patterns	+5 to 26% +16 to 63%	(Salvati et al., 2020)
Modena	1 year	Observation	TRNSYS	Library (office)	+8 to 10%	(Magli, Lodi, Lombroso, Muscio & Taggi, 2015)
Nanjing	1 day in summer, 1 day in winter	ENVI-met	EnergyPlus	Generic urban pattern	9.2% and 16.4 %	(Zhang & Gao, 2021)
Abu Dhabi	1 year	TEB	Regression		+15%	(Afshari & Liu, 2017)
Hong Kong	1 day	UMM (validated)	HTB2	District	+15%	(Huang et al., 2020)
Nanjing	1 typical year	Observation	EnergyPlus	Typical building (residential) Typical building (office)	+12 to 24% +9 to 14%	(Yang et al., 2020)
Barcelona	Winter and summer	Observation	EnergyPlus	Typical building (residential)	+18 to 28%	(Salvati, Roura & Cecere 2017)
Rome	1 year	Observation	TRNSYS	Typical building (residential)	+12 to 46%	(Zinzi & Carnielo, 2017)
London	Winter and summer	UWG	Thermal model IESVE	Typical building (office) in a generic urban pattern featuring 3 different materials	+16, +26, 30%	(Gunawardena et al., 2019)
Rome	1 year	Observation	TRNSYS	Typical building	+30%	(Guattari, Evangelisti & Balaras, 2018
Rome	July and January	UWG	EnergyPlus	Typical building across 6 urban patterns	+30%	(Boccalatte et al., 2020)

>>>

TABLE 6.1 Key studies on urban climate related cooling penalty

City	Period of analysis	Climate method	Energy method	Type of building	Change in cooling (%)	Reference
Antwerp	1 month	CFD simulation	EnergyPlus	Typical building (office) Typical building (residential)	+31% +90%	(Toparlar et al., 2018)
London	1 year	Observation	Cooling degree hours	Typical building	+32 to 42%	(Kolokotroni, Davies, Croxford, Bhuiyan, & Mavrogianni, 2010)
Rome	1 year	Observation	TRNSYS	Typical building (office) Typical building (residential)	+53% +74%	(Zinzi, Carnielo & Mattoni, 2018)
European cities	1 typical year	CIM	CitySim	Typical building	Up to 60%	(Krafess et al., 2019)
San Francisco	1 year	Observation	EnergyPlus	Typical building (hotel) Typical building (office)	+65%	(Hong et al., 2021)

While the methods and geographical contexts of the studies in Table 6.1 do not allow for a holistic comparison, one can still derive some insight by contextualising the Rotterdam results. First, in terms of function, office buildings typically exhibit lower climate-related cooling demand than residential buildings. Toparlar et al. (2018) and Zinzi et al. (2018) found cooling demand increases in residential buildings of 90% and 74% and increases in office buildings of 31% and 53%, respectively. The energy modelling of the Rotterdam archetypes assumes a residential function; incorporating other functions could produce lower cooling penalties. Second, as the large majority of existing studies evaluate a typical building without considering the surrounding urban fabric, microscale climate processes are generally neglected. This is problematic, as the consideration of buildings' surroundings appears to be critical to achieving an accurate understanding. According to Allegrini, Dorer and Carmeliet (2012), cooling demand is higher among buildings in street canyons than among stand-alone buildings. The role of buildings' surroundings can be largely explained by two main mechanisms in the urban climate: radiation exchange between surfaces and the influence of wind sheltering on convective heat transfer. Additionally, only very few studies have analysed the impact of building form on cooling demand variability (e.g., A. Salvati et al., 2020). Thus, by analysing both buildings and their context types at the microclimate scale, this study on Rotterdam enlarges the literature's understanding of the morphological variables involved in urban thermal processes.

6.6 Relationship between cooling demand, urban form and climate characteristics

As proven by the literature review in Chapter 2, there is great interest in the ability of form characteristics and parameters to indicate buildings' energy-consumption levels. This study found that the relationship between urban form and energy demand is twofold. An 'intrinsic' role of form lies in the direct effect of building shape on thermal losses and gains, which influence energy loads, while an 'extrinsic' role of form lies in the indirect effect of urban fabric on local climate processes and, in turn, on the contextual conditions in which a building performs. Chapter 5's regression analysis identified the significant form and climate variables that explain diurnal cooling demand of the Rotterdam archetypes. Since theoretical and empirical studies have generally acknowledged the relationship between urban form and building energy performance in urban environments, it is possible to compare these results with the findings of the Rotterdam statistical analysis. From a

microclimate perspective, as shown in Table 5.5, the most relevant predictor of building cooling demand is average diurnal outdoor air temperature. Relative humidity and wind speed play a secondary—but still significant—role. Similar correlations were found by Fung, Lam, Hung, Pang and Lee (2006). Additionally, a recent empirical study by Su, Ngarambe, Santamouris and Yun (2021) confirmed positive correlations between average daytime UHI and building cooling demand and between outdoor air temperature and building cooling demand. Average outdoor air temperature was found to be highly determinative of maximum cooling energy loads (Yi & Peng, 2019).

From a morphological perspective, this thesis found that all three of the studied variables describing building form (height, footprint, surface-to-volume ratio) are significantly correlated with building cooling loads. In this study, building height was found to be a relevant predictor for both the mild first day and the warmer second day demand. The relation has a positive sign, meaning that as building height increases, so too does cooling demand. These results are not consistent with the negative correlation uncovered between building height and outdoor temperature in Chapter 3. However, air temperature is only one of several components that affect energy loads; since high-rise buildings have more exposed surface area, solar gains may play a larger role in their total thermal balance. While some studies have observed decreases in annual cooling alongside increasing height (Gui et al., 2021), these comparisons were based not only on the difference between urban and rural

conditions but also on the number of cooling degree days. Furthermore, on the second day analysed in the Rotterdam case, surface-to-volume ratio (StoV) was also found to be positively correlated with cooling loads. Buildings with high StoV are less compact, meaning that their cooling demand is higher on account of solar gains stemming from their larger exposed envelope. Importantly, this parameter is sensitive to dimensions, so the correlation may also depend on building size. On the first day studies, another parameter found significantly correlated with cooling demand was building footprint area.

Additionally, in the Rotterdam case, density and roughness parameters describing context characteristics were found to be significantly correlated with urban cooling demand on the first day. While there is extensive research on the negative correlation between heating demand and these variables (e.g., Rode et al., 2014; Rodríguez-Álvarez, 2016), only a few recent studies have looked at cooling demand (Trepci, Maghelal & Azar, 2021). For example, regarding Floor Space Index (FSI) and Ground Space Index (GSI), which describe building intensity and building coverage, respectively, the Rotterdam case study revealed a negative correlation between GSI and cooling loads but a positive correlation between FSI and cooling loads. The results pertaining to GSI have been confirmed in a Barcelona case study by Salvati, Coch and Morganti (2017), where, Including UHI in the energy model, cooling demand was found to decrease alongside increases in site coverage ratio. Zhang and Gao (2021) found that cooling load is negatively correlated with both GSI and FSI on a typical day. However, in the case of Rome A. Salvati et al. (2020) uncovered a positive correlation between GSI and cooling demand when considering UHI despite finding a negative correlation between them when only considering shadow contribution. Generally, high intensity and high compactness mean that there is higher shadow density, reducing daytime solar gains during summers. Contextual mean building height was also found to be significantly negatively correlated with cooling demand in the Rotterdam case. This relation has a negative sign, corroborating that as average building height of an area increases, cooling consumption decreases (Mangan, Koclar Oral, Erdemir Kocagil & Sozen, 2021; A. Salvati et al., 2020).

In contrast, grass and tree coverage area were found non-significantly correlated with cooling loads. Still, the beneficial effects of green areas and urban parks on energy savings have been widely acknowledged as shown in Chapter 2. According to Ca, Asaeda and Abu (1998), proximity of a building to an urban park can result in daytime energy savings of up to 15%. Toparlar et al. (2018) found similar results for both residential and office buildings (14% and 11%, respectively). Thus, it is generally agreed upon that greenery reduces urban temperatures and, in turn, building cooling demand. Huang and Li (2017) estimate that the dense planting of

trees at two-meter intervals in an urban canyon results in a drop in cooling energy consumption of up to 1.73W/m2. Shading by trees on facades boosts the potential for cooling energy savings of up to 54% depending on planting patterns and foliage density (Palme, Privitera & La Rosa, 2020; Stella Tsoka, Leduc & Rodler, 2021). Additionally, city-scale scenarios for major European capitals highlight the cumulative cooling potential of greenery, demonstrating a potential reduction in annual cooling demand of up to 34% (Houmani et al., 2019). This thesis, however, classified local climate types based on two parameters - grass coverage and tree crown area - and did not find a statistically significant difference in cooling demand across types. The sensitivity analysis confirmed the non-significance of these two variables. There may be two reasons for this. First, the radius of influence used in this analysis—25m for tree crown area and 50m for grass coverage area—may be too small to capture the full impact of parks and densely vegetated areas. Second, since CEA is unable to consider the shadows created by trees in the radiation calculation module, the impact of trees adjacent to building façades on solar gains is not captured.

As shown, building height and local air temperature were both found to be significant predictors of cooling demand on the days under study. However, the number and significance of the other predictors vary by day, suggesting that there is no absolute explanation of cooling loads based on these factors. Thus, it appears that the energy-relevance of both local climate and form characteristics depends on the overall weather conditions, suggesting that the thermal mechanisms triggered by urban form possess high temporal variability and may be a function of weather-related temperature thresholds.

This Rotterdam case study sought an understanding of the morphological factors affecting cooling loads during a hot summer period. A more general evaluation of the balance between cooling and heating needs on a yearly base is beyond the scope of this thesis. However, other researchers have argued that higher internal gains are indicative of larger annual shifts from heating to cooling (Maria Kolokotroni, Zhang & Watkins, 2007). Thus, the contextual properties of building intensity, compactness and mean height that influence solar access may reverse their influence on heating loads.

6.7 Potential applications of the results

The literature review in Chapter 2 developed a comprehensive list of energy-relevant form attributes, including those that modify the local climate of building contexts. Chapters 3,4 and 5 adopted a predictive, analytical perspective with the aim of informing design and planning practices. The overall attempt of this thesis was to identify which morphological characteristics at the city scale can help reducing energy consumption. In other words, it was to determine the types of buildings and contexts that boost energy performance to the greatest degree. However, defining generalised guidelines is challenging without a deep, multiscale understanding of local conditions and the instruments to analyse their complexity.

The Rotterdam case study showed that the LCT classification method and the coupled assessment method, both of which were developed in this thesis, are powerful instruments for achieving a greater understanding of the relationship between urban form and cooling demand in urban climates. In discussing their limitations, however, this chapter has highlighted paths for further methodological improvements: to validate the unit size for context classifications; to evolve the LCT classification for mapping types at the wide city scale; and to extend the analysis of the relationship between urban form and night-time temperatures. Furthermore, the contextualisation of the Rotterdam results showed that the relationship between energy performance and the form characteristics of buildings and their context has a high spatial and temporal variability. Beyond geographical and climate-zone-related aspects, urban climate processes and the microscale trade-offs between buildings and their immediate context can lead to different energy performance levels. Additionally, form-related building loads are strongly influenced by seasonal, daily and hourly microclimate variations in radiation income, air temperature, wind velocity and humidity, adding another layer of complexity.

While the findings in the Rotterdam case offer some worthwhile reflections, results and recommendations are not generalisable and cannot be extended directly to similar locations in the same climate zone, nor to other climate or geographical conditions without further studies. As shown in Chapter 5, high-rise building cooling demand is less sensitive to changes in climate and morphological context, while low-rise buildings are highly sensitive to them. Thus, the latter may be more vulnerable to climate warming while the rising number of cooling days and the spread of low-rise buildings may drive drastic rises in energy consumption during summers in the future. However, this does not mean that urban development should completely be oriented towards the construction of high-rise buildings; rather, it should pay

greater attention to morphological and climate contextual conditions when designing low-rise buildings, as more compact urban fabrics and established heat-mitigation measures would considerably reduce their cooling loads. Traditionally passive and vernacular architecture highlight the use of fabric compactness as a heat-mitigation strategy. Still, the matter of translating these measures for the Dutch temperate climate remains; it would require the preservation of solar access (and, in turn, internal gains) during the heating season as well as reducing it during summer while allowing cool wind flow infiltration into the urban fabric.

References

Afshari, A., & Liu, N. (2017). Inverse modeling of the urban energy system using hourly electricity demand and weather measurements, Part 2: Gray-box model. Energy and Buildings, 157 (2017), 139–156. https://doi.org/10.1016/j.enbuild.2017.01.052

Allegrini, J., Dorer, V., & Carmeliet, J. (2012). Influence of the urban microclimate in street canyons on the energy demand for space cooling and heating of buildings. Energy and Buildings, 55 (2012),823–832. https://doi.org/10.1016/j.enbuild.2012.10.013

Alonso, L., & Renard, F. (2020). A new approach for understanding urban microclimate by integrating complementary predictors at different scales in regression and machine learning models. Remote Sensing, 12(15). https://doi.org/10.3390/RS12152434

Barlow, J. F. (2014). Progress in observing and modelling the urban boundary layer. Urban Climate, 10(P2), 216–240. https://doi.org/10.1016/j.uclim.2014.03.011

Boccalatte, A., Fossa, M., Gaillard, L., & Menezo, C. (2020). Microclimate and urban morphology effects on building energy demand in different European cities. Energy and Buildings, 224 (2020), 110–129. https://doi.org/10.1016/j.enbuild.2020.110129

Ca, T. V., Asaeda, T., & Abu, E. M. (1998). Reductions in air conditioning energy caused by a nearby park. Energy and Buildings, 29(1), 83–92. https://doi.org/10.1016/s0378-7788(98)00032-2

Conry, P., Sharma, A., Potosnak, M. J., Leo, L. S., Bensman, E., Hellmann, J. J., & Fernando, H. J. S. (2015). Chicago's heat island and climate change: Bridging the scales via dynamical downscaling. Journal of Applied Meteorology and Climatology, 54(7), 1430–1448. https://doi.org/10.1175/JAMC-D-14-0241.1

Du, S., Li, Y., Wang, C., Tian, Z., Lu, Y., Zhu, S., & Shi, X. (2020). A cross-scale analysis of the correlation between daytime air temperature and heterogeneous urban spaces. Sustainability (Switzerland), 12(18), 1–22. https://doi.org/10.3390/su12187663

Ellena, M., Breil, M., & Soriani, S. (2020). The heat-health nexus in the urban context: A systematic literature review exploring the socio- economic vulnerabilities and built environment characteristics. Urban Climate, 34(September), 100676. https://doi.org/10.1016/j.uclim.2020.100676

Fung, W. Y., Lam, K. S., Hung, W. T., Pang, S. W., & Lee, Y. L. (2006). Impact of urban temperature on energy consumption of Hong Kong.
Energy, 31(14), 2623–2637. https://doi.org/10.1016/j.energy.2005.12.009

Godoy-Shimizu, D., Steadman, P., & Evans, S. (2021). Density and morphology: From the building scale to the city scale. Buildings and Cities, 2(1), 92–113. https://doi.org/10.5334/bc.83

Guattari, C., Evangelisti, L., & Balaras, C. A. (2018). On the assessment of urban heat island phenomenon and its effects on building energy performance: A case study of Rome (Italy). Energy and Buildings, 158, 605–615. https://doi.org/10.1016/j.enbuild.2017.10.050

Gui, C., Yan, D., Hong, T., Xiao, C., Guo, S., & Tao, Y. (2021). Vertical meteorological patterns and their impact on the energy demand of tall buildings. Energy and Buildings, 232, 110624. https://doi.org/10.1016/j.enbuild.2020.110624

Gunawardena, K., Kershaw, T., & Steemers, K. (2019). Simulation pathway for estimating heat island influence on urban/suburban building space-conditioning loads and response to facade material changes. Building and Environment, 150(2019), 195–205. https://doi.org/10.1016/j.buildenv.2019.01.006

Hassid, S., Santamouris, M., Papanikolaou, N., Linardi, A., Klitsikas, N., Georgakis, C., & Assimakopoulos, D. N. (2000). Effect of the Athens heat island on air conditioning load. Energy and Buildings, 32(2), 131–141. https://doi.org/10.1016/S0378-7788(99)00045-6

Heusinkveld, B. G., Steeneveld, G. J., Hove, L. W. A. van, Jacobs, C. M. J., & Holtslag, A. A. M. (2014). Spatial variability of the Rotterdam urban heat island as influenced by urban land use. Journal of Geophysical Research, 131–146. https://doi.org/10.1002/2012JD019399

Hong, T., Xu, Y., Sun, K., Zhang, W., Luo, X., & Hooper, B. (2021). Urban microclimate and its impact on building performance: A case study of San Francisco. Urban Climate, 38(March), 100871. https://doi.org/10.1016/j.uclim.2021.100871

Houmani, C., Krafess, I., Coccolo, S., Mauree, D., Perera, A. T. D., Mohajeri, N., & Scartezzini, J. L. (2019). Urban greening archetypes at the European scale. Journal of Physics: Conference Series, 1343(2019) 012024. https://doi.org/10.1088/1742-6596/1343/1/012024

Huang, J., Jones, P., Zhang, A., Peng, R., Li, X., & Chan, P. (2020). Urban Building Energy and Climate (UrBEC) simulation: Example application and field evaluation in Sai Ying Pun, Hong Kong. Energy and Buildings, 207 (2020) 109580. https://doi.org/10.1016/j.enbuild.2019.109580

Huang, K. T., & Li, Y. J. (2017). Impact of street canyon typology on building's peak cooling energy demand: A parametric analysis using orthogonal experiment. Energy and Buildings, 154, 448–464. https://doi.org/10.1016/j.enbuild.2017.08.054

Hwang, R. L., Lin, T. P., & Lin, F. Y. (2020). Evaluation and mapping of building overheating risk and air conditioning use due to the urban heat island effect. Journal of Building Engineering, 32(May), 101726. https://doi.org/10.1016/j.jobe.2020.101726

Jin, H., Cui, P., Wong, N., & Ignatius, M. (2018). Assessing the effects of urban morphology parameters on microclimate in Singapore to control the urban heat island effect. Sustainability, 10(1), 206-224. https://doi.org/10.3390/su10010206

Kolokotroni, M., Davies, M., Croxford, B., Bhuiyan, S., & Mavrogianni, A. (2010). A validated methodology for the prediction of heating and cooling energy demand for buildings within the urban heat island: Case study of London. Solar Energy, 84(12), 2246–2255. https://doi.org/10.1016/j.solener.2010.08.002

Kolokotroni, M., Zhang, Y., & Watkins, R. (2007). The London heat island and building cooling design. Solar Energy, 81(1), 102–110. https://doi.org/10.1016/j.solener.2006.06.005

Krafess, I., Houmani, C., Mauree, D., Coccolo, S., Perera, A. T. D., & Scartezzini, J. L. (2019). Local climate impact on the energy demand: An analysis at the European scale. Journal of Physics: Conference Series, 1343(1), 012013. https://doi.org/10.1088/1742-6596/1343/1/012013

Lauzet, N., Rodler, A., Musy, M., Azam, M. H., Guernouti, S., Mauree, D., & Colinart, T. (2019). How building energy models take the local climate into account in an urban context – A review. Renewable and Sustainable Energy Reviews, 116(September), 109390. https://doi.org/10.1016/j.rser.2019.109390

Leng, H., Chen, X., Ma, Y., Wong, N. H., & Ming, T. (2020). Urban morphology and building heating energy consumption: Evidence from Harbin, a severe cold region city. Energy and Buildings, 224 (2020), 110143. https://doi.org/10.1016/j.enbuild.2020.110143

Li, X., Zhou, Y., Yu, S., Jia, G., Li, H., & Li, W. (2019). Urban heat island impacts on building energy consumption: A review of approaches and findings. Energy, 174 (2019), 407–419. https://doi.org/10.1016/j.energy.2019.02.183

Loibl, W., Vuckovic, M., Etminan, G., Ratheiser, M., Tschannett, S., & Österreicher, D. (2021). Effects of densification on urban microclimate — A case study for the city of Vienna. Atmosphere, 12(4), 511-534. https://doi.org/10.3390/atmos12040511

Magli, S., Lodi, C., Lombroso, L., Muscio, A., & Teggi, S. (2015). Analysis of the urban heat island effects on building energy consumption.

International Journal of Energy and Environmental Engineering, 6(1), 91–99. https://doi.org/10.1007/s40095-014-0154-9

Mangan, S. D., Koclar Oral, G., Erdemir Kocagil, I., & Sozen, I. (2021). The impact of urban form on building energy and cost efficiency in temperate-humid zones. Journal of Building Engineering, 33(2021), 101626. https://doi.org/10.1016/j.jobe.2020.101626

Middel, A., Häb, K., Brazel, A. J., Martin, C. A., & Guhathakurta, S. (2014). Impact of urban form and design on mid-afternoon microclimate in Phoenix local climate zones. Landscape and Urban Planning, 122 (2014), 16–28. https://doi.org/10.1016/j.landurbplan.2013.11.004

Mirzaei, P. A. (2021). CFD modeling of micro and urban climates: Problems to be solved in the new decade. Sustainable Cities and Society, 69(March), 102839. https://doi.org/10.1016/j.scs.2021.102839

Ouyang, W., Morakinyo, T. E., Ren, C., & Ng, E. (2020). The cooling efficiency of variable greenery coverage ratios in different urban densities: A study in a subtropical climate. Building and Environment, 174(February), 106772. https://doi.org/10.1016/j.buildenv.2020.106772

Palme, M., Privitera, R., & La Rosa, D. (2020). The shading effects of green Infrastructure in private residential areas: Building performance simulation to support urban planning. Energy and Buildings, 229 (2020),110531. https://doi.org/10.1016/j.enbuild.2020.110531

Ratti, C., Baker, N., & Steemers, K. (2005). Energy consumption and urban texture. Energy and Buildings, 37(7), 762–776. https://doi.org/10.1016/j.enbuild.2004.10.010

Rode, P., Keim, C., Robazza, G., Viejo, P., & Schofield, J. (2014). Cities and energy: Urban morphology and residential heat-energy demand. Environment and Planning B: Planning and Design, 41,138–162.

Rodríguez-Álvarez, J. (2016). Urban Energy Index for Buildings (UEIB): A new method to evaluate the effect of urban form on buildings' energy demand. Landscape and Urban Planning, 148 (2016), 170-187. https://doi.org/10.1016/j.landurbplan.2016.01.001

Saaroni, H., Amorim, J. H., Hiemstra, J. A., & Pearlmutter, D. (2018). Urban Green Infrastructure as a tool for urban heat mitigation: Survey of research methodologies and findings across different climatic regions. Urban Climate, 24(October 2017), 94–110. https://doi.org/10.1016/j.uclim.2018.02.001

Salata, F., Golasi, I., de Lieto Vollaro, R., & de Lieto Vollaro, A. (2016). Urban microclimate and outdoor thermal comfort. A proper procedure to fit ENVI-met simulation outputs to experimental data. Sustainable Cities and Society, 26, 318–343. https://doi.org/10.1016/j.scs.2016.07.005

Salata, F., Golasi, I., Petitti, D., de Lieto Vollaro, E., Coppi, M., & de Lieto Vollaro, A. (2017). Relating microclimate, human thermal comfort and health during heat waves: An analysis of heat island mitigation strategies through a case study in an urban outdoor environment. Sustainable Cities and Society, 30, 79–96. https://doi.org/10.1016/j.scs.2017.01.006

Salvati, A., Palme, M., Chiesa, G., & Kolokotroni, M. (2020). Built form, urban climate and building energy modelling: Case-studies in Rome and Antofagasta. Journal of Building Performance Simulation, 13(2), 209–225. https://doi.org/10.1080/19401493.2019.1707876

Salvati, A., Coch, H., & Morganti, M. (2017). Effects of urban compactness on the building energy performance in Mediterranean climate.

Energy Procedia, 122 (2017), 499–504. https://doi.org/10.1016/j.egypro.2017.07.303

Salvati, A., Coch Roura, H., & Cecere, C. (2017). Assessing the urban heat island and its energy impact on residential buildings in Mediterranean climate: Barcelona case study. Energy and Buildings, 146(2017), 38–54. https://doi.org/10.1016/j.enbuild.2017.04.025

Salvati, A., Monti, P., Coch Roura, H., & Cecere, C. (2019). Climatic performance of urban textures: Analysis tools for a Mediterranean urban context. Energy and Buildings, 185(2019) 162–179. https://doi.org/10.1016/j.enbuild.2018.12.024

Santamouris, M. (2020). Recent progress on urban overheating and heat island research. Integrated assessment of the energy, environmental, vulnerability and health impact. Synergies with the global climate change. Energy and Buildings, 207. https://doi.org/10.1016/j.enbuild.2019.109482

Skelhorn, C., Lindley, S., & Levermore, G. (2014). The impact of vegetation types on air and surface temperatures in a temperate city: A fine scale assessment in Manchester, UK. Landscape and Urban Planning, 121(2014), 129–140. https://doi.org/10.1016/j.landurbplan.2013.09.012

Stewart, I. D., & Oke, T. R. (2012). Local climate zones for urban temperature studies. Bulletin of the American Meteorological Society. https://doi.org/10.1175/BAMS-D-11-00019.1

Steemers K., Ramos M., Sinou M. (2004). Urban diversity. In K. Steemers, & M. A. Steane (Eds.), Environmental diversity in architecture. Spon Press.

Su, M. A., Ngarambe, J., Santamouris, M., & Yun, G. Y. (2021). Empirical evidence on the impact of urban overheating on building cooling and heating energy consumption. IScience, 24(5), 102495. https://doi.org/10.1016/j.isci.2021.102495

Takebayashi, H. (2017). Influence of urban green area on air temperature of surrounding built-up area. Climate, 5(3), 60-72. https://doi.org/10.3390/cli5030060

Taleghani, M., Kleerekoper, L., Tenpierik, M., & Van Den Dobbelsteen, A. (2015). Outdoor thermal comfort within five different urban forms in the Netherlands. Building and Environment, 83, 65–78. https://doi.org/10.1016/j.buildenv.2014.03.014

Tian, L., Li, Y., Lu, J., & Wang, J. (2021). Review on urban heat island in China: Methods, its impact on buildings energy demand and mitigation strategies. Sustainability (Switzerland), 13(2), 1–31. https://doi.org/10.3390/su13020762

Toparlar, Y., Blocken, B., Maiheu, B., & van Heijst, G. J. F. (2018). Impact of urban microclimate on summertime building cooling demand: A parametric analysis for Antwerp, Belgium. Applied Energy, 228(April), 852–872. https://doi.org/10.1016/j.apenergy.2018.06.110

Trepci, E., Maghelal, P., & Azar, E. (2021). Urban built context as a passive cooling strategy for buildings in hot climate. Energy and Buildings, 231(2021), 110606. https://doi.org/10.1016/j.enbuild.2020.110606

Tsoka, S., Theodosiou, T., Tsikaloudaki, K., & Flourentzou, F. (2018). Modeling the performance of cool pavements and the effect of their aging on outdoor surface and air temperatures. Sustainable Cities and Society, 42(June), 276–288. https://doi.org/10.1016/j.scs.2018.07.016

Tsoka, S., Leduc, T., & Rodler, A. (2021). Assessing the effects of urban street trees on building cooling energy needs: The role of foliage density and planting pattern. Sustainable Cities and Society, 65(2021), 102633. https://doi.org/10.1016/j.scs.2020.102633

Willmott, C. J. (1982). Some comments on the evaluation of model performance. Experimental Techniques, 7(5), 20–21. https://doi.org/10.1111/j.1747-1567.1983.tb01755.x

Yang, X., Peng, L. L. H., Jiang, Z., Chen, Y., Yao, L., He, Y., & Xu, T. (2020). Impact of urban heat island on energy demand in buildings: Local climate zones in Nanjing. Applied Energy, 260(30), 114279. https://doi.org/10.1016/j.apenergy.2019.114279

Yang, X., Zhao, L., Bruse, M., & Meng, Q. (2013). Evaluation of a microclimate model for predicting the thermal behavior of different ground surfaces. Building and Environment, 60(2013),93–104. https://doi.org/10.1016/j.buildenv.2012.11.008

Yi, C. Y., & Peng, C. (2019). An archetype-in-neighbourhood framework for modelling cooling energy demand of a city's housing stock. Energy and Buildings, 196(2019) 30–45. https://doi.org/10.1016/j.enbuild.2019.05.015

Zhang, M., & Gao, Z. (2021). Effect of urban form on microclimate and energy loads: Case study of generic residential district prototypes in Nanjing, China. Sustainable Cities and Society, 70(March), 102930. https://doi.org/10.1016/j.scs.2021.102930

Zinzi, M., & Carnielo, E. (2017). Impact of urban temperatures on energy performance and thermal comfort in residential buildings. The case of Rome, Italy. Energy and Buildings, 157(2017), 20–29. https://doi.org/10.1016/j.enbuild.2017.05.021

Zinzi, M., Carnielo, E., & Mattoni, B. (2018). On the relation between urban climate and energy performance of buildings. A three-years experience in Rome, Italy. Applied Energy, 221(March), 148–160. https://doi.org/10.1016/j.apenergy.2018.03.192

7 Conclusions

This dissertation concludes by answering the main research question stated in Section 1.5.

How does urban form influence building cooling demand in urban microclimate conditions, and how can the magnitude of the relationship be assessed?

This main question is answered by addressing the research sub-questions. Additionally, this chapter offers some recommendations for future research, design and planning practices.

7.1 Answering the research sub-questions

7.1.1 Sub-questions 1 and 2

What urban form characteristics influence building cooling demand? What thermal mechanisms drive this influence?

As shown in the literature review, there has been a great interest in energy-related form characteristics and the development of corresponding descriptive parameters. Chapter 2 analysed urban form characteristics based on transdisciplinary literature (urban morphology, climatology and energy-related fields) on three units of analysis: building, street canyon and urban fabric. It was found that a large body of literature exists on cooling-related form characteristics for the street canyon and urban fabric units; the literature on the building unit, however, focuses largely on heating-related form characteristics, meaning that further cooling-oriented studies are necessary. Additionally, the literature review focused on the thermal and aerodynamic processes influenced by urban form that drive both cooling and heating demand and it found that urban form characteristics play a twofold role in determining building energy demand. The 'intrinsic' role of form lies in building characteristics, which directly

influence energy loads by impacting thermal gains and losses. The 'extrinsic' role of form lies in the indirect effect of canyon and urban fabric on local climate conditions (e.g., through altering mesoscale wind flows, radiation, sensible heat fluxes) and, in turn, on the contextual conditions in which a building energy system operates.

The literature review identified a total of 9 energy-related form attributes and 54 parameters for their quantification. As energy research traditionally focuses on individual buildings, energy performance is generally investigated in relation to the geometrical characteristics of the building envelope and the space enclosed by it. The form attributes of building *size, orientation and compactness* were found to influence the thermal exchange between indoor and outdoor spaces and thus the balance between thermal gains and losses which determine cooling energy loads. Street canyon is an aggregative unit comprising buildings and street profiles; it is traditionally used in climatological studies and was later adopted in energy-related studies to observe thermal trade-offs between street surfaces and buildings. The street canyon is characterised by the attributes of *proportion* and *direction*, which influence urban climate phenomena and, indirectly, building energy performance. The aggregative unit urban fabric conveys the spatial relation between buildings and multiple land-division units (e.g., plot, block, island, fabric, district). At the urban fabric unit, attributes of *density, vertical openness, surface roughness* and *greenery* influence buildings' energy performance via urban climate phenomena. From a microclimate perspective, the constitutive attributes of street canyon and urban texture influence incoming short-wave radiation, long-wave radiation trapping, wind speed and convective heat transfer from building façades. The combination of and interactions among these form-dependent mechanisms create the climate conditions that influence thermal gains and losses and, in turn, determine cooling loads.

7.1.2 Sub-question 3

How to assess urban microclimate conditions influenced by urban form characteristics?

In urban climatological studies, two main morphological approaches are employed to quantify the influence of urban form on climate phenomena. The first, mainly employed in parametric and comparative studies, entails the qualitative selection of homogeneous or generic form patterns limiting the description of morphologically complex contemporary cities. The second, mainly used for urban climate mapping, entails supervised classification techniques to identify zones with different climate characteristics using large aggregative units, which are unable to capture microscale thermal behaviours.

Addressing these limitations and exploring the potential of quantitative morphological approaches in urban climatology, Chapter 3 developed and tested a method to obtain numerically defined morphological types and a method to assess their urban microclimate conditions. To assess urban microclimate conditions on a morphological basis, four conditions must be satisfied. First, the morphological approach should allow a multi-variable description of the urban fabric since multiple form attributes can influence solar accessibility, air and surface temperatures, wind flows and humidity levels. Second, the approach should offer a multi-scale description of urban form. This is necessary because urban elements' thermal and aerodynamic influences vary by proximity (the distance from an urban element). For example, shadow patterns can be observed in the close vicinity of an object, while dense green areas can influence air temperatures for several hundred metres. Third, an analytical spatial unit capable of describing proximity should be used for each microclimate-related mechanism. Fourth, the classification and selection of representative form patterns should acknowledge the heterogeneity of the urban fabric to describe the complexity of existing cities.

The morphological classification method enables to identify building types and context types via cluster analysis. The combinations of these building and context types lead to the identification of local climate types (LCTs), allowing to describe conditions of heterogeneity in the urban fabric. The LCTs distinction is based on the unsupervised hierarchical classification of multiple form characteristics of buildings and their surroundings. Among the attributes identified in the literature review, eight were selected to describe building and context characteristics that impact thermal behaviours. Building height, footprint area and surface-to-volume ratio convey building size and compactness, which determine thermal exchange between outdoor and indoor conditions. GSI, FSI, mean building height, grass coverage and tree crown area reflect contextual density, roughness and vegetation coverage, which determine shadow, wind and temperature patterns. Additionally, building contexts are described not through the measurement of absolute values based on ownership division (e.g., blocks, plots) but through values relative to each building context measured in units of spatial continuity equidistant from each building facet. In other words, the form parameters of context characteristics are calculated within buffer areas at multiple distances from the buildings. Two radii are used to satisfy the condition of multi-scalarity. GSI and tree crown area are calculated in a buffer area with a 25-metre radius that captures the characteristics of the tangent street canyons; mean building height, FSI and grass coverage area are calculated in a buffer area with a 50-metre radius that describes the structure of the surrounding.

The assessment method allows the analysis of thermal and aerodynamic behaviours in local climate types. This assessment entails the selection of a combination of archetypical buildings and contexts, for which microclimate simulations are

conducted via ENVI-met, a well-established and validated urban climate model. The modelling allows for the isolation of the impacts of urban form on the microclimate by keeping all other model inputs—including material properties—constant. The analysis of thermal trade-offs through microclimate simulations enhances the understanding of building types' sensitivity to local climate conditions as well as thermal patterns stemming from contextual form characteristics. The testing of this framework in the Rotterdam case is discussed further in Section 7.1.4

7.1.3 Sub-question 4

How and to what extent do urban form characteristics influence summer outdoor and indoor thermal conditions in the Rotterdam case?

Understanding and quantifying urban form's influence on urban climate phenomena in the Rotterdam case study based on the previously described two-step framework. The first step consisted of the classification of similar spatial conditions, while the second step entailed the use of computational modelling to uncover climate behaviour associated with these spatial conditions. Based on the building attributes of size and compactness and the context attributes of density, roughness and greenery, the novel data-driven LCT classification method applied in the Rotterdam case identified five building types and five context types. The microclimate simulations carried out for the resultant 25 combined archetypes offered insights into the relationship between form variations and diurnal thermal processes. The simulations were performed in ENVI-met for two representative consecutive hot days with clear sky, that reached a maximum temperature of 25°C and 28°C respectively at the rural weather station of Rotterdam Airport.

Outdoor temperatures were generally higher in the urban archetypes than in the rural environment, while wind speed and relative humidity were generally lower. These factors resulted in a strong UHI effect ranging between 0.5°C and 3°C during the studied period. Variation in the eight urban form characteristics resulted in up to a 2.5°C change in urban air temperature, 3m/s change in wind speed and 5% change in relative humidity. Additionally, as indoor air temperature varies as a function of outdoor conditions, higher outdoor temperatures resulted in higher indoor temperatures. In fact, it was found that morphological variables accounted for average diurnal indoor temperature change between 1.8 °C on the first (milder) day and 3.2 °C on the second (hotter) day.

Generally, high-rise and high-density contexts with a mean height above 15 metres, FSI above 2.0 and GSI above 0.48 provided the coolest outdoor environments. During the daytime, these are the major form characteristics responsible for enhancing shading potential and reducing envelope exposure to solar radiation. A regression analysis further highlighted that, during daytime hours, building height and FSI collectively explain between 77% (day 2) and 85% (day 1) of outdoor air temperature values. The negative sign of the correlation means that the lower the height of the building and the built intensity of its context, the warmer the air layer around building facades. Differently, vegetation appears to have a minor effect on urban temperatures during the daytime.

The analysis of indoor temperatures also highlights that building form influences buildings' sensitivity to outdoor conditions. In low-rise buildings (< 9 metres), the context change determines a variation in the average diurnal indoor temperature between 1.4°C and 3.2 °C. Variation between 0.7°C and 1°C is found in mid-rise buildings (9–19 metres) characterised by small footprints (< 139m^2). Differently, a high building footprint (> 1650m^2) for mid-rise buildings results in low temperature variation (0.4–0.5°C), suggesting that contextual conditions only affect the balance between thermal gains and losses of this building type to a minor degree. Finally, in high-rise buildings (> 19 metres), average indoor temperature demonstrates a minor variation (0.2-0.3°C), suggesting that the indoor environments of towers and skyscrapers are less affected by urban warming mechanisms and the influence of the urban form of their surroundings. Notably, the Rotterdam case showed that 50% of diurnal indoor temperature variation can be explained by building footprint size and mean contextual building height. Indoor environments are warmer as footprint area increases and cooler as mean contextual building height increases.

7.1.4 Sub-question 5

How to include the effects of urban microclimate in the assessment of building cooling demand?

Traditionally, building energy modelling (BEM) employ 'typical meteorological year' data from rural weather stations as climate boundary conditions, ignoring the climate effects of the urban environment. However, in the last few decades, two approaches have been developed with a focus on the UHI effect on energy consumption. The first is based on using temperature measurements at urban weather stations as inputs to model the energy needs of reference buildings removed from their spatial context. The second is based on advanced simulation techniques

and integrated workflows between climate (meso/micro) and energy models for the analysis of single buildings and, oftentimes, generic urban patterns.

Advancements in climate and energy modelling have enabled to estimate building energy demand and urban climate phenomena with an increased level of detail. The main advantage of simulations over measured data is that they can generate explicit information for distinct parameters and help to assess potential scenarios and parametric changes during the design process. In particular, advanced coupling procedures between BEM and microclimate models enable the evaluation of the influence of urban climate on energy demand by assessing the effects of overheating mechanisms—caused by radiation interreflection, heat-trapping, reduced wind velocity and evapotranspiration—on energy loads. Additionally, coupling methods are more suitable for assessing the influence of morphological and material characteristics on both urban microclimate and energy consumption patterns.

The potential of simulation models to provide a deep understanding of the thermal trade-offs between buildings and their surroundings and a detailed characterization of urban areas' energy needs, however, depend on their computational capacities. The models should be capable to address the district scale, to accurately represent the heterogeneity of urban areas (materials, form, vegetation) and compute the cooling loads. Similarly, the models should provide results in a high time resolution to account for the effects of urban overheating and daily cycles on peak energy demand.

Fulfilling these requirements, Chapter 4 developed an integrated simulation method by coupling the existing ENVI-met and city energy analyst (CEA) models. The coupling enables the calculation of building energy loads using climate boundary conditions (e.g., air temperature, relative humidity, wind speed) resulting from microclimate simulations. In this way, the CEA model considers the microclimate around buildings when estimating space cooling demand. More specifically, to consider urban microclimate effects in building cooling demand assessment, the CEA model calculates: i) sensible loads as a function of the simulated local outdoor air temperature, ii) latent loads as a function of the difference between the urban outdoor and building indoor humidity levels and iii) air infiltration and convective heat transfer at the building surfaces using simulated wind speed at façade. The high resolution of the ENVI-met microclimate model enables the averaging of the resulting hourly values in the air layer near the façade of each building. Similarly, the computational characteristics of the CEA model enable the consideration of material and form variety in real built environments and the simulation of building energy demand at the district scale.

The comparison of the coupled microclimate-energy model results with a baseline case aids in observing the sensitivity of cooling demand to climate conditions. For the baseline case, data from a rural weather station are used as boundary conditions for energy simulation in the CEA model. Thus, this comparison allows for the assessment of the magnitude of the cooling penalty caused by urban temperature, wind speed and relative humidity. The novelty of this method lies in its capacity to analyse reciprocal influences between a group of buildings at the district level. Finally, the application in the Swiss case study of Zurich showed that the integrated method is capable of assessing mutual thermal and aerodynamic influences between buildings and their consequent impact on sensible and latent cooling loads in a hot summer period.

7.1.5 Sub-question 6

How and to what extent do urban microclimate and urban form impact building cooling demand in the Rotterdam case?

Urban overheating is highly correlated with cooling energy consumption, as the increase in urban temperature increases demand for space cooling. The coupling of the ENVI-met and CEA models detailed in Chapter 4 was applied to Rotterdam LCTs to analyse the influence of urban microclimate on cooling loads across 25 representative cases (Chapter 5). The results of the coupled simulations (Microclimate Scenario) were compared against simulations using rural climate data as boundary conditions (Baseline Scenario). During the two representative days under study, average daily cooling demand across the 25 cases ranges from 64 Wh/m2 (day 1) to 85 Wh/m2 (day 2) in the Baseline Scenario and from 94 W/m2 to 111 W/m2in the Microclimate Scenario . Compared to rural climate, the warmer microclimate conditions and reduced wind velocity in the urban environment result in higher energy demand. On average, daily cooling demand was found to increase by 24–32%. Among the analysed buildings, the load increase in urban conditions varied from 3.6% to 100%. Notably, the higher the temperature at the rural weather station, the lower the difference in cooling load between the rural and urban microclimate.

In the Rotterdam case, the analysis of the relationship between form characteristics and microclimate-related cooling loads shows that building form considerably influences impact size. Generally, the effect of urban overheating on space cooling demand is a function of building height: the taller the building, the lower the climate-related cooling load. This is because, near the ground, temperatures are higher due

to the release of heat (convection) from paved surfaces, and wind flows have a lower dissipation capacity. Overall, cooling loads in low-rise buildings (< 9 metres) are the most sensitive to urban overheating, followed by mid-rise buildings (9–19 metres) and high-rise buildings (> 19 metres).

Due to microclimate conditions, average energy demand for space cooling rises by up to 58% in low-rise buildings with a StoV under 0.47 and up to 42% in low-rise buildings with a StoV above 0.53. More compact buildings (with a lower StoV) have a lower proportion of envelope exposed to convective processes; thus, building surfaces release heat accumulated through the absorption of short-wave radiation more slowly. Energy cooling demand increases by up to 34% in mid-rise buildings characterised by a footprint lower than 139m^2 and up to 21% in mid-rise buildings with a footprint higher than 1650 m^2. The latter have the greatest average cooling load among types. However larger footprints correspond to larger roof areas and, in turn, prolonged incident solar radiation during the day which plays a greater role compared to air temperature change due to urban microclimate conditions. Finally, high-rise buildings increase their cooling need, on average, by 13%.

The morphological conditions of surroundings also considerably affect buildings' energy performance. Air temperature in the canyons around buildings is influenced by surface temperatures, as energy is mainly transferred through radiative and convective processes. Thus, in high-density (GSI > 0.48, FSI > 2), high-rise (mean height > 15 metres) contexts, low surface temperatures (due to high shadow cast) and low wind speeds collectively contribute to reducing local air temperatures during the daytime. Consequently, all building types performing in this context demonstrate a lower increase in microclimate-related energy loads. In high-density, high-rise contexts, relative to the average energy demand increase for each building type, cooling load is up to 35–60% lower for low-rise buildings, 43-68% lower for mid-rise buildings, and 54–59% lower for high-rise buildings.

Beyond addressing the influence of microclimate processes on building cooling demand across various building and context types, Chapter 5 employs multiple linear regression analysis to better understand the extent to which morphological and local climate variables are related to variation in space cooling. The results show that the eight form parameters (building height, footprint area, surface-to-volume ratio, GSI, FSI, mean building height, grass coverage and tree crown area) and the three variables of air temperature, wind speed and relative humidity explain 76–79% of the variance in diurnal cooling loads. However, different predictors were found to be significant across the two representative hot days (section 5.3), suggesting that the relationship is a function of the overall starting conditions at the rural weather station. The most important predictors across both days are diurnal average urban

air temperature and building height, confirming the previously described findings. On the milder day (T_{max} 25°C at the rural weather station) the other significant predictors of cooling variance are mean building height, FSI, GSI, building footprint and relative humidity. On the warmer day (T_{max} 28°C at the rural weather station), only wind speed and building compactness (StoV) are significant predictors.

7.2 Main research question

How does urban form influence building cooling demand in urban microclimate conditions, and how can the magnitude of the relationship be assessed?

The main research question is structured around two foci. The first part of the question addresses the relationships between urban form characteristics, urban microclimate processes and cooling demand, while the second part focuses on the methodological instruments that can support an understanding of their complex interrelationships.

Regarding the first part of the main research question, it can be concluded that urban form characteristics play both intrinsic and extrinsic roles in shaping building cooling loads. The former is determined by building's form and mechanisms of thermal losses and gains, while the latter is determined by the form of the surrounding urban fabric, or in other words, the building context, which modifies the thermal conditions in which a building operates. Air and surface temperatures are generally higher in cities than in rural environments, and UHI magnitudes can vary significantly at the microscale due to urban form characteristics (e.g., roughness, density, land cover). As a result, building cooling demand is generally higher in urban environments than in rural environments. Still, the cooling penalty values can have a large range. In fact, this study found that, on average, daily cooling demand increased by up 32% in Rotterdam, and the diversity of form characteristics in 25 archetypical cases resulted in a cooling demand increase of between 3% and 100%.

This wide range of cooling penalties, observed among archetypes by comparing the results of energy simulation using rural and urban microclimate boundary conditions, is not exclusively the consequence of the UHI magnitude created by the surrounding fabric. Form attributes of buildings substantially influence the degree of sensitivity

to urban overheating. Among the building types assessed in Rotterdam, high-rise buildings are the least sensitive to urban temperatures, followed by mid-rise buildings and then low-rise buildings; cooling loads increase by up to 13% in high-rise, 34% in mid-rise and 58% in low-rise buildings. Additionally, the relationship between form and cooling demand demonstrates high temporal variability, as a result of atmospheric variations. In other words, the higher the daily average temperature at the rural weather station, the lower the daily cooling penalty due to urban microclimate conditions. This finding aligns with the results of a sensitivity analysis carried out for the 25 cases in Rotterdam, which showed that form and climate factors vary their statistical significance in cooling load prediction for the two days of focus. This variance of significance indicates that the role of form characteristics might change in line with UHI contribution to total demand, demonstrating the high complexity of the trade-off between form and cooling demand in urban climate environments.

The second part of the main research question pertains to the conceptual and methodological instruments with which to quantify the impacts of urban form on cooling energy demand. In this regard, it can be concluded that the multidisciplinary nature of the problem requires structural frameworks to facilitate the classification of morphological patterns and the joint assessment of microclimate and energy performance.

Morphological approaches employed in climatology have proven themselves to be of great support to analysing urban-climate patterns. On this basis, the thesis developed the quantitative morphological method of local climate type (LCT), to separately classify and assess building and context types enabling an understanding of the thermal trade-off between them. The LCT classification allows for the description of heterogeneous conditions at the urban microscale and is based on the unsupervised hierarchical classification of multiple form variables, calculated for analytical units of proximity, at multiple scales. The assessment of LCTs through ENVI-met microclimate modelling allowed to analyse the thermal behaviours of building and context types in the test case.

Regarding cooling demand assessments, energy models' main advantage is that morphological components can be analysed independently of occupant behaviours, energy systems and material factors. However, energy models' accuracy in urban environments can be further increased by using microclimate data as climate boundary conditions. Thus, this thesis developed a coupling method between two existing tools (ENVI-met and CEA) to assess the cooling demand of buildings at the district level. Coupled microclimate and energy simulations, allow for the consideration of the distinctive local variables of air temperature, wind speed and

relative humidity when estimating energy loads. The main limitation of this method is the high computational requirements of CFD, which currently prohibits full-year assessments. Therefore, representative days for analysis must be selected with care. The methods developed in this thesis build a novel framework which enables a more accurate assessment and a greater understanding of urban form's influence on building cooling demand in urban environments. The application of the framework on the Rotterdam case allowed to identify building and context types, and estimate their performance during two representative hot days. The results finally suggest that microclimate patterns and building cooling demand are largely determined by urban form characteristics. However, this relationship is dynamic due to the phenomena's high temporal and spatial variability. In other words, some building and context characteristics can be more determinant than others at a specific point in time depending on temperature values.

7.3 Recommendations

7.3.1 Recommendations for future research

The thesis contributes to advance the bridging between the urban morphology, urban climatology and energy-related fields, providing integrated approaches and instruments to better understand the complexity of thermal mechanisms in the urban environment. As previously stated, this thesis focuses on the development of a new methodological framework and methods to support the deeper understanding of the relationship between form and cooling demand in urban climate conditions. The framework allows 1) the classification of LCTs, 2) their microclimate assessment and 3) the assessment of climate-related cooling demand through a coupling approach. Throughout the research, reflections on limitations, processes and findings have indicated potential future research developments. The following lists highlight the major recommendations for future research:

LCT method

The novel local climate type method should be considered as an exploration of the use of a data-driven morphological classification in urban climatology. Further development of this classification method should improve the following aspects:

- While hierarchical clustering allows for an understanding of interrelations among types, this classification method is limited in its applicability to large datasets. The use of a significant sample of the full data population does result in a representative description of classes but limits full-city mapping and, in turn, an understanding of the spatial distribution of types. Other clustering classification methods with a higher capacity to process large datasets should be tested to identify types and allow for their visualization at the full-city level.
- The microclimate assessment of morphological types does not clearly indicate temperature variations due to greenery changes (measured via tree crown area and grass coverage area). One potential explanation is that the effect of vegetation concentration and contiguity is not captured by the dimension of the buffer area around buildings. Further empirical and theoretical studies are necessary to assess the scales of influence of vegetation on climate variables, and test parameters that might be more effective in describing green compactness and the cumulative effect of concentrated or dispersed vegetation elements.
- Water features contribute to shape climate in cities, altering the level of humidity and air temperature. Future testing of the LCT method should include parameters that describe water coverage and characteristics of water features (e.g., depth, level of motion).
- This study assumes buildings' and surfaces' material characteristics to be constant. However, in future research, the method should admit a larger number of parameters in the type-classification procedure and allow for further inclusion of material variation in the mapping of types and their climate assessment. Data on materials is difficult to obtain, but the effort in retrieving and storing data and in increasing the level of detail in 3D city models might in turn, support this improvement in the LCT classification.

Microclimate and energy assessment of LCTs

- The simulation study of two representative hot days with clear sky suggested that there may be ambient air-temperature thresholds at which point the relationship between form characteristics and microclimate is modified. This finding opens a new research line in a prospective of climate change and the resultant increase in air temperatures. Analyses of urban form performance should focus on how the urban form influences urban microclimate at different ambient temperature thresholds.

- Despite the ENVI-met model being validated against the measured data of two urban weather stations in Rotterdam, measured climate data should be collected for all 25 archetypes to verify climate patterns and their correspondence with potential cooling demand.
- This study's methodological framework should be applied to other geographical and climatic contexts to test its level of transferability and the accuracy of the results in different contexts. The LCT classification is intended as a tool with which to understand local relationships. Its overall aim is not to identify global morphological types and their performance but to describe the specific climatic, morphological and environmental components of a 'locus'.
- Current energy modelling in CEA has the downside of neglecting trees in the radiation module. Although this tool is one of the few capable of performing district- and city-scale energy simulations, it neglects urban open spaces, their material and green coverage characteristics in the modelling of thermal processes. Advancements in CEA and other energy models to integrate these aspects would further enable an understanding of the trade-offs between buildings and their surroundings.
- This study employs many assumptions to define the inputs for energy modelling, including assumptions regarding window-to-wall ratio, building materials and the type of energy systems for cooling purposes. While CEA is already able to accept variation in these inputs, many cities lack a comprehensive dataset with this information. Regarding the future development of energy assessments in CEA and other energy modelling tools—as well as that of the LCT method—advancements in 3D city models and specifically the increase in level of detail (LOD) might provide more accurate inputs for climate and energy simulations, allowing for more accurate predictions.
- CEA employs an indoor set point temperature and a humidity range for the calculation of cooling demand and thus no adaptive comfort limits are considered in this study. Further development of the method should address a wider indoor comfort range and human's capability of thermal adaptation.
- This study focuses on understanding the urban form characteristics that influence cooling loads during a hot summer period. A more general evaluation of the balance between cooling and heating demand on an annual basis is beyond the scope of this thesis. More research is needed into the suitability of the LCT classification for such analysis, as well as into the climate and energy coupling modelling for an annual assessment. The eight form parameters derived from the literature for the LCT classification have been confirmed by previous studies to be able to convey also heating-related mechanisms. Although CEA can perform yearly energy estimations, ENVI-met and other CFD models for microclimate assessment are strongly limited in computational capacity—annual simulations currently seem to be unfeasible. However, a selection of representative seasonal days could help to achieve a new understanding of the effect of urban and building form on heating loads under

climate change and UHI effect. Additionally, increasing computational capacity could facilitate an enhanced assessment process and lower the cost of climate modelling.

7.3.2 Recommendations for planning and design

Developed on transdisciplinary grounds, this research does not directly address the implications of urban form's cooling energy performance for planning and design. However, it shows that quantitative form parameters and spatially oriented climate classification can offer meaningful diagnoses of urban climate and energy behaviours.

From this perspective, the review of energy-related form characteristics and the LCT classification method are meant to facilitate an understanding of microclimate and cooling demand patterns by offering planners and designers basic insight into the mechanisms trigged by decisions on urban composition and configuration. In planning and design applications, the use of proximity units conveys the collective effort necessary to make integrated interventions for a carbon-neutral urban environment. As highlighted, buildings' individual energy performance largely depends on intrinsic geometrical characteristics and extrinsic climate conditions influenced by the surrounding urban fabric. As a result, each design choice for a single building has the power to modify the performance of all other buildings in its proximity and vice-versa; thus, re-development and densification processes modify the context in which existing buildings perform. Designers and planners have a clear responsibility for effective climate and energy transitions and, therefore, should more seriously consider the potential impacts of their interventions and ensure coherence, or in other words 'performative' integration, between energy saving and heat mitigation measures applied on buildings and their surroundings.

For urban planning, the LCT method offers the possibility of addressing complex heterogeneous characteristics of the urban fabric in processes of urban transformation. An understanding of form-related performance can effectively guide the framing of climate-sensitive planning regulations for existing and new developments. For example, a full-city LCTs mapping can serve as a powerful tool to understand the spatial distribution of risks pertaining to urban overheating and related energy consumption, enabling practitioners to employ more effective strategies of intervention. On the one hand, the fine spatial scale offered by LCTs facilitates the development of climate adaptation guidelines and energy-efficiency measures based on common spatial conditions between context types, facilitating standardization in the implementation phase. The building focus, on the other hand, supports prioritization and the fair distribution of beneficial interventions by

revealing the sensitivity levels of buildings to UHI and potential cooling demand increases. LCTs mapping could also find applications in a wide range of climate-sensitive planning instruments, extending beyond explanation to prescription. Further analysis should be conducted to assess the potential of such a classification method in heat-exposure and vulnerability analysis as well as the nascent field of heat-stress management.

In urban design, LCT classification can serve as a fundamental tool to guide decisions in an early design stage, by offering an overall understanding of the status quo and indicating performance levels that can be achieved through morphological choices. Uncovering the correlation between environmental properties of the built environment and both urban climate and building cooling demand could reinforce the long-term systemic integration of decisions in the practice of climate- and energy-sensitive design. For example, an analysis of the status quo through LCT classification can indicate buildings at risk of reaching high temperatures and loads, encouraging designers to apply heat-mitigation measures and passive cooling measures. The evolution of LCT classification in a catalogue of integrated solutions or in an integrated assessment procedure should be considered. In fact, in taking design decisions, interventions aimed at energy reduction and those aimed at climate adaptation should reinforce each other. However, combined analyses are necessary to align such measures to avoid the selection of measures with negative repercussions for other pursuits. Energy-assessment procedures that consider local urban climate conditions (such as those outlined in this thesis) would support an integrative design process in this direction.

7.4 Final words

This thesis aims to support the integration of knowledge between urban morphology, urban climatology and energy-related fields. It offers a novel methodological framework and methods to develop an understanding of the relationship between urban form and building cooling demand in urban climate conditions. By doing so, the thesis contributes to the conceptualization and understanding of both intrinsic and the extrinsic energy role of urban form and to increasing the assessment accuracy of urban form-related climate and energy performance.

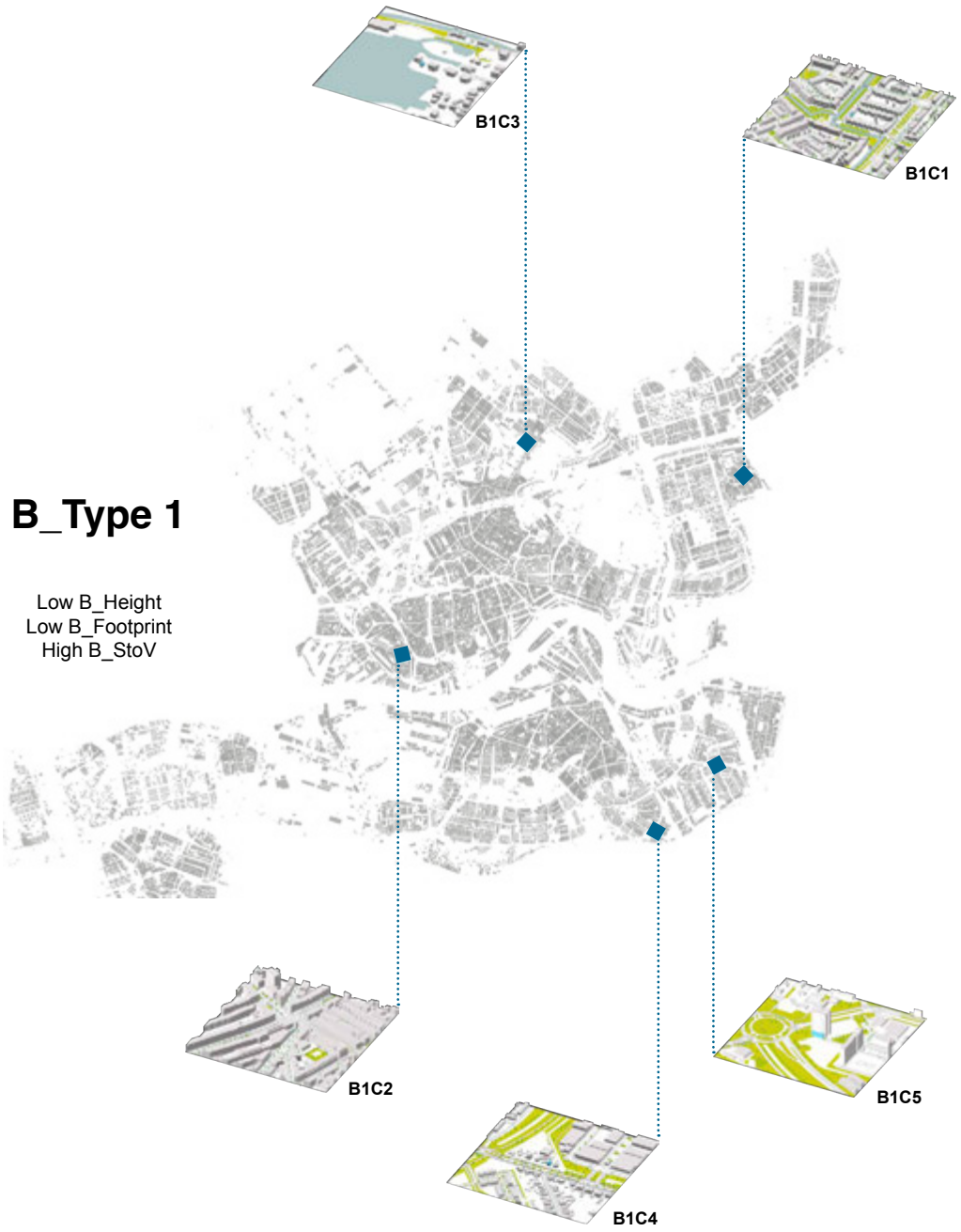
First, the thesis demonstrated the potential of quantitative morphological approaches in environmental analysis, offering a comprehensive review of form attributes and parameters for building cooling- and microclimate-oriented analysis. Second, it addressed the micro-scale mechanisms behind urban climate by developing an explorative method for LCT classification. Thirdly, it stressed the importance of using microclimate boundary conditions to estimate building cooling demand and developed an integrated method for such a combined assessment. Finally, the thesis also indicates the limitations of microclimate and energy models, highlighting that further work should aim at improving the modelling approaches and calculation methods.

The high spatial and temporal variability of urban form's impact on cooling demand suggests that standardized guidelines and strategies aimed at reducing building energy consumption would be unsuccessful if they overlook urban microclimate conditions. The use of the classification and assessment methods developed in this thesis in future research, planning and design practice is expected to contribute to acknowledging the importance of urban form and microclimate factors in defining and implementing energy transition measures.

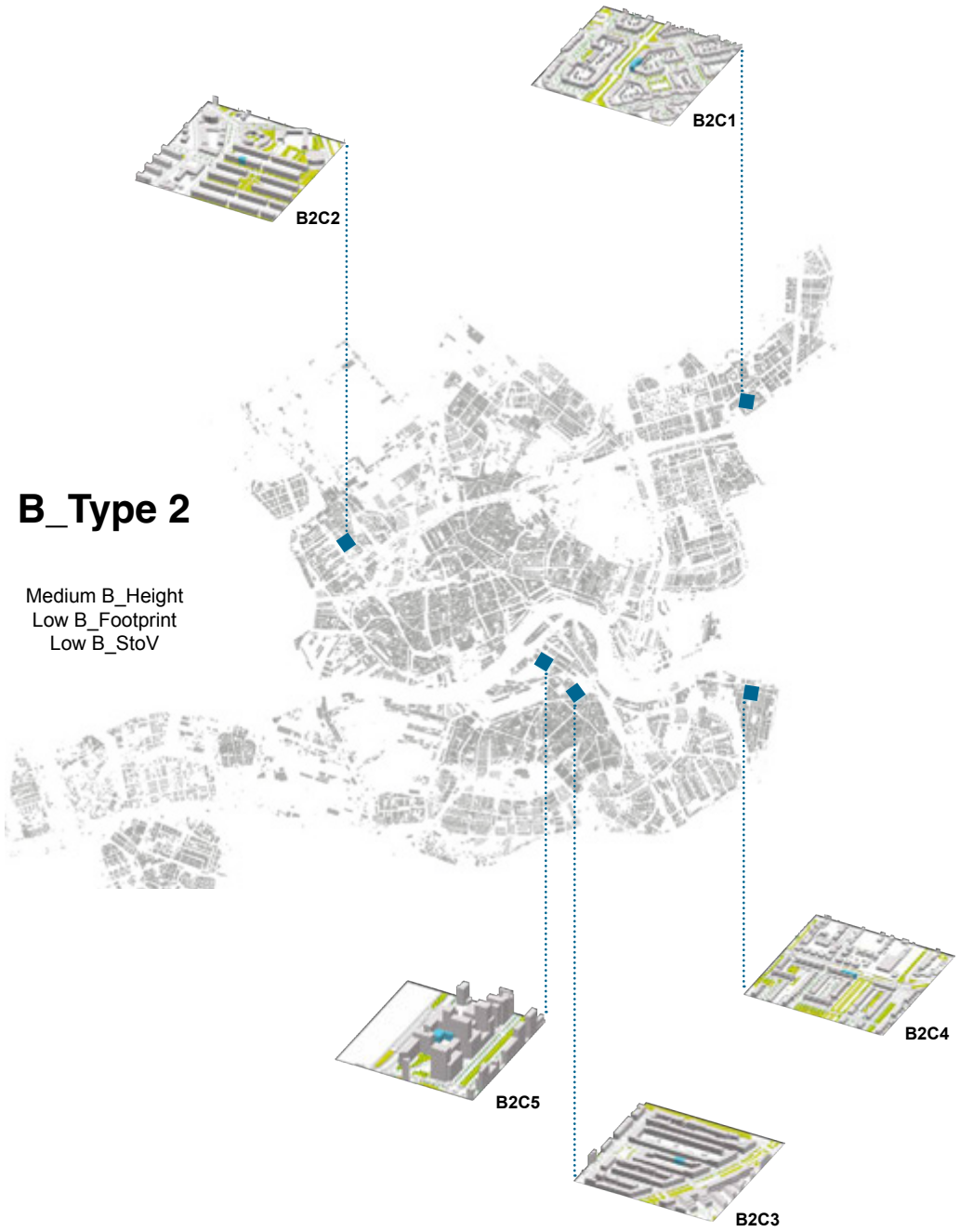
Finally, the application of the proposed framework to the Rotterdam case study contributes to developing a deeper understanding of building cooling demand in temperate climates and raising awareness about the potential energy impacts of urban form and urban warming phenomena.

Appendix

TOC


B1C3
B1C1
B_Type 1
Low B_Height
Low B_Footprint
High B_StoV
B1C2
B1C5
B1C4

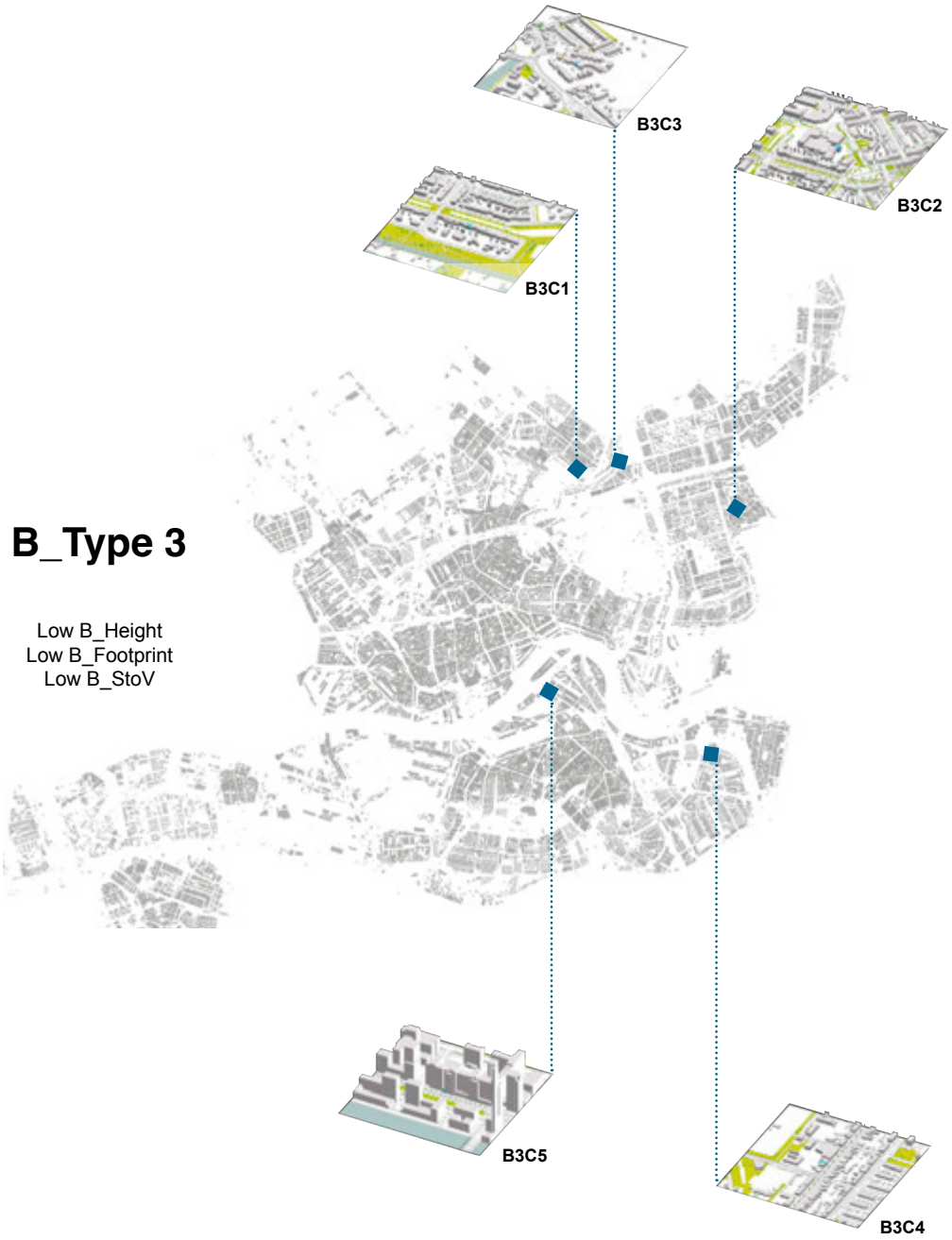
TOC


B2C1
B2C2
B_Type 2
Medium B_Height
Low B_Footprint
Low B_StoV
B2C4
B2C5
B2C3

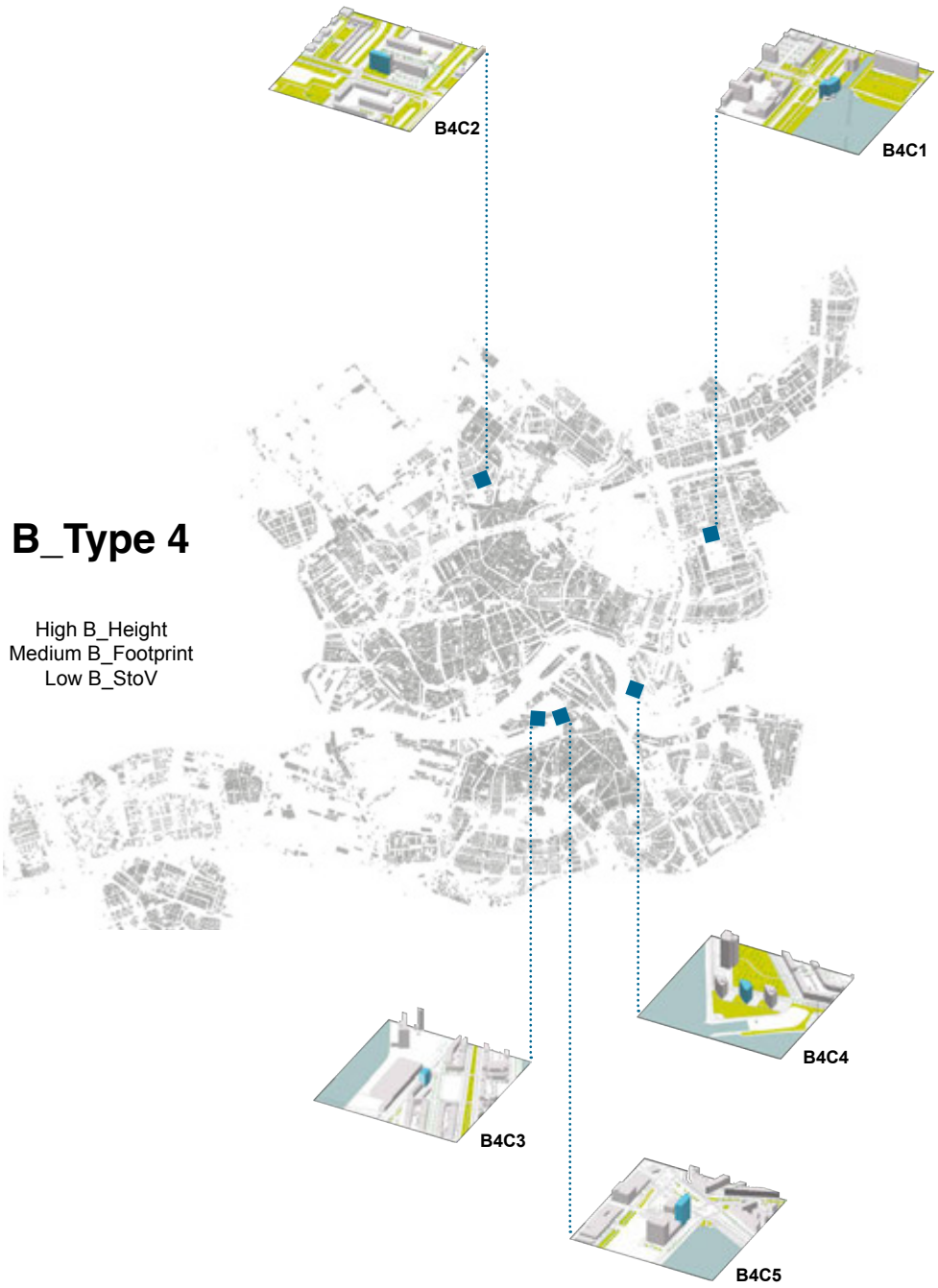
TOC

B_Type 3

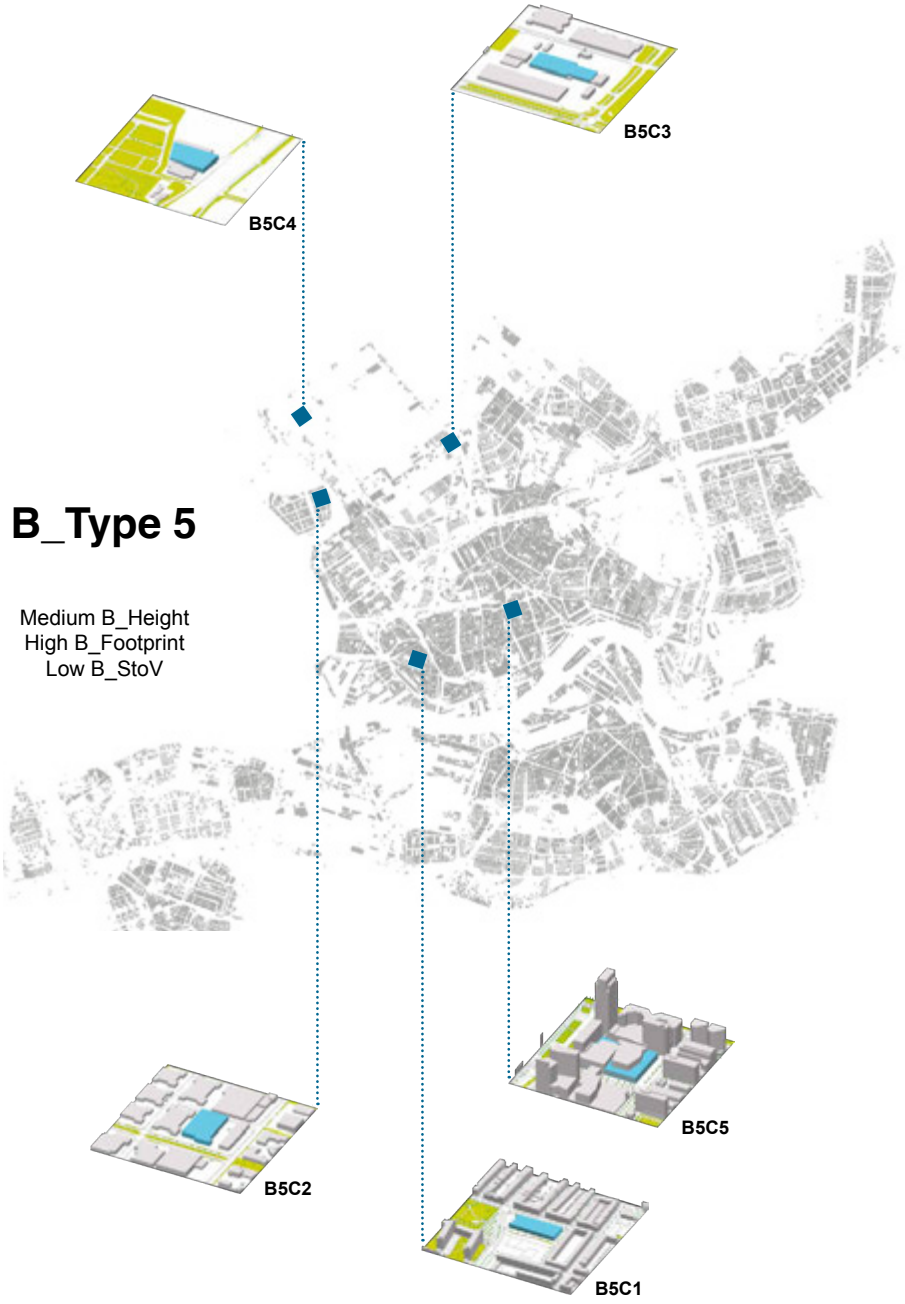
Low B_Height
Low B_Footprint
Low B_StoV



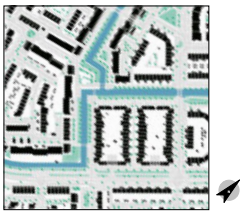
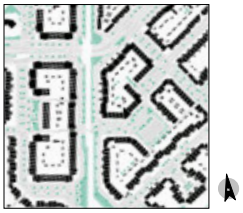
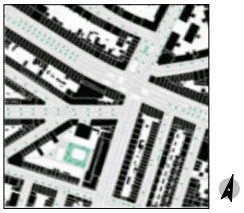
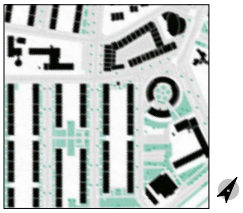
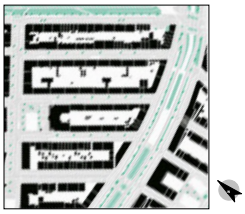
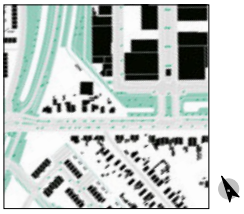
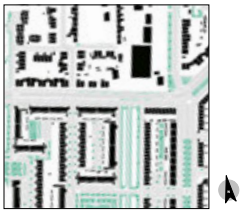
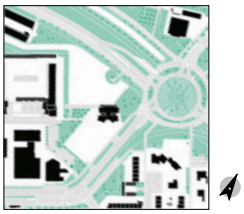
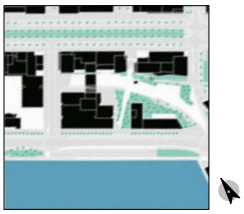
TOC


B4C2
B4C1
B_Type 4
High B_Height
Medium B_Footprint
Low B_StoV
B4C4
B4C3
B4C5

TOC


B5C4
B5C3
B_Type 5
Medium B_Height
High B_Footprint
Low B_StoV
B5C2
B5C5
B5C1

TOC

	BUILDING TYPE 1 Low B_Height Low B_Footprint High B_StoV	BUILDING TYPE 2 Medium B_Height Low B_Footprint Low B_StoV
CONTEXT TYPE 1 Low-Medium MeanH Low GSI Low FSI High TArea Medium GArea		
CONTEXT TYPE 2 Medium MeanH Medium GSI Medium FSI Low TArea Low GArea		
CONTEXT TYPE 3 Low MeanH Low GSI Low FSI Low TArea Low GArea		
CONTEXT TYPE 4 Low MeanH Low GSI Low FSI Low TArea Medium GArea		
CONTEXT TYPE 5 High MeanH Medium-High GSI High FSI Low TArea Low GArea		

TOC

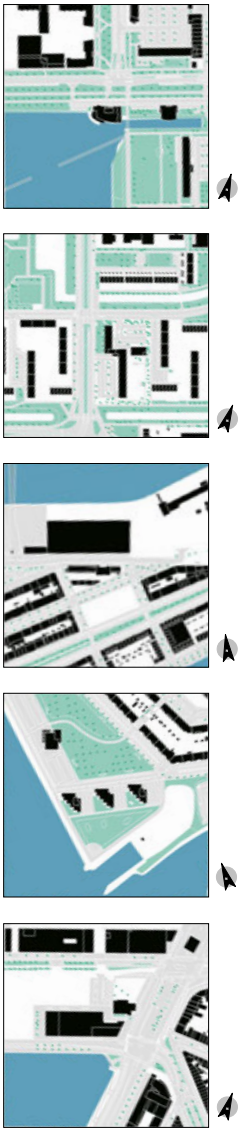
BUILDING TYPE 3

Low B_Height
Low B_Footprint
Low B_StoV



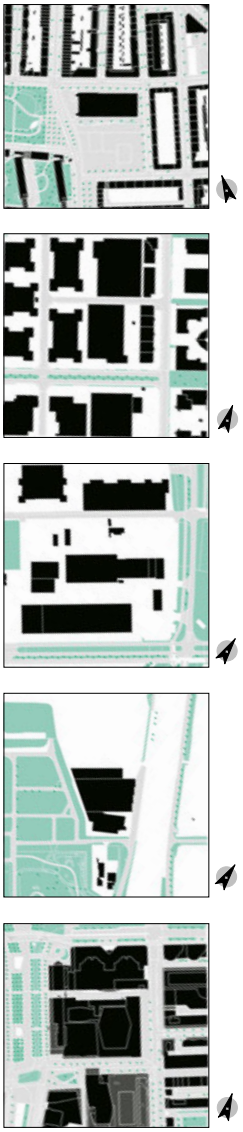
BUILDING TYPE 4

High B_Height
Medium B_Footprint
Low B_StoV



BUILDING TYPE 5

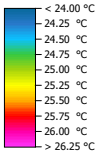
Medium B_Height
High B_Footprint
Low B_StoV



TOC

Day 1

Air Temperature
(16.00h)



BUILDING TYPE 1

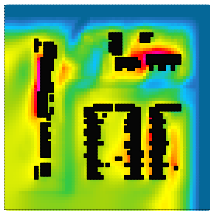
Low B_Height
Low B_Footprint
High B_StoV

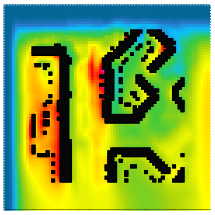
BUILDING TYPE 2

Medium B_Height
Low B_Footprint
Low B_StoV

CONTEXT TYPE 1

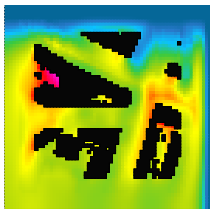
Low-Medium MeanH
Low GSI
Low FSI
High TArea
Medium GArea

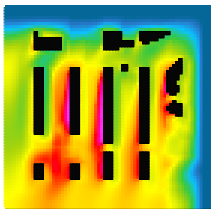




CONTEXT TYPE 2

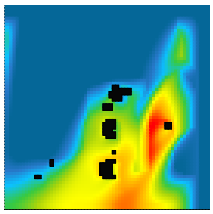
Medium MeanH
Medium GSI
Medium FSI
Low TArea
Low GArea





CONTEXT TYPE 3

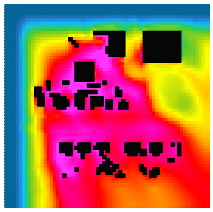
Low MeanH
Low GSI
Low FSI
Low TArea
Low GArea

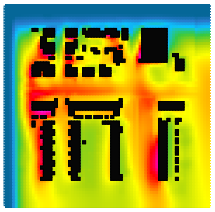




CONTEXT TYPE 4

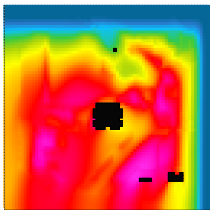
Low MeanH
Low GSI
Low FSI
Low TArea
Medium GArea

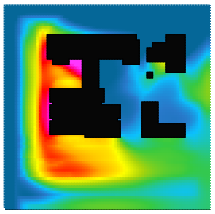




CONTEXT TYPE 5

High MeanH
Medium-High GSI
High FSI
Low TArea
Low GArea

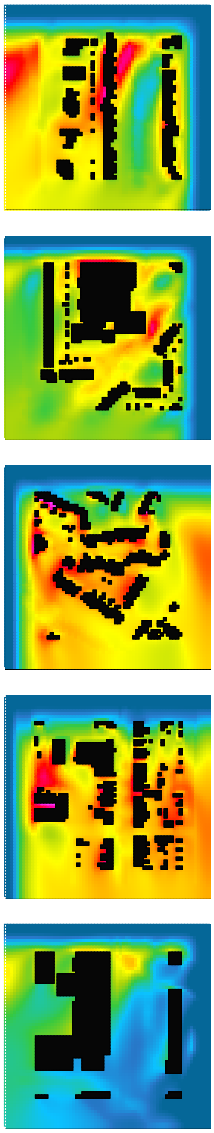




TOC

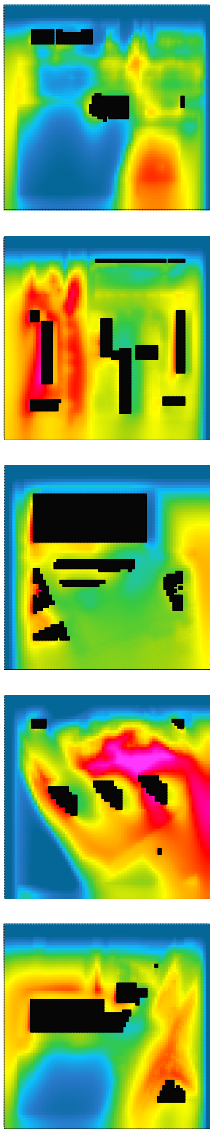
BUILDING TYPE 3

Low B_Height
Low B_Footprint
Low B_StoV



BUILDING TYPE 4

High B_Height
Medium B_Footprint
Low B_StoV



BUILDING TYPE 5

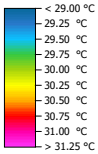
Medium B_Height
High B_Footprint
Low B_StoV



TOC

Day 2

Air Temperature
(16.00h)



BUILDING TYPE 1

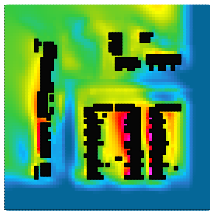
Low B_Height
Low B_Footprint
High B_StoV

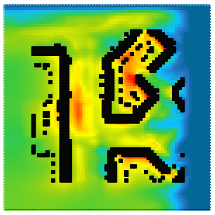
BUILDING TYPE 2

Medium B_Height
Low B_Footprint
Low B_StoV

CONTEXT TYPE 1

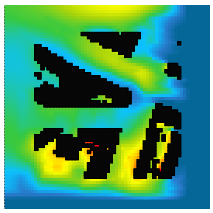
Low-Medium MeanH
Low GSI
Low FSI
High TArea
Medium GArea

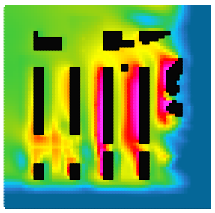




CONTEXT TYPE 2

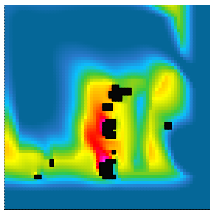
Medium MeanH
Medium GSI
Medium FSI
Low TArea
Low GArea

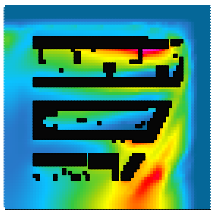




CONTEXT TYPE 3

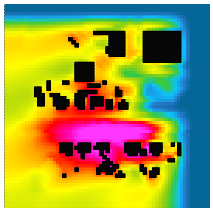
Low MeanH
Low GSI
Low FSI
Low TArea
Low GArea

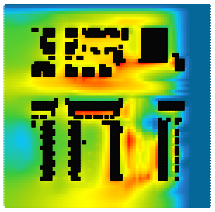




CONTEXT TYPE 4

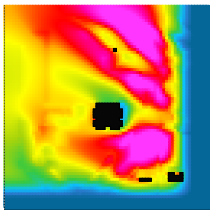
Low MeanH
Low GSI
Low FSI
Low TArea
Medium GArea

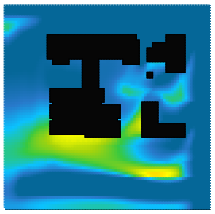




CONTEXT TYPE 5

High MeanH
Medium-High GSI
High FSI
Low TArea
Low GArea

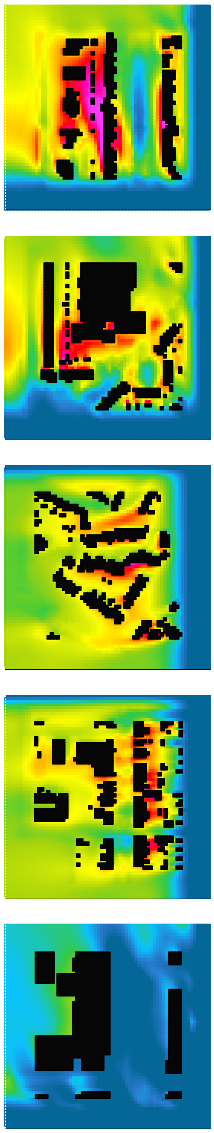




TOC

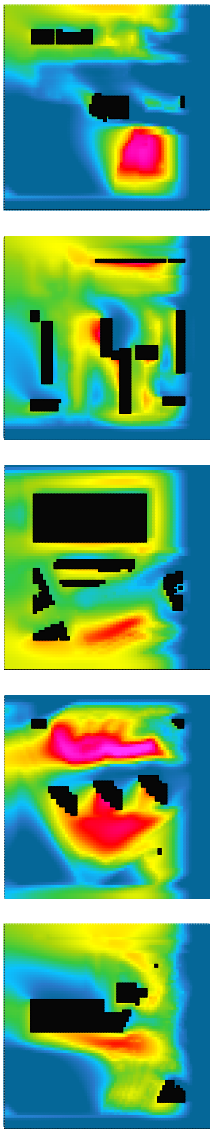
BUILDING TYPE 3

Low B_Height
Low B_Footprint
Low B_StoV



BUILDING TYPE 4

High B_Height
Medium B_Footprint
Low B_StoV



BUILDING TYPE 5

Medium B_Height
High B_Footprint
Low B_StoV



TOC

Day 1

Relative Humidity
(16.00h)

< 52.00 %
52.50 %
53.00 %
53.50 %
54.00 %
54.50 %
55.00 %
55.50 %
56.00 %
> 56.50 %

BUILDING TYPE 1

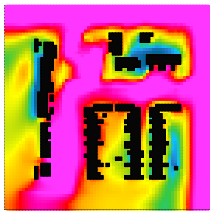
Low B_Height
Low B_Footprint
High B_StoV

BUILDING TYPE 2

Medium B_Height
Low B_Footprint
Low B_StoV

CONTEXT TYPE 1

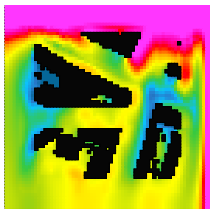
Low-Medium MeanH
Low GSI
Low FSI
High TArea
Medium GArea

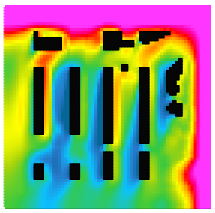




CONTEXT TYPE 2

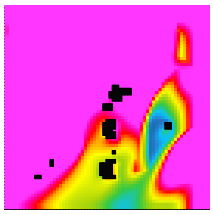
Medium MeanH
Medium GSI
Medium FSI
Low TArea
Low GArea

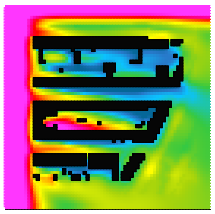




CONTEXT TYPE 3

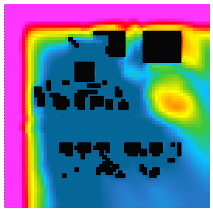
Low MeanH
Low GSI
Low FSI
Low TArea
Low GArea

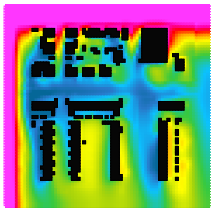




CONTEXT TYPE 4

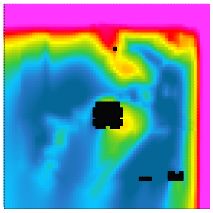
Low MeanH
Low GSI
Low FSI
Low TArea
Medium GArea

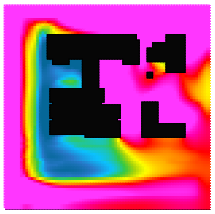




CONTEXT TYPE 5

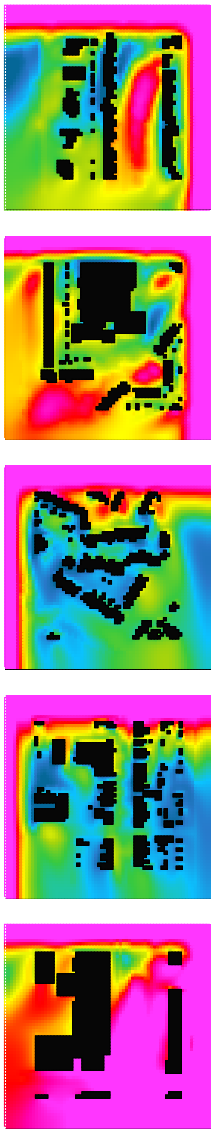
High MeanH
Medium-High GSI
High FSI
Low TArea
Low GArea





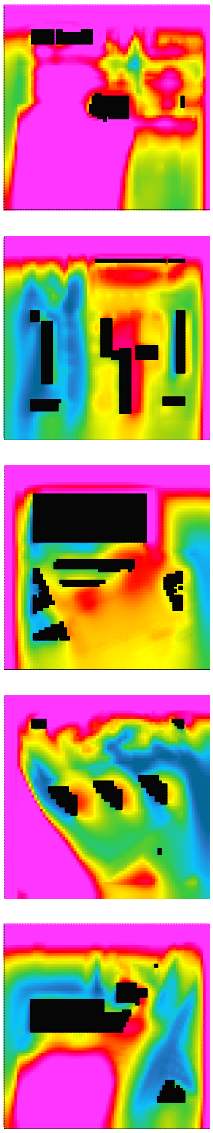
BUILDING TYPE 3

Low B_Height
Low B_Footprint
Low B_StoV



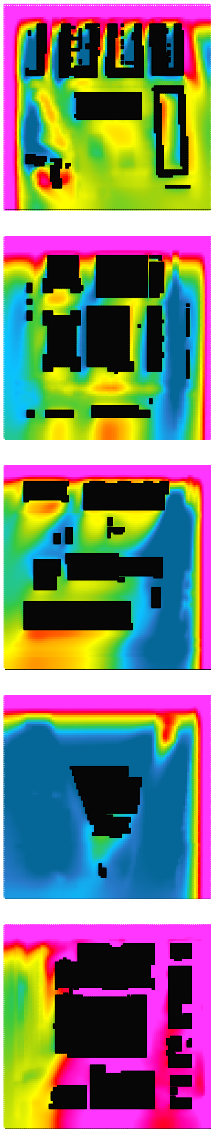
BUILDING TYPE 4

High B_Height
Medium B_Footprint
Low B_StoV



BUILDING TYPE 5

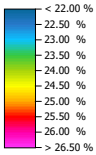
Medium B_Height
High B_Footprint
Low B_StoV



TOC

Day 2

Relative Humidity
(16.00h)



BUILDING TYPE 1

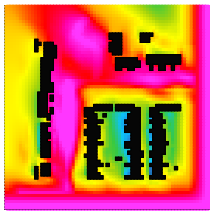
Low B_Height
Low B_Footprint
High B_StoV

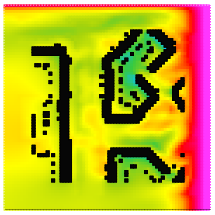
BUILDING TYPE 2

Medium B_Height
Low B_Footprint
Low B_StoV

CONTEXT TYPE 1

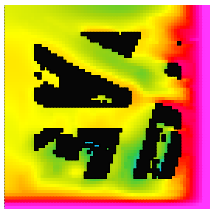
Low-Medium MeanH
Low GSI
Low FSI
High TArea
Medium GArea

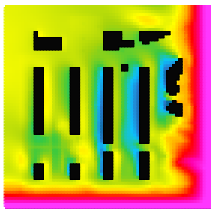




CONTEXT TYPE 2

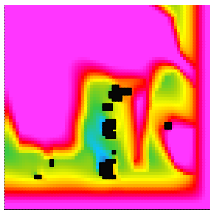
Medium MeanH
Medium GSI
Medium FSI
Low TArea
Low GArea





CONTEXT TYPE 3

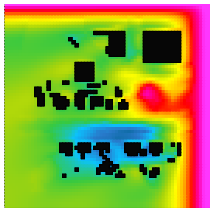
Low MeanH
Low GSI
Low FSI
Low TArea
Low GArea

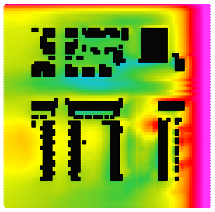




CONTEXT TYPE 4

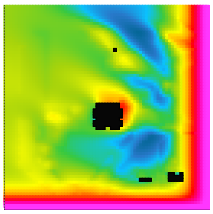
Low MeanH
Low GSI
Low FSI
Low TArea
Medium GArea

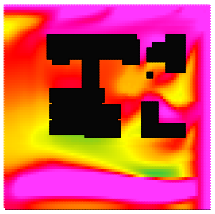




CONTEXT TYPE 5

High MeanH
Medium-High GSI
High FSI
Low TArea
Low GArea

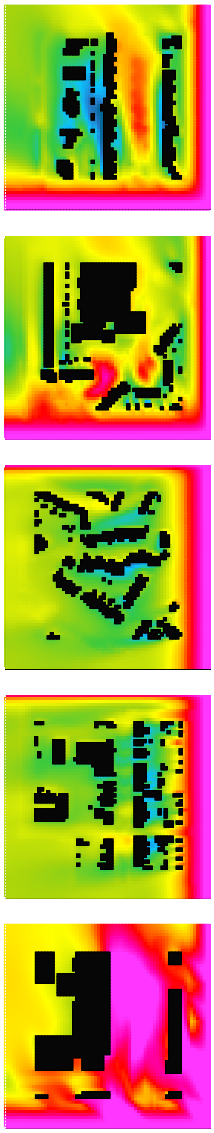




TOC

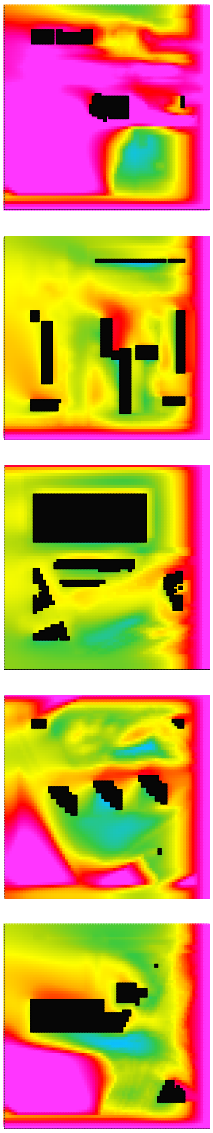
BUILDING TYPE 3

Low B_Height
Low B_Footprint
Low B_StoV



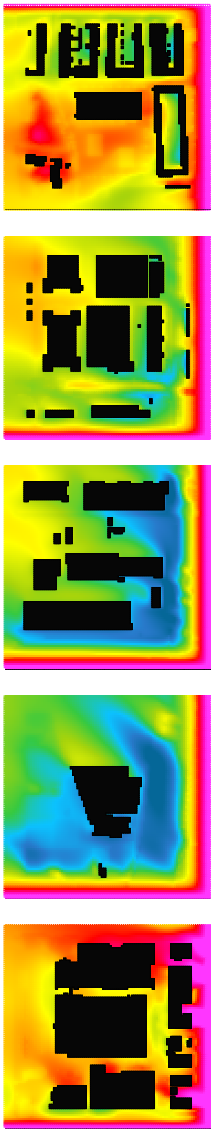
BUILDING TYPE 4

High B_Height
Medium B_Footprint
Low B_StoV



BUILDING TYPE 5

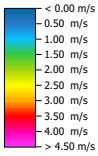
Medium B_Height
High B_Footprint
Low B_StoV

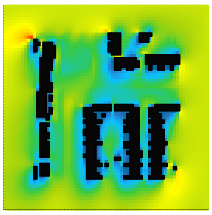
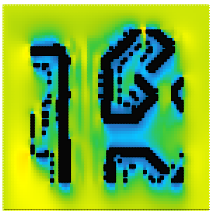
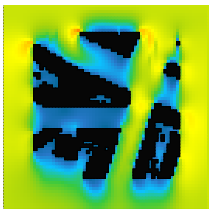
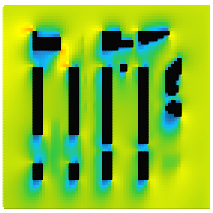
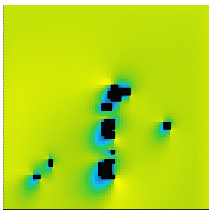
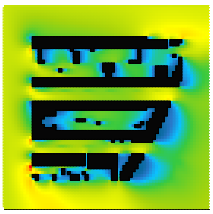
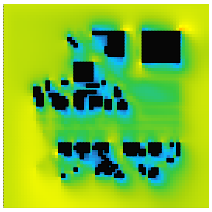
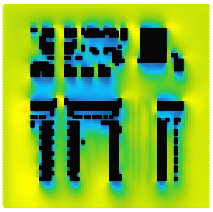
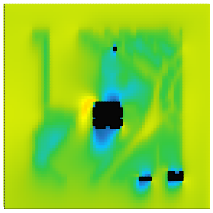
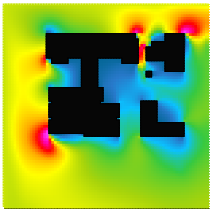


TOC

Day 1

Wind Speed
(16.00h)

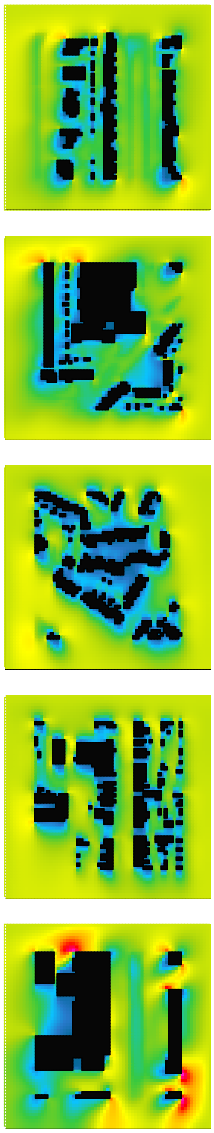


	BUILDING TYPE 1 Low B_Height Low B_Footprint High B_StoV	**BUILDING TYPE 2** Medium B_Height Low B_Footprint Low B_StoV
CONTEXT TYPE 1 Low-Medium MeanH Low GSI Low FSI High TArea Medium GArea		
CONTEXT TYPE 2 Medium MeanH Medium GSI Medium FSI Low TArea Low GArea		
CONTEXT TYPE 3 Low MeanH Low GSI Low FSI Low TArea Low GArea		
CONTEXT TYPE 4 Low MeanH Low GSI Low FSI Low TArea Medium GArea		
CONTEXT TYPE 5 High MeanH Medium-High GSI High FSI Low TArea Low GArea		

TOC

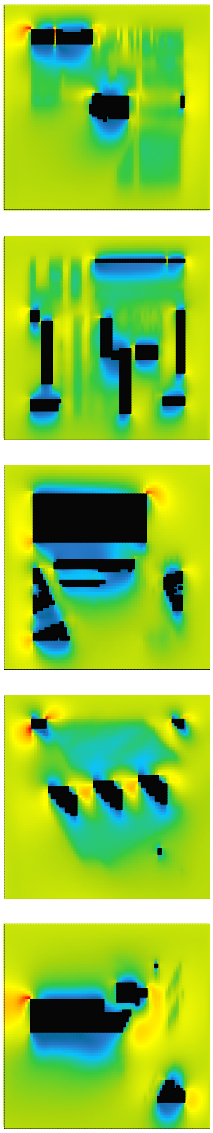
BUILDING TYPE 3

Low B_Height
Low B_Footprint
Low B_StoV



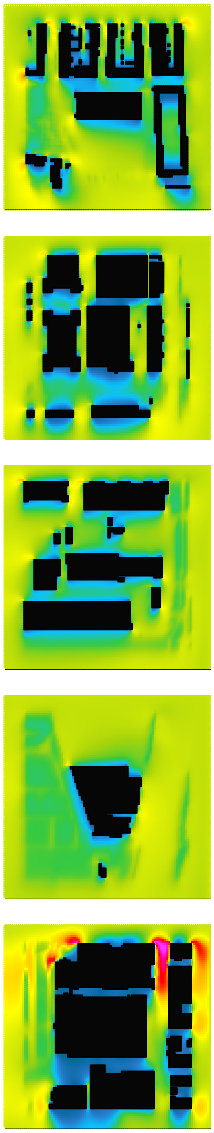
BUILDING TYPE 4

High B_Height
Medium B_Footprint
Low B_StoV



BUILDING TYPE 5

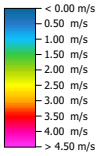
Medium B_Height
High B_Footprint
Low B_StoV

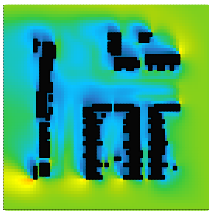
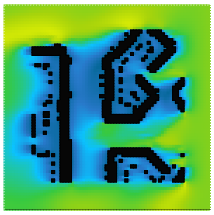
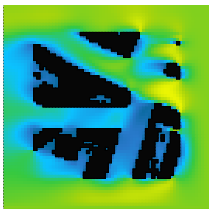
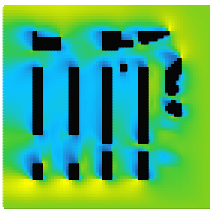
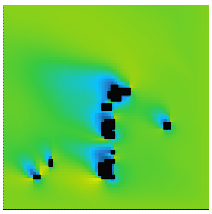
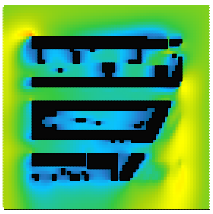
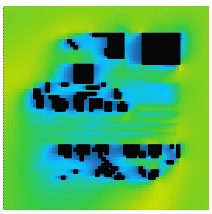
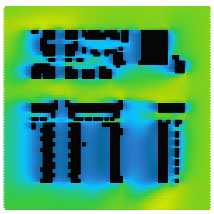
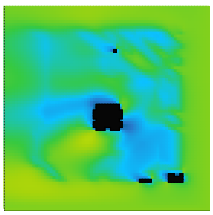
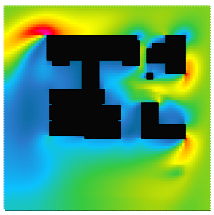


TOC

Day 2

Wind Speed
(16.00h)

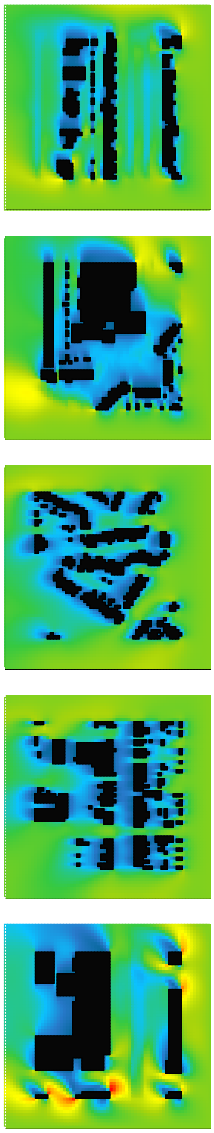


	BUILDING TYPE 1 Low B_Height Low B_Footprint High B_StoV	**BUILDING TYPE 2** Medium B_Height Low B_Footprint Low B_StoV
CONTEXT TYPE 1 Low-Medium MeanH Low GSI Low FSI High TArea Medium GArea		
CONTEXT TYPE 2 Medium MeanH Medium GSI Medium FSI Low TArea Low GArea		
CONTEXT TYPE 3 Low MeanH Low GSI Low FSI Low TArea Low GArea		
CONTEXT TYPE 4 Low MeanH Low GSI Low FSI Low TArea Medium GArea		
CONTEXT TYPE 5 High MeanH Medium-High GSI High FSI Low TArea Low GArea		

TOC

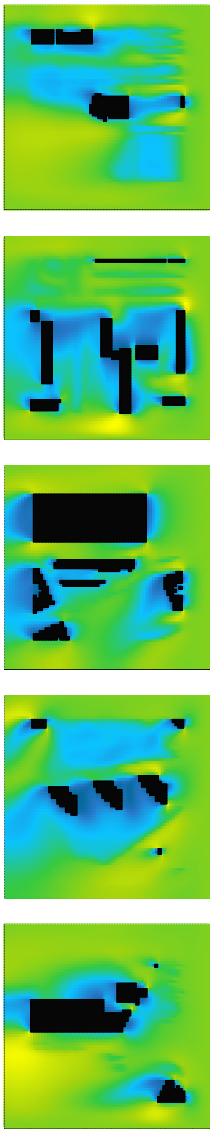
BUILDING TYPE 3

Low B_Height
Low B_Footprint
Low B_StoV



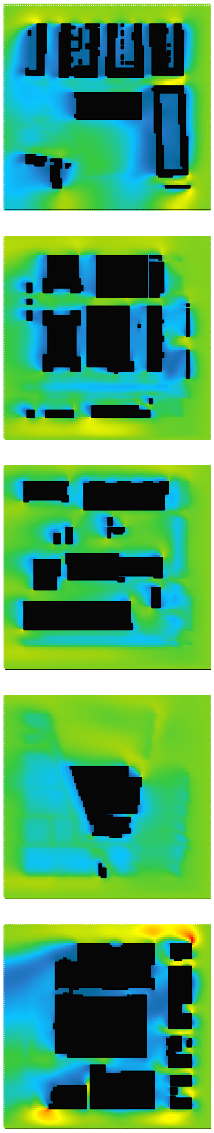
BUILDING TYPE 4

High B_Height
Medium B_Footprint
Low B_StoV



BUILDING TYPE 5

Medium B_Height
High B_Footprint
Low B_StoV



TOC

TOC

Curriculum vitae

Daniela Maiullari



Education

2016 – 2023 **Doctoral Education Programme**
Delft University of Technology, Faculty of Architecture & the Built Environment, Department of Urbanism, Chair of Environmental Technology & Design

2014 **LLP LEONARDO DA VINCI DYF Programme**
Host Organization: Delft University of Technology, Faculty of Architecture & the Built Environment, Department of Urbanism, Chair of Environmental Technology & Design.
Project: JPI Urban Europe 'Green/Blue Infrastructure for Sustainable, Attractive Cities'
Coordinators: Prof.Arjan van Timmeren,Taneha Kuzniecow Bacchin

2010 – 2013 **ClaM.Arch. Master in Architecture:** degree CUM LAUDE, at the University IUAV Venice, Faculty of Architecture.
Title of the thesis: 'Metropolitan reactions. Transport oriented urban development in the Venice Metropolitan Area'. Mentor: Prof. Arch. Alberto Cecchetto

2009 **Specialization Course: Energetic House and Bio-climatic Architecture**
Fellowship by European Social Fund and Ministry of Labour and Social Affairs, En.A.I.P. Puglia, Bari, IT.

2006 – 2009 **ClaSa. Bechelor in Architecture:** Bechelor degree at University IUAV Venice, Faculty of Architecture.

Academic experience

2022 – 2023 Research Fellow | Delft University of Technology, Faculty of Architecture & the Built Environment, Department of Urbanism, Section of Landscape Architecture.

2021 – 2023 Research Fellow | Chalmers University of Technology, Faculty of Architecture and Civil Engineering, Section of Architectural Theory and Methods.

2016 – 2023 PhD candidate | Delft University of Technology, Faculty of Architecture & the Built Environment, Department of Urbanism, Chair of Environmental Technology and Design.

2020 Researcher within the project funded by the AMS Institute and Gemeente Haarlemmermeer, 'Make some Noise. Acustic, microclimate and energy scenarios for flexible housing in Rijsenhout'.
Role: Responsable for microclimate modelling and measurement campaign.

2016 – 2020 Coordinator of the international research project 'SPACERGY. Space-Energy patterns for smart energy infrastructures, community reciprocities & related governance' (JPI Urban Europe).

2014 – 2015 Research assistant in the project JPI Urban Europe 'GREEN BLUE CITIES: Green/ Blue Infrastructure for Sustainable, Attractive Cities'. Coordinators: Prof.Arjan van Timmeren,Taneha Kuzniecow Bacchin

Teaching experience

2021 – 2023 Lecturer | ARK500: Geographical information analysis in the Degree of Business development and entrepreneurship, Department of Architecture and Civil Engineering, Chalmers University of Technology.

2020 – 2021 Lecturer | R&D Studio: Designing Urban Environments (AR1U100), MSc Urbanism, Faculty of Architecture & the Built Environment, Delft University of Technology.

2019 – 2020 Lecturer and tutor | Course for Metropolitan Solutions: Climate Proof Quay Walls (YMS-60312), MSc Made, Amsterdam Institute for Advanced Metropolitan Solutions (AMS).

2019 – 2020 Lecturer and tutor | R&D Studio: Designing Urban Environments AR1U100, MSc Urbanism, Faculty of Architecture & the Built Environment, Delft University of Technology.

2017 – 2021 Graduation mentor | Faculty of Architecture & the Built Environment, Delft University of Technology.

2017 – 2018 Reviewer | MSc3 AR3U022 - Theory of Urbanism, Faculty of Architecture & the Built Environment, Delft University of Technology.

2016 – 2018 Tutor | Urban Metabolism Graduation Studio, Faculty of Architecture & the Built Environment, Delft University of Technology.

TOC

Publications

2022

Maiullari, D., Palm, A., Wallbaum, H., & Thuvander, L. (2022, September). Pathways towards carbon neutrality: A participatory analysis of the Gothenburg's energy plan. In IOP Conference Series: Earth and Environmental Science (Vol. 1085, No. 1, p. 012041). IOP Publishing.

Maiullari, D., Palm, A., Wallbaum, H., & Thuvander, L. (2022, September). Matching energy targets, stakeholders' needs and modelling choices in developing urban energy scenarios. In IOP Conference Series: Earth and Environmental Science (Vol. 1078, No. 1, p. 012087). IOP Publishing.

Maiullari, D. and Pijpers-van Esch, M. and Aldakheelallah, A. and Cannatella, D. (2022) The microclimate performance of urban form : a quantitative morphological approach. In: Annual Conference Proceedings of the XXVIII International Seminar on Urban Form. University of Strathclyde Publishing, Glasgow, pp. 625-633. ISBN 9781914241161

2021

Gherri, B., Maiullari, D., Finizza, C., Maretto, M., & Naboni, E. (2021). On the Thermal Resilience of Venetian Open Spaces. Heritage, 4(4), 4286-4303. https://doi.org/10.3390/heritage4040236

Maiullari D., Pijpers-van Esch M. and van Timmeren A. (2021). A Quantitative Morphological Method for Mapping Local Climate Types. Urban Planning, 6(3), 240-257. https://doi.org/10.17645/up.v6i3.4223

Maiullari D., Gherri B., Finizza C., Maretto M., Naboni E. (2021). Climate Change and Indoor Temperature Variation in Venetian Buildings: the Role of Density and Urban Form. Conference CISBAT 2021- Carbon Neutral Cities - Energy Efficiency & Renewables in the Digital Era, Journal of Physics: Conference Series, 8 September 2021, Lausanne, Switzerland.

Gherri B., Maiullari D., Finizza C., Maretto M., Naboni E. (2021). On Venetian Campi Resilience to Climate Change, Conferenza Internazionale Sustainable Built Heritages – SBE 21, Design, construction and operation of solutions for climate change resilience, Aprile 14 2021, Bolzano, Italia.

Maretto M., Finizza C., Monacelli A., Naboni E., Gherri B., Maiullari D., Iannantuono M. (2021). Regenerative deisgn processes in urban morphology, XXVIII International Seminar on Urban Form ISUF2021: URBAN FORM AND THE SUSTAINABLE AND PROSPEROUS CITIES, 29 June -3 July 2021, Glasgow.

2020 Mosteiro-Romero M., Maiullari D., Pijpers-van Esch M. and Schlueter A. (2020). An Integrated Microclimate-Energy Demand Simulation Method for the Assessment of Urban Districts. Front. Built Environ. 6:553946. doi: 10.3389/fbuil.2020.553946

Maiullari D., Pijpers-van Esch M., Mosteiro-Romero M., and van Timmeren A. (2020). Modelling the Impact of Vegetation on Building Space Cooling. PLEA 2020, Sustainable Architecture and Urban Design, Planning Post Carbon Cities: Proceedings of the 35th International Conference on Passive and Low Energy Architecture, University of A Coruña (UDC), Coruña, Spain.

2019 Maiullari D., Mosteiro-Romero M., de Koning R., van Timmeren A., van Nes A., & Schluter A. (2019). SPACERGY: Space-Energy Patterns for Smart Energy Infrastructures, Community Reciprocities and Related Governance. BK BOOKS,TU Delft. ISBN 978-946-366-2147.

Natanian J., Maiullari D., Yezioro A., & Auer T. (2019). Synergetic urban microclimate and energy simulation parametric workflow Synergetic urban microclimate and energy simulation parametric workflow. Journal of Physics: Conference Series, 1343. https://doi.org/10.1088/1742-6596/1343/1/012006

Mosteiro-Romero M., Maiullari D., Collins F., & Schlueter A. (2019). District-scale energy demand modeling and urban microclimate : A case study in The Netherlands. Journal of Physics: Conference Series, 1343. https://doi.org/10.1088/1742-6596/1343/1/012003

Maiullari D., van Timmeren A., Mosteiro-Romero M., (2019). Spatial Negotiation and Energy Transition management: the University campus Zurich Case. International Conference: the Reciprocity of Space and Energy, TU Delft, Delft.

2018 Maiullari D., Mosteiro-Romero M., & Pijpers-van Esch M. (2018). Urban Microclimate and Energy Performance: An Integrated Simulation Method. In E. Ng, S. Fong, & C. Ren (Eds.), PLEA 2018 Smart and Healthy Within the Two-Degree Limit: Proceedings of the 34th International Conference on Passive and Low Energy Architecture; Chinese University of Hong Kong, Hong Kong, China (Vol. 1, pp. 384-389).

Maiullari D. (2018). Microclimatic performance of urban form: an analytic method in energy-sensitive urban design (Abstract). International Seminar on Urban Form ISUF 2018, Krasnoyarsk, Russia.

Maiullari D., & Mosteiro-Romero M. (2018). The impact of microclimate on building energy demand: A district scale simulation method. Poster session at CITY + 2018: The International Conference for PhD Students and Early Career Researchers on urban Studies, London, United Kingdom.

2017

Maiullari D. and van Timmeren A. (2017). Building Scenarios in Urban Energy Transition: A trans-disciplinary method for integrated spatial energy design. PLEA 2017, Design to Thrive: Proceedings of 33rd PLEA International Conference, Edinburgh, UK, NCEUB, 2017, vol.I, pp. 1438-1445

Maiullari D. (2017). Energy and Space Reciprocity. A Morphological Approach for urban design in energy transition (PhD Go / No Go report), Delft University of Technology, Faculty of Architecture & the Built Environment, Department of Urbanism, Chair of Environmental Technology & Design.

Maiullari D.,Mosteiro Romero M., van Timmeren A., (2017), Space-Energy Development Scenarios for the Zurich Hochschulquartier, JPI Urban Europe - Report for the project SPACERGY, TU Delft.

2016

Maiullari D., Wandl A., Pijpers-van Esch M., van Timmeren A. (2016). Smart Cities and Socio-technical Utopias in the transition towards a carbon-free society. International conference GIORNATA DI STUDIO BERNARDO SECCHI- Utopia and the project for the City and the Territory. 17 -18 November 2016, Venice, IT.

TOC

23#04

Urban form influence on microclimate and building cooling demand

An analytical framework and its application on the Rotterdam case

Daniela Maiullari

Urban form plays a critical role when planning city transitions toward decarbonization. However, in urban climate conditions the complex relationship between urban form and cooling demand remains understudied. This thesis develops integrated approaches and knowledge in the transdisciplinary domain of urban morphology, urban climatology and energy-related fields while addressing the question: *'How does urban form influence building cooling demand in urban microclimate conditions, and how can the magnitude of the relationship be assessed?'*.

By answering this main research question, the thesis delivers a threefold contribution. First, it contributes to the conceptualization and understanding of both the intrinsic and the extrinsic role of urban form, by identifying urban form characteristics that directly influence building cooling demand, and indirectly contribute to shaping urban microclimate conditions in buildings' surroundings. Second, the thesis contributes to increasing the assessment accuracy of urban form-related climate and energy performance. It does so by developing a quantitative morphological method to identify Local Climate Types (LCTs) and by developing a modelling method that enhances the use of microclimate data as boundary conditions for energy demand assessments. Thirdly, for the city of Rotterdam, the testing of these novel methods provides an understanding of how and to what extent the form of buildings and contexts influence building cooling demand.

A+BE | Architecture and the Built Environment | TU Delft BK